Chemical valorization of bio-oil resulting from biomass pyrolysis for green polymer synthesis

Jie Xu

Normandie Université

THESE

Pour obtenir le diplôme de doctorat

Spécialité génie de procède

Préparée au sein de « INSA Rouen Normandie »

Chemical valorization of bio-oil resulting from biomass pyrolysis for green polymer synthesis

Présentée et soutenue par
Jie XU

Thèse soutenue publiquement le 28/04/2022 devant le jury composé de		
Mme Sophie DUQUESNE	Professeure / ENSCL / Unité Matériaux et Transformations / Lille	Rapporteur
M. Guillain MAUVIEL	Professeur / Université de Lorraine / LRGP / Nancy	Rapporteur
M. Jack LEGRAND	Professeur Emérite / Université de Nantes / GEPEA / Saint Nazaire	Examinateur
M. Boulos YOUSSEF	MCF / INSA Rouen Normandie / Laboratoire PBS / Rouen	Examinateur
M. Nicolas BRODU	MCF / Université de Rouen Normandie / LSPC / Rouen	Co-encadrant de thèse
M. Bechara TAOUK	Professeur / INSA Rouen Normandie / LSPC / Rouen	Directeur de thèse

Thèse dirigée par Bechara TAOUK et Nicolas BRODU, Laboratoire de Sécurité des Procédés Chimiques - LSPC

INSA INSTITUT NATIONAL DES SCIENCES APPLIQUÉES ROUEN NORMANDIE

ED 591 PSIME

LSPC Laboratoire de sécurité des procédés chimiques

Never give up

永不言弃

Acknowledgments

My doctoral thesis is supported by the cooperation program between China scholarship council (CSC) and UT- INSA (France) from 2018-2022. First of all, I would like to thank CSC for supporting me to allowing me to have my Ph.D. in France. And also, thanks for our lab LSPC (Laboratoire de Sécurité des Procédés Chimiques) in INSA Rouen Normandie for the technical support.

My deepest gratitude goes to my thesis director Prof. Bechara Taouk for his patient guidance and supervision. He is always gentle, kind, calm demeanor, meticulous, has great knowledge, and broad vision, and always calms me down when I am anxious. In my first year of my Ph.D., each time I encounter problems with the experimental setup, he always came to the lab to help me and guided me on how to do it immediately. Whenever I need to discuss I can always find him in the office, he always spares time and patiently helps me. His encouragement and help made me more confident and more passionate about scientific research and chemical process engineering.

The profound gratitude should go to my thesis co-supervisor Dr. Nicolas Brodu for all the things he did in these three years for this doctoral thesis. He has a wealth of knowledge and a keen sense of scientific research, and he can always easily help me solve all the problems encountered in the experiment. He has a strong sense of responsibility and can always encourage, care for, and help me appropriately so that I can stabilize my mood and regain my confidence. He gave me great instructions and advice in the process of selecting topics, designing experiments, writing papers and articles, and perfecting outlines and arguments. The thesis could not be finished without his patient guidance.

I would like to thank all of the jury members of my doctoral thesis defense: Sophie Duquesne, Guillain Mauviel, Jack Legrand, and Boulos Youssef for evaluating my thesis and for their questions and valuable comments on it.

I would also like to thank all the staff from LSPC, PBS, and COBRA. Thanks for their kind help to me. In particular, I would like to thank Lokmane Abdelouahed and Boulos Youssef for their insightful comments on my experiment and articles, which provide me with many enlightening ideas. I would like to thank Alain Ledoux, Laurent Balland, Lionel Estel, Maria Pereira De Araujo, Fabien Boust, Jeremy Deshais, Isabelle Delaroche, Raphaël Delamare,

Sylvie Poubelle and Jean-Pierre Hébert for their help for my experiments. I would like to thank CSI members Lokmane Abdelouahed and Laurence Lecamp. Especially, I would like to thank Bruno Daronat, for his kindness and help in my experience and reactor. I would also express my sincere gratitude to Christine Devouge-Boyer and Mélanie Mignot from COBRA for your help in chemical analysis.

Therefore, I would like to thank all my Ph.D. and master colleagues in LSPC. I'm very happy I can work together with all of you for these three years. I would like to thank Xiaoshuang Cai Chetna Mohabeer, Yanjun Wang, Jundong Wang, Xiaojia Lu, Isabelle Lahoud, Luis Reyes Alonzo, Silvia De Los Santos Meran, Elizabeth Garcia Hernandez, Michael Jabbour, Balkydia Campusano Mercedes, Jose Delgado Liriano, Rosy Valdez Lorenzo, Leonela Martes Hernandez, Daniele Di Menno Di Bucchianico, Sindi Baco (my amazing neighbor), Yudong Meng. I would also like to thank some colleagues in PBS for their kind help: Xuelian Liu, Bo Jiang, Yuzhen Lou, Vincent Valette, Vincent Gonnot, Klara Jastak, Di Wang, and Bao Ding. In particular, I want to express my gratitude to my friends for their three years of accompanying and helping in Rouen: Ruiping Yang, Linlin Jia, Jing Zhang, Ling Chen, Chao Ren, Xuefei Wang, and Ce Zhang.

I would like to thank my supervisors during my master's study, Prof. Zhongwen Liu, and Prof. Jinqiang Jiang. Thanks for supporting me apply for the CSC/UT-INSA and guiding me during my master's. I would like to thank my master's colleagues and friends: Huan Wang, Fang Yin, Guoqing Yang, Xiaoyong Zhang, Mengxiao Yan, Ning Du, Yuanbao Zhang, Yang He, etc. Thanks a lot for your kind help.

Finally, I would like to give my greatest thanks to my parents, who always support me and encourage me at any time and in any situation. I never feel scared because knowing you are here, standing behind me. I would also like to thank my best friend Jieru Zeng, you have always been able to encourage me and comfort me in my most difficult times. We have been best friends for 16 years and we will be best friends for life.

Contents

List of Figures

◆ Figures of GENERAL INTRODUCTION

◆ Figures of chapter 1

◆ Figures of chapter 2

◆ Figures of chapter 3

◆ Figures of chapter 4

◆ Figures of chapter 5

◆ Figures of general conclusion and perspective

◆ Figures of Appendix 1

◆ Figures of Appendix 2

◆ Figures of Appendix 3

◆ Figures of Appendix 4

List of Tables

◆ Tables of chapter 1

◆ Tables of chapter 2

◆ Tables of chapter 3

◆ Tables of chapter 4

◆ Tables of chapter 5

◆ Tables of Appendix 2

◆ Tables of Appendix 3

◆ Table of Appendix 4

List of Abbreviations

A: the pre-exponential factor (min^{-1})

A: 0.2 mol/L NaOH volume (mL) for the blank

ATR-FTIR: Attenuated total reflectance-Fourier transform infrared spectroscopy

B: 0.2 mol/L NaOH volume (mL) for the prepolymer

BPA: bisphenol A

BPF: bio-oil phenol formaldehyde resin

BOA: bio-oil acetaldehyde resin

BOG: bio-oil glyoxal resin

BW: Beech wood

C: constant of Flynn–Wall–Ozawa method

C_A: the concentration at any time t ($mol \cdot L^{-1}$).

C_{A0}: the initial concentration ($mol \cdot L^{-1}$),

C_p: the heat capacity of the reaction mixture (J/g/K)

$C_{NaOH:}$ Molar concentration of 0.2 mol/L NaOH solution

Co-1, Co-2 and Co-3: The first, second and third condenser

Di: distribution ratio of a particular component

DCM: dichloromethane

DGEBA: Bisphenol A type epoxy resin

DMSO-D^6: Dimethyl sulfoxide-d^6

DPA: 2,6-dimethylphenol acetaldehyde resin

DSC: Differential scanning calorimeter

DTG: Derivative thermogravimetry

DTR: Drop tube reactor

E_a: the activation energy (J/mol)

ECH: Epichlorohydrin

ECN: effective carbon number method

EEW: Epoxy equivalent weight

EGA: 4-ethylguaiacol acetaldehyde resin

FCC: Fluidized catalytic cracking

FS: Flax shives

FWO: Flynn–Wall–Ozawa method

k: reaction rate constant (s^{-1})

GC-MS: Gas chromatography-mass spectrometry

GC-FID: Gas chromatography-flame ionization detection

GC-TCD: Gas chromatography-thermal conductivity detection

GVL: γ-valerolactone

GPC: Gel permeation chromatography

^{1}H-NMR: the nuclear magnetic resonance

HDO: Hydro de-oxygenation

HHV (Higher Heating Value)

HMF: 5-(Hydroxymethyl) furfural

HMTA: Hexamethylenetetramine

HPLC: High-performance liquid chromatography

IRTF : Infrarouge à transformée de Fourier

KF: Karl Fischer titration method

KOH: potassium hydroxide

L: the weight of the dried OIL1WI

M_n: number average molecular weight

M_w: weight average molecular

MCA: m-cresol acetaldehyde resin

Mimic: mimic phenol acetaldehyde resin

mol. %: percentage, on molar basis

MPA: model phenol acetaldehyde resin

MTSR: Maximum temperature of synthesis reaction

n: reaction order

NCG: Non-condensable gases

OCA: o-cresol acetaldehyde resin

OHN: The hydroxyl number

Oil-1, Oil-2, and Oil-3 (OIL1, OIL2 and OIL3): The oil fractions collected from the condensation setup is a three-stage condensation including three condensers (Co-1, Co-2, and Co-3, respectively).

Oil-S (OILS): the oil collected from the condensation setup is a single condenser and single flask held in a cold bath at -11 °C.

Oil-S-WS, Oil-1-WS and Oil-2-WS (OILSWS, OIL1WS and OIL2WS): the water-soluble fraction of Oil-S, Oil-1, and Oil-2

Oil-S-WI, Oil-1-WI and Oil-2-WI (OILSWI, OIL1WI and OIL2WI): the water-insoluble fraction of Oil-S, Oil-1, and Oil-2

OILSA, OIL1A, OIL2A, OILSWIA, OIL1WIA, and OIL2WIA: bio-oil acetaldehyde resin using various bio-oil products

P = BOE resin weight (g)

PA: phenol acetaldehyde resin

PF: phenol formaldehyde resin

Ph: phenyl group

PHMF: phenol–hydroxymethylfurfural resin

PTFE: polytetrafluoroethylene

q: the specific heat release rate

R: the gas constant (8.314 J/mol/K)

R^2: Pearson's correlation coefficient ($0 \leq R^2 \leq 1$)

R_{800}: the residue percentage at 800℃

r_A: the reaction rate ($mol \cdot L^{-1} \cdot s^{-1}$)

S: the weight of the dried BOE

T_{D24}: Temperature at which TMR_{ad} is 24 hours

T_{d5}: the initial degradation temperature for 5% weight loss

T_g: glass transition temperature

T_i: onset temperature

$T_{max:}$ temperature of maximum decomposition rate

T_p: temperature of the maximum reaction rate or peak temperature

TEBAC: benzyltriethylammonium chloride

TGA: Thermogravimetric analysis

TMR_{ad}: the time to maximum rate under adiabatic conditions

TPP: Triphenylphosphine

wt. %: percentage, on mass basis

X_A: the fractional conversion

Xi.aq: the ratio of the equilibrium mass fraction of a particular component in the aqueous extract phase

Xi.org: the ratio of the equilibrium mass fraction of a particular component in the organic

β: heating rate (K/min)

ΔH: the specific enthalpy of reaction (J/g)

ΔT_{ad}: the adiabatic temperature increase

Abstract

Biomass, in particular wood and wood residues, is the most common form of renewable energy source. Bio-oil, the main product of biomass pyrolysis contains over 400 different chemical compounds. The complexity of their composition makes their direct use difficult. In this study, the combination of two environmentally friendly methods was successfully studied to separate target chemicals from pyrolytic bio-oil of beech wood. Firstly, the fractional condensation of pyrolysis oil was carried out using a system with three condensers at three different temperatures. Then, the water extraction was carried out to further the separation of the products of the different condensers. The stability during the storage of bio-oil was also examined. Each chemical compound of the bio-oil fractions before and after storage was identified and quantified using GC-MS and GC-FID and the yield of the target chemicals was calculated. The phenolics and sugars were mainly found in the first condenser. Separation by water allowed recovering phenolics in the water-insoluble fraction (70.6 wt%) with good stability.

The polymerization of model phenol, a mimic mixture of bio-oil, and the obtained phenol-rich bio-oil fraction of bio-oil with some reactive aldehydes were investigated to produce bio-oil based novolac resin. The aim was to demonstrate the feasibility of using bio-oil instead of petroleum-derived phenol during the manufacture of these resins. Then, the novolacs were cured with commercial and bio-based epoxy resin for preparing bio-based green polymers. The biochar was also applied as an additive to the curing process. The kinetic parameters of the curing reaction were obtained with model-free methods (Kissinger, Flynn–Wall–Ozawa (FWO), Crane) using data from a differential scanning calorimeter (DSC). The curing activation energies of bio-oil resin and phenol resin were very close (95.5 and 94.9 kJ/mol). The risk assessment of the reaction was finally investigated. The results showed that using bio-oil glyoxal resin, bio-oil epoxy resin and biochar for resin curing reaction can significantly reduce the runaway risk.

Résumé

La biomasse, en particulier le bois et ses résidus, est la forme de source renouvelable la plus courante. La bio-huile, principal produit de la pyrolyse de la biomasse, contient plus de 400 composés chimiques différents. La complexité de la composition des bio-huiles rend très difficile leur utilisation directe. Dans cette étude, le couplage de deux méthodes respectueuses de l'environnement a été étudiée avec succès pour séparer les produits chimiques cibles de la bio-huile pyrolytique issue du bois de hêtre. Dans un premier temps, la condensation fractionnée de l'huile de pyrolyse a été réalisée à l'aide d'un système à trois condenseurs à trois températures différentes. Ensuite, l'extraction à l'eau a été effectuée pour améliorer la séparation des produits des différents condenseurs. La stabilité pendant le stockage de la bio-huile a également été examinée. Chaque composé chimique des fractions de bio-huile avant et après stockage a été identifié et quantifié à l'aide de GC-MS et GC-FID et le rendement des produits cibles a été calculé. Les composés phénoliques et les sucres sont recueillis principalement dans le premier condenseur. La séparation à l'eau a permis de récupérer les composés phénoliques dans la fraction des produits insolubles dans l'eau (70,6 % en poids) avec une bonne stabilité.

La polymérisation du phénol, d'un mélange modèle de bio-huile et de la fraction de bio-huile riche en phénols obtenue avec certains aldéhydes réactifs a été étudiée pour produire de la résine novolaque. L'objectif était de démontrer la faisabilité de l'utilisation de la bio-huile à la place du phénol dérivé du pétrole lors de la fabrication de ces résines. Les résines novolaques préparées ont été durcies avec une résine époxy pour préparer des polymères verts biosourcés. Le biochar a également été appliqué comme additif du processus de durcissement. Les paramètres cinétiques de la réaction de durcissement ont été obtenus à l'aide de différentes méthodes (Kissinger, Flynn – Wall – Ozawa (FWO), Crane) en utilisant les données de calorimétrie différentielle à balayage (DSC). Les valeurs de l'énergie d'activation du durcissement de la résine bio-huile et de la résine phénol sont très proches (95,5 et 94,9 kJ/mol). L'évaluation du risque de la réaction a finalement été abordée. Les résultats ont montré que l'utilisation de résine bio-huile -glyoxal, de résine bio-huile-époxy et de biochar pour la réaction de durcissement de la résine peut réduire de manière significative le risque d'emballement.

List of publications and conferences

- **Publications:**
  1. **Xu J**, Brodu N, Mignot M, Youssef B, Taouk B. Synthesis and characterization of phenolic resins based on pyrolysis bio-oil separated by fractional condensation and water extraction. ***Biomass Bioenergy*** 2022;159.
  2. **Xu J**, Brodu N, Abdelouahed L, Taouk B. Investigation of the combination of fractional condensation and water extraction for improving the storage stability of pyrolysis bio-oil. ***Fuel*** 2022;314.
  3. **Xu J**, Brodu N, Wang J, Abdelouahed L, Taouk B. Chemical characteristics of bio-oil from beech wood pyrolysis separated by fractional condensation and water extraction. ***Journal of the Energy Institute*** 2021; 99:186-97.
  4. Wang J, Abdelouahed L, **Xu J**, Brodu N, Taouk B. Catalytic Hydrodeoxygenation of Model Bio-oils Using HZSM-5 and Ni2P/HZM-5 Catalysts: Comprehension of Interaction. ***Chemical Engineering & Technology*** 2021;44(11):2126-38.
- **The article in preparation:**
  5. **Xu J**, Brodu N, Youssef B, Taouk B. Synthesis and characterization of bio-oil-glyoxal novolac resins curing with bisphenol a diglycidyl ether and biochar. ***Green chemistry*** (under review).
  6. **Xu J**, Brodu N, Christine D. Boyer, Youssef B, Taouk B. Biobased novolac resins cured with DGEBA using water-insoluble fraction of pyrolysis bio-oil: Synthesis and characterization. ***Journal of the Taiwan Institute of Chemical Engineers*** (under review)
- **Conferences:**
  1. **Xu J**, Brodu N, Christine D. Boyer, Youssef B, Taouk B. Synthesis and characterization of novel epoxy resins from pyrolysis bio-oil as a curing agent of bio-oil phenol glyoxal novolac resin. ACS Spring 2022, March 20-24, 2022. **Oral presentation**
  2. **Xu J**, Brodu N, Youssef B, Taouk B. Synthesis and characterization of bio-oil-glyoxal novolac resins curing with bisphenol a diglycidyl ether and biochar. ACS Spring 2022, March 20-24, 2022. **Oral presentation**
  3. **Xu J**, Brodu N, Christine D. Boyer, Youssef B, Taouk B. Biobased novolac resins cured with DGEBA using water-insoluble fraction of pyrolysis bio-oil: Synthesis and characterization. 10th Edition of Global Conference on Catalysis, Chemical Engineering and Technology, March 28-30, Singapore, 2022, **Oral presentation**
  4. **Xu J**, Brodu N, Abdelouahed L, Taouk B. The new routine of green polymer synthesis based on pyrolysis bio-oil separated by fractional condensation and water extraction. 4th Seminar of the GDR Thermobio "Thermochemical conversion Biomass and Waste" 30th November –1st December 2021, **Oral presentation**
  5. **Xu J**, Brodu N, Mignot M, Youssef B, Taouk B. Synthesis and characterization of phenolic resins based on pyrolysis bio-oil separated by fractional condensation and water extraction. 29th European Biomass Conference and Exhibition. 26th to 29th April 2021, Marseille, France. **Poster presentation**
  6. **Xu J**, Brodu N, Abdelouahed L, Taouk B. Chemical characteristics of bio-oil from beech wood pyrolysis separated by fractional condensation and water extraction. Pyro 2022, May 15-20, 2022. Het Pend, Ghent, Belgium**. Poster presentation**

GENERAL INTRODUCTION

Nowadays, fossil-based energy resources, such as petroleum, coal, and natural gas, are responsible for about three-quarters of the total the world's primary energy consumption. More than 90% of organic chemicals

in the world are still derived from fossil fuels alone, releasing a large amount of dangerous and greenhouse gases into the atmosphere. In addition, due to the larger consumption of organic chemicals and energy, fossil fuel resources are expected to decline inexorably until 2050. Therefore, it is motivation to explore renewable resources for sustainable production of organic chemicals, polymers, heat, fuels, and electricity [1]. Alternatives to fossil-based energy resources are nuclear power (5%), hydropower (6%), and biomass (13%), representing currently about one-quarter of the world's primary energy consumption [2-4]. Since it is considered that the biomass system and derivatives as sub-systems do not contribute to the greenhouse effect due to the CO_2 neutral conversion, biomass becomes an abundant and carbon-neutral renewable resource to produce biofuels and valuable chemicals [5] (**Figure 0. 1**).

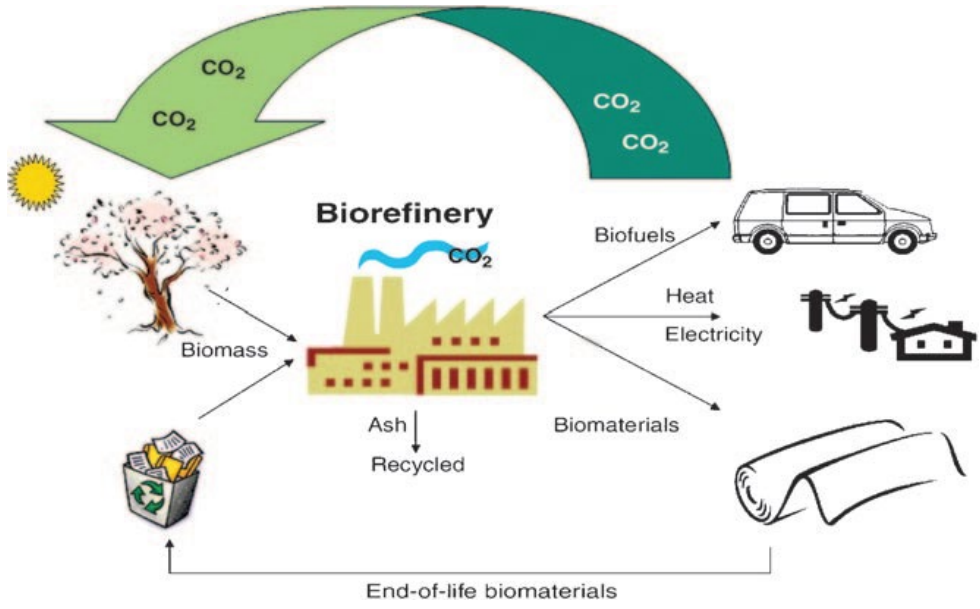

Figure 0. 1 Sustainable technology in an integrated biorefinery[6]

Biomass, in particular wood and wood residues, is the most common form of renewable source. Lignocellulosic biomass typically consists of three major components: 35–50 wt% cellulose, 20–35 wt% hemicellulose, and 10–25 wt% lignin [7]. It can be used directly as a fuel, or be processed into other types of fuel or chemicals. Three thermochemical processes can convert biomass to biofuel or chemicals: pyrolysis, gasification, and liquefaction [8]. The products of biomass pyrolysis are classified into three groups: gas, liquids (bio-oil), and carbon solid residues. Bio-oils contain over 400 different chemical compounds, resulting in the complexity

of their direct use. The strong acidity (pH = 2.5), water content and high oxygen content (35–40 wt%) of bio-oils also lead to a 50% lower energy density than conventional fuels and immiscibility with hydrocarbon fuels [9]. This has an impact on the fuel quality of bio-oils and therefore limits their applications. To improve the physicochemical properties of bio-oil for its practical application in the field of bio-fine chemicals, upgrading is necessary [10]. In recent years, bio-oil has often been used as a substitute for phenol and to synthesize bio-based renewable resins [11, 12].

The aim of this work was to first study the fractional condensation of pyrolysis bio-oil of beechwood as an upgrading method, then to use the water extraction method to separate the bio-oil products into the water-insoluble and water-soluble fractions. Next, the valorization of the obtained phenol-rich bio-oil fraction with some aldehyde crosslinkers was performed to produce resins. The bio-based novolac resin will be cured with commercial and bio-based epoxy resin for preparing bio-based green polymer, as illustrated in Figure 0. 2. The safety parameters of greener synthesis were determined and compared with conventional process reactions.

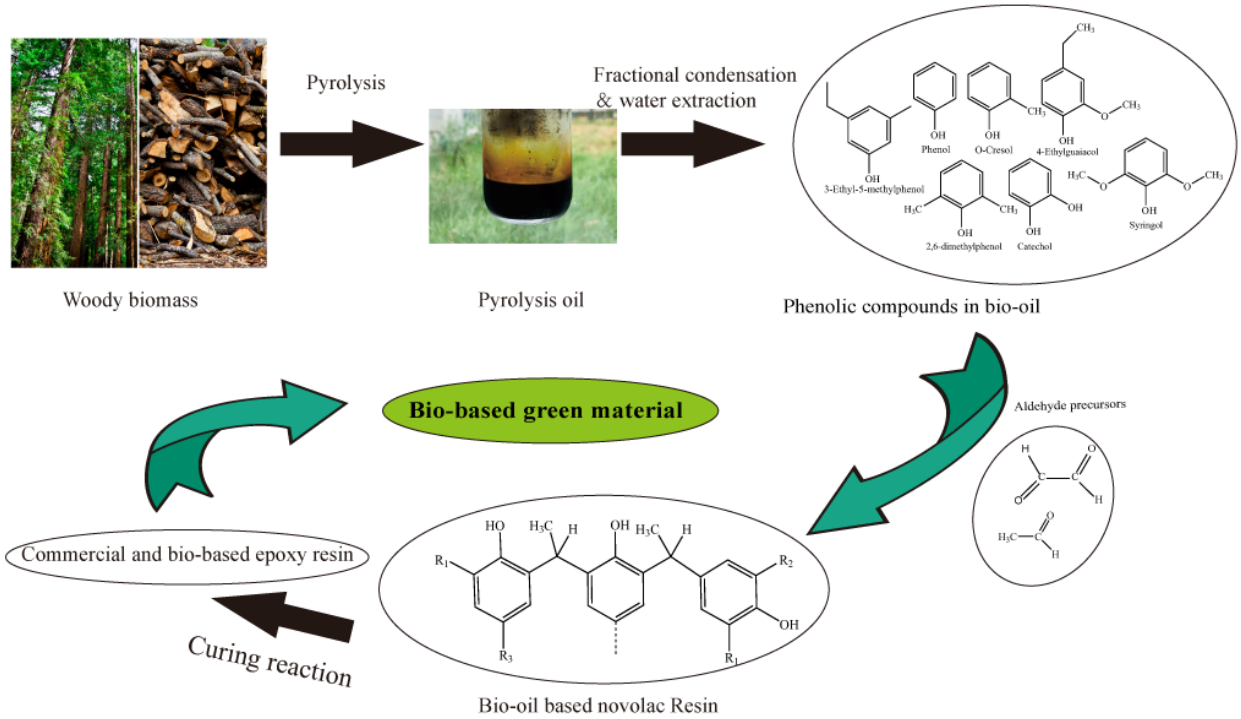

Figure 0. 2 The carries out route design of this work

This manuscript is structured as follows:

Chapter 1 provides a literature review of both main topics of my thesis. Firstly, biomass and upgrading and stability of biomass pyrolysis bio-oil were reviewed, including the physical-chemical characterization of biomass, its conversion processes and technology utilized; the upgrading methods and the storage stability of pyrolysis bio-oil. Secondly, the production of bio-based green polymers based on upgraded bio-oil is then presented, involving: an introduction to renewable bio-based resins; the production of bio-based novolac resins; the selection and synthesis of green curing agent for bio-based novolac resins. Finally, a section dealing with the kinetic study of resinification and curing reaction was discussed.

In Chapter 2, the combination of two environmentally friendly methods was successfully performed to separate target chemicals from the beechwood pyrolytic bio-oil. Firstly, the fractional condensation pyrolysis oil was carried out using a system with three condensers. The effect of the temperature of the first and second condensers was studied. Water extraction was realized to further the separation of products recovered from the three condensers. Each chemical compound of the bio-oil products was identified and quantified using GC-MS and GC-FID. Distribution ratios of the target chemicals were calculated and discussed.

In Chapter 3, the physicochemical properties and composition variation of bio-oil during aging at different storage temperatures and different storage times were studied and compared to that of fresh bio-oil.

In Chapter 4, the polymerization of phenol models (phenol, o-cresol, 2,6-dimethylphenol, m-cresol, and 4-ethylguaiacol) was studied to produce novolac model phenol acetaldehyde resins and mimic acetaldehyde resin. Bio-oil fractions obtained were added to synthesize bio-oil phenol acetaldehyde resins. DGEBA was used for the first time as a formaldehyde-free cross-linker for curing bio-oil based novolac resins. The kinetic parameters of the curing reaction using data obtained from DSC were determined. The physicochemical and thermal properties of resins before and after curing were compared to evaluate the potential of bio-oil products to effectively replace commercial phenols.

In Chapter 5, the polymerization of commercial phenol, mimic phenols and the water-insoluble part of bio-oil fractional condensation products were used to produce the novolac type resins with glyoxal (PG, MPG and BOG). The polymerization of the water-insoluble fraction of bio-oil was also used to synthesize the bio-oil based epoxy resin (BOE). The chemical structure of BOE was characterized by different methods. In a second step, DGEBA and biochar were used

as curing agents for novolac resins. In addition, the BOE will gradually replace DGEBA to use as a bio-based formaldehyde-free cross-linker for bio-based glyoxal novolac resin curing to build a “greener” material. The physicochemical and thermal properties of prepared resins before and after curing were compared. Moreover, polymerization of renewable novolac resins using glyoxal with phenol and bio-oil was conducted in DSC and their reaction mechanism was discussed. Then, a thermal kinetic study was performed to evaluate the safety parameters. Secondly, the safety parameters of the curing reaction of renewable novolac resins (PG and BOG) with 40% DGEBA and 5% biochar were determined. The effect of biochar addition and phenol precursor on the safety of the reaction was discussed.

Chapter I

Literature review

1.1 Introduction

This chapter provides a literature review of both main topics of my thesis. Firstly, the upgrading and stability of biomass pyrolysis bio-oil were reviewed, including the physical-chemical characterization of biomass, its conversion processes and technology utilized, the upgrading methods, and the study of storage stability of bio-oil. Secondly, the production of bio-based green polymers based on upgraded bio-oil was summarized, involving: an introduction of renewable bio-based resins; the production of bio-based novolac resins; the selection and synthesis of green curing agent for bio-based novolac resins. Finally, a section dealing with the kinetic study of resinification and curing reaction was discussed, in particular, the assessment of safety parameters is presented.

1.2 The composition and conversion of biomass

1.2.1 Biomass

Biomass is a complex biogenic organic-inorganic solid product generated by natural and anthropogenic processes and comprises: (i) natural constituents originating from growing land and water-based vegetation via photosynthesis or generated via animal and human food digestion, and (ii) technogenic products derived via processing of the above natural constituents. The general classification of biomass varieties can be divided preliminary and roughly into several flowing groups according to the literature [13-16] (**Table 1. 1**). Lignocellulosic biomasses, which are the most abundant and renewable biomass on earth and lowest cost, have crucial advantages over other biomass supplies because they are the non-edible portion of the plant and therefore, they do not interfere with food supplies. Moreover, disposal of the biomass wastes in the soil or landfill causes serious environmental problems. It could be utilized as a promising alternative to produce biofuels, biomolecules, and biomaterials [17-19].

Table 1. 1 General classification of biomass varieties as solid fuel resources according to their biological diversity, source, and origin. [5]

Biomass groups	Biomass sub-groups, varieties, and species
1. Wood and woody biomass	Coniferous or deciduous; angiospermous or gymnosperms; soft or hard; stems, branches, foliage, bark, chips, lumps, pellets, briquettes, sawdust, sawmill, and others from various wood species
2. Herbaceous and agricultural biomass	Annual or perennial and field-based or processed-based such as: Grasses and flowers (alfalfa, arundo, bamboo, banana, brassica, cane, cynara, miscanthus, switchgrass, timothy, others) Straws (barley, bean, flax, corn, mint, oat, rape, rice, rye, sesame, sunflower, wheat, others) Other residues (fruits, shells, husks, hulls, pits, pips, grains, seeds, coir, stalks, cobs, kernels, bagasse, food, fodder, pulps, cakes, others)
3. Aquatic biomass	Marine or freshwater algae; macroalgae (blue, green, blue-green, brown, red) or microalgae; seaweed, kelp, lake weed, water hyacinth, others
4. Animal and human biomass wastes	Bones, meat-bone meal, chicken litter, various manures, others
5. Contaminated biomass and industrial biomass wastes (semi-biomass)	Municipal solid waste, demolition wood, refuse-derived fuel, sewage sludge, hospital waste, paper-pulp sludge, waste papers, paperboard waste, chipboard, fireboard, plywood, wood pallets and boxes, railway sleepers, tannery waste, others
6. Biomass mixtures	Blends from the above varieties

1.2.2 Composition of lignocellulosic biomass

Lignocellulosic biomass, referring to most plants or plant-based materials, is composed of three main structural constituents (**Figure 1. 1**): hemicellulose (25 –35%), cellulose (40 – 50%), and lignin (15 – 20%). It also includes some non-structural components (minerals, extractives, moisture)[20]. The relative weight proportions of cellulose, hemicellulose, and lignin depending on the type of biomass, have a distinct effect on the quality and the quantity of the produced bio-oil [20-23].

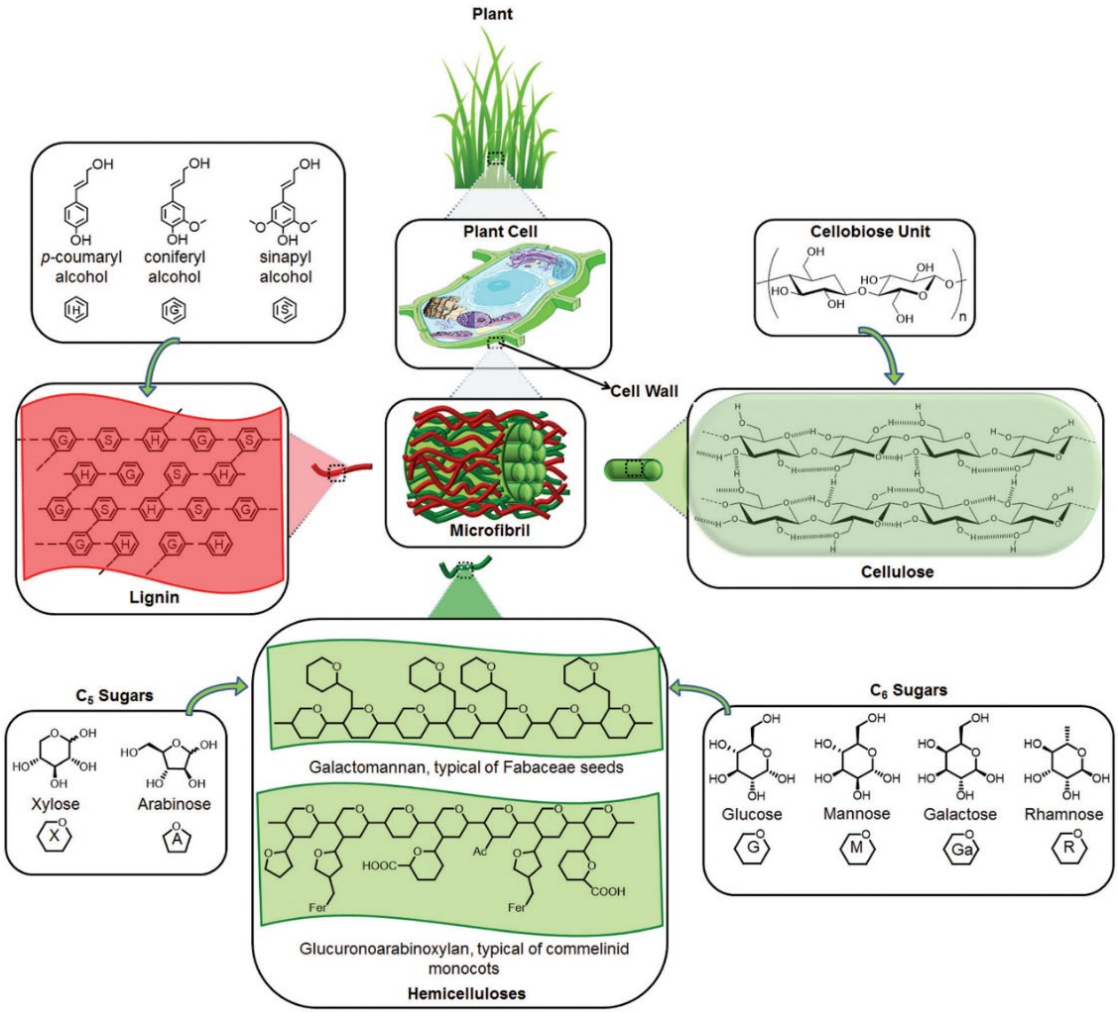

Figure 1. 1 The structure of main components of lignocellulosic biomass [18]

Cellulose: The major component of lignocellulosic biomass is cellulose. Unlike glucose in other glucan polymers, cellulose is a high molecular weight linear polymer of β-(1-4)-d-glucopyranose units linked together by (1-4) glycosidic bonds. These repeating units are cellobiose units (two glucose units)[4, 18]. Its structure consists of extensive intramolecular and intermolecular hydrogen bonding networks, which tightly bind the glucose units (**Figure 1. 1**). Cellulose has a crystalline structure including amorphous regions. Its variable degrees of polymerization can reach several thousand [21]. Groups of cellulose chains make microfibril sheets which are the basis of complex fibers. Since about half of the organic carbon in the biosphere is present in the form of cellulose, the conversion of cellulose into fuels and valuable chemicals has paramount importance [2].

Hemicellulose: Hemicellulose is the second most abundant bio-polymer. Unlike cellulose, hemicellulose has a random and amorphous structure, which contains five-carbon sugars (usually xylose and arabinose) and six-carbon sugars (galactose, glucose, and mannose), all of

which are highly substituted with acetic acid. The most abundant building block of hemicellulose is xylan (a xylose polymer linked at the 1 and 4 positions). Hemicellulose is amorphous because of its branched nature and it is relatively easy to hydrolyze to its monomer sugars compared to cellulose [2].

Lignin: Lignin constitutes the third main component of lignocellulosic biomass, and is an amorphous, three-dimensional polyphenolic material with no exact structure. Lignin fills the spaces in the cell wall between the cellulose and hemicellulose. It is covalently linked to hemicellulose and confers mechanical strength to the cell wall and by extension the plant. As shown in **Figure 1. 1**, the three main structural units occurring in lignin correspond to coniferyl, sinapyl and p-coumaryl alcohol [20].

1.2.3 Conversion of biomass

Lignocellulosic biomass is acknowledged as the largest source of renewable energy available in the world. Conversion of biomass to energy is undertaken using two main process technologies: thermo-chemical and bio-chemical/biological. Bio-chemical conversion encompasses two process options: anaerobic digestion (production of biogas, a mixture of mainly methane and carbon dioxide) and fermentation (production of ethanol) [8, 24, 25]. Of the biotechnological methods of biomass conversion, anaerobic fermentation is the most used.

Concerning thermo-chemical conversion, six process options are available: combustion, pyrolysis, gasification, liquefaction, carbonization, and torrefaction [22, 24, 26-28]. The main differences between each method are summarized in **Figure 1. 2**. The operations of these methods depend on oxygen supply and reaction temperature, while solid, liquid, and gas biofuels are produced, except for combustion [27]. Biofuels produced from lignocellulosic biomass via thermochemical technologies are gaining increasing interest as alternatives to petroleum-based fuels due to their economic and environmental benefits [29]. Pyrolysis and liquefaction are two main thermochemical biomass-to-liquid conversion methods used to obtain bio-oils from biomass.

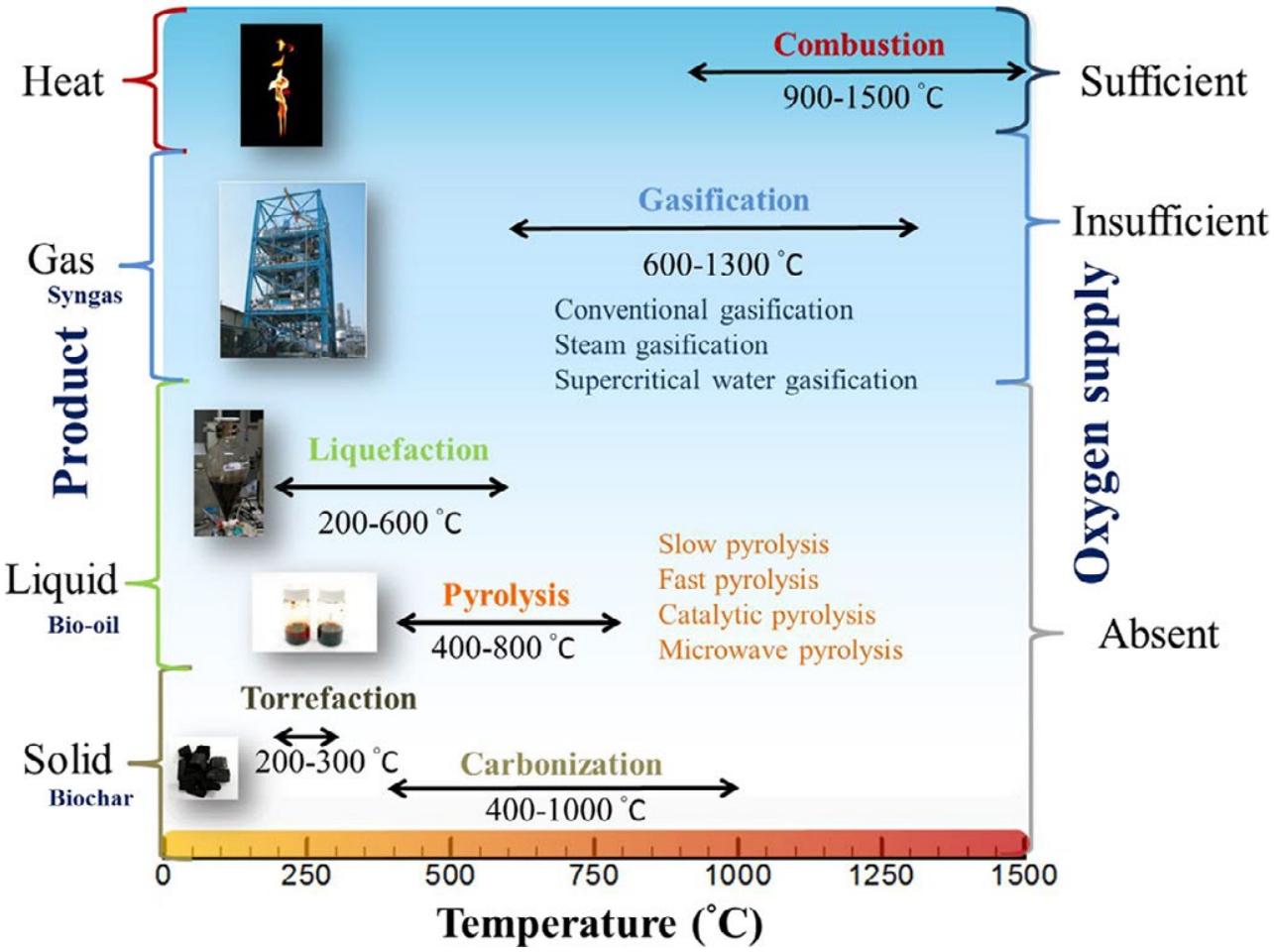

Figure 1. 2 A schematic description of biomass thermochemical conversion methods [27]

1.2.3.1 Pyrolysis of biomass

1.2.3.1.1 Types of pyrolysis

The word — Pyrolysis, results from two Greek words: 'pyro', which means fire, and 'lysis', which means disintegration into integral parts. [28]. Pyrolysis can be defined as thermal degradation (devolatilization) in the absence of an externally supplied oxidizing agent. The pyrolysis products are mainly bio-oil, biochar, and low molecular weight gases. The biomass is selected based on various properties such as moisture content, lignocellulosic composition, particle size, etc. In addition, temperature, heating rate, inert gas flow rate, residence time, pressure, and reaction time are all operating variables that affect the distribution and properties of the products formed [30, 31].

Pyrolysis can mostly be classified into three types (**Table 1. 2**): fast, intermediate and slow. Compared to slow pyrolysis which yields higher amounts of biochar, fast pyrolysis results in maximum yields of bio-oil due to a faster heating rate, shorter vapor residence time and rapid

quenching of hydrocarbon vapors [32].

Table 1. 2 Summary of different pyrolysis process conditions and products yield [26, 30, 33]

Mode	Process temperature (°C)	Heating rate (°C/s)	Vapor residence time	Biomass size	Bio-oil	Biochar	Syngas
Fast/flash	~500°C	>1000	< 1 s	Finely ground	50–70	10–30	15–20
Intermediate	~ 400-500°C	1-1000	10–30 s	Corse/chopped/ finely ground	35–50	25–40	20–30
Slow	~ 300-500°C	Up to 1	>30 s	Briquette/whole	20–50	25–35	20–50

1.2.3.1.2 Reactors utilized for biomass pyrolysis

Nowadays, pyrolysis technologies are developed based on already existing reactor concepts. The reactor type is classified by the movement of the feedstock, the means of heat transfer, and the assisted media. The reactors used in commercial companies or scale-up laboratories consist of (1) fixed bed reactor; (2) Rotary drum reactor; (3) Fluidized bed reactor; (4) Auger reactor; (5) microwave reactor; (6) Torbed reactor (rotary fluidized bed); (7) Ablative reactor. The advantages and disadvantages of the reactors are shown in **Table 1. 3**. The selection of adapted reactor design is essentially based on the given feedstock [26-28].

In addition to the reactors mentioned above, there is also a common laboratory-scale continuous reactor for the pyrolysis of biomass, the drop tube reactor (DTR), also known as the free fall reactor (**Figure 1. 3**).

Recently, it has been applied in research by many scholars and a lot of work has been centered on the influence of material types and pyrolysis conditions (temperature, biomass particle size, gas residence time) on the distribution and properties of pyrolysis products [34-37]. The reactor temperature (450–600°C) and particle size (370–640 mm) were found to have a major influence on the pyrolysis product distribution whereas they were not found to have a significant influence on the bio-oil properties, such as acidity [38]. In addition, the optimum reactor temperature for maximizing bio-oil yield is in the range of 350-450°C. About 70 wt% of bio-oil yield could be obtained at a reactor temperature of 450 °C [39].

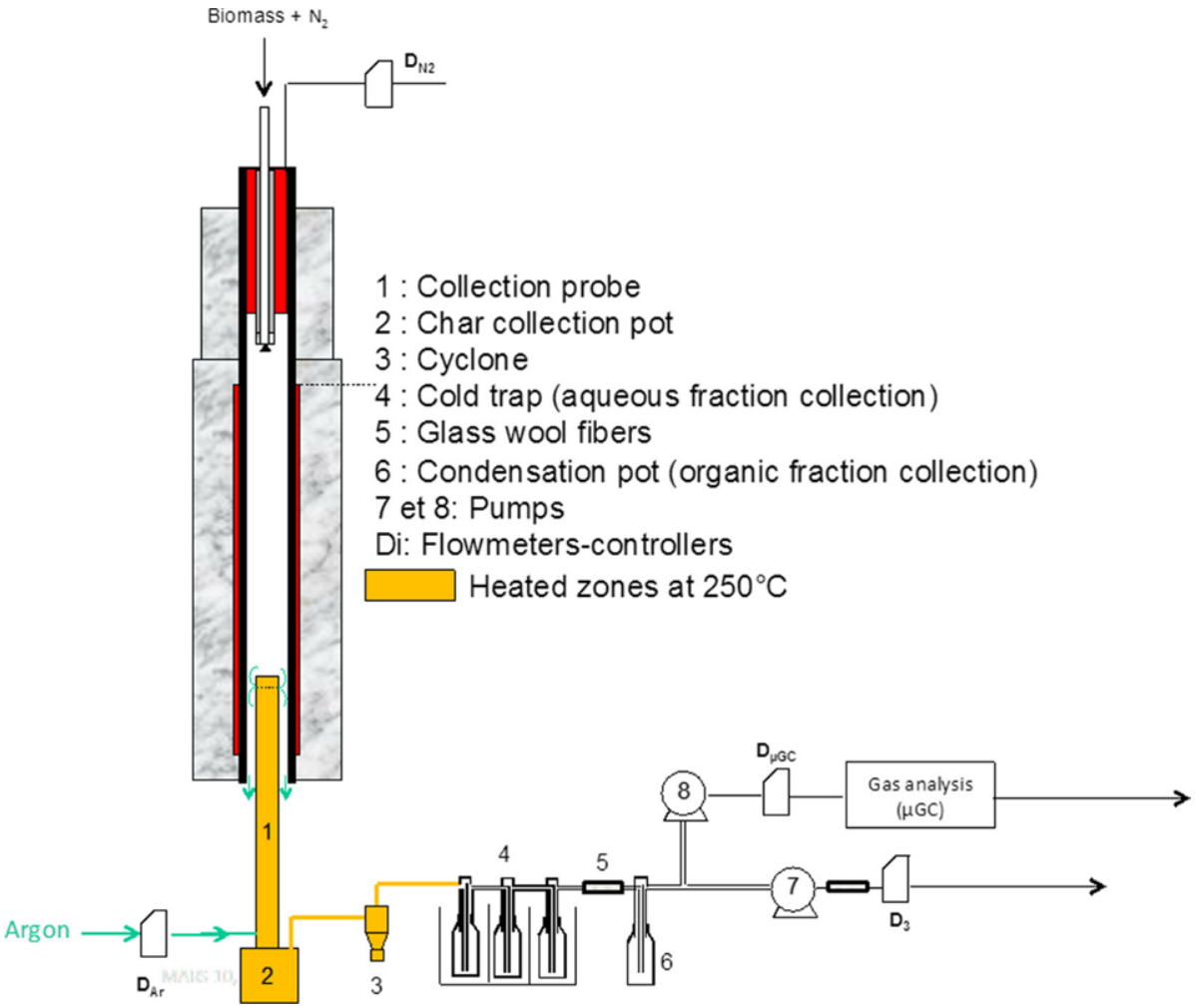

Figure 1. 3 Schematic representation of the biomass pyrolysis experimental set-up.

Table 1. 3 Summary of the main reactors used for biomass pyrolysis

Reactor	Advantages	Disadvantages	Reference
Fixed bed reactor	• Low cost of construction, operation, and maintenance • Suitable for any biomass particle size	• Difficult temperature controlling • Lower carrier gas flow rate	[40-42]
Rotary drum reactor	• Low cost of construction, operation, and maintenance • Large capacity and continuous operation • High operating flexibility	• Difficult installation and removal • Low thermal efficiency • Limited scalability	[43, 44]
Fluidized bed	• Rapid and intense heat transfer • Scalable technology	• Limited particle size	[45, 46]
Auger reactor	• Proven technology • Suitable for any biomass particle size	• Poor heat transfer between the feedstock • Limited scalability • Axial dispersion and blockages may occur	[47, 48]
Microwave reactor	• Better heat transfer within the feedstock • Suitable for any biomass particle size • Shorter residence time	• Non-uniform heating with large particle	[49, 50]
Torbed reactor (rotary fluidized bed)	• Rapid and intense heat transfer • More homogeneous product	• Higher energy consumption	[51]
Ablative reactor	• Possibility of large particle sizes • High mechanical char abrasion from biomass Compact design • Heat transfer gas is not required • Carrier has not always been a necessity	• Scaling is less effective • The reactor is mechanically driven • Limited by the rate of heat supply	[26]

1.2.3.1.3 Lignocellulosic biomass pyrolysis oil

The liquid product from pyrolysis, also named bio-oil, is a complex mixture of water and organic species. It can be stored until required or readily transported to where it can be most effectively utilized. Bio-oil is usually a dark brown, free-flowing liquid, having a distinctive

smoky odor. It can be used both as an energy source and a feedstock for chemical production [52].

Bio-oil also contains many different chemical compounds. The diversity and complexity of bio-oil composition make an accurate analysis of their specific chemical composition a very complicated task. Gas chromatography (GC) is commonly used to identify by detecting the relative mass contents (MS detector) and quantify (using FID detector) substances present in an organic liquid. By comparing the peak areas and the relative abundance in terms of area percentage, different types of chemical compounds were detected [9, 10, 29, 34, 39, 53-55]. For example, the bio-oil of pyrolyzed flax shives at 500°C contained a total of more than 255 compounds as shown on the chromatogram in Figure 1. 4.

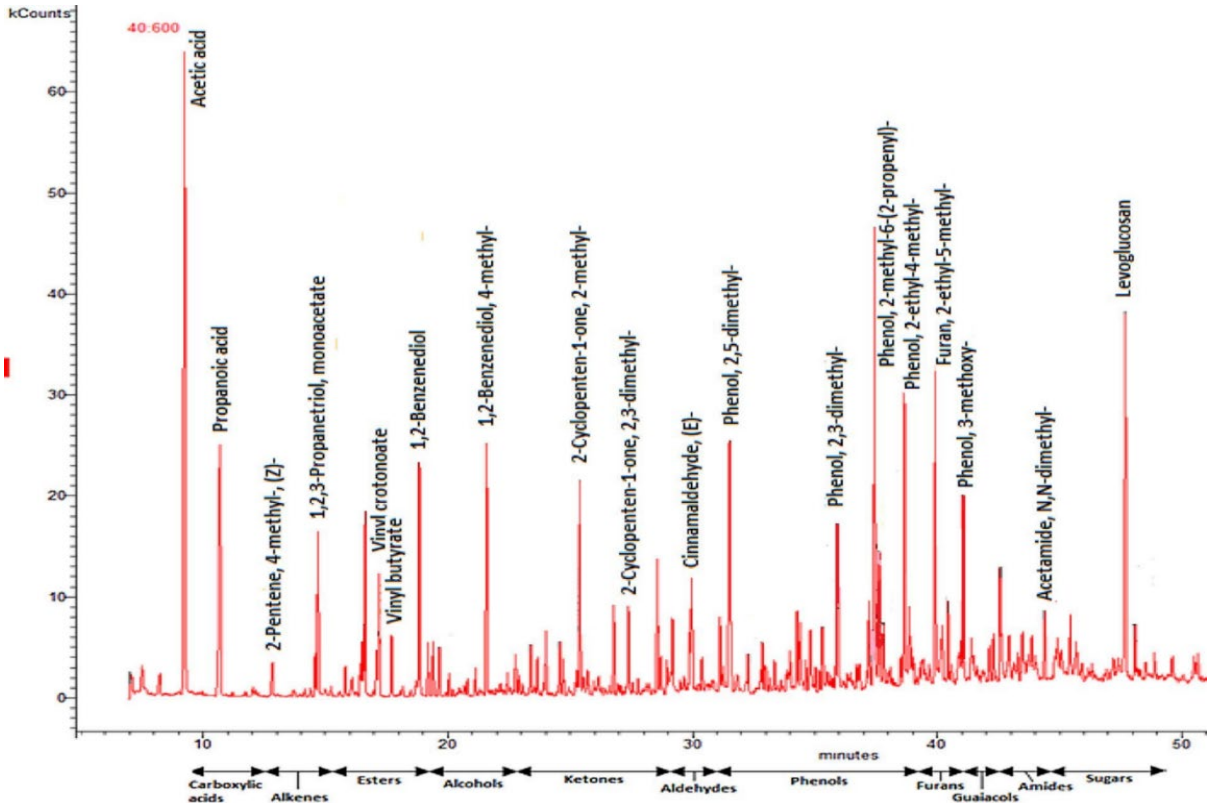

Figure 1. 4 GC–MS chromatogram of flax shives pyrolytic oil obtained at 500 °C [7]

All the compounds were grouped into 12 major chemical families: Carboxylic acids, phenols, guaiacols, ketones, esters, alcohols, sugars, aldehydes, furans, amides, alkenes, and alkanes.

Table 1. 4 shows the chemical composition and yield of bio-oil from pyrolysis of different types of woody biomass. The yield of bio-oil is between 36% and 77%. Regardless of the influence of other pyrolysis parameters such as temperature and reactor design, the type of biomass feedstock can have a significant influence not only on bio-oil yield but also on the

chemical composition. As shown in **Table 1. 4**, sugars, phenolics, carboxylic acids, and ketones are the major detected bio-oil components in the woody biomass.

Table 1. 4 Chemical compositions of bio-oil from pyrolysis of different woody biomass [56].

Biomass	Processing conditions	Bio-oil yield (%)	Main components (relative abundance) of bio-oil
Poplar	Slow pyrolysis conditions, fixed bed, 650 ℃	36.5	Sugars > phenols > lignin > carboxylic acids > furans > aldehydes > ketones and alcohols
Lignin	Flash pyrolysis, centrifuge reactor, 550 ℃	43	Guaiacols > syringols > acetic acid > sterols > hydrocarbons > ketones > phenols > furans
Wheat straw	Fast pyrolysis, bench-scale circulating fluidized-bed, 400 ℃	46	Acids > ketones > alcohols
Poplar (Populus nigra)	Flash pyrolysis, pilot plant, 455 ℃	69	Acids > ketones > phenolics
Pinewood waste (Pinus insignis)	Flash pyrolysis, bench-scale plant, 500 ℃	77	Phenolics > ketones > saccharides > furans, alcohols, acids, and aldehydes
Pinewood sawdust	Flash pyrolysis, pilot plant, 500 ℃	75	Phenolics > ketones > saccharides > furans, alcohols, acids, and aldehydes
Typical bio-oil (from lignocellulosic)			Sugars (20-35%) > phenolics (15-30%) > aldehydes (0-10%) > acids (4-15%) > alcohols, furans, ketones

Among these chemical families, the chemicals such as acetic acid, formic acid, furfural, lactic acid, and levoglucosan result in strong acidity (pH = 2.5) and high oxygen content (35–40 wt%) of bio-oils [54].

Physicochemical properties, including water content, solid content, pH, heating value, elemental composition, acid value, density, etc., are indicatives of the characteristics and interactions of the chemical mixture that constitutes the bio-oil [9]. Table 1. 5 indicates the physical properties of six different woody biomass pyrolysis oils. These properties are decisive in the bio-oils potential to be used for combustion in boilers or engines. The properties of heavy petroleum fuel oil are also presented in **Table 1.5**.

Table 1. 5 Characteristics of bio-oils from different woody biomass pyrolysis compared to petroleum oil

Characteristics Of bio-oil	pyrolytic lignin bio-oil [39]	eucalyptus bark bio-oil [36]	Oak wood bio-oil [57]	Beech wood bio-oil [57]	Pine wood bio-oil [57]	Heavy petroleum fuel oil [58]
Water content (wt%)	15-30	32.86	22.1	43.6	30.5	0.1
Solid content (wt%)	0.2-1	0.45	-	-	-	0.1
pH	2.5	2.87	3.2	3.0	2.6	-
Specific gravity	1.2	1.14	1.230	1.165	1.175	0.94
Elemental composition (wt%, as-produced basis)						
Carbon	54-58	-	44.06	34.96	43.52	85
Hydrogen	5.5-7.0	-	5.79	5.94	6.31	11
Nitrogen	0-0.2	-	0.08	0.11	0.07	0.3
Oxygen	35-40	-	48.68	58.70	50.07	1.0
Ash	0-0.2	0.23	1.38	0.28	0.03	1
Heating value (MJ/kg, as-produced basis)						
HHV	16-19	12.23	18.21	15.87	18.16	40

All the bio-oils have undesirable properties such as high water content, high viscosity, high ash content, high oxygen content, and high acidity [58]. This leads to a 50% lower energy density than conventional fuel and immiscibility with hydrocarbon fuels [9]. This has an impact on the fuel quality of bio-oils and therefore limits their applications. However, these chemicals have great potential in the field of bio-fine chemicals. In recent years, biomass has often been used as a fractional substitute for phenol and to synthesize bio-based phenolic resin. Polyesters can be prepared by polymerization of bio-based acids, alcohols, or lactones [11, 12].

1.3 Upgrading of pyrolysis bio-oil

The deleterious properties of high viscosity, thermal instability and corrosiveness present many obstacles to the industrial application, in particular, the substitution of fossil-derived fuels for bio-oils. So, an upgrading process by reducing the oxygen content and improving the physicochemical properties of bio-oil for its practical application is required [9].

Bio-oil can be upgraded in many ways, physically, chemically, and catalytically, using approaches such as filtration, emulsification, hydrogenation, hydrodeoxygenation, catalytic pyrolysis, steam reforming, molecular distillation, extraction using supercritical fluids, etc. These technologies can significantly improve the properties of the bio-oil (Table 1. 6).

Table 1. 6 Bio-oil upgrading methods

Upgrading method	Reaction conditions	Reaction process	Advantages	Disadvantages	Ref.
Filtration (Physical)	filter temperature (450 °C), residence time (3s)	Use hot gas filtration with a ceramic (Dia-Schumalith sintered ceramic powder) filter	reduce alkali and alkaline earth metals and total solids of bio-oil	limited information available on the performance or operation of hot vapor filters	[26, 59]
Emulsification (Physical)	Mild conditions need surfactant	Bio-oil is miscible with diesel fuels with the surfactants	Simple, less corrosive	The cost of surfactants; the high energy required	[56]
One-step hydrogenation–esterification (OHE) (Catalytic and chemical)	Mild conditions, catalysts (bifunctional)	To convert acids and aldehydes to stable and combustible components	have properties of hydrogenation and esterification	Have higher requirements on reaction conditions	[60, 61]
Hydrodeoxygenation (Catalytic)	High pressure, temperature (3 MPa ,300–450 °C), and catalyst (HZSM-5 and Ni2P/HZM-5)	Hydro-deoxygenation, hydrogenation without simultaneous cracking or with partial cracking	Oxygen is removed as H_2O and CO_2, and then the energy density is elevated.	needs complicated equipment, superior techniques, and excess cost; catalyst deactivation and reactor clogging.	[62, 63]
Catalytic pyrolysis (Catalytic)	atmospheric pressure, catalyst (HZSM-5 zeolite)	Catalytic deoxygenating	Cheaper lowered the oxygen content of the bio-oils and increased the calorific values	Catalyst deactivation, reactor clogging, coke production and high-water content in bio-oils	[64]
Steam reforming (chemical)	High temperature (800–900), need catalyst (e.g., Ni)	Catalytic steam reforming + water–gas shift	Produces H_2 as a clean energy resource	Complicated, requires steady, dependable, fully developed reactors	[65, 66]
Liquid/liquid extraction (Physical)	In mild conditions, polar solvents needed such as water, methanol, ethanol, and furfural	Solvent extraction, distillation, or chemical modification	Extract valuable chemicals	Low-cost separation and refining techniques are still needed	[23, 58, 67]

1.3.1 Fractional condensation

The main drawback of the upgrading methods is the low liquid yield, which makes the processes economically unattractive. Since pyrolysis oil consists of very complex compound groups having a large range of dew points, fractional condensation can be simpler, lower cost and more efficient approach to producing liquid fuels and chemicals compared with treating all the oil [68, 69].

Chai et al. [70] studied the fractionation of pine sawdust pyrolysis vapor. Phenols, acids, and furans tend to be distributed at high temperatures, with the highest HHV (Higher Heating Value). Sui et al. [71] set four condensers arranged in sequence at 300 °C, 100 °C, 0 °C, and −20 °C: over 90% of small molecules were gathered in the 0 °C condensers, and phenols were collected in the 100 °C condensers. Yin et al.[72] used five condensers in a relatively close temperature range (36,85°C - 13,85 °C) and they obtained bio-oils with different properties and compositions. Wang et al. [73] studied the effect of the condensation temperature on the composition of bio-oil at condensation temperatures from 17 °C to 97 °C. When the temperature of the first stage condenser increased, the condensing efficiency of the condensers and the moisture of the bio-oil decreased significantly. In the above studies, different condensation systems and various condensation temperature groups were set to obtain bio-oil, but the influence of the dew point, which is closely linked to the boiling point of each component, on the condensation temperature and the enrichment of compounds was rarely mentioned [74, 75]. From a more scientific perspective, an extremely high or low condensing temperature for the fractional condensation system will damage the economy of biomass pyrolysis processes and is meaningless [73, 76].

1.3.2 Solvent extraction

Bio-oil is a mixture of many chemical compounds and not all the chemicals have the same affinity with the solvent. Liquid/liquid extraction methods are used for separating the pyrolysis bio-oil in fractions with different polarities. The relative content of these fractions will control bio-oil multiphase nature and phase stability [23]. Some information on common solvents used for extraction were shown in Table 1. 7. The polarity index is defined as a measure of the ability of the solvent to interact with various test solutes [77].

The addition of water is considered the simplest and greenest method to extract and separate chemical compounds [78, 79]. Oasmaa and Kuoppala [80] found that it was much more efficient

to use water and centrifuge to divide pyrolysis liquid into water-soluble (WS) and water-insoluble (WI) fractions. Ren et al. [81] separated the crude bio-oil by adding water, and 61 wt% of the organic compounds (acetic acid, propionic acid, and levoglucosan) were distributed into the aqueous phase. Besides, the phenolic compounds in the crude bio-oil were extracted to the organic phase.

Table 1. 7 Solvents used for extraction [23]

Solvent	Polarity index	Application	Ref.
pentane	0.0	nonpolar to less-polar compounds (e.g., hydrocarbons, olefins)	[82]
n-hexane	0.1	nonpolar to less-polar compounds (lignin monomers and sugar-like compounds)	[83]
cyclohexane	0.2	nonpolar to less-polar compounds	[52]
toluene	2.4	less or moderately polar compounds (e.g., wood extractive-derived compounds	[81]
benzene	2.7	less or moderately polar compounds (e.g., phenols and oxygenated compounds; aliphatic, aromatic, and polyaromatic hydrocarbons, neutral oxygen compounds, and basic and acidic oxygenated compounds)	[82]
diethyl ether	2.8	moderate polar compounds (e.g., phenolic compounds)	[84]
dichloromethane	3.1	less to moderately polar compounds (e.g., aldehydes, ketones, phenols, and furans)	[84]
ethyl acetate	4.4	polar compounds (e.g., phenolic fraction, ketones and aldehydes, and lignin-rich fractions)	[81]
acetone	5.1	strongly polar compounds (e.g., sugars and acids)	[85]
methanol	5.1	strongly polar compounds (e.g., sugars and acids, solid determination)	[86]
ethanol	5.2	phenolic compounds, lipid extracts	[87, 88]
water	10.2	precipitation of lignin oligomers (syringol guaiacol, and furfural)	[89]

1.4 Storage stability of pyrolysis bio-oil

1.4.1 The storage stability problem of pyrolysis bio-oil

Bio-oil is an intermediate product that is generated by first thermal degradation of biomass at a very rapid heating rate and then condensation of vapors and aerosols into liquid at a fast quenching rate, and the process does not reach a thermodynamical equilibrium [90].

Therefore, bio-oil contains many oxygenated organic compounds with a wide range of molecular weights and some of the species are still highly active. During storage, the chemical composition of the bio-oil changes toward thermodynamic equilibrium, and some aging reactions take place under storage conditions, resulting in some undesirable changes in physical and chemical properties of bio-oil (viscosity, molecular weight, and co-solubility) [91].

However, most projected uses of bio-oil require that it retains these initial physical properties during storage, shipment, and use. Unfortunately, some bio-oils rapidly become more viscous during storage at room temperature (**Figure 1. 5**). In addition, the single-phase bio-oil can separate into a various tarry, sludgy, waxy, and thin aqueous phases during aging. Tarry sludges and waxes still in suspension cause rapid clogging of fuel filters. Bio-oil appears to be more unstable during storage than petroleum-derived fuel oil [91].

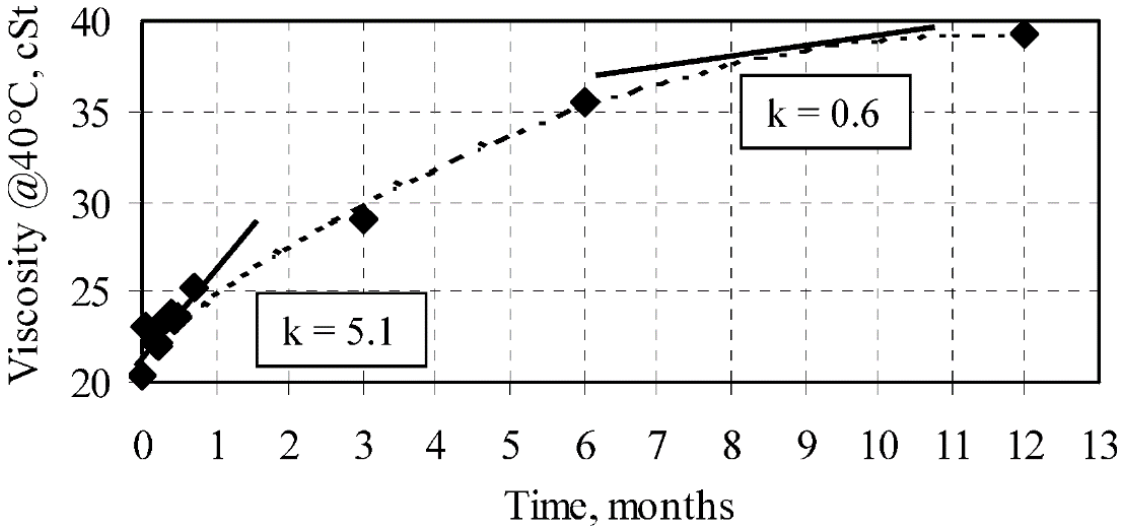

Figure 1. 5 Viscosity increases of forestry residue liquids during one year of storage at room temperature[92]

1.4.2 Methods to slow aging in Bio-oils

It is critical to developing effective approaches to maintain the stability of bio-oil during storage and transport because unstable bio-oil with high viscosity creates challenges in pumping and handing the bio-oil during storage and transportation to the biorefinery or end-use application. The decrease in viscosity, the content of highly active organic compounds, acidity and solid carbon residues are the main keys to improving the stability of bio-oil. Bio-oil stabilization technology is divided into physical and chemical methods and is discussed in **Table 1. 8**.

Table 1. 8 Summary of current technologies to slow aging in bio-oils

Methods	Reaction mechanism	Function	Refs.
Solvent addition	adding low-viscosity water, methanol, or acetone to dilute the polymers being formed.	reduce the viscosity of the mixtures; more effective at higher storage temperature	[93]
Emulsification	emulsification of pyrolysis oils with mineral oils	produce stable emulsions with higher quality than the original pyrolysis oils	[94]
Limiting Access to Air and Antioxidants	Limiting the access to air minimizes the possibility of forming peroxides that catalyze olefinic polymerization. Adding a small quantity of an antioxidant such as hydroquinone to stabilize the olefins in bio-oil	Reduce Viscosity and Aging Rates	[95]
Removal of solid char residue	Removed the alkali metals retained in char particles that act as catalysts triggering reactions	Reduce reactions such as polymerization and condensation	[96]
Esterification	Chemical reactions between acids and Alcohols	Applicable to improve oil qualities with low cost	[90]
Mild hydrodeoxygenation	Hydrogenation under mild conditions	Reduced hydrogen input, reduced handling cost of stabilized intermediates	[90]
Catalytic cracking	Crack large molecules into small molecules through decarboxylation and decarboxylation	No hydrogen input, low cost	[90]

1.4.3 Methods to measure the stability of bio-oil

Many researchers have worked on the storage stability of bio-oils, especially bio-oil obtained by one-step pyrolysis [97, 98]. Few studies have focused on the stability of fractional condensation bio-oil and their water extraction fractions. During the storage, bio-oil can undergo various kinds of changes in its chemical and physical properties, such as phase separation, viscosity increase leading to an increase in molecular weight, and change in water content [90]. These changes are due to the polymerization reactions of the chemical compounds, frequently occurring in the early storage period and usually between highly reactive and polar organic functional families (such as aldehydes, alcohols, carboxylic acids, and phenols). Moreover, the main factors that have a significant impact on the performance of bio-oil during aging are exposure to air, storage time, and temperature [91, 98]. The storage temperature can determine whether the polymerization reaction will take place and the extent of the reaction. For example, the esterification reaction usually occurs at 50 °C. Therefore, it is very important to set an appropriate aging temperature. Moreover, the temperature associated with the storage time can be a powerful method for evaluating the effect of aging on the changes in the fraction of each bio-oil product in an accelerating way. For instance, heating bio-oil between 40 to 100 °C could correspond to storage at 25 °C for 12 months [97]. Czernik et al. [99] pointed out that the viscosity of bio-oil aged for three months at room temperature is equivalent to 9 days at 60 °C. Oasmaa et al. [92] indicated that aging bio-oil for 6 h at 80 °C or 1 week at 40 °C was equivalent to aging for 3–4 months at room temperature. It can be found that as the aging temperature increases, it takes less time for the bio-oil to reach the same degree of aging.

According to the composition changes of the chemical family of each bio-oil product after water extraction, it is speculated that the stability of the water extraction fraction will be affected significantly. Therefore, studying the stability of the water extraction fraction of fractional condensation pyrolysis oil is essential and can also help us to know the probable polymerization reactions of pyrolysis oil.

1.5 Bio-based green materials

Biomass is one of the most important renewable resources to produce value-added products and energy. As shown in **Figure 1. 6**, polymers from biomass can be classified into three main groups: natural polymers (e.g., cellulose starch and protein); synthetic polymers derived from natural monomers (e.g., polylactic acid) and polymers from microbial fermentation (e.g.,

polyhydroxybutyrate). To foster and promote sustainability, synthetic polymers from bio-based monomers such as poly (lactic acid), furan derivatives, sugars, lignin, and fatty acids derivatives, offer a new route to develop green polymers from renewable resources [100].

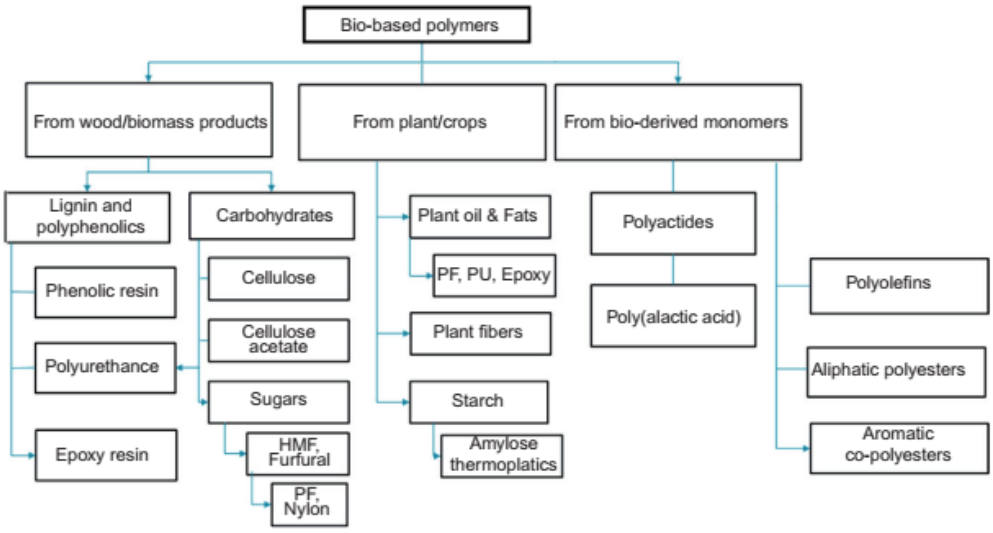

Figure 1. 6 Classification of the common bio-based resins developed from various bioresources [100]

In the latter field, three major challenges should be well addressed: (1) relatively high cost of some biomass feedstocks and related biorefinery technologies; (2) mechanical and thermal properties, processability, barrier properties, durability, and other physical properties that are often not competitive with fossil-fuel derived plastics; and (3) the lack of universally accepted quantitative metrics on economical sustainability [101].

1.5.1 Type of renewable bio-based materials

Resins or thermosets constitute a wide class of synthetics that are used in composites, binders (for plate materials), adhesives, inks, paints, and coatings. Thermosetting polymers and related materials, such as polyester resins, polyurethanes, phenolic resins, urea-formaldehyde resins, and epoxy resins, are well-known worldwide [101, 102]. Nowadays, many bio-based thermosets are synthesized by partially or completely replacing the traditional fossil fuel resource material with renewable raw materials. Furthermore, the resins synthesized from renewable resources offer similar properties compared to their petroleum-based counterparts [102].

1.5.1.1 Bio-based carbonaceous materials

It is more favorable to produce carbonaceous materials from biomass considering the environmental impact and the sustainability of the feedstock. The production of activated carbon from biomass has been intensively investigated for many years, which is also a mature technology for commercialization. Activated carbon featured abundant micropores and mesopores, rendering it good performance for use as an adsorbent. Nevertheless, the highly developed porous structure of activated carbon also leads to low mechanical strength, except for some specific types of biomass such as coconut shells and bamboo [103]. Hu et al.[104] developed a method to produce carbon materials from bio-oil and bio-char with the aid of a polymerization agent (furfural) at 170–280°C biomass with high yields. Furfural effectively promoted the cross-polymerization of bio-oil and biochar, which "bonded" bio-oil and biochar together, forming cross-linking structures.

1.5.1.2 Bio-based polyesters

Polyesters constitute a variety of materials with different chemical structures and mechanical properties that are widely used in laminates, industrial construction and installation, molding compounds, coatings, and adhesives [105]. To replace petroleum source, an alternative pathway for obtaining sustainable polyester have been intensively developed. Polyesters can be prepared through a polycondensation reaction by different renewable biomass-based monomers such as sugars, vegetable oils, lactic acid, 2,5-furandicarboxylic acid, carbohydrates, isosorbide, mannitol, galactic acid, 5-Hydroxymethylfurfural (HMF), terpene, betulin, and vanillin. [1, 105-109]. Moreover, among bio-based polyesters, polyhydroxyalkanoatesolyacid (PHAs) are totally synthesized in microbes and used in the production of bio-plastics, biodegradable implants and controlled drug delivery systems [110].

1.5.1.3 Bio-based polyurethanes

Polyurethane represents a versatile class of polymeric materials in which repetitive structures are linked by carbamate (urethane). Polyurethanes have been widely used in construction, packaging, insulation, bedding, upholstery, footwear, vehicle parts, panting, etc. The synthesis of conventional polyurethane consists of the reaction between diisocyanates and polyols, defined as compounds with at least two hydroxyls (OH) groups. Recently, traditional petrochemical polyol has begun to be replaced by polyol from vegetable oils [111-114]. Lee et al. [115] produced a non-isocyanate polyurethane elastomer with two different biomasses

(lignin and soybean oil) for the synthesis of sustainable polyurethane. The incorporation of biomaterial such as cellulose nanocrystals is studied to produce a material with enhanced thermal and mechanical properties in a solvent-free process [116].

1.5.1.4 Bio-based epoxy resins

Epoxy resins are the most significant polymers among the thermosetting polymers with excellent properties, such as high corrosive resistance and adhesion strength, favorable processing ability, low curing shrinkage, and excellent mechanical, thermal, and electrical properties. Epoxy resins are widely used in coatings, adhesives, composites, and constructions [101, 102, 117, 118].

There are various types of epoxy resins on the market depending on the molecular weight, epoxy equivalent weight, and viscosity. Bisphenol A glycidyl ether (DGEBA) is the most widely used epoxy resin, accounting for more than 90% of the global epoxy resin market, and is expected to be worth US$34 billion by 2022 [119]. However, DGEBA is derived from bisphenol A (BPA) which is toxic and petroleum-derived. Hence, the replacement of BPA with alternatives derived from sustainable and renewable resources bio-based polyphenols would be highly promising [120-124].

Researchers focus on developing a bio-based epoxy monomer or oligomer prepared from a variety of renewable resources, such as vegetable oils (soybean oil, linseed oil, palm oil, and castor oil) [125-129]. Moreover, several promising results have been reported by applying wood biomass to the production of epoxy resin [130]. Indeed, lignin source [131] and bio-oil from wood biomass pyrolysis [132] were used successfully to prepare epoxy resin with outstanding viscosity and mechanical properties.

1.5.1.5 Bio-based phenolic resins

Since the discovery of phenol-formaldehyde (PF) resins in the early twentieth century, [133], the phenolic resin has become an irreplaceable material that can be used in selective high technology applications offering high reliability under severe circumstances [134]. It has been widely used in electronics, adhesives, carbon foams, molding compounds, thermal insulation materials, and composite materials among others, due to its low cost, thermostability, and chemical durability [135].

However, in recent years, traditional non-renewable petroleum-based phenol and formaldehyde

have been recognized as unfavorable effects on the safety, environment and human health [136]. Indeed, Since both phenol and formaldehyde are mutagenic, carcinogenic, and reprotoxic, this creates significant constraints during the manufacturing process for PF resins, and expensive safety measures are necessary to prevent worker exposure [137]. Furthermore, residual formaldehyde can remain in the PF resin products, leading to the potential for low-level, long-term exposure in homes and offices.

The increased environmental awareness and stringent environmental laws underscore the need for the development of sustainable phenolic resins. [137, 138]. Chen et al. [139] used the direct bio-oil obtained from Eastern white pine to partly replace phenol (0% to 75%) in the synthesis of bio-oil-phenol-formaldehyde (BPF) resol resins. When the proportion of bio-oil is increased, the molecular weight of the resin increases. Yang et al.[135] successfully used lignin-derived monomers with oxalic acid as the catalyst to synthesize renewable phenolic resins which have a similar performance as the commercial novolac phenolic resin (**Figure 1. 7**).

1.6 Production of bio-based phenolic resin

There are two types of phenolic resins (novolac and resole), which are synthesized by acid or base-catalyzed reactions between phenols and aldehydes. Due to the toxicity of formaldehyde used and the petrochemical origin of phenol, the replacement of these raw chemicals is necessary [137, 138]. Novolac resin can be cured to improve its mechanical properties.

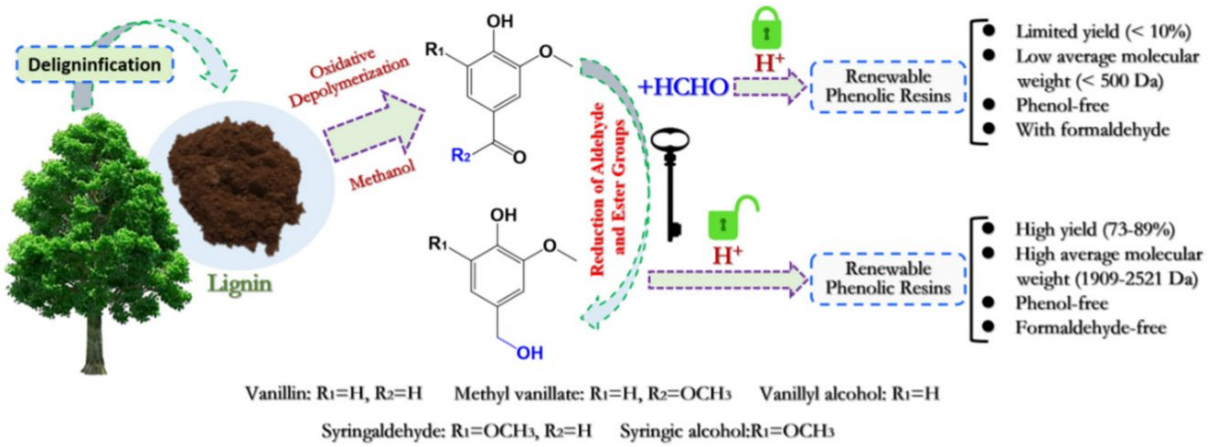

Figure 1. 7 Schematic illustrations of the renewable phenolic resin synthesis based on lignin-derived monomers [135]

1.6.1 Bio-based phenol alternatives

Phenol is solid and appears as a white amorphous material at ambient temperature with a melting point of 40.9°C and a boiling point of 181.8°C. The chemical properties of phenol are unique due to the presence of a hydroxyl group and an aromatic ring which are complementary to each other by facilitating both electrophilic and nucleophilic reactions with the aldehyde. To produce phenolic resins, mostly mono-hydroxybenzenes, especially phenol, are used. Furthermore, alkylphenols (cresols and xylenols), resorcinol (di-hydroxybenzene) and bisphenol are used sparingly to produce phenolic resins [133].

For this reason, the replacement of phenol in conventional phenol-formaldehyde resins by the

phenol fraction extracted from biomass has been proposed. In the literature, three main strategies have been studied for the use of a phenolic fraction of bio-oil: (i) bio-based individual phenol models or mimic of bio-oil, (ii) natural resource phenol-rich extraction of monomers and chemicals from biomass (lignin, tannin, and cardanol) or (iii) phenolic-rich oil from woody biomass pyrolysis oil.

1.6.1.1 Bio-based individual phenol models or mimic of bio-oil

Due to the complexity of biomass extracts, some scholars have generated a single bio-oil mimic based on the previous literature or the data of phenolic bio-oil in their laboratory. The mimic is usually composed of phenolic compounds (phenol, guaiacol, catechin, etc.) in an appropriate ratio in order to better understand the reaction between aromatic compounds and aldehydes.

Patel et al.[140] studied the condensation of o-cresol with furfural catalyzed by potassium carbonate at 135°C for 5h. A dark-colored solid was obtained after washing with a yield of 74%. It has a soft point in the range of 145–150°C and was soluble in common organic solvents.

Xu et al. [141] studied the cross-polymerization of the furfural and aromatic compounds in bio-oil (Guaiacol and Eugenol) was conducted to understand the impact of structures of the aromatic compounds on their tendencies towards polymerization (**Figure 1. 8**).

The results showed that the cross-polymerization existed and the reactivity depended on the electron density of their benzene ring. The weak acid (acetic acid) showed an insignificant effect on promoting the polymerization, while the strong acid (H_2SO_4) could remarkably promote

cross-polymerization.

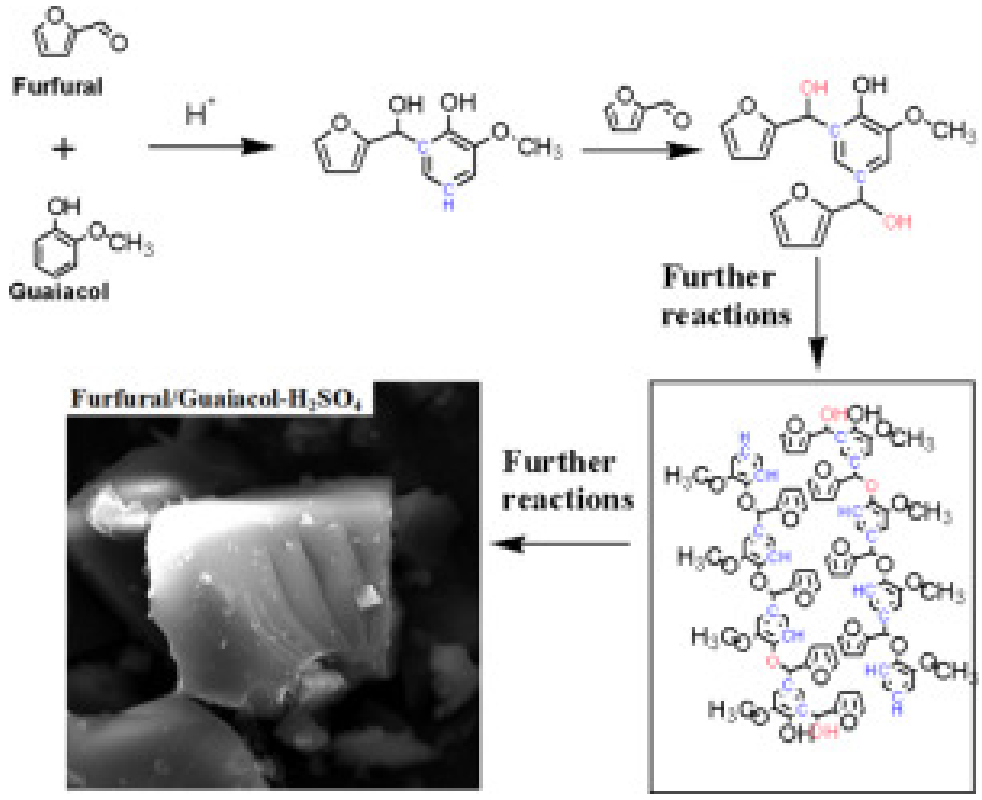

Figure 1. 8 The cross-polymerization of the furfural and Guaiacol[141]

1.6.1.2 Natural resource phenol extraction of monomers and chemicals from biomass

Nowadays, there are some potential eco-friendly substitutes for phenol that are generally applied in resin synthesis. They are all promising biomass extracts such as lignin, cardanol, and tannin. The chemical structures of these complicated extracts were shown in **Figure 1. 9**. The various cardanol, lignin, and tannin substituted resins and their associated properties are summarized in Table 1. 9 [142]. Cardanol has been used to synthesize novolac resin, whereas most of the studies referenced focus on the production of resole resins for lignin and tannin chemicals.

Cardanol is a naturally occurring phenolic compound issued from cashew nutshell liquid. Its chemical structure is interesting because cardanol is bearing a phenolic hydroxyl function and an unsaturated alkyl chain in meta. Numerous chemical reactions can thus be considered for their chemical modification [143]. In addition, cardanol can react with formaldehyde to form cardanol–formaldehyde resins which have key properties such as high-temperature resistance,

modulus retention at elevated temperatures, resistance to chemicals and detergents, high surface hardness, and low cost [144]. Campaner et al.[144] used cardanol from cashew nut shell liquid to synthesize cardanol-based novolac resin. The condensation reaction between cardanol (35 wt % and 20 wt %) and paraformaldehyde has been carried out using oxalic acid as a catalyst. Rahmawati et al. [145] also used cardanol isolated from cashew nut shell liquid and formaldehyde by addition of citric acid as a catalyst for preparing cardanol-based novolac resin. The thermal stability of resin showed high degradation temperature at 282°C.

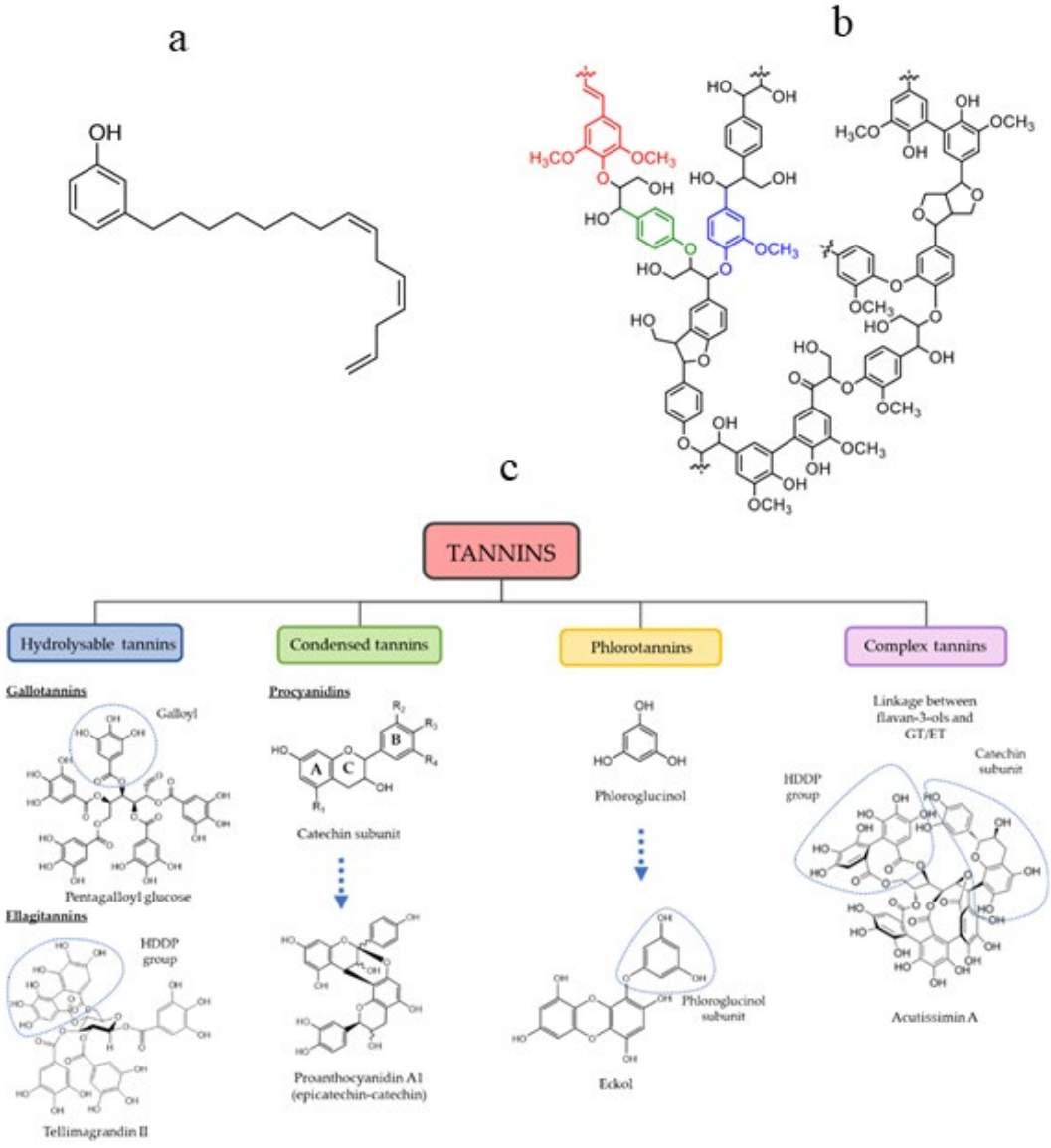

Figure 1. 9 The structures of a. cardanol, b. lignin and c. tannin

Tannins are polyphenolic compounds historically utilized in the textile and adhesive industries, but also in traditional human and animal medicine or foodstuffs [142]. Naturally distributed

tannins are oligomeric compounds containing multiple structure units with a range from 500 to greater than 20,000 in molecular weight. Tannin possesses numerous phenolic hydroxyl groups which make it possible to substitute phenol in the preparation of PF resin [146-148]. Li et al. [146] prepared phenol–tannin–urea-formaldehyde (PTUF) resins by copolymerization of tannin, urea, phenol, and formaldehyde. Plywood bonded with those resins was prepared as well. Despite the bonding strength test, the optimized PTUF resin presents a promising substitution for PF resin in some aspects of the wood industry. Legal et al.[149] used hydrolyzable chestnut tannin extracts to partially replace phenol in PF resins for phenolic rigid foams. The obtained foams, tested for thermal conductivity, show slightly worse than that of pure PF foams but are better in mechanical properties and water absorption.

Table 1. 9 Cardanol, lignin and tannin substituted phenolic resins.

Phenol precursor	Substitution/%	Resin Type	Reaction conditions	Achievement	Ref.
Cardanol	35 wt % and 20 wt %	Novolac	100℃, 6 h.	As an effective epoxy curing agent.	[144]
Cardanol	100 wt %	Novolac	1 wt % citric acid, 120℃, 5 h.	High degradation temperature of 282°C	[145]
Tannin	10–40 wt %	Resole	85℃, 1h.	A promising substitution of PF resin in some aspects of the wood industry	[146]
Tannin	30 wt %	Resole	85℃, 2h.	Better performance in mechanical and water absorption.	[149]
Lignin	25 to 75 wt.%	Resole	80℃, 4h.	Though purifying lignin to improve the thermal stability of the resin	[150]
Lignin	30 wt %	Resole	80℃, 3h. and 70℃, 15 min.	Use as a fast-curing biobased phenolic resin for the plywood industry.	[151]
Alkaline-lignin, dealkaline lignin, and lignin sulfonate	100 wt %	Resole	80℃exceeded 200 cps	Resin with a shorter gel time and had lower exothermic peak temperature	[152]

Lignin has been incorporated into wood adhesives due to its similar structure to PF resins [153]. Many units of aldehydes and phenols in the lignin structure, and the active hydrogen in the benzene ring structure, which has not been replaced, can undergo hydroxymethylation and condensation polymerization with formaldehyde [154]. Wang et al.[150] extracted lignin from white pine sawdust by using hot-compressed at 180 °C with ethanol-water solvent. Then, the

bio-based phenol-formaldehyde resole resins were synthesized, and catalyzed by sodium hydroxide, using the resultant lignin as the replacement of petroleum-based phenol at varying ratios from 25 to 75 wt.%. Li et al.[151] studied four types of demethylation reagents to sever the methoxy bonds of lignin to increase its reactivity. The modified lignin was served to prepare lignin-phenol-formaldehyde resin. Lee et al. [152] used liquefied lignin as raw material to prepare resole-type phenol-formaldehyde resins. A lower gel time was observed than those of conventional resol PF resin.

1.6.1.3 Phenolic-rich oil from fractions of woody biomass pyrolysis oil

Due to the complexity of bio-oil, its direct use as a substitute for phenols will complicate the polymerization reaction. Moreover, bio-oil phenolic fraction includes a wide variety of phenolic compounds. An upgrading step for concentrating phenolic fraction can be an interesting alternative. Fractional condensation is an efficient approach to producing a phenol-rich liquid product compared with untreated oil [68, 69]. The high-temperature fraction mainly includes phenolic compounds and sugars. In addition, the extraction of bio-oil by adding solvent is considered the simplest method to extract phenol.

Since both separation methods (fractional condensation and water extraction), many kinds of phenol rich bio-oil precursors can be chosen by using: (i) the whole bio-oil to substitute petroleum-derived phenol, (ii) the bio-oil obtained from fractional condensation, or (iii) the water-insoluble fraction of the bio-oil obtained from extraction. The various Bio-oil based substituted resins and their associated properties are summarized in **Table 1. 10**.

Yu et al. [155] studied applying the whole bio-oil as a substitute for phenol (10, 20, and 30 wt%) to synthesize bio-oil phenol-formaldehyde resin. The result showed that adding bio-oil reduced the initial and final equilibrium formaldehyde emission values, by 12–49% and 25–51%, respectively. The components of bio-oil, the chemical structure, the mechanical performances, and the morphological and thermal properties of bio-oil phenolic foam were investigated. The good flame-retardant, thermal stability, and thermal isolation properties were maintained.

Chaouch et al. [156] synthesized renewable bio-oil-based resins by replacing 25, 50, and 75% of phenol with bio-oil from two-stage fractional condensation. The results obtained showed that substitution degrees up to 50% provided reactivity and performance equal or superior to the pure PF resin. Also, good storage stability, improved shear strength, and thermal stability compared to the pure PF were observed.

Kokten et al.[157] investigated the chemical, physical, thermal and mechanical properties of bio-oil-phenol–formaldehyde resin synthesized with catalyzed and uncatalyzed pyrolysis oil at 10 to 50 wt% phenol replacement levels. Resins synthesized with catalytic bio-oils showed better thermal stability than resins synthesized with non-catalytic bio-oil. Aslan et al. [158] have modified resole phenol-formaldehyde adhesive by an increasing amount of the phenol-rich fraction extracted from crude bio-oil up to 40 wt%, keeping similar properties to conventional adhesive.

Table 1. 10 Bio-oil based substituted phenolic resins.

Phenol precursor	Pyrolysis condition	% Substitution	Resin Type	Reaction conditions	Achievement	Ref.
The whole bio-oil	Fast pyrolysis at fluidized bed at 550 °C for 2–3 s	10, 20, and 30 wt%	Resole	90°C, 1.5h. and 40°C, 20 min.	Reduce the cost and formaldehyde emission.	[155]
The whole bio-oil and catalytic bio-oils	Vacuum catalytic pyrolysis; 500°C; 30 min 10 kPa	10 wt% to 50 wt%	Resole	60°C, 1h. and 90°C, 1h.	Catalytic bio-oils showed better thermal stability	[157]
Fractional condensation and extracted with diethyl ether	Fixed-bed reactor 500°C; 30 min	up to 40 wt%	Resole	room temperature for 10 min	The phenol-rich bio-oil could be partially substituted for phenol in PF adhesives	[158]
Fractional condensation bio-oil	Fast pyrolysis in a Lab-scale Auger reactor at 500 and 400°C	25, 50, and 75 wt %	Resole	9°C to viscosity (180 -300 cP)	Good storage stability, improved shear strength, and thermal stability compared to the pure PF	[156]
The whole bio-oil	Fast pyrolysis at fluidized bed at 550 °C for 2–3 s	Up to 30 wt.%	Resole	90°C, 0.5h. and 80°C, 1h.	All bio-oil resins maintained good flame-retardant properties, thermal stability, and thermal isolation	[159]
Solvent extraction Oil	Fluidized bed reactor; 500°C	100 wt %	Novolac	125°C, 24h.	Similar properties to phenol resin	[160]

Vithanage et al [160] yielded a bio-oil by lignin fast pyrolysis, then methylene chloride was used as a solvent to extract a phenol-rich monomer mixture. In addition, the extracted bio-oil was added to formaldehyde to produce novolac type phenolic resins and then the synthesized resins had properties similar to those from phenol.

The extraction of bio-oil by adding water is considered the simplest and greenest method to extract phenol into the water-insoluble fraction [78, 79]. The separated and purified bio-oil fractions will become a very attractive substitute for commercial phenols in the field of phenolic resin production [161].

1.6.2 Bio-based formaldehyde alternatives

Formaldehyde, the second major reagent for PF resins, is produced on a large scale via the catalytic oxidation of (fossil-derived) methanol. The former is a hazardous chemical and has been classified as a "probable human carcinogen". Thus, there are many undesirable factors restricting the manufacture or consumption of formaldehyde [133, 162].

The phenolic resins using bio-based formaldehyde alternatives were summarized in Table 1. 11. Regardless of aldehyde with a single functional group, the increase in carbon number causes a decrease in its solubility and its reactivity. Acetaldehyde is miscible with water and most common organic solvent [133]. Acetaldehyde, naturally present, is produced on a large scale in the industry. It is also the main product of bio-oil [7] and is selected to replace formaldehyde as an aldehyde monomer due to its low cost and high activity with phenol. Casiraghi et al.[163] prepared all-ortho phenol-acetaldehyde novolac resins with the uniform constitution by bromomagnesium ion mediated reaction of phenol with acetaldehyde derivatives with a resin yield (91%). The C_3 through C_{11} aldehydes are highly flammable and explosive, colorless liquids with a pungent odor. They are miscible with most organic solvents, for example, acetone, ethanol, or toluene, but are only slightly soluble in water [133]. Higher aldehydes react with phenol at significantly slower rates compared to formaldehyde. Butyraldehyde is produced by the oxo reaction of propylene in the presence of cobalt or rhodium catalysts. Moreover, except for acetaldehyde, butyraldehyde also has had limited commercial success in resin manufactory.

Nowadays, researchers focus on selecting greener bioresources raw materials to be substituted for formaldehyde. For example, HMF, furfural, benzaldehyde, vanillin, and glyoxal have all been reported as potential substitutes to provide formaldehyde-free materials. The chemical structures of bio-based formaldehyde alternatives are shown in **Figure 1. 10**. HMF contains

both furfural and hydroxymethylfuran groups, can be effectively converted from glucose by catalytic conversion. It also can polymerize with phenol or bio-phenolic compounds to form novolac resins under acidic conditions for replacing formaldehyde [138, 164, 165]. Yuan et al.[166] synthesized phenol-5-hydroxymethyl furfural resins by reacting phenol with 5-hydroxymethyl furfural generated in situ from glucose at 120 °C catalyzed by both $CrCl_2/CrCl_3$ and tetraethylammonium chloride. The resin was found to have a relative weight average molecular weight of 700–900 g mol^{-1} and a similar structure to novolac phenol-formaldehyde (PF) resin.

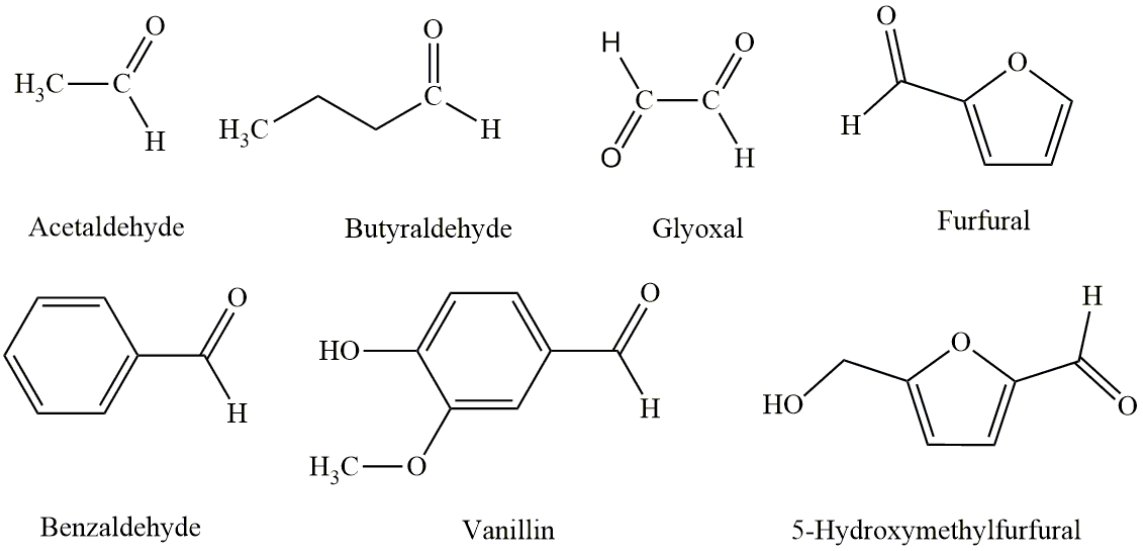

Figure 1. 10 The chemical structures of bio-based formaldehyde alternatives

Among all the heteroaryl aldehyde furfural components in bio-oil. Furfural, as the most representative compound of furans, has reactive carbonyl and furan ring with high electron density, which could activate it toward polymerization reaction [140, 167]. Srivastava et al.[168] focused on the condensation reaction of cardanol with furfural in the presence of an oxalic acid catalyst for the synthesis of novolac resin. The progress of the reaction was monitored by determining the free formaldehyde and free phenol content. The prepared cardanol–furfural-based novolac resins were found to have better mechanical and thermal properties than PF resin. Oliveira et al.[169] prepared resole type resins in alkaline conditions using furfural obtained by acid hydrolysis of abundant renewable resources from agricultural and forestry waste residues.

Vanillin produced by lignin depolymerization was used as a renewable building block to develop a platform of biobased compounds for polymer chemistry [170]. Yang et al.[135] used vanillin and syringic alcohols to polymerize renewable lignin-derived polymers catalyzed by oxalic acid, in absence of aldehydes. The synthesized resins have similar thermal properties and

adhesion properties to the commercial phenolic resins. The described method provides an alternative synthetic route to renewable phenolic resins.

Based on the literature studies detailed in **Table 1. 11**, the relatively complex structures of bio-based aldehydes (HMF, furfural, benzaldehyde, and vanillin), resulting in low reactivity and steric hindrance can only react under severe conditions (high pressure, high reaction temperature and long reaction time) [135].

Table 1. 11 Phenolic resins using bio-based formaldehyde alternatives

Aldehyde precursor	Resin Type	Catalyst	Reaction conditions	Advantages	Ref.
Acetaldehyde	Novolac	$MgBr^+$	80°C, 20h.	High yield 90%	[163]
HMF	Novolac	$CrCl_2$, $CrCl_3.6H_2O$, and TEAC	120°C, 5h, in a glass pressure reactor	Similar or better tensile strength than conventional PF resin.	[166]
Furfural	Novolac	Oxalic acid 1%	120°C, 6h	better mechanical and thermal properties than PF resin.	[168]
Furfural	Resole	Potassium carbonate	135°C, 3.25h	Displayed excellent adhesion between resin and fiber.	[169]
Benzaldehyde,	Resole	Sodium hydroxide	130°C, 0.5h	Higher thermal stability and char yield properties.	[171]
Vanillin	Novolac	Oxalic acid 10 wt%	110°C, 12h	Excellent adhesion strength, glass transition temperature and thermal stability	[135]
Glyoxal	Resole	Potassium hydroxide	100°C, 2h	Have an excellent mechanical property	[172]

Glyoxal, composed of two aldehyde groups, has high reactivity, is a nontoxic aldehyde and is classified as non-volatile [173]. Glyoxal is already proved to be an ideal substitute for formaldehyde in various applications [172]. Indeed, a cured biobased phenolic resin has been synthetized, using glyoxal, phenol and resorcinol. The glyoxal–phenol thermoset resin was confirmed to have an excellent mechanical property[172].

1.6.3 Catalyst selection

As it has seen mentioned above, the phenolic resin can be classified into novolac or resole resin based on the type of catalyst and phenol to formaldehyde ratio used in the reaction. Generally, novolac type resin is formed under acidic conditions when the molar amount of formaldehyde is less than that of phenol. Under the acid condition, phenol has an extremely high reactivity of its ring toward electrophilic substitution to form novolac type resin. In addition, due to the acidity of phenol, it can be converted into more reactive (more nucleophilic) phenate or phenate

ions for reaction under alkaline conditions to synthesize resole type resin in which the molar amount of formaldehyde exceeds that of phenol. They are thermosetting resins with methylol and hydroxyl groups capable of forming a cross-linked network without the use of additional curing agents[133, 137]. Their schematic is shown in **Figure 1. 11**.

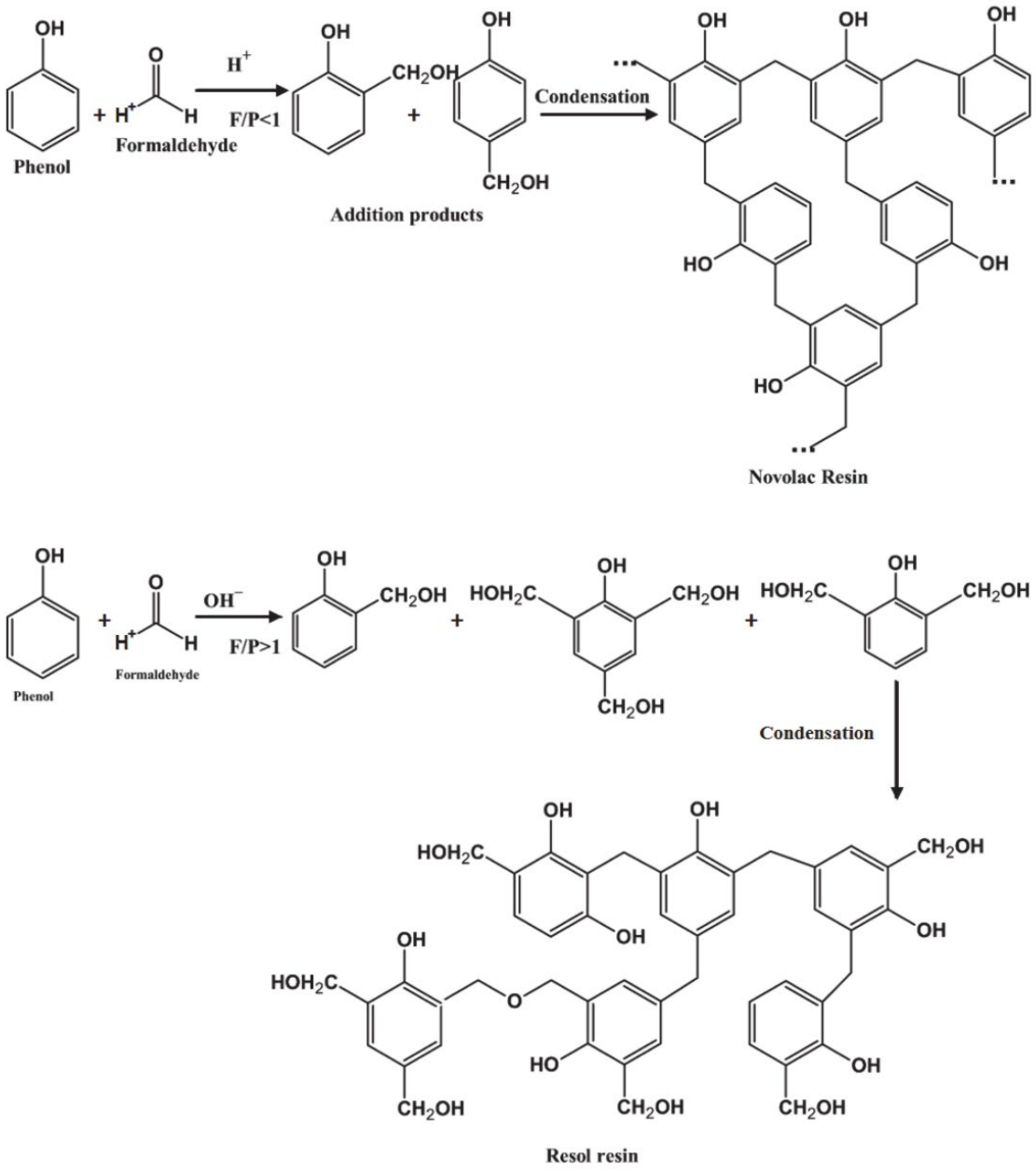

Figure 1. 11 Schematic representation of novolac and resole resins synthesis [137]

For novolac type resin synthesis, oxalic acid [160], hydrochloric acid, and sulfuric acid are common catalysts. Oxalic acid is generally used to catalyze the reaction between formaldehyde and phenol and loses its acidic activity at elevated temperatures (>180°C) by decomposing into carbon dioxide as the novolac is devolatilized and recovered. Sulfuric acid and hydrochloric

acid are strong acids and are used under special conditions when using raw materials with weak reactivity. However, the use of sulfuric acid leads to thermally unstable novolacs since this acid will remain in the resin whereas oxalic and hydrochloric acids are both volatile enough to be removed on vacuum stripping [160].

The basic catalysts are usually strongly alkaline such as NaOH [155, 157, 174] and KOH [171]. At the same time, there are also relatively mild base salts like K_2CO_3 [175] and Na_2CO_3. Therefore, the selection of catalysts also depends on the reactivity of the raw material.

1.7 The selection of green curing agents for bio-based novolac resin

Compared with resole resins, novolac resins have higher shelf life and stability [137]. Since the mole ratio of aldehyde to phenol is less than one, novolac resins are permanently soluble and fusible. An additional curing agent is required to crosslink novolac resins.

1.7.1 Traditional curing agent

Hexamethylene tetramine (HMTA) is the most common compound currently used for curing novolac-type phenolic resins [138]. It is prepared from formaldehyde and ammonia according to **Equation 1.1**.

$$6CH_2O + 4NH_3 \rightleftharpoons (CH_2)_6N_4 \;\; 6\,H_2O$$

Equation 1. 1

Since the reaction **Equation 1. 1** is reversible, HMTA will decompose into ammonia and formaldehyde during heating [100]. The curing reaction of novolac with HMTA was commonly conducted for a novolac/HMTA weight ratio of 80/20, 88/12, and 94/6. In addition, the curing reaction will occur in two main stages (see **Figure 1. 12**). Firstly, some initial intermediates (benzoxazines and benzyl amines) are formed. Then, the decomposition, oxidation, and/or further reactions of these initial intermediates into methylene bridges between phenolic rings take place [176, 177].

1.7.2 The more environment-friendly curing agent of novolac resin

As the emissions of ammonia and formaldehyde bring adverse effects to the environment, therefore, the selection of non-formaldehyde or non-hexa curing agents are being examined and consist of quinone, hydroxymethyl derivatives of phenol, bisoxazolines, bisbenzoxazines, solid resole, epoxy resins, isocyanate, urea, melamine glyoxal, resorcinol, tannins, organosolv lignin,

or kraft lignin [133, 138, 176-181]. In some cases, these curing agents require less energy and have better performance for curing phenolic resins than that HMTA.

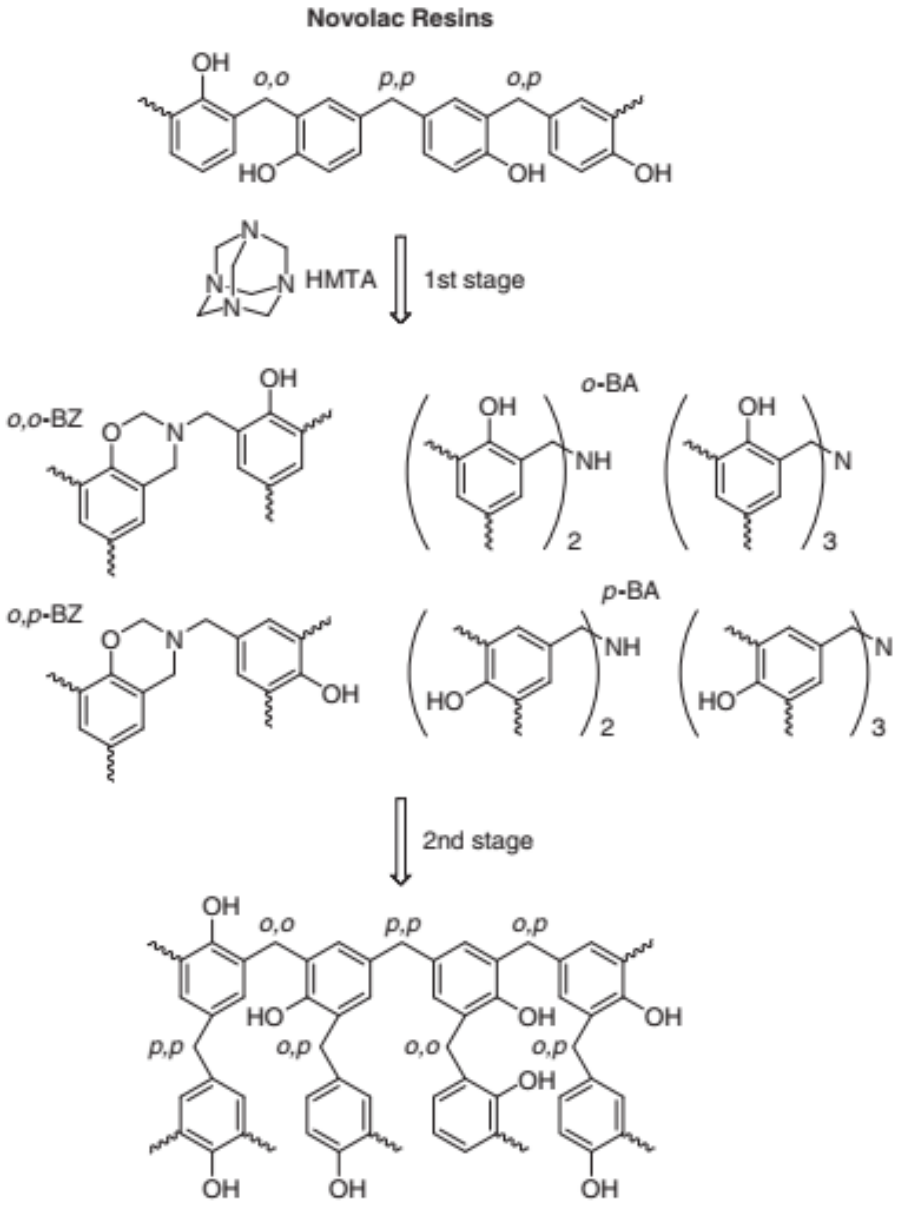

Figure 1. 12 Curing mechanism of novolac resin and HMTA [180]

Tejado et al [181] used a diisocyanate as a curing agent for novolac-type lignin–phenol-formaldehyde (LPF) resins, instead of HMTA. Similar results were shown between the curing reaction with diisocyanate and HMTA, and the curing reaction with diisocyanate is faster than HMTA and easier to proceed at a lower temperature.

Organosolv lignin is obtained from wood or other lignocellulosic biomass by extraction with various organic solvents. Kraft lignin is the byproduct generated in a large amount worldwide

from the Kraft pulping process. Zhang et al.[138] used a green curing agent organosolv lignin or Kraft lignin for curing phenol-5-hydroxymethylfurfural resin. An improvement of thermal stability and mechanical properties demonstrated that organosolv lignin and Kraft lignin could be promising curing agents.

Oxazolines and oxazines are the five- and six-member cyclic imino ethers (imitates), respectively. Culbertson et al.[178] proposed that there are significant opportunities to use oxazoline or oxazine functionalized monomers, oligomers and polymers (e.g. phenolic resin) to produce new materials for a variety of applications.

1.7.3 Epoxy resin as a curing agent of novolac resin

In previous work, epoxy resin was usually used as a curing agent of novolac type phenolic resin by making use of the OH–epoxy reaction to produce low moisture absorbing and void-free products for various electronic applications. Thus, the novolac-epoxy curing system has also received extensive attention [179, 182-184].

1.7.3.1 Synthesis

Generally, there are three main methods for epoxy resin synthesis[185].

- From Epichlorohydrin ECH. (ECH is used in significant excess and the reaction is carried out in an aqueous solution of sodium hydroxide)
- From Double Bond Oxidation. (The peroxidation of a carbon−carbon double bond requires the use of hydrogen peroxide or m-chloroperbenzoic acid)
- From Glycidyl (Meth)acrylate. (Though a free radical polymerization reaction of glycidyl methacrylate with other monomers carrying a vinyl or (meth)acrylic double bond)

Currently, the most common synthesis method of phenol-type epoxy is to etherify the hydroxyl groups using epichlorohydrin (ECH) [186] as shown in **Figure 1. 13**.

In principle, phenolic compounds contained at least one phenolic hydroxyl group that can be converted to epoxy groups through O-glycidylation by reacting with ECH under an alkaline condition. As shown in **Figure 1. 13**, in method A, NaOH acts as the catalyst and reactant and ECH as the reactant and solvent, by which epoxy monomers and oligomers produce simultaneously. In method B, a phase transfer catalyst is required, to better control epoxy values, reduce organochlorine, oligomer contents and side reactions likely by decreasing the reaction

temperature and reaction time [101]

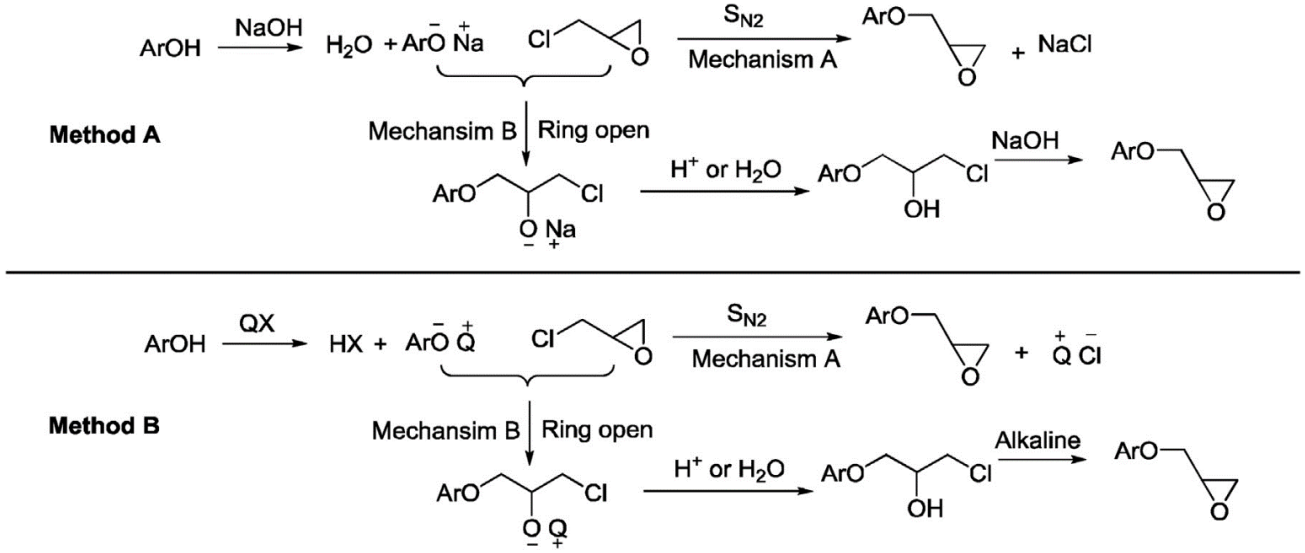

Figure 1. 13 O-glycidylation mechanisms of phenolic compounds in the absence (Method A) and presence (Method B) of a phase transfer catalyst (QX). [101]

1.7.3.2 Commercial epoxy resins as a curing agent

Kim et al [184] investigated the cure kinetics of epoxy resin (YX-4000H, EOCN-1020, XP-2030 and XD-1000) with different novolac resin as curing agents, and analyzed in respect of the network structure. The conversion rates of novolac epoxy resins with phenyl and dicyclopentadiene moiety were higher than biphenyl epoxy resin and o-cresol novolac epoxy resin systems. Among commercial epoxy resin, Bisphenol A diglycidyl ether (DGEBA) has been used as a formaldehyde-free curing agent and was shown to be an effective cross-linker compared with HMTA. Indeed, both curing agents obtained similar curing reaction curve and peak temperatures [187, 188]. Kim et al. [184] studied the curing kinetics of the epoxy/novolac resin systems and found that regardless of the type of epoxy resin a cure reaction, a curing reaction can be achieved. In addition, bisphenol A diglycidyl ether (DGEBA) was used as a formaldehyde-free curing agent and was shown to be an effective cross-linker compared with HMTA, obtained similar curing reaction curve and peak temperature, and the curves obtained from DSC are shown in **Figure 1. 14**. However, commercial epoxy resins such as DGEBA is derived from bisphenol A (BPA) which is toxic and petroleum-derived. Hence, the replacements for BPA with alternatives derived from sustainable and renewable resources bio-based polyphenols would be highly desired [120-124, 126, 127].

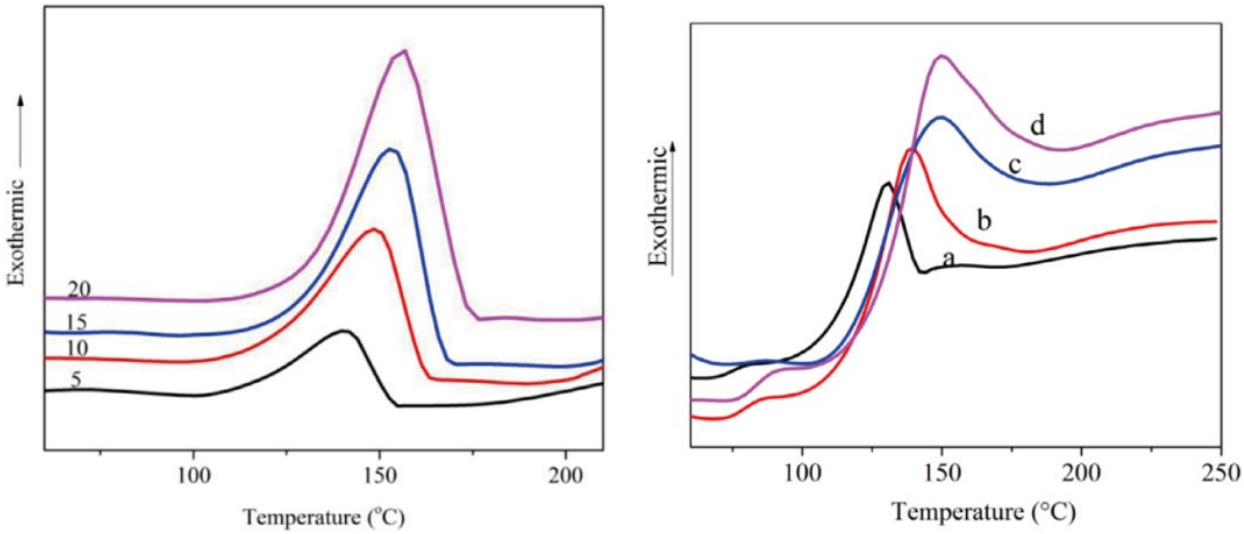

Figure 1. 14 DSC curves of the PHMF resin cured with 20 wt% DGEBA (left) and HMTA (right) at different heating rates: 5 (a), 10 (b), 15 (c), and 20 (d) °C/min [188]

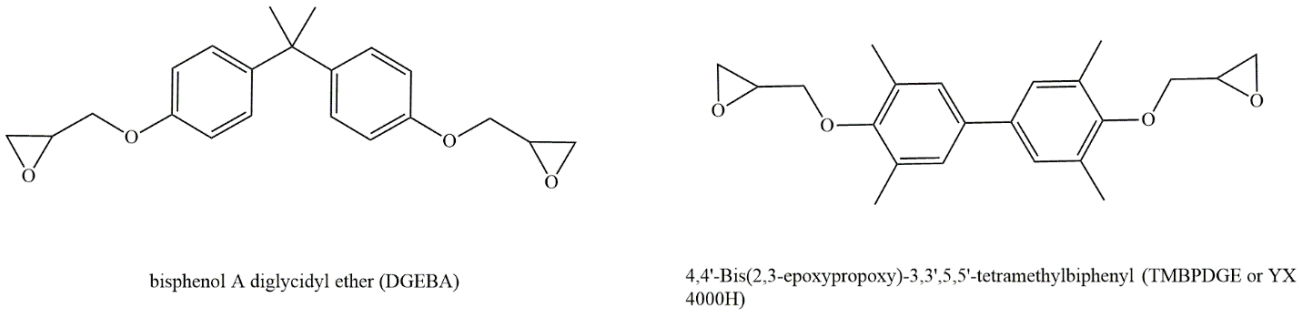

bisphenol A diglycidyl ether (DGEBA)

4,4'-Bis(2,3-epoxypropoxy)-3,3',5,5'-tetramethylbiphenyl (TMBPDGE or YX 4000H)

Figure 1. 15 Chemical structures of commercial epoxy resins.

1.7.3.3 Bio-based epoxy resin

Nowadays, researchers focus on developing a bio-based epoxy monomer or oligomer

1.7.3.3.1 Bio-based epoxy resin synthesis

The bio-based epoxy resins have been prepared from a variety of largely utilized renewable resources which can be clarified in the following four catalogs and some of them are summarized in **Table 1. 12.**

- Vegetable oils [125, 128, 129] (soybean oil, linseed oil, palm oil, and castor oil),
- Lignocellulosic biomass (lignin, vanillin, and eugenol) [130]
- Polyphenols, tannins, and cardanol (resorcinol, tannins, catechin, gallic acid and cardanol)
- Starch and sugar (glycerol, sorbitol, maltitol, levulinic acid, itaconic acid and furans)

Plant oils which are eco-friendly, low-cost, biodegradable and easily available materials have often been used in different applications, but their inferior strength and rigidity of them need to be enhanced by further modifications[189]. Kim et al.[128] investigated the development of thermoset plastics from several plant oils (linseed, soybean, cottonseed, oilseed radish, and peanut oils) using an optimal process of solvent-free epoxidation by reacting the double bonds of fatty acids with hydrogen peroxide. Epoxidized linseed oil promises the highest modulus and impact resistance due to the largest number of double bonds.

Table 1. 12 Bio-based epoxy resin from various bio-based precursors

Bio-based precursor	Epoxidation reagent	catalyst	EEW	Ref.
Plant-based oils (e.g., linseed, soybean, cottonseed, oilseed radish, and peanut oils)	hydrogen peroxide	ion-exchange resin.	-.	[128]
Eugenol	m-CBPA in ethyl acetate	-.	-	[127]
Vanillyl Alcohol	Epichlorohydrin	TEBAC and NaOH	193 g/eq.	[124]
Lignin, demethylated lignin, phenolated lignin, and hydroxymethylated lignin	Epichlorohydrin	TBAB and NaOH	-	[131]
Lignin hydrogenolysis product	Epichlorohydrin	NaOH	359 g/eq.	[190]
4-methylcatechol, gallic acid, protocatechuic acid, pyrogallol and resorcinol	Epichlorohydrin	TEBAC and NaOH.	-	[191]
Tara tannins extract	Epichlorohydrin	TEBAC and NaOH.	8.48×10^{-3} mol/g	[192]
Resveratrol	Epichlorohydrin	NaOH.	280 g/eq.	[193]
Itaconic acid	m-CBPA in dichloromethane	-	1.16	[194]
Bio-oil (hydrothermal liquefaction of loblolly pine)	Epichlorohydrin	TEBAC and NaOH	About 250 g/eq	[120]
Bio-oil (fast pyrolysis of biomass)	Epichlorohydrin	TEBAC and NaOH	333 g/eq	[195]
Bio-oil (fast pyrolysis from hardwood)	Epichlorohydrin	TEBAC and NaOH	314 g/eq	[196]

Therefore, several promising results have been reported by applying lignocellulosic biomass products to the production of epoxy resin. Chen et al.[127] prepared bio-based epoxy compounds by a two-step procedure from eugenol. The first step is the esterification of eugenol with succinyl, adipoyl, suberoyl, and 2,5-furan chloride, respectively, in ethyl acetate using triethylamine as a base catalyst, forming intermediated. The second step is the oxidation of the allylic groups by m-CBPA in ethyl acetate, forming epoxy compounds.

Vanillyl alcohol, a lignin-derived aromatic diol, is a potential platform chemical for the production of renewable epoxy thermosets. Hernandez et al.[124] successfully prepared

diglycidyl ether of bisguaiacol by synthesizing bisguaiacol and epichlorohydrin according to known glycidylation procedures. Wang et al.[197] successfully condensed bisguaiacol from vanillyl alcohol and guaiacol and then synthesized vanillin derivative-based epoxy resin.

In recent years, various modification methods such as demethylation, phenolation, and hydroxymethylation have been introduced as effective pre-treatment strategies to enhance the reactivity and compatibility of raw lignin [131]. Zhang et al. [131] prepared epoxy grouting resin using lignin as an underutilized by-product of the forestry industry with outstanding viscosity and mechanical properties. van de Pas and Torr [190] synthesized of novel epoxy resins from native lignin in pine wood hydrogenolysis products. These were blended with bisphenol A diglycidyl ether or glycerol diglycidyl ether and cured with diethylenetriamine or isophorone diamine as sustainable biobased polyols in the synthesis of high-performance epoxy resins (**Figure 1. 16**).

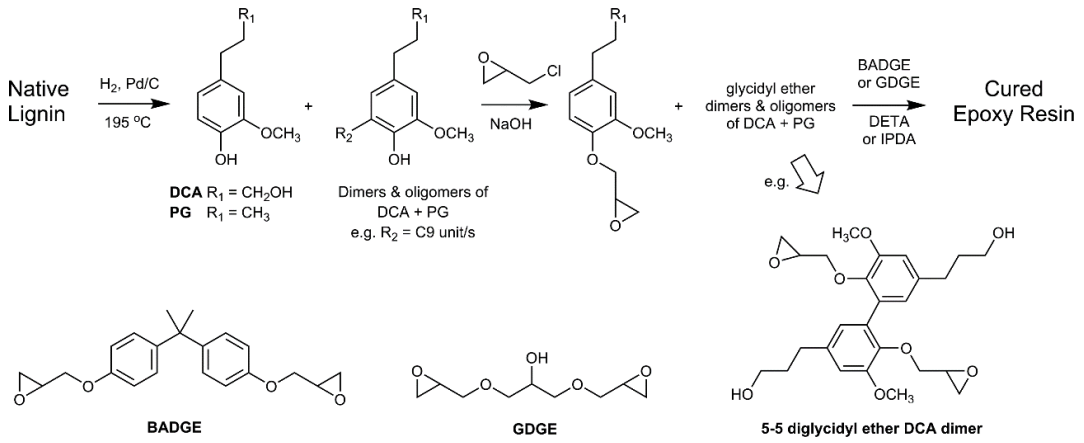

Figure 1. 16 Approach used to prepare cured epoxy resins from lignin hydrogenolysis products [190].

Polyphenols and more specifically condensed tannins, extracted from wastes produced by the wood and wine industries can be an alternative to BPA to produce epoxy resins [198]. Aouf et al.[191] conducted the O-alkylation reaction by epichlorohydrin of some natural phenolic compounds (4-methylcatechol, gallic acid, protocatechuic acid, pyrogallol and resorcinol). The O-alkylated products obtained in this reaction could be further used as bisphenol A substitutes in the synthesis of epoxy resin pre-polymers. The next year, they successfully prepared thermosetting epoxy polymer with tara pod powder using the same method [192]. Shang et al [193] also focused on the renewable resveratrol deriving from tannins to synthesize the bio-based epoxy resin which is named triglycidyl ether of resveratrol. Ma et al.[194] proposed a bio-based epoxy resin with high epoxy value (1.16) and low viscosity (0.92 Pa s, 25°C) was synthesized from itaconic acid and its chemical structure was confirmed by ^{1}H NMR and ^{13}C

NMR spectroscopy.

1.7.3.4 Synthesis of upgraded woody biomass pyrolysis oil-based epoxy resin

Another potential eco-friendly substitute for BPA is using bio-oil from wood biomass [132]. As it mentioned above, bio-oil is a complex mixture that contains over 255 different chemical compounds [7]. It can be used as a source of phenolic compounds in the production of a bio-based polymeric network. Celikbag et al [120] applied bio-oil produced by hydrothermal liquefaction of loblolly pine as the bio-based phenol precursor in the synthesis of bio-oil-based epoxy resin, the resulting resin is a black viscous liquid. Sibaja et al.[195] used bio-oil from fast pyrolysis of biomass to react with epichlorohydrin in an alkaline medium using benzyltriethylammonium chloride as a phase transfer catalyst to produce bio-based epoxy resin and the measured epoxy equivalent weight (333 g/eq) is approx. the half of commercial epoxy resins. Barde et al.[196] synthesized epoxy resins from fast pyrolysis bio-oil derived from hardwood found that bio-oil based epoxy resins have structural and chemical similarities with petroleum-derived ones and can also be cross-linked by the existing amine hardeners.

However, the application of phenol in pyrolysis oil is limited due to fewer reactive sites and steric hindrance, it is very necessary to update bio-oil for better use in resin synthesis [63, 132, 139, 158, 199, 200].

The combination of both separation and purification methods (factional condensation and water extraction) was accomplished. Based on the above discussion, many kinds of phenol rich bio-oil precursors obtained from woody biomass pyrolysis oil were chosen in the bio-based phenolic resin synthesis and they also can be chosen in bio-based epoxy resin synthesis as (1) the whole bio-oil to substitute petroleum-derived phenol, (2) the bio-oil obtained from fractional condensation, or (3) the water-insoluble fraction of the bio-oil obtained from fractional condensation.

Previously, the researchers have accomplished to use bio-oil from fast pyrolysis biomass to synthesize bio-oil based epoxy resin and obtain similar properties compared with commercial epoxy resin. Since there is not a lot of scholars focusing on using phenol-rich fraction from fractional condensation or water extraction pyrolysis oil for bio-based epoxy resin synthesis. Thus, the high purity bio-oil fraction with a large yield of phenolics will become a very effective alternative for commercial BPA [201].

1.8 Safety study of resinification and curing reaction

1.8.1 Techniques for thermal hazard analysis

The commonly used thermal hazard analysis techniques and equipment can be divided into five categories:

- thermal analysis technology (DSC, DTA),
- isothermal calorimetric technology (TAM III),
- adiabatic calorimetric technology (VSP2, ARC),
- reaction calorimetric technology (RC1, C80),
- emergency relief control technology (VSP2, RSST).

These techniques can be used to experimentally measure the intrinsic hazard data of hazardous or unknown substances used in manufacturing processes, including the thermal stability, incompatibility, lowest exothermic temperature, and hazardous consequence analysis, to determine the hazardous properties and to provide references for protective process safety design [202]. A comparison of these thermal hazard analysis techniques were summarized in Table 1. 13.

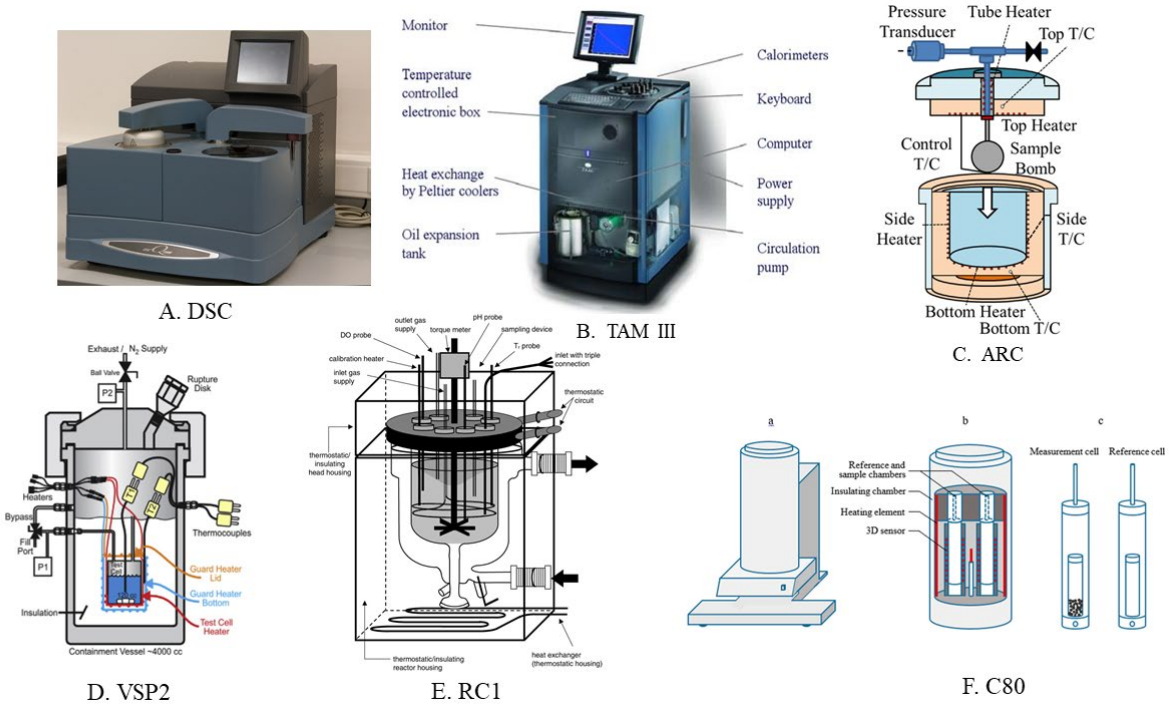

Figure 1. 17 The structure of commonly used thermal hazard analysis techniques

Table 1. 13 Comparison of commonly used thermal hazard analysis techniques [203]

Techniques	Measuring principles	Application field	Sample size	Temperature range	Sensitivity (Wkg^{-1})	Ref
Differential scanning calorimetry (DSC)	Differential, ideal flux, or isoperibolic	Screening and secondary reactions	1–50mg	−50 to 500 ◦ C	2–10	[204-206]
Reaction calorimeter Thermal activity monitor (TAM)	Differential, ideal flux	Secondary reactions, storage stability	0.5–3 g	30–150 ◦C	0.01	[202, 207-209]
Vent Sizing Package (VSP)	Ideal accumulation	Main and secondary reactions	50–100 g	30–350 ◦C	0.2	[206, 210-212]
Accelerating rate calorimeter (ARC)	Ideal accumulation	Secondary reactions	0.5–3 g	30–400 ◦C	0.5	[213-215]
Calvet C80	Differential, ideal flux	Main and secondary reactions	0.1–3 g	30–300 ◦C	0.1–1	[202, 216]

DSC has long been proven a powerful technique for measuring the variation of polymerization rate as a function of time (isothermal mode) or temperature (non-isothermal mode) due to the various advantages it offers [202, 203, 205-207]:

- To identify potential exothermic hazards in the process units, the thermophysical properties of the chemicals and reaction conditions must be explored[217]. The shape of a DSC thermogram gives important information for hazard identification. A sharp rise due to a rapid energy release with temperature indicates that the chemical may be thermally unstable. Furthermore, dynamic temperature-programmed screening is conducted to determine the onset temperature (T_i), exothermic temperature rise (ΔT), and heat of reaction (ΔH).

- The use of DSC to investigate the polymerization of a variety of monomers has been reported in the literature (Table 1. 14**)**, including the well-studied vinyl acetate monomer,

phenol-formaldehyde, and epoxy acrylic resin as well as the curing of novolac-epoxy resins. Chen et al [217] employed DSC to perform the non-isothermal experiments of vinyl acetate monomer producing a variety of copolymer products, and the calculations of the kinetic parameters from temperature-programmed DSC curves have been evaluated by the isoconversional method. Lin et al.[218] used DSC to investigate the basic characteristics of thermal polymerization of phenol-formaldehyde resin for eliminating hazards associated with manufacture. The work of Wang et al. [205] aims to test and ascertain the effect of the catalyst in terms of its dosage on the runaway reaction of the epoxy acrylic resin. Zhang et al.[188] studied the curing reaction of bisphenol A type epoxy resin and a phenolic novolac resin based on data acquired from DSC and the kinetic parameters were evaluated.

Table 1. 14 Experimental conditions used in the investigation of the polymerization reaction by DSC

Reaction type	Crucible type	Sample size	Ramp	Temperature range	Ref
self-polymerization of Vinyl acetate monomer	gold-plated high-pressure crucible	4–5 mg	1, 2, 4, and 10 K min^{-1}	room temperature to 400 °C	[217]
phenol-formaldehyde polymerization in pH (5-9)	high pressure crucible 10 MPa	<10 mg.	0.01 to 100 °C / min^{-1}	0 °C to 725 °C	[218]
autocatalytic reaction of benzoyl peroxide	high pressure crucible 10 MPa	5mg	4 °C / min^{-1}	30 and 300 °C	[219]
phenol–formaldehyde polymerization with acid catalyst	stainless steel sealed crucible 10 MPa	5–10mg	4°C /min^{-1}	30 and 250 °C	[210]
epoxy acrylic resin polymerization	high pressure crucible 10 MPa	3 mg	1, 2, 4, 6 and 8 °C /min^{-1}	0 °C to 725 °C	[205]
Dicumyl peroxide polymerization	high pressure crucible 10 MPa	3 to 10 mg	1, 2, 4, and 10 °C /min^{-1}	30 °C to 300 °C	[206]
curing of novolac-epoxy resins	stainless steel sealed crucible 10 MPa	5–10mg	5, 10, 15 and 20 °C/min^{-1}	30 and 250 °C	[188]

1.8.2 Kinetic models

Non-isothermal differential scanning calorimetry techniques are commonly applied to study the curing behavior and kinetics of resins and polymers. The results of DSC measurements are then used for the evaluation of kinetics parameters with different models. Actually, following famous scientists, such as Kissinger, Ozawa, Augis, and Bennett, we acquired thermo-kinetic parameters via their well-known kinetic equations. They offered useful results of thermo-kinetic parameters and also satisfy further application because f(α) is independent of the heating rate when used to determine E_a. Thus, these formulas are more suitable for simplified first-order reactions (n = 1) [188, 205, 217, 218, 220, 221].

The kinetic models, mainly include:

- model-free methods (Kissinger, Flynn–Wall–Ozawa (FWO) methods, Crane equation Friedman model, and Kisinger–Akahira–Sunose (KAS))
- model-fitting method (autocatalytic model)

1.8.3 Analysis of experimental results and assessment of safety parameters

The chosen approach was to obtain the beneficial kinetics and reliable parameters of the thermal reaction that included the kinetic parameters and inherently safe properties, reaction order (n), activation energy (E_a), time to maximum rate (TMR), and maximum temperature of synthesis reaction (MTSR).

The cooling failure scenario (**Figure 1. 18**) commonly uses the temperature scale for the assessment of severity and the time scale for the probability assessment including the time to maximum rate under adiabatic conditions (TMR_{ad}), Maximum temperature of synthesis reaction (MTSR) and Temperature at which TMR_{ad} is 24 hours (TD_{24}). [203, 212].

After the assessment of both risk components' severity and probability of occurrence by the adiabatic temperature rise and time to maximum rate under adiabatic conditions, the risk linked with a runaway reaction can be assessed. Then, an assessment matrix using levels low, medium, and high on each coordinate is proposed (**Figure 1. 19**) [203].

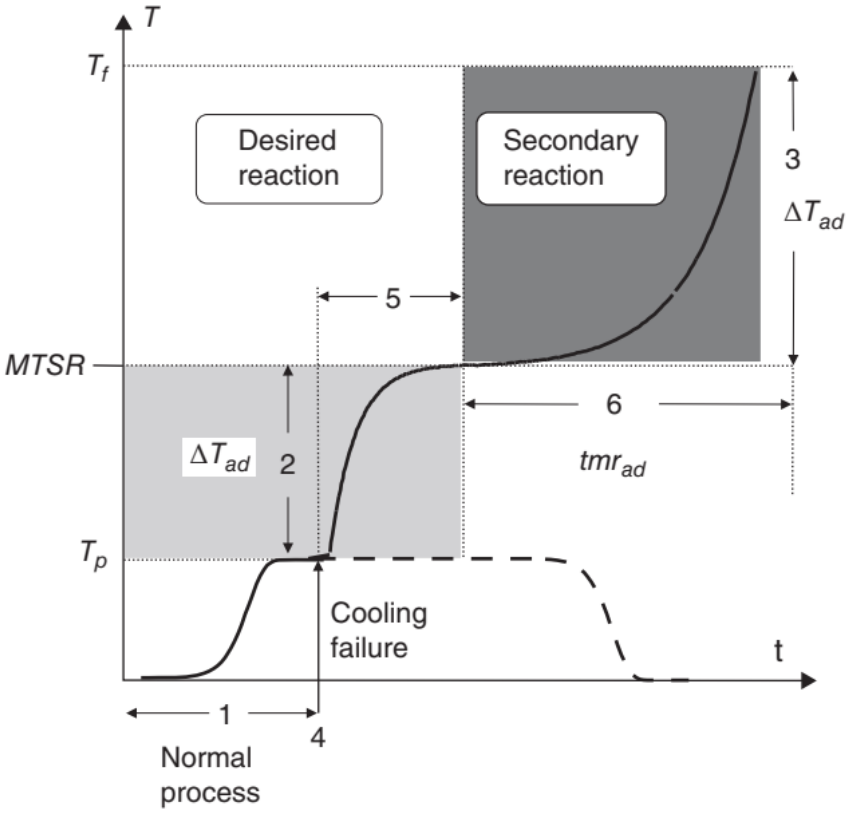

Figure 1. 18 Cooling failure scenario [203]

Severity	High	$\Delta T_{ad} > 200$ K	Medium	High	High
	Medium	50 K < ΔT_{ad} < 200 K	Medium	Medium	High
	Low	$\Delta T_{ad} < 50$ K	Low	Low	Low
Runaway risk assessment			$TMR_{ad} \geq 24$ h	8 h < TMR_{ad} < 24	$TMR_{ad} \leq 8$ h
			Low	Medium	High
			Probability		

Figure 1. 19 Runaway risk assessment matrix [203]

1.9 Conclusions

This literature review has provided knowledge on how to produce, upgrade and apply biomass feedstock in the field of green sustainable synthesis. Actually, it is a completed system of biomass application valorization, since this subject starts from the immediate pyrolysis of woody biomass; then, the upgrading of biomass pyrolysis oil; next, the production of a bio-based green polymer by using the obtained phenol-rich fraction from pyrolysis oil; at last, the kinetic study of the reaction.

In this literature review, a large number of scientific articles and books on biomass conversion, biomass pyrolysis, fractional condensation, solvent extraction, oil storage stability, resin synthesis, resin curing reaction, and kinetic study of the reaction as well as reaction risk assessment, have been consulted to better carry out this work and obtain a comprehensive academic perspective in this field, and further for better innovation. Simultaneously, the investigation of the research background and references shows the feasibility and possibility of this topic. It is worth mentioning that the scientific community has researched these topics. They have compared and analyzed many recent works, some of these studies are still not complete and systematic, especially for specific reactions that lack precise reaction conditions and operating methods. The purpose of this survey is to

understand these themes more clearly, and to obtain more favorable reaction conditions and innovative methods for future work.

Chapter II

Chemical characteristics of bio-oil from beech wood pyrolysis separated by fractional condensation and water extraction

Abstract:

The biomass pyrolysis was carried out using a drop tube reactor system equipped with three-stage condensers, each set to a different temperature for the fractional condensation of bio-oil. Beechwood was used as feedstock. The effect of the temperature of the first and second condensers was examined. The obtained bio-oil fractions were analyzed to determine the distribution and the yield of the chemical compounds collected. A second upgrading step of bio-oil previously obtained from the first and second condensers was performed by extraction and separation using water. Finally, the changes in the main representative components are discussed.

A part of this study has been published as an article (Xu J, Brodu N, Wang J, Abdelouahed L, Taouk B. Chemical characteristics of bio-oil from beech wood pyrolysis separated by fractional condensation and water extraction. J Energy Inst 2021; 99:186-97. https://doi.org/10.1016/j.joei.2021.09.006)

2.1 Introduction

To improve the physicochemical properties of bio-oil for its practical application, upgrading is necessary [10]. Since pyrolysis oil consists of very complex compound groups having a large range of dew points, fractional condensation can be a simpler, lower cost, and more efficient approach to producing liquid fuels and chemicals compared with treating all the oil [68, 69].

Bio-oil is a mixture of many chemical compounds and not all the chemicals have the same affinity with the solvent. The extraction of bio-oil in different solvents is used for upgrading the bio-oil. Adding water is considered the simplest and greenest method to extract and separate chemical compounds [78, 79].

Both fractional condensation and water extraction have been studied extensively as a single separation method. In this study, the combination of these methods was studied in order to improve the separation by chemical family.

2.2 Experimental section

2.2.1 Materials

The beechwood (BW) used for this study was provided by ETS Lignex Company and its average fractional size was 400 µm. The beechwood was dried at 105 °C for 12 h before use to remove moisture. The proximate analysis and elemental analysis of beech wood are shown in Table 2. 1.

Table 2. 1 Proximate analysis and elemental analysis of beech wood.[7]

Proximate analysis (% w : w)	**Humidity**	**Volatile matter**	**Fixed carbon**	**Ash**
Beech wood	7.44	74.19	17.52	0.85
Elemental analysis (% w : w)	**Carbon**	**Hydrogen**	**Nitrogen**	**Oxygen**
Beech wood	47.38	6.11	<0.01	46.51

2.2.2 Biomass pyrolysis–condensation setup

The experimental runs in this study were performed in a continuous drop tube reactor (DTR) coupled with a three-stage condensation unit in series, as illustrated in **Figure 2. 1.** The operating conditions of the DTR are chosen to have an optimal yield of bio-oil. Two cyclones were placed at the vapor exit of the char collector to separate some of the fine particles that tend to get entrained by the gas/vapor flow. The vapor coming through was condensed to be recovered as bio-oil fractions by the three-stage condenser.

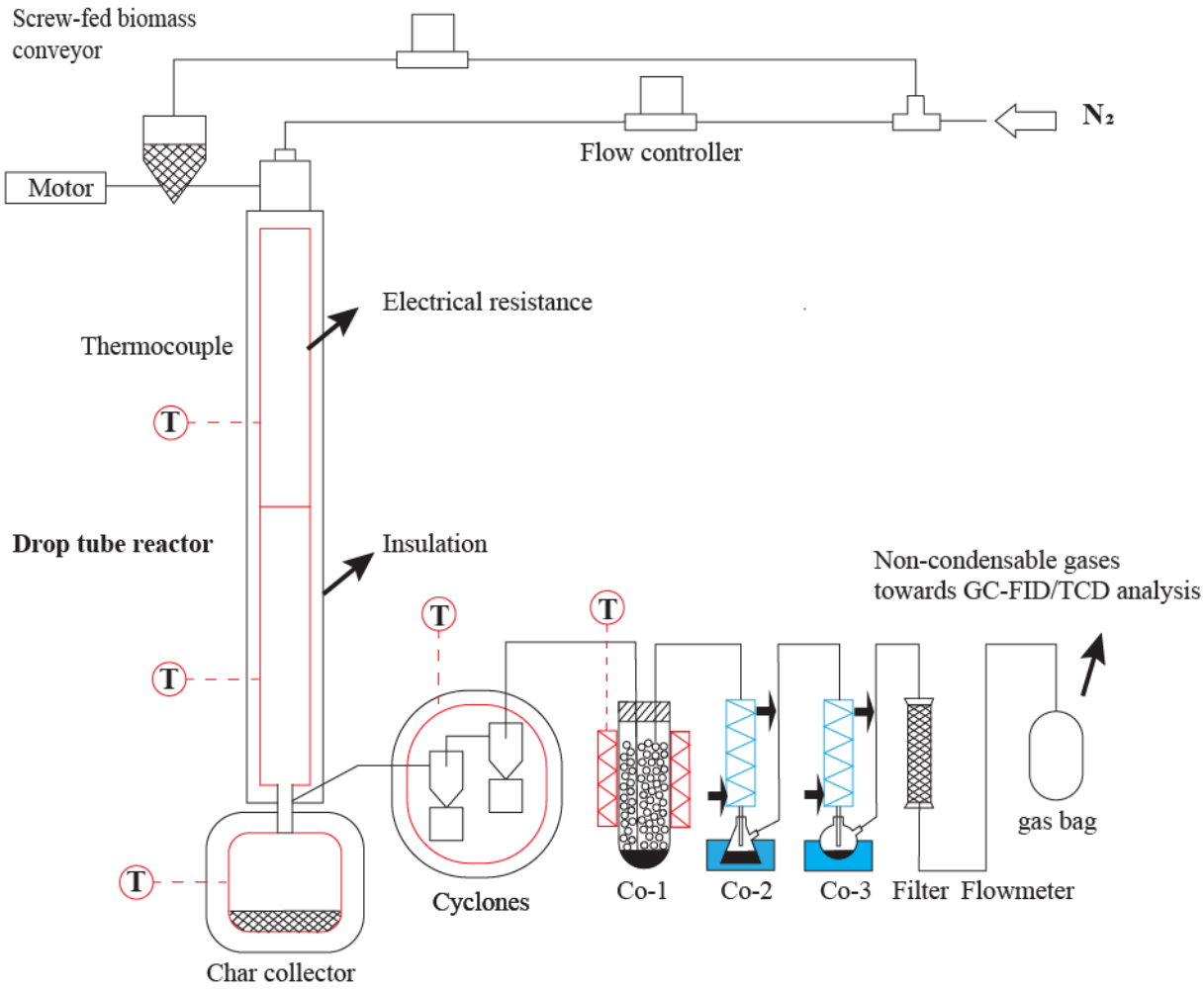

Figure 2. 1 Experimental setup of drop tube reactor and three-condensation system.

The first condenser (Co-1) was designed to be filled with glass beads to increase the contact surface area and optimize the condensation of heavy components of pyrolysis vapor. A furnace shell covered the glass flask and its internal temperature was controlled using a thermocouple. The second and third stages of the condensation setup (Co-2 and Co-3) were two condensers and two flasks held in two cold baths of two recirculating coolers (JULABO). The non-condensable gases, at the exit of a silica wool filter, consisting of CO, CO_2, CH_4, H_2, C_2, and C_3 hydrocarbons, were then sent on to the analytical setup to be analyzed. For the experiments,

the temperature of all the heaters was set as indicated in **Table 2. 2**. The nitrogen flow rate was 500 mL/min, corresponding to the gas residence time of 9.77 s. The DTR was fed with 1.28 g/min of biomass using a spiral conveyor. The biomass particle residence time in the reactor was 2.20 s, which was much lower than the gas residence time[222]. The oil fractions (Oil-1, Oil-2, and Oil-3) were condensed into the condensers (Co-1, Co-2, and Co-3, respectively). A single condensation pyrolysis experiment was carried out for comparison with the three-stage condensation of liquid pyrolysis products, under the same pyrolysis temperature and nitrogen flow rate. The condensation setup is a single condenser and single flask held in a cold bath at -11 °C, and the collected oil was named Oil-S. The physical-chemical properties of Oil-1, Oil-2 and Oil-3 will be compared with those of Oil-S. The analysis results of Oil-S can be used as a reference. Each experiment was repeated three times, the experimental repetitive errors were reported and average values were calculated. The analysis is based on the wet matter of oil.

Table 2. 2 The temperatures used at different positions of the experimental setup

[a] present: the Co-2 set as 20℃ when varying the Co-1 temperature

Unit	DTR	Cyclones	Char collector	Co-1[a]	Co-2[b]	Co-3
Temperature (°C)	500	300	300	110-80	30-10	-11

[b] present: the Co-1 set as 100℃ when varying the Co-2 temperature

2.2.3 Water extraction experiment

After fractional condensation, three fractions of pyrolysis oils were recovered into sealed glass bottles and then stored in the fridge. Approximately 10 g of pyrolysis oils (Oil-1 and Oil-2) wet samples were taken in a flask and 10–70 wt% of deionized (DI) water was added to them. Upon the addition of water to the pyrolysis oil, shaking a few times for better mixing and storing in the refrigerator for 12h, phase separation takes place until equilibrium is reached. The latter depends on the nature of the pyrolysis oil. The samples were centrifuged at 4,000 rpm for 20 min (REMI R-12C Plus centrifuge), the upper portion is less viscous and the lower portion is thick. After centrifugation, the water-soluble fraction (Oil-1-WS and Oil-2-WS) on top was collected carefully with the help of a 5 ml syringe and concentrated through rotating evaporation until its water content reached approximately 15 wt%, leaving the water-insoluble fraction (Oil-1-WI and Oil-2-WI) on the bottom. All the samples were collected and analyzed further.

2.2.4 The pyrolytic product analysis method

2.2.4.1 GC analysis

The analysis of the recovered bio-oil was performed using a gas chromatograph-mass spectrometry instrument GC-MS (Varian 3,900-Saturn 2100T). The column was a VF-1701ms (Agilent) (60 m × 0.25 mm × 0.25 µm film thickness). The oven was held at 45 °C for 4 min then heated to 280 °C with a heating rate of 4 °C and held for 20 min. The carrier gas was helium with a constant flow of 1 mL/min. 1 µL of the bio-oil sample diluted in pure acetone was directly injected into the heated split injector (split ratio 30:1) at 250 °C. The MS electron ionization energy was 70 eV. The detection was performed in full scan mode. The analyzed components were identified with Varian WS (Work Station) and NIST 2,002 software by comparing the mass spectrum obtained to mass spectra from the NIST library. Kovats retention indices of the identified peaks were then calculated and compared to reference values to confirm their identity.

Once the identity of the peaks was confirmed, a GC-FID Scion 456-GC Bruker instrument was used to quantify the components. The column used was the same as the one used for the GC-MS and the temperature program was also the same except that the final temperature was 240 °C instead of 280 °C. These compounds were then grouped into chemical "families", each family having the same main functional group. A pure reference compound for each family was used for calibration of all peaks of the corresponding family. Standard solutions of each of these reference compounds were prepared by dissolving them in acetone. Five-point straight line calibration curves (with $R^2 > 0.99$) were established for these pure compounds [7], using nonane as the internal standard. Considering the differences in the response factor from the selected reference compound, the relative response factors were calculated by using the effective carbon number (ECN) method [223].

2.2.4.2 Karl Fischer (KF) titration method and density test method

The volumetric KF titrations were performed with a Metrohm 870 KF Titrino Plus apparatus. An Aqualine sodium tartrate solution was used as a titrating agent, along with Hydranal Composite 5 and Hydranal Methanol Rapid as working media. The sample weight used was in the range of 0.17–0.20 g.

The density of bio-oil is measured using a pycnometer (10 ml). Bio-oil was homogenized for 1 min by vibration before introducing the sample into the pycnometer. The temperature of the bio-oil was maintained at 20°C using a water bath. Then, after weighing, the sample was replaced by water. The mass of bio-oil was divided by that of water to obtain the density.

2.2.4.3 ATR-FTIR

The use of FTIR can give a quantification by the peak area ratio analysis, and is the most powerful technique to identify the functional groups present in bio-oils [224]. Attenuated total reflectance-Fourier transform infrared spectroscopy (ATR-FTIR) was used to analyze the organic functional groups present in the bio-oil samples before and after the separation and extraction by water. The water-insoluble samples were vacuum dried before use. A SHIMADZU IRTracer-100 spectrometer with a resolution of 4 cm^{-1} was used for analyzing the samples. The spectrum was developed in reflectance mode with a wavenumber range of 450–4,000 cm^{-1}.

2.3 Experimental results and discussion

2.3.1 Influence of experimental conditions on the distribution of products yield

The effect of the temperatures of Co-1 and Co-2 on the distribution of the bio-oil in the three condensers was studied (**Figure 2. 2**). Concerning the temperature of the Co-1, the results show that the amount of Oil-2 increased as the temperature rose, whereas the yield of Oil-1 decreased at the same time. However, for the yield of Oil-3 no significant changes were observed, because the specified temperature of Co-2 was enough to condensate the same fraction in each run. The increase in temperature leads to a decrease in the condensing efficiency of the first condenser [73]. Meanwhile, more and more low dew point molecules condensed in the relatively low-temperature condenser.

Concerning the effect of the condensation temperature of Co-2 on the distribution of oil products, the results show that as the temperature of Co-2 increases, the yield of Oil-2 decreases, whereas Oil-3 indicated an opposite trend to that of Oil-2. Meanwhile, Oil-1 did not seem to be affected by the temperature of Co-2. It is logical and can be expected as long as the temperature of Co-1 didn't change, its yield stays at the same level. Ma et al. [76] studied the effect of the temperature of Co-2 from 80 °C to 0 °C and a similar result was obtained.

The temperature of the condenser also had a slight influence on the distribution of bio-oil, biochar and biogas. When the temperature of the condenser increases, the yield of total bio-oil production decreases slightly, whereas the yield of char and gas products increases. It was shown the same changes in Co-1 and Co-2 (see **Figure A 1. 1**).

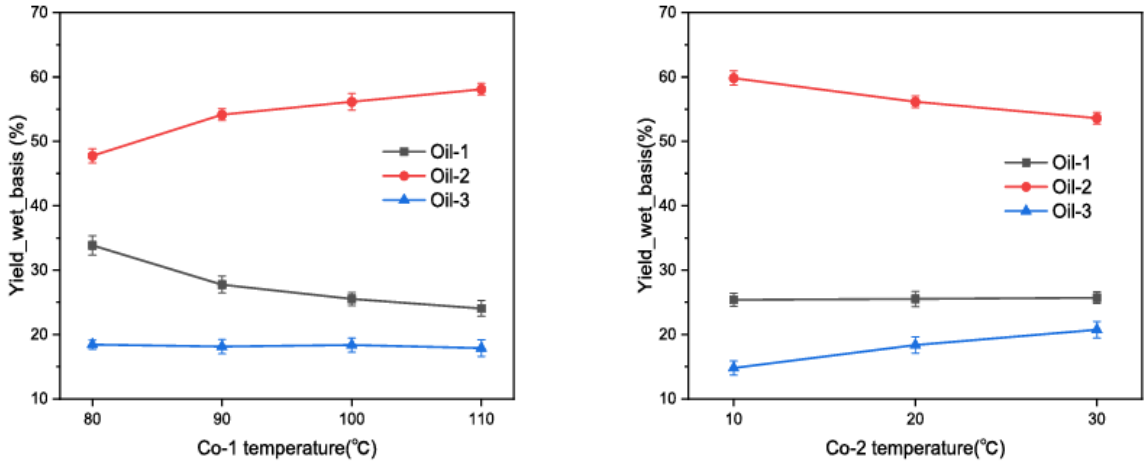

Figure 2. 2 Distribution of bio-oil fraction in the function of temperature: on the left condenser 1 (Co-2 set as 20 °C) and on the right condenser 2 (Co-1 set as 100 °C)

2.3.2 Physical properties of liquid products

2.3.2.1 Water content and density

The water content values in the oil products are shown in **Figure 2. 3 a, b**. The water contents of Oil-S, Oil-1, Oil-2, and Oil-3 collected from the single condenser (-11 °C), Co-1 (110 °C), Co-2 (20 °C), and Co-3 (-11 °C), are 33.33 wt%, 1.44 wt%, 37.37 wt%, and 71.22 wt%, respectively. The water present in the bio-oil comes from the original moisture of the feedstock (7.44 wt%) and from dehydration reactions as by-products during biomass pyrolysis.

It is evident that the water content of the pyrolysis bio-oil through three-stage condensation has changed greatly compared with single condensation, and there are also large differences between the stages of condensation. The water content of Oil-1 is weak, whereas most of Oil-3 is composed of water. It should be also mentioned that the water content of Oil-2 is similar to that of Oil-S. With the increase in temperature of Co-1 from 80 °C to 110 °C, the water content of Oil-1 decreased from 11.24 wt% to 1.44 wt%, whereas that of Oil-2 and Oil-3 increased slightly. When the temperature increased, in particular above the boiling point of water, this resulted in a reduction of the water in Oil-1, while the excess water is condensed in the Co-2 and Co-3 condensers.

For the measurement of the density, the results (**Figure 2. 3 c, d**) show an opposite trend compared to the water content, and an obvious difference between the density of Oil-S, Oil-2,

Oil-3, and Oil-1 (1.13, 1.12, 0.93, and 1.29 g·cm^{-3}, respectively) is observed. When the temperature of Co-1 increases, the density of Oil-1 increases and the density of Oil-3 decreases, but the change of Oil-2 is not clear. High water content means low kinematic viscosity [70].

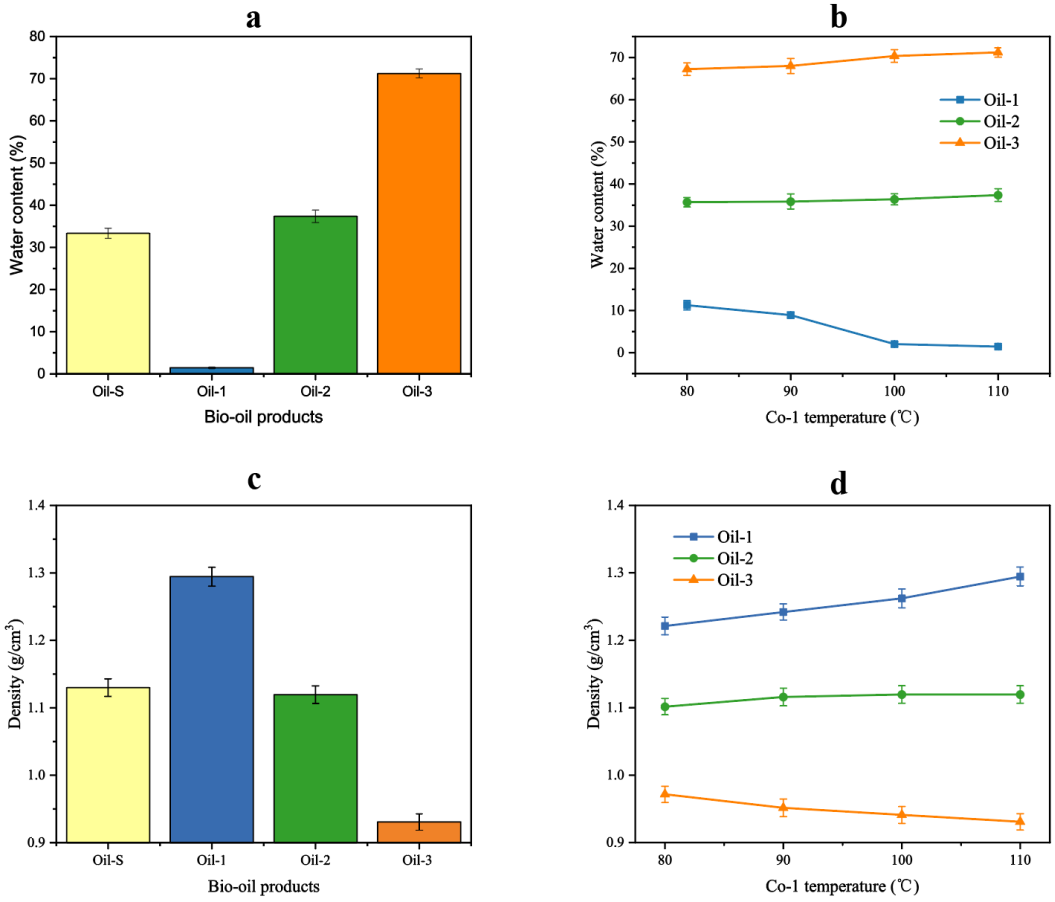

Figure 2. 3 The water content (a) and density_wet_basis (c) of fractional bio-oils and the water content (b) and density (d) evolution of fractional bio-oil samples as function of Co-1 temperature

2.3.3 Chemical distribution of liquid products

2.3.3.1 Identification and quantification of bio-oil components

To ensure the accuracy of the results, GC-MS was used to identify individual peaks of the Oil-S, Oil-1, Oil-2, and Oil-3 samples, and found 270, 106, 139, and 97 compounds respectively. After the identification of each peak, the quantification of the compounds that appeared was performed. All the compounds were grouped into 11 major chemical families and reference compounds were used for calibration.

Figure 2. 4 shows GC-MS chromatograms of bio-oil collected in different condensers. From the comparison of the shapes and intensities of the peaks, it can be noted that the pyrolysis oil products are effectively separated by the three-stage condensation system. The peak at 8.5 min

corresponds to acetic acid, and Oil-1 has the smallest peak area. The peaks starting from 25 min are identified as phenols, guaiacols, sugars, and some heavy compounds of other families. The peak area in Oil-1 is much larger than that in Oil-2, but no peak was detected in Oil-3. **Table 2. 3** gives the number of chemical compounds and their yield in the three oil products. The calculation is based on the wet matter of oil and neglects the non-GC-detectable portion of the oil. Globally, 63.54 wt% of phenolics and 71.41 wt% of sugars are collected in Co-1 and 96.82 wt% of carboxylic acids were obtained by Co-2 and Co-3.

To establish a relationship between the chemical composition of each oil fraction obtained and the temperature of the condensers, the boiling points of the main compounds of each family are collected in **Table 2. 3** and discussed. Compared with Oil-S, Oil-1 and Oil-3 have fewer chemical compounds and showed an obvious separation effect. (See clearly in **Figure A 1. 2**) Approximately 71.41 wt% of sugars, 59.38 wt% of phenols, and 73.12 wt% guaiacols of the organic part of the GC-detectable portion of the total bio-oil were captured at 110 °C (Oil-1). This is certainly due to the high boiling points of the compounds in these chemical families, ranging from 182 to 675 ºC. The average molecular weight of Oil-1 was as high as 148.78 g/mol with a carbon atom number of 6 to 12 (C_6–C_{12}). The main phenols and their derivatives, such as phenol, 2,4-dimethylphenol, catechol, 4-ethylguaiacol, syringol, and others, have great prospects in the field of fine chemicals and materials. Some of these phenols are mainly collected in Oil-1, such as 2,5-dimethylresorcinol, 4-ethylguaiacol, 4-methylcatechol, and isoeugenol.

However, the pyrolysis steam vapor exhibits a high-speed movement with the carrier gas and it is a mixture of all the compounds so that some compounds cannot be condensed completely at their boiling point [75]. Those phenolics were not completely condensed as Oil-1 but were captured as Oil-2, such as phenol (67.74 wt%), guaiacol (100.00 wt%), 2,4-dimethylphenol (60.57 wt%) and O-cresol (68.95 wt%). The hydroxyl and methoxy functional groups affect the separation that benzenediol and monomethoxy phenols can pass through the whole bio-oil condensing system as vapors. The hydroxyl functional group increases the polarity of benzenediol with a relatively low molecular weight, which also increases the boiling point and water solubility of phenolic compounds. It is easily carried by vapor and condenses in Oil-2 or even Oil-3. These results are consistent with previous works [69, 71]. All the sugars have a high boiling point, from 317 to 675 °C. Levoglucosan, the main product of sugars, is mainly recovered in Oil-1 (72.84 wt%) but was present only slightly in Oil-2 (22.56 wt%) and Oil-3 (4.60 wt%). This indicates that some levoglucosan may exist as an aerosol that keeps the

levoglucosan vapor in the condensation system.

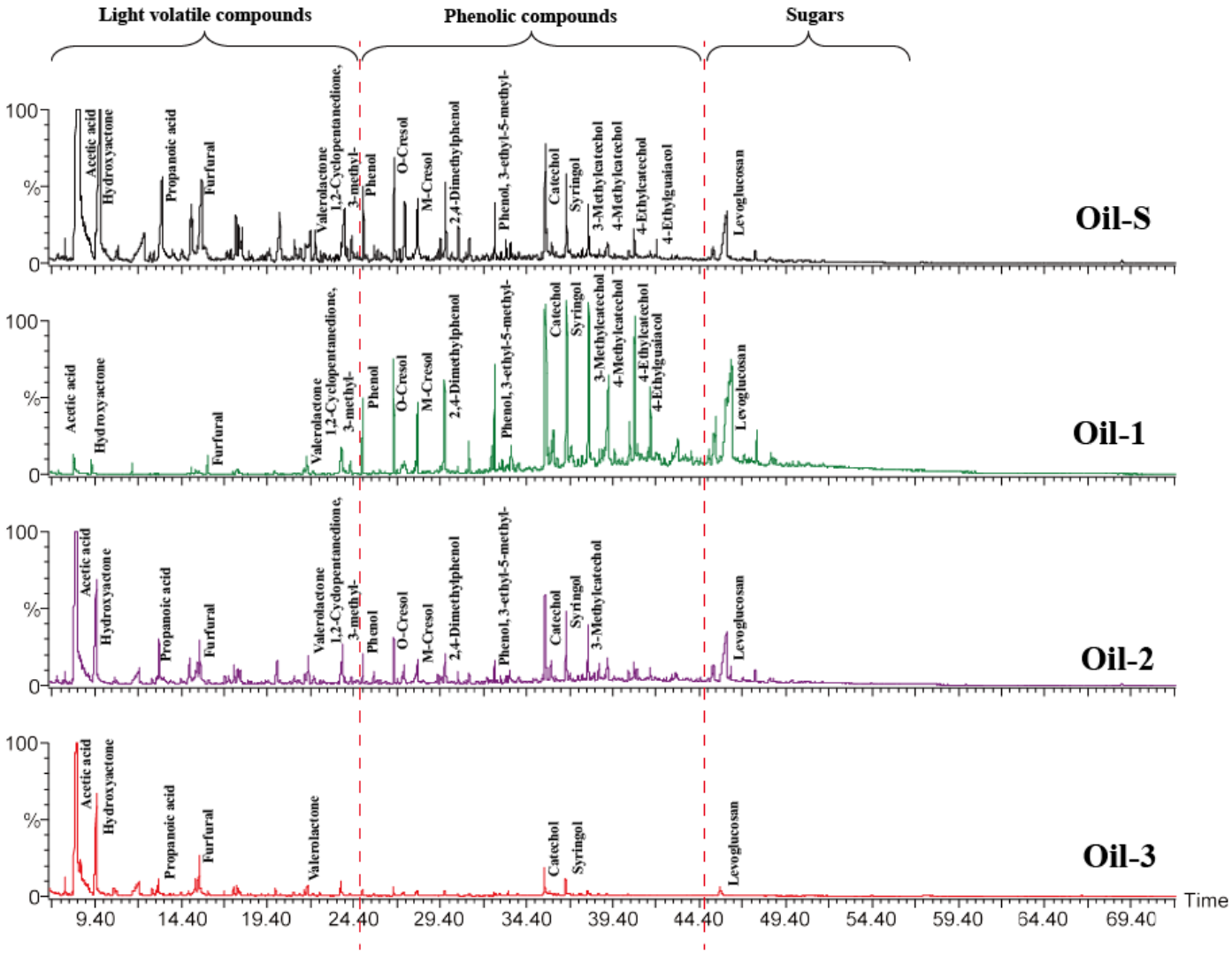

Figure 2. 4 GC-MS chromatograms of bio-oil (Oil-S, Oil-1, Oil-2, and Oil-3) obtained in single and three-stage condensation at temperatures of -11 ºC, 110 ºC, 20 ºC, and -11ºC, respectively.

The bio-oil condensed at 20 °C (Co-2), as a mid-fraction, contains the similar composition to those in Oil-S, except for some high boiling point compounds. Since the condensation process of the pyrolysis steam is not an equilibrium process [71], the pyrolysis vapor will have insufficient condensation in Co-1. Co-2 has a buffering effect on compounds that have a higher boiling point (over 80 °C) but are not recovered in Co-1 due to incomplete condensation [76]. As a consequence of the presence of Co-1, its compounds have a lower boiling point range. Aldehydes including glycolaldehyde (bp 131 °C), and succindialdehyde (bp 145 °C) were mainly lumped in Oil-2. Due to the relatively high boiling point and molecular weight (bp 161 °C and MM 96 g/mol), furfural was collected mainly in condensers 1 and 2. Ketones (such as hydroxyacetone) and a large number of esters and alcohols were found in Oil-2 as well.

Table 2. 3 The amount (g) and yield (wt%) of chemical compounds present in Oil-1, Oil-2, and Oil-3 (Co-1 (110 °C), Co-2 (20 °C), and Co-3 (-11 °C))

Compound	Chemical formula	MM (g/mol)	BP (℃)	Oil-1		Oil-2		Oil-3	
				mass/g	wt%	mass/g	wt%	mass/g	wt%
Carboxylic acids									
Acetic acid	$C_2H_4O_2$	60	118	0.17	2.91	4.69	81.01	0.93	16.08
Propanedioic acid	$C_3H_4O_4$	104	135	-	-	0.15	71.90	0.06	28.10
Propanoic acid	$C_3H_6O_2$	74	141	0.05	7.99	0.47	78.42	0.08	13.58
Esters									
Allyl acetate	$C_5H_8O_2$	100	103	-	-	0.08	81.68	0.02	18.32
Acetic acid, (acetyloxy)-	$C_4H_6O_4$	118	142	-	-	0.20	83.88	0.04	16.12
Pentanoic acid, ethyl ester	$C_7H_{14}O_2$	130	145	-	-	0.05	75.07	0.02	24.93
2(5H)-Furanone	$C_4H_4O_2$	84	204	0.06	45.18	0.06	44.84	0.01	9.98
Valerolactone	$C_4H_6O_2$	86	230	0.11	38.67	0.14	52.20	0.02	9.12
Phenols									
Phenol	C_6H_6O	94	182	0.08	25.20	0.20	67.74	0.02	7.06
O-Cresol	C_7H_8O	108	191	0.09	25.15	0.24	68.95	0.02	5.89
M-Cresol	C_7H_8O	108	202	0.07	33.61	0.12	58.26	0.02	8.13
2,6-Dimethylphenol	$C_8H_{10}O$	122	203	0.09	39.43	0.14	60.57	-	-
2,4-Dimethylphenol	$C_8H_{10}O$	122	210	0.30	53.68	0.23	41.71	0.03	4.60
Phenol, 4-ethyl-2-methyl-	$C_9H_{12}O$	136	223	0.13	63.41	0.07	36.59	-	-
Phenol, 3-ethyl-5-methyl-	$C_9H_{12}O$	136	233	0.09	57.52	0.07	42.48	-	-
Phenol, 4-ethyl-3-methyl-	$C_9H_{12}O$	136	235	0.12	100.00	-	-	-	-
2-Allyl-4-methylphenol	$C_{10}H_{12}O$	148	240	0.12	73.14	0.05	26.86	-	-
3-Methylcatechol	$C_7H_8O_2$	124	241	0.22	76.06	0.07	23.94	-	-
Catechol	$C_6H_6O_2$	110	245	0.21	65.23	0.09	28.56	0.02	6.21
4-Methylcatechol	$C_7H_8O_2$	124	251	0.16	100.00	-	-	-	-
2,5-Dimethylresorcinol	$C_8H_{10}O_2$	138	264	0.22	100.00	-	-	-	-
4-Ethylcatechol	$C_8H_{10}O_2$	138	273	0.16	100.00	-	-	-	-
Methylhydroquinone	$C_7H_8O_2$	124	278	0.11	100.00	-	-	-	-
1,3-Benzenediol, 4-propyl-	$C_9H_{12}O_2$	152	287	0.12	100.00	-	-	-	-
Guaiacols									
Guaiacol	$C_7H_8O_2$	124	205	-	-	0.14	100.00	-	-
Creosol	$C_8H_{10}O_2$	138	221	0.16	63.50	0.09	36.50	-	-
3-Methoxy-2-methylphenol	$C_8H_{10}O_2$	138	234	0.15	62.46	0.09	37.54	-	-
4-Ethylguaiacol	$C_9H_{12}O_2$	152	235	0.16	100.00	-	-	-	-
Syringol	$C_8H_{10}O_3$	154	265	0.32	64.50	0.14	28.88	0.03	6.63
Isoeugenol	$C_9H_{12}O_3$	168	266	0.17	100.00	-	-	-	-
2,4-Dimethoxyphenol	$C_8H_{10}O_3$	154	268	0.14	100.00	-	-	-	-
trans-4-Propenylsyringol	$C_{11}H_{14}O_3$	194	305	0.23	100.00	-	-	-	-
Alcohols									
1-Propanol, 2-methyl-	$C_4H_{10}O$	74	108	-	-	0.08	87.60	0.01	12.40
1,2-Cyclopentanediol, trans-	$C_5H_{10}O_2$	102	136	0.10	40.68	0.11	47.18	0.03	12.14

1,2,4-Butanetriol	$C_4H_{10}O_3$	106	190	-	-	0.13	78.41	0.04	21.59
1,2-Ethanediol	$C_2H_6O_2$	62	198	0.07	56.34	0.04	32.29	0.01	11.36
Aldehydes									
Glycolaldehyde	C_4H_6O	70	131	0.04	6.09	0.65	90.33	0.03	3.57
Succindialdehyde	$C_4H_6O_2$	86	154	-	-	0.18	86.93	0.03	13.07
Furfural	$C_5H_4O_2$	96	161	0.05	26.28	0.13	61.43	0.03	12.29
Ketones									
Hydroxyacetone	$C_3H_6O_2$	74	146	0.05	3.71	1.23	91.68	0.06	4.61
1,2-Cyclopentanedione	$C_8H_{12}O_2$	140	170	0.10	34.08	0.17	55.79	0.03	10.13
1,2-Cyclopentanedione,3-methyl-	$C_6H_8O_2$	112	218	0.13	50.06	0.12	46.07	0.01	3.87
Sugars									
Levoglucosan	$C_6H_{10}O_5$	162	385	2.31	72.84	0.72	22.56	0.15	4.60
d-Mannose	$C_6H_{12}O_6$	180	411	0.36	71.23	0.15	28.77	-	-
Galacto-heptulose	$C_7H_{14}O_7$	210	527	0.35	70.99	0.14	29.01	-	-
Lactose	$C_{12}H_{22}O_{11}$	342	668	0.35	65.43	0.18	34.57	-	-
l-Gala-l-ido-octose	$C_8H_{16}O_8$	240	675	0.65	68.85	0.29	31.15	-	-
Furans									
Furan, 2,5-dimethyl-	$C_6H_{10}O$	98	92	0.09	49.62	0.05	27.21	0.04	23.17
The total mass of oil product				10.17		24.59		7.57	

- represents mass less than 0.01g and mass percentage not calculated.

Acetic acid is the most abundant carboxylic acid in pyrolysis oil (21.71 wt% in Oil-S), with a high contribution of low boiling point and acidity. This separation of acetic acid is effective because only 2.91 wt% of the whole acetic acid accumulates in Oil-1, whereas it represents 81.01 wt% and 16.08 wt% in Oil-2 and Oil-3, respectively.

Oil-3 is a light fraction and consists of small molecular compounds, such as alcohols, carboxylic acids, esters, and aldehydes, which have comparatively low boiling points. 23.17% furan 2,5-dimethyl- with the family group of furans were also present in Oil-3.

These results indicated clearly that the fractional condensers had a major effect on the distribution of the bio-oil compounds and are beneficial to the selection of some specific compounds by controlling the condenser temperature. Oil-1 permits the separation of the relatively high boiling point compounds (bp>180 °C), whereas Oil-2 and Oil-3 have the capability to collect relatively low boiling point compounds (bp< 120 °C). And TGA graph of Oil-1, Oil-2 and Oil-3 also confirmed the previous statement (Appendix **Figure A 1. 4**).

2.3.3.2 Effect of the temperature of the condenser on the composition of liquid product

The distribution of the chemical compounds in each chemical family group when increasing

the temperature of Co-1 is shown in **Table 2. 4**. Some of these families in Oil-1 decrease gradually as the temperature increases: carboxylic acids from 5.76 wt% to 2.18 wt%, where the changes are 62.15 wt%. Moreover, ketones, alcohol, esters and aldehydes also decreased as well. As a consequence, the content of the other family groups in Oil-1 such as sugars, phenols, and guaiacols increases when the temperature of condensation rises. Sugars increased gradually from 35.61 wt% to 47.54 wt%, phenolic compounds increased gradually from 30.37 wt% to 38.03 wt%. The amount of the predominant phenolic compounds in Oil-1 is also illustrated graphically in **Figure 2. 5.** The curves of all products show an upward trend, other than phenol. The polyhydric or methoxy phenols, for example, syringol, 3-methylcatechol, 2,5-dimethylresorcinol, and catechol, have increased significantly, but compounds like 2,4-dimethylphenol with two methyl groups grow slowly and fluctuate. However, 4-ethylguaiacol and isoeugenol have similar changing trends based on their similar structural formula.

Table 2. 4 Effect of Co-1 temperature on the composition of liquid products (Co-2 set as 20 ℃)

Chemical group in bio-oil	wt. % *												
	Oil-S	Oil-1				Oil-2				Oil-3			
		80°C	90°C	100°C	110°C	80°C	90°C	100°C	110°C	80°C	90°C	100°C	110°C
Carboxylic acids	26.12	5.76	3.16	2.74	2.18	44.67	39.10	38.20	36.02	44.84	46.20	50.04	50.37
Esters	6.43	6.49	4.83	4.42	0.48	6.81	7.53	7.44	7.30	7.17	7.47	7.40	6.93
Phenols	14.39	23.43	22.98	24.62	24.76	8.15	9.69	10.79	10.36	8.02	7.67	3.99	4.77
Guaiacols	6.66	6.94	12.31	12.04	13.27	2.76	2.85	2.94	2.97	1.63	1.60	1.55	1.50
Alcohols	6.43	2.48	2.50	1.45	1.57	5.78	5.30	5.18	5.22	8.13	7.48	9.38	10.70
Aldehydes	7.20	5.81	5.79	3.08	2.84	7.32	8.75	7.71	7.98	6.08	5.86	6.02	5.60
Ketones	9.51	10.82	6.69	5.73	6.14	9.29	10.84	13.32	15.40	11.51	10.74	11.56	10.81
Sugars	19.86	35.61	38.89	43.17	47.54	11.95	12.64	11.14	11.45	10.30	10.62	7.73	6.70
Furans	1.31	0.94	0.88	0.84	0.80	1.62	1.60	1.49	1.53	1.55	1.53	1.56	1.84

* The calculation is based on dry matter of oil and neglecting the non-GC-detectable portion of the oil.

The distribution of each chemical family in Co-2 (20 °C) has not changed obviously, except for carboxylic acids. When the Co-1 temperature increases, only the fraction of carboxylic acids decreases from 44.67 wt% to 36.02 wt%, corresponding to a relative change of 19.36 wt%. The families of phenols, guaiacols, ketones, and sugars increase in varying degrees and the distribution of each family are similar to Oil-S. In Co-3, it should be mentioned that carboxylic acids dominate the distribution, and increase from 44.84 wt% to 50.37 wt% as the Co-1 temperature increases. In addition, the content of other families shows a decreasing trend, such as esters, phenols, ketones, and sugars.

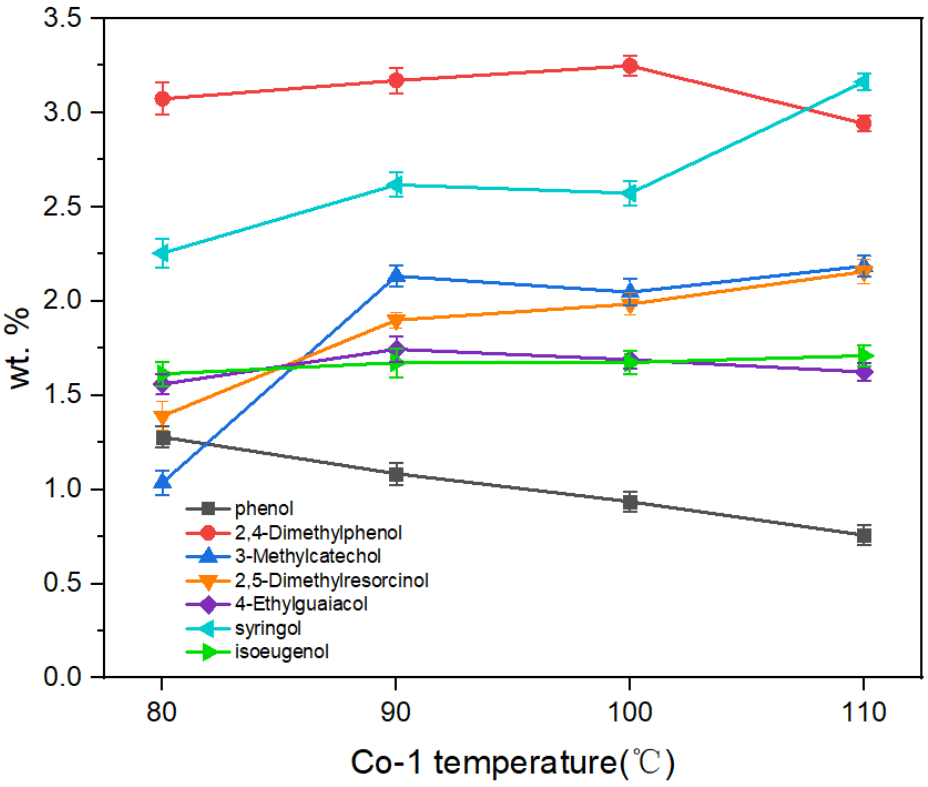

Figure 2. 5 The content of the major phenolic compounds in Oil-1 as a function of Co-1 temperature

Table 2. 5 shows the composition of Oil-1, Oil-2, and Oil-3 as a function of the temperature of intermediate condenser Co-2, which was varied (10, 20 and 30 °C). The distribution of Oil-1 is not affected by the temperature of Co-2. Carboxylic acids, alcohols, and aldehydes diminished in Co-2, whereas other chemical families increased, such as phenols, guaiacols and sugars. This was explained by the fact that the boiling point of phenolic products and sugars was higher than other small volatile compounds. Caused by the wide range of boiling points for ketones and furans, their content in the three condensations always fluctuates slightly, without obvious regularity.

Table 2. 5 Effect of Co-2 temperature on the composition of liquid product (Co-1 set as 100 °C)

The chemical group in bio-oil	wt. %*									
	Oil-S	Oil-1			Oil-2			Oil-3		
		Co-2 temperature (°C)			Co-2 temperature (°C)			Co-2 temperature (°C)		
		10°C	20°C	30°C	10°C	20°C	30°C	10°C	20°C	30°C
Carboxylic acids	26.12	3.21	2.74	2.81	39.05	38.20	34.11	49.90	50.04	50.78
Esters	6.43	5.46	4.42	4.83	7.91	7.44	9.60	7.39	7.40	7.19
Phenols	14.39	24.05	24.62	24.43	9.45	10.79	11.38	4.65	3.99	3.68
Guaiacols	6.66	11.13	12.04	12.73	1.07	2.94	2.86	1.63	1.55	1.57
Alcohols	6.43	2.85	1.45	2.06	8.90	5.18	5.32	9.21	9.38	10.40
Aldehydes	7.20	2.61	3.08	5.13	9.87	7.71	7.36	5.78	6.02	6.46
Ketones	9.51	5.98	5.73	6.83	12.54	13.32	13.88	11.47	11.56	9.81
Sugars	19.86	43.08	43.17	42.85	8.44	11.14	11.90	7.86	7.73	6.98
Furans	1.31	0.62	0.84	0.78	1.53	1.49	1.68	1.46	1.56	2.50

* The calculation is based on dry matter of oil and neglecting the non-GC-detectable portion of the oil.

Unlike changing the temperature of Co-1, the temperature changes of increasing Co-2 are less obvious. There is a huge temperature difference between the cyclone (300 °C) and the following Co-1 (110 °C). According to **Table 2. 3** most chemical compounds have boiling points above 110 °C and some others are close to it. Since the condensation process of the pyrolysis steam is not an equilibrium process [71], the pyrolysis vapor will have insufficient condensation in Co-1.

Hence, changing the temperature of Co-1 has a significant impact on the separation system and product composition. Co-2 has a buffering effect on compounds that have a higher boiling point (over 80 °C) but are not recovered in the first condenser due to incomplete condensation [76]. Globally, a slight difference is observed with the change of the Co-2 temperature from 10 to 30 °C because all the boiling points are above 80 °C. Due to the Co-2 temperature increasing,

Oil-2 yielded less oil but consisted of more heavy compounds. Therefore, it is possible in this kind of way to collect only water, acid and more light chemical compounds in the final stage of condensation.

2.3.4 Additional water extraction

As it has been noted that water solubility has an impact on separation in different fractions, the oil product obtained from different condensers was separated further by adding water. The effect of the proportion of water on the efficiency of separation has been observed. It can be seen that when 70 wt% of water was added, phase separation begins to occur and there is no significant change from adding more water. Vitasari et al. [225] claimed that 50 wt% is a minimum water-to-oil ratio to achieve complete phase separation.

The FTIR spectra with the wavenumber range of 450–4,000 cm^{-1} of WS and WI fractions for Oil-1 and Oil-2 are presented in Fig. 2.6, while the main functional groups are listed in **Table 2. 6**. The wide absorbance band at around 3,338 cm^{-1} is due to O-H stretching (3,300–3,400 cm^{-1}), related to the presence of sugars, alcohols, carboxylic acids, and water in the bio-oil [226]. Its peak intensity of both oil-1 and oil-2 WS fractions increased compared with the WI fraction and proves that there is a large number of sugars, carboxylic acids, alcohols, and water in the WS fractions. The sharp peak at 1,713 cm^{-1}, correlated with carboxylic acids, esters, aldehydes, and ketones [227], is observed in the WS fraction of Oil-1 and Oil-2, whereas its intensity is weaker in the case of the WI fraction.

The peaks around 2,960 cm^{-1} are due to the C-H stretching of aromatics [228] and only appeared in the WI fraction. Alternatively, the peaks observed between 1,650–1,600 cm^{-1} and 1,530–1,430 cm^{-1}, and 1,470–1,350cm^{-1} are attributed to Ph-C=C stretching, C-C stretching of aromatics and symmetric deformation of C-H in methyl families of aromatics, respectively [35]. Assuming the weak concentrations of furans and aldehydes (see Table 2.5), all these peaks are mainly assigned to phenols and guaiacols, and it is obvious that the WI fractions of Oil-1 and Oil-2 have stronger peaks intensities in these regions compared with the WS fractions. The peaks located in the range 1,300–1,030 cm^{-1} are assigned to the C-O stretching and appear in the compounds in the bio-oil as guaiacols, phenols, alcohols, furans, and esters. An intense band at 1,089 cm^{-1} indicates the presence of stretching vibration of C-O-C bands, which may result from guaiacols. Both WI fractions have an obvious peak at this position, but the peak in Oil-1 is stronger than that in Oil-2, which means that the WI fraction of Oil-1 contains more guaiacols.

Some functional groups of phenols and guaiacols are also observed at 900–600 cm^{-1}, which are attributed to O-H bending and aromatic C-H bending and could confirm this hypothesis

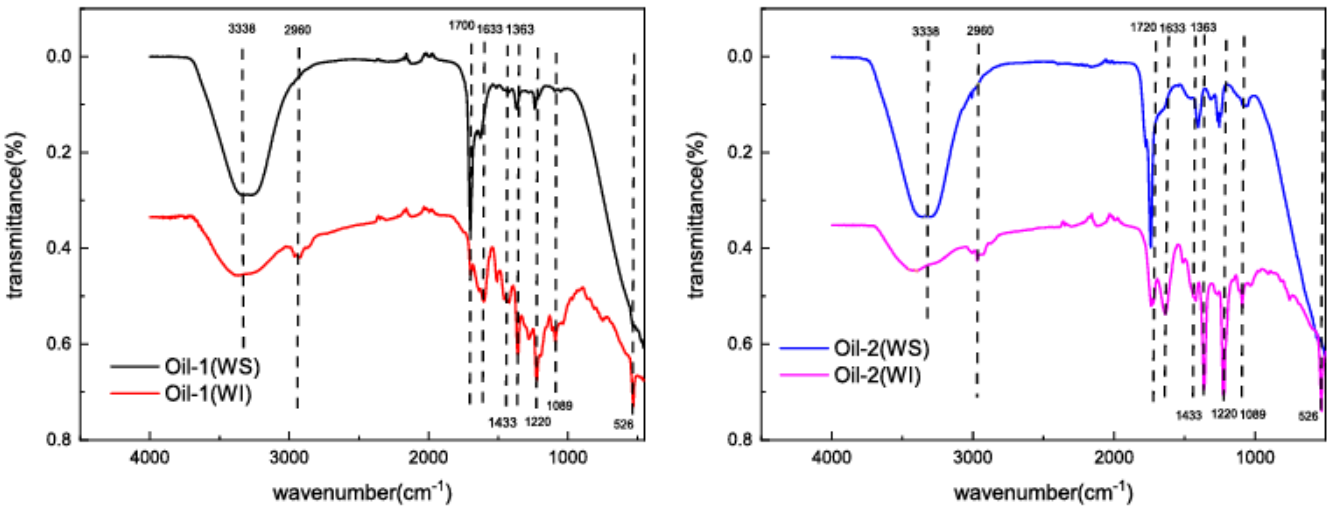

Figure 2. 6 FT-IR spectra of the water-soluble (WS) fraction and the water-insoluble (WI) fraction of Oil-1 and Oil-2

Table 2. 6 Functional group frequencies of the WI and WS samples

Wavenumber/cm^{-1}	Functional families	Compounds
3,400-3,300	O-H stretch	Water, sugars, carboxylic acids, alcohols
2,960-2,850	C-H stretch of aromatics	Phenols, guaiacols, aldehydes, furans
1,780-1,650	C=O stretching vibration	Carboxylic acids, esters, aldehydes, and ketones
1,650-1,600	Aromatic C=C ring, skeletal vibrations, C-O stretching vibrations.	Furans, ketones, phenols, guaiacols, aldehydes, and esters
1,530-1,430	C-C stretch of aromatics	Phenols, guaiacols, aldehydes, furans
1,470-1,350	symmetric deformation of C-H in methyl families of aromatic	Phenols, guaiacols, aldehydes, furans
1,300-1,030	C-O stretch vibration	Guaiacols, phenols, alcohols, furans, esters,
1,000-500	C–H in-plane benching of aromatics	Phenols, guaiacols

Figure 2. 7 shows the weight distribution of chemical families present in the WS and WI fractions of Oil-1 and Oil-2 based on the result of GC-FID. Water extraction upgrading has hugely changed the composition of the chemical families. In Oil-1, some chemical families are more preserved in WI fractions such as phenols (64.77 wt%), guaiacols (68.64 wt%) and furans (74.85 wt%) than in WS fraction. Furan is not detected by chromatography in the case of water fractions. This result shows that most phenolics compounds and furans are poorly soluble in water. The major families of Oil-1 in WS fraction include carboxylic acids, esters, alcohols, aldehydes, and sugars. In particular, 74.99 wt% and.77.17 wt% of carboxylic acids sugars can be found in the WS fraction respectively because of the large water solubility of acids and sugars in water.

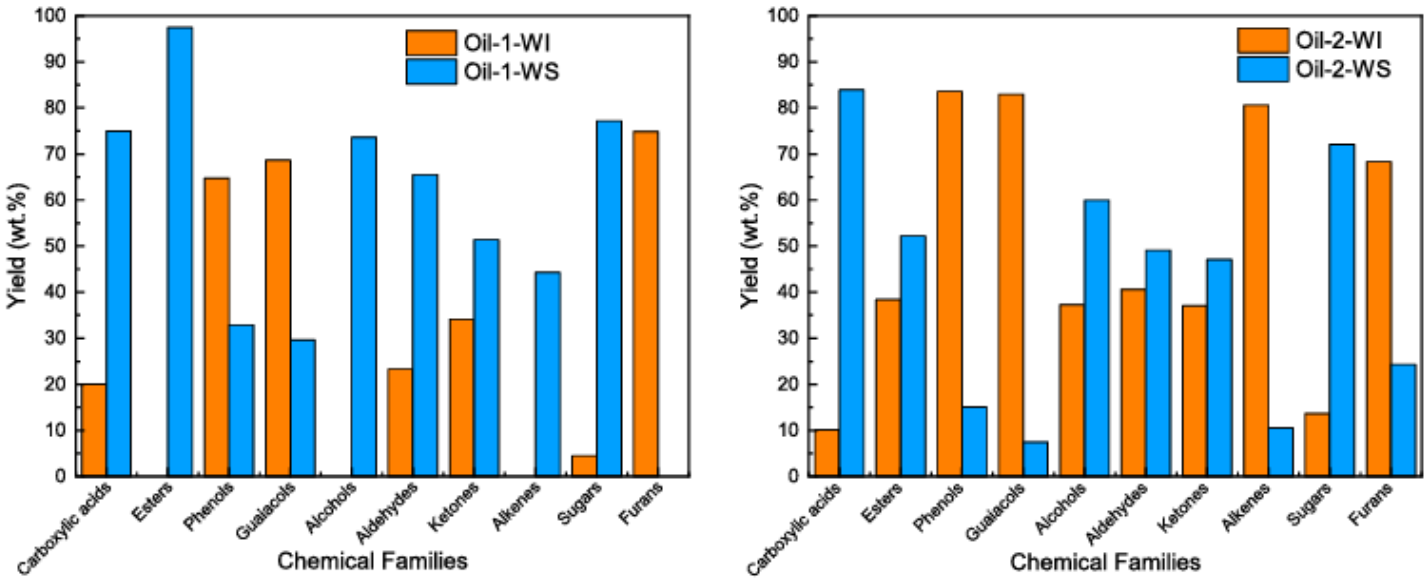

Figure 2. 7 The weight distribution of chemical families presented in the water-soluble (WS) fraction and the water-insoluble fraction (WI) concerning oil-1 (left) and oil-2 (right).

Concerning Oil-2, carboxylic acids have the largest change among all the family groups in the chemical composition. Indeed, 83.88 wt% have been recovered in the WS fraction. As observed in Oil-1, sugar is mainly present in the WS fraction (72.03 wt%) whereas the major family groups in the WI fraction are phenols (83.56 wt%), guaiacols (82.95 wt%), and furans (68.32 wt%). Regarding the chemical families of esters, alcohols, aldehydes, and ketones, which are selectively soluble in water, their overall mass distribution in the WS fraction is higher than in WI fraction.

According to the results from GC, it appears that the extraction capability can be denoted as a distribution ratio of a particular component (Di) defined as the ratio of the equilibrium mass

fraction of that component in the aqueous extract phase (Xi.aq) and the organic raffinate phase (Xi.org) [225]. The higher the value Di is, the more hydrophilic it is

$$Di = Xi.aq/Xi.org$$

Equation 2. 1

The results are shown in Table 2. 7, for some representative compounds from each family. Carboxylic acids in bio-oil products have a high extraction capability in water, especially for acetic acid (Di = 3.39 in Oil-2). As representatives of aldehydes, glycolaldehyde, and succindialdehyde, relied on the strong polarity because of their C=O function, and have their Di values superior to 1, whereas furfural has a Di value inferior to 1 due to its furan ring. Hydroxyacetone, 1,2-cyclopentanedione, and 1,2-cyclopentanedione, 3-methyl- are the main ketones in the pyrolysis oil. With the contribution of the hydroxyl group, hydroxyacetone has a higher Di value than the other two ketones, and the Di value of 1,2-cyclopentanedione, 3-methyl- is smaller relating to its additional methyl group. Most esters are slightly soluble in water, but valerolactone and 2(5H)-furanone have a strong extraction capability in water due to their internal lactone structure.

The yield of phenols and guaiacols in both Oil-1, WS and WI fractions showed that most of them remain in the WI fraction as same as reported in the literature [226]. The number and type of substituents on the benzene ring of phenolic compounds are important factors affecting its performance on the extraction capacity. In Oil-1, the Di value of this group follows the rank, 4-ethylcatechol < 2,5-dimethylresorcinol < methylhydroquinone < 3-methylcatechol < catechol, owing to the number of alkyl groups and the chain length. For phenols with one or two hydroxyl groups, the highly polar hydroxyl groups make them have good water solubility. For instance, in phenols that have one or two alkyl groups like O-cresol, M-cresol, and 2,4-dimethylphenol, the additional methyl on the benzene ring increases their hydrophobicity and the Di value decreases. Since alkyl (methyl or ethyl) groups are hydrophobic groups and they can prevent interactions between the hydroxyl groups on the monophenols with water and reduce the water solubility of the compound [224]. In Oil-2, the Di value of catechol is the largest in the phenol group and 3-methylcatechol has a lower Di value than it due to an extra methyl group. Guaiacols have at least one methoxy group and even an alkyl group. With the increase of these hydrophobic functional groups, the structure becomes more complex, the steric hindrance increases, and consequently, the water solubility becomes worse.

Table 2. 7 weight ratio of chemical compounds collected in the WS and WI fractions from Oil-1 and Oil-2 and the associated distribution ratio (Di)

Compound	Oil-1			Oil-2			Compound	Oil-1			Oil-2		
	WI	WS	Di	WI	WS	Di		WI	WS	Di	WI	WS	Di
	wt%	wt%		wt%	wt%			wt%	wt%		wt%	wt%	
Acetic acid	28.15	71.85	2.55	22.77	77.23	3.39	Phenol	61.03	38.97	0.64	60.19	39.81	0.66
Propanoic acid	28.94	71.06	2.46	20.79	79.21	3.81	O-Cresol	68.48	31.52	0.46	68.37	31.63	0.46
Pentanoic acid. ethyl ester	-	-	/	18.26	81.74	4.48	M-Cresol	58.66	41.34	0.70	64.57	35.43	0.55
Levoglucosan	14.13	85.87	6.07	17.30	82.70	4.78	2.4-Dimethylphenol	71.36	28.64	0.40	78.25	21.75	0.28
Valerolactone	-	100	/	38.95	61.05	1.57	3-Methylcatechol	60.22	39.78	0.66	65.22	34.78	0.53
2(5H)-Furanone	-	100	/	47.15	52.85	1.12	Catechol	52.41	47.59	0.91	58.02	41.98	0.72
Hydroxyacetone	14.74	85.26	5.78	15.43	84.57	5.48	2,5-Dimethylresorcinol	63.04	36.96	0.59	-	-	/
Furan, 2,5-dimethyl-	100	-	0	63.96	36.04	0.56	4-Ethylcatechol	67.97	32.03	0.47	-	-	/
Glycolaldehyde	39.22	60.78	1.55	15.04	84.96	5.65	Methylhydroquinone	63.93	36.07	0.56	-	-	/
Succindialdehyde	36.80	63.20	1.72	38.76	61.24	1.58	4-Ethylguaiacol	70.11	29.89	0.43	-	-	/
Furfural	57.35	42.65	0.74	57.72	42.28	0.73	Syringol	69.10	30.90	0.45	71.43	28.57	0.40
1,2-Cyclopentanedione	59.30	40.70	0.67	61.04	38.96	0.64	Isoeugenol	71.68	28.32	0.40	-	-	/
1,2-Cyclopentanedione, 3-methyl-	61.13	38.87	0.64	60.98	39.02	0.64	trans-4-Propenylsyringol	74.98	25.02	0.33	-	-	/

- represents non-detectable

/ represents can not calculate

The extraction capability seems to depend on polarity and solubility. Polar compounds move to the aqueous phase while non-polar ones remain in the organic phase. Since water is a polar solvent and has a symmetrical molecular structure, theoretically the more polar and the more symmetrical compounds are the most soluble in water. The polarity ranking of the functional groups increases as follows: alkanes < ethers < esters < ketones < aldehydes < alcohols < phenols < carboxylic acids. This ranking is applied to compounds with a single functional

group. However, the polarity of complex bio-based compounds with multiple functional groups is affected in many ways. According to the data from the Hansen solubility parameters [229], the order of polarity is 2(5H)-furanone < acetic acid < levoglucosan <hydroxyacetone < furfural. Although levoglucosan is not as polar as furfural and hydroxyacetone, it has a better water extraction capability because of a weak hydrogen bond interaction between levoglucosan and water.

For the same compound, the value of Di can vary between Oil-1 and Oil-2. The distribution of each family in Oil-1 and Oil-2 obtained through fractional condensation is different leading to the different concentrations of each chemical component. The initial concentrations and composition of the oil products seem to influence the extraction capability. In the case of levoglucosan, its value of Di of Oil-1 (6.07) is higher than Oil-2 (4.78) because levoglucosan has a different initial concentration in the WS fraction (47.54 wt% in Oil-1, 11.45 wt% in Oil-2).

2.3.5 Global efficiency of the combination of both upgrading methods

The recovery yield of each chemical family in variations bio-oil fraction by using both separation methods successively are shown in **Figure 2. 8**. The yield is not 100% due to the loss by the process of water evaporation and the undetectable of GC chromatography. Most chemical families can be unequally separated in several specific bio-oil fractions. Carboxylic acids are mainly presented in Oil-2-WS (67.80 wt%), whereas only 1.33 wt% of them were collected in Oil-1-WI. Due to the hydrophilic nature of sugars, they are more likely to be collected in water-soluble fractions (74.12 wt%), especially in Oil-1-WS with a sugar yield up to 55.10 wt%. Totally 70.59 wt% of phenolic compounds were collected in water-insoluble fractions, of which 42.09 wt% in Oil-1-WI. Moreover, there are some families whose content is drastically reduced in certain bio-oil fractions to be undetectable. For example, esters and alcohols cannot be detected in Oil-1-WI and furans disappeared in the Oil-1-WS.

By observing the distribution of bio-oil fractions in **Figure 2. 9**, it is clear that additional separation is effective to obtain fractions concentrated with chemical families. Oil-1-WI and oil-2-WI to a lesser extent are mainly composed of phenolic compounds (guaiacol and phenol). Sugars are a major family of Oil-1-WS. After both steps separation, Oil-2 WS has a chemical close to Oil-3. Regardless of Oil-3, recovery yield using fractional condensation is weak. Carboxylic acids represent the largest content of this fraction as water is mainly recovered in

the third condensers, in which the solubility and low boiling point of carboxylic acids promote the recuperation. The other chemical families occupy a small part of this fraction.

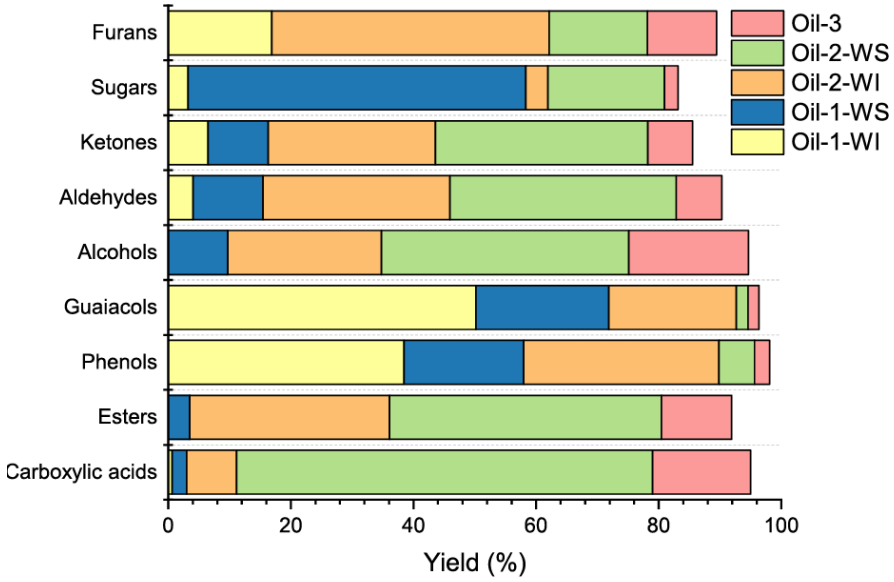

Figure 2. 9 The yield of chemical families presented in bio-oil fractions by the combination of two methods

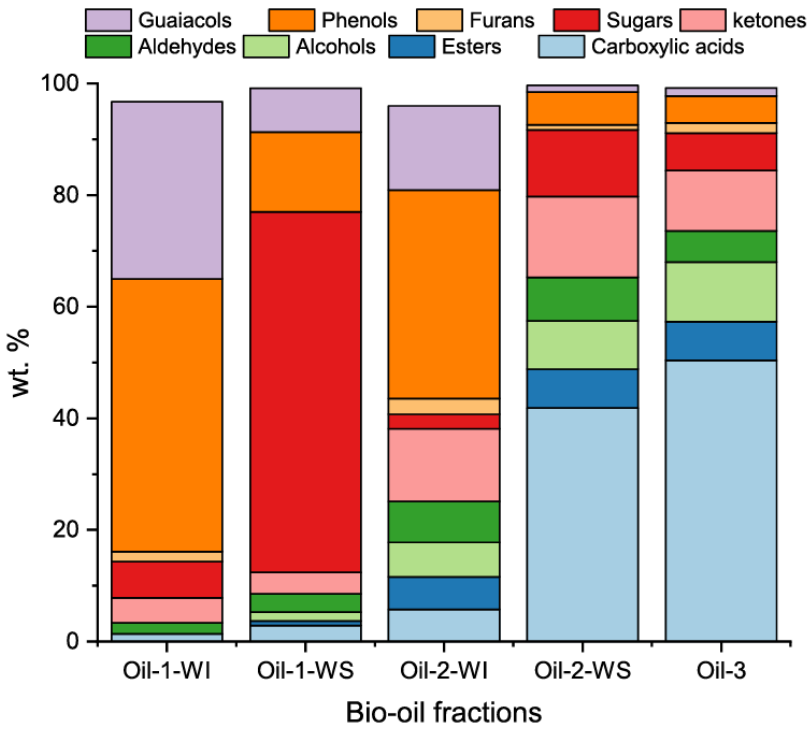

Figure 2. 8 The distribution of bio-oil fractions

2.4 Conclusion

Combining fractional condensation and water extraction has been proven to be an efficient and interesting method for the separation and purification of bio-oil due to both the dew points and the solubility in water of chemical compounds.

Compared with the single-stage condensation, a significant difference in the physicochemical properties of the bio-oil is noticed when using the three-stage condensation system. Water is mainly recovered in the second and the third condensers, in which the solubility and low boiling point of carboxylic acids promote the recuperation. Phenolic compounds and sugars are mainly found in the first condenser (63.54 wt% and 71.41 wt%, respectively). An increase in the first condenser temperature promotes the selectivity for sugars and phenolic compounds in Oil-1 to 33.52 wt% and 25.21 wt% respectively. Unlike changing the temperature of Co-1, the increase in temperature of the second condenser Co-2 induces a slightly higher selectivity for carboxylic acids, alcohols, and aldehydes in the third condenser.

The effect of additional separation of bio-oil by water was more beneficial for the fraction of the first condenser. Sugars can be separated efficiently in the WS fraction (74.12 wt%), whereas phenolics remain in the WI fractions (70.59 wt%). In the second condenser, carboxylic acids are in the majority present in the WS fractions (67.80 wt% in Oil-2-WS), allowing the acidity of the WI fractions to be reduced.

Chapter III

Investigation of the improvement of the storage stability of pyrolysis bio-oil

Abstract:

Many researchers have been working on the storage stability of bio-oils, especially bio-oil obtained by one-step pyrolysis [97, 98]. Few studies have focused on the stability of fractional condensation bio-oil and its water extraction fractions.

The bio-oil products resulting from the single and three-stage condensers (temperature set at 110 ℃, 20 ℃, and -11 ℃) and their water extraction fractions studied in chapter 1 will be used to investigate the stability. The bio-oil stability was evaluated by comparing the physicochemical and compositional variation of aged bio-oils to that of fresh bio-oil and between aged bio-oils recovered from different condensers. The objective was to assess the effects of different storage temperatures (4 ℃, room temperature-18 ℃, and 50 °C) and different storage times (1, 2, 3, and 4 weeks) on the bio-oil products obtained from fractional condensation and their water extraction fractions during aging.

A part of this study has been published in the article: Xu J, Brodu N, Abdelouahed L, Taouk B. Investigation of the combination of fractional condensation and water extraction for improving the storage stability of pyrolysis bio-oil. Fuel 2022;314. 10.1016/j.fuel.2021.123019.

3.1 Introduction

Based on the improvement in the bio-oil composition using upgrading methods, storage and transportation stability are also important characteristics that hinder the successful use of bio-oil for fuel, chemicals, and power production [90]. During storage, bio-oil can undergo various kinds of changes in its chemical and physical properties, such as phase separation, viscosity increase leading to an increase in molecular weight, and change in water content [90]. Otherwise, it is speculated that the stability of the water extraction fractions will be affected significantly [230].

The storage temperature can determine whether the polymerization reaction will take place and the extent of the reaction. Moreover, accelerating aging by storing bio-oil at high temperatures for a short time can predict the possible changes in bio-oil during long-term storage at room temperature [231]. Therefore, it is very important to set an appropriate aging temperature to study the effect of storage time on the changes of each bio-oil product. It will help us to know the probable polymerization reactions of the water extraction fractions of fractional condensation pyrolysis oil.

3.2 Materials and methods

3.2.1 Materials

The bio-oil products resulting from the single and three-stage condensers (Oil-S, Oil-1, Oil-2, and Oil-3) and the water-insoluble fractions (Oil-S-WI, Oil-1-WI and Oil-2-WI) were obtained according to the method described in **Chapter II**.

3.2.2 Aging method

Figure 3. 1 illustrates the experimental procedure. The pre-weighed fresh bio-oil (about 10 g) and water extraction samples (about 2 g) were placed in sealed glass bottles, and the gap between the cap and the bottle was sealed with PTFE thread seal tape, then put in polypropylene sealed bags. All bio-oil products are uniformly mixed without phase separation before aging. The bio-oil samples were stored at different aging temperatures (4 °C, room temperature [18 °C], 50 °C) for 1, 2, 3, and 4 weeks. An accelerated stability study has been done for 4 weeks using a temperature of 50 °C that would correspond to the storage of 1 year at room temperature [232]. After the storage period, the weight of the aged bio-oil was measured to determine the loss of volatile compounds during storage. In each case, the weight loss of the aged bio-oil was less

than 1.0 wt%. The variations in certain pivotal physicochemical parameters were measured, and the composition of organic compounds was analyzed before and after storage.

The aging index of each property was calculated by following **Equation 3. 1**, where P stands for a particular property of bio-oil [97]. All the aging experiments were repeated three times, the experimental repetitive errors were reported and average values were calculated. In addition, the aging index was calculated by the average value of each property.

$$\text{Aging index} = (P_{\text{aged-sample}} - P_{\text{fresh-sample}}) / P_{\text{fresh-sample}} * 100\%$$

Equation 3. 1

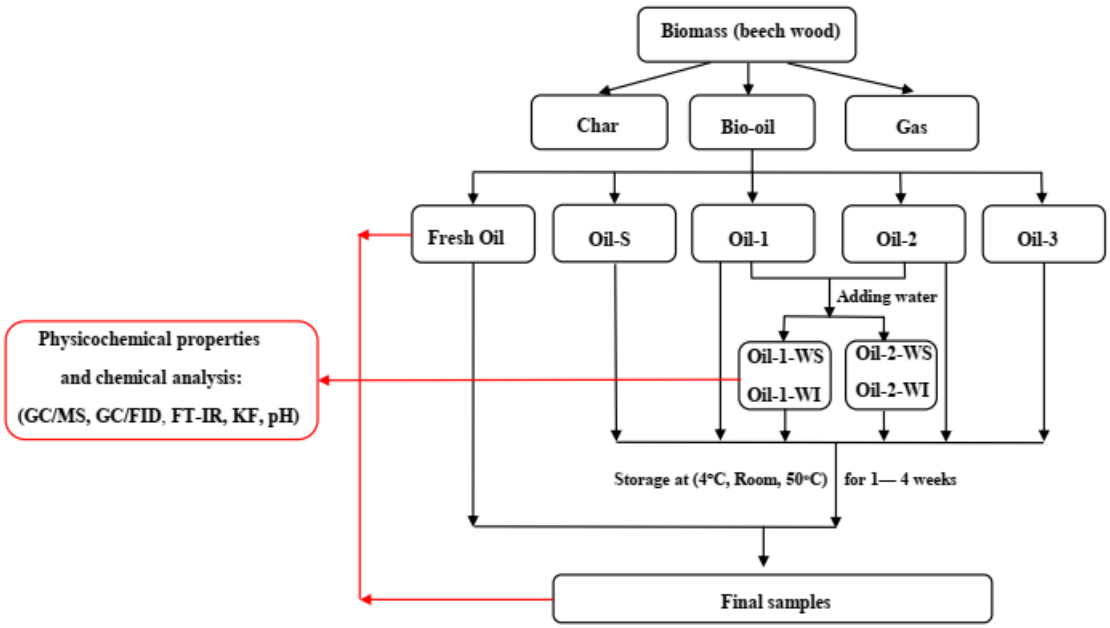

Figure 3. 1 Overview of the experimental procedure

3.2.3 Analytical methods

3.2.3.1 Organic components

The identification and quantification of organic compounds were carried out using GC-MS and GC-FID, respectively. Attenuated total reflectance-Fourier transform infrared spectroscopy (ATR-FTIR) was used to analyze the organic functional groups present in the bio-oil samples before and after aging. The details of each analytic method have been discussed in Chapter II (**2.2.4**).

3.2.3.2 pH and water content

The water content was measured using Karl Fischer (KF) titration method (Refer to Chapter II, section **2.2.4.2**).

The pH of the bio-oil samples before and after aging was determined by a Cole-Parmer P200-02 pH Meter Kit. It was calibrated by using buffer solutions of pH (4, 7, and 10) to ensure reliability in the measurements.

3.2.3.3 TGA

The thermal stability of bio-oil samples was analyzed by using TGA (TA Instrument ExplorerQ600). 5 to 10 mg sample was placed in a ceramic crucible under a 50 mL/min nitrogen flow. The char sample was then heated up to 900°C with a heating rate of 10 °C/min.

3.3 Experimental results and discussion

3.3.1 The effect of aging temperature on fractional condensation bio-oil products

3.3.1.1 Physicochemical properties of aged bio-oil

Analysis results of water content and pH values are powerful pieces of information to assist in understanding the effect of temperature changes. **Table 3. 1** shows the water content and pH values of the bio-oil stored for 4 weeks at various temperatures (4 °C, room temperature, and 50 °C). The water content values of the four bio-oil samples before and after aging decrease as follows: Oil-3 > Oil-S > Oil-2 > Oil-1. The water in the bio-oil comes from the original moisture of the feedstock (7.44 wt%) and is the by-product of dehydration reactions during biomass pyrolysis. During storage of bio-oil, water can also be produced through aging reactions, mainly from the esterification of acids and alcohols, polycondensation reaction of aldehydes and alcohols, as well as polycondensation reaction of aldehydes and phenolics [91, 98].

The pH measurement is a rapid method for determining the acidity level of pyrolysis liquids [233]. The ranking of the pH values of fresh oil is Oil-1 > Oil-S > Oil-2 > Oil-3, and the same ranking was obtained after 4 weeks of age at 50 °C. Therefore, all the pH values of the oil products decreased, which is consistent with the results of other researchers [234, 235].

The aging index in water content and pH after storage are shown in **Figure 3. 2**. When the oil was stored at 4 °C for 4 weeks, the value was less than 1%. There was only a slight change when the oil was stored at room temperature, and at 50 °C, the aging produced a significant change in the physical properties. Among each bio-oil fraction, Oil-1 had the slowest decline rate in each temperature environment.

Table 3. 1 Water content and pH values of different oil samples at different aging temperatures after 4 weeks

Property	Bio-oil	Pre-age	Aging temperature		
			4 °C	Room temperature	50°C
Water content wt%	Oil-S	33.33 ± 1.21	33.35 ±0.89	33.80 ±0.75	35.33 ±1.19
	Oil-1	1.44 ± 0.20	1.44 ±0.52	1.45 ±0.33	1.48 ±0.11
	Oil-2	37.37 ± 1.51	37.38 ±1.02	37.57 ±0.77	38.91 ±0.60
	Oil-3	71.22 ± 1.10	71.26 ±0.11	71.69 ±0.82	76.81 ±0.61
pH	Oil-S	4.05 ±0.01	4.01 ±0.05	3.99 ±0.02	3.89 ±0.01
	Oil-1	4.26 ±0.03	4.26 ±0.03	4.24 ±0.01	4.19 ±0.02
	Oil-2	2.46 ±0.02	2.44 ±0.01	2.40 ±0.00	2.35 ±0.01
	Oil-3	2.43 ±0.01	2.42 ±0.01	2.41 ±0.02	2.32 ±0.01

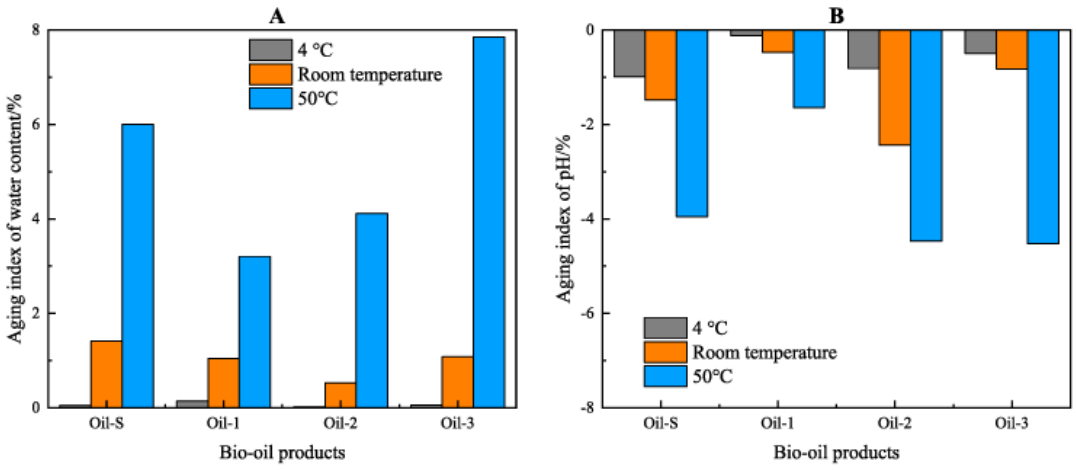

Figure 3. 2 The aging index of (A)water content and (B) pH value of 4 weeks aged bio-oil products at various aging temperatures (4 °C, room temperature, 50 °C)

3.3.1.2 FTIR analysis

FTIR spectra with the wavenumber range of 4,000–500 cm^{-1} are presented in **Figure 3. 3.** The O-H stretching indicates the presence of water, alcohols, phenols, organic acids, and other hydroxyl groups [236, 237]. Herein, the peaks of the broad O-H stretching vibration of all the aged bio-oil samples increased in intensity, whereas the changes in the samples aged at 4 °C and room temperature were smaller than the changes at 50 °C. The enhancement of the transmittance peak is relatively small in the case of Oil-1. These changes can be attributed to the increase in water and acid content during aging, as mentioned above.

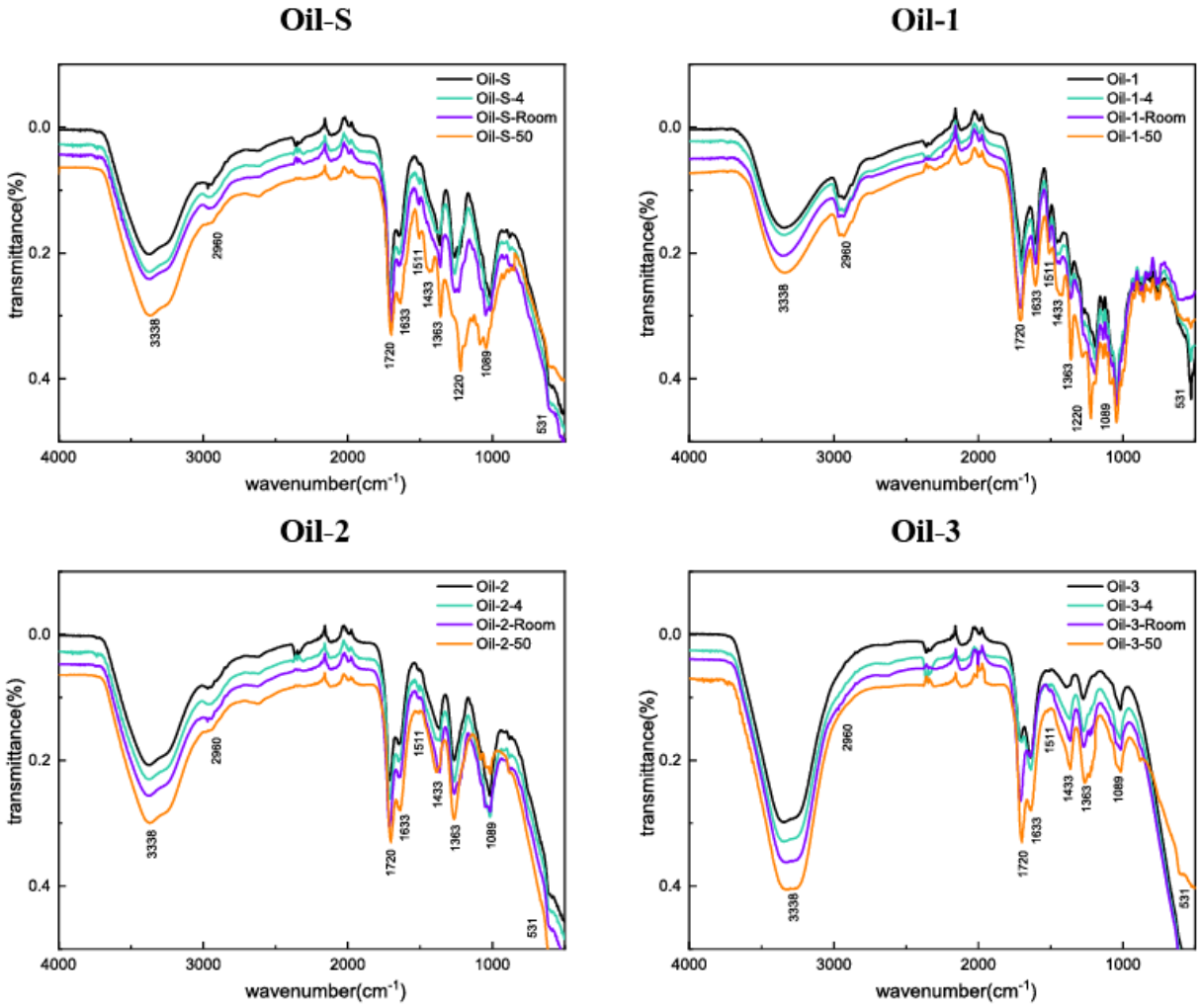

Figure 3. 3 FITR spectra of pre-aging and post-aging bio-oil products at aging temperatures of 4 °C, room temperature, and 50 °C stored for 4 weeks

The C=O stretching vibration, indicates the presence of carboxylic acids, aldehydes, ketones, and esters. After aging at 50 °C, the peak of the carbonyl group (1,780–1,630 cm^{-1}) of the aged bio-oils was much higher than before aging. In particular, the peak intensity of Oil-3 increased

significantly, which is mainly due to the decomposition of sugars to form carboxylic acids during aging.

Alternatively, for all the products, no obvious intensity change was observed for the peak of the C-C stretch of aromatics. An increase in the peak of the symmetric deformation of C-H in the methyl families of aromatics simultaneously occurred, which means that more and more unsaturated bonds of aromatic hydrocarbons were oxidized into saturated bonds. Among them, the higher absorbance at 1,220 cm^{-1} (C-O-C stretching) and the lower absorbance at 1,089 cm^{-1} (C-O-H stretching) suggest the formation of ethers or esters in the bio-oils during aging, producing water as a by-product [235]. An increase in the peak of C-O-C stretching is detected when bio-oil products are aged at 50 °C.

According to the results of FTIR, an increase in the concentration of carbonyl, ester, and ether families of aging bio-oils is associated with oxidation. Unlike the notable change in Oil-S and Oil-3, Oil-1 demonstrates high stability, confirming that fractional condensation helps improve the bio-oil stability.

3.3.1.3 Chemical composition by GC-MS and GC-FID

The pre-aging and post-aging oil product analysis methods require the combination of the analytical data of GC-MS and GC-FID. Thanks to GC-MS analysis, 270, 106, 139, and 97 compounds have been identified for Oil-S, Oil-1, Oil-2, and Oil-3 samples, respectively. All the compounds were grouped into 11 major chemical families, and the calibration curve of the reference compounds was used for the quantification [7].

Figure 3. 4 shows the changes in the content of some chemical families in bio-oils at different aging temperatures (4 °C, room temperature, and 50 °C) after 4 weeks. To see clearly, the aging index of the content of chemical families of pre-aging and post-aging bio-oil products were shown in **Figure 3. 5**. Compared to the fresh oil, the content of the aged bio-oil stored at 4 °C has almost no change. A slight change is observed when bio-oil is stored at room temperature.

The yield of carboxylic acids, esters, and furans families increases during aging, while the other chemical families (such as phenols, guaiacols, alcohols, aldehydes, ketones, and sugars) decrease with aging. Regarding aging at 50 °C, the trends of chemical change in the families are similar to those observed at room temperature, but the yield differences compared to fresh bio-oil are more significant. Additionally, the content of esters undergoes obvious changes at

this temperature compared to other aging temperatures, especially for Oil-3. It indicates that the esterification reaction, which also produces water as a by-product as well as the decomposition reaction of levoglucosan, are more likely to happen above 50 ℃

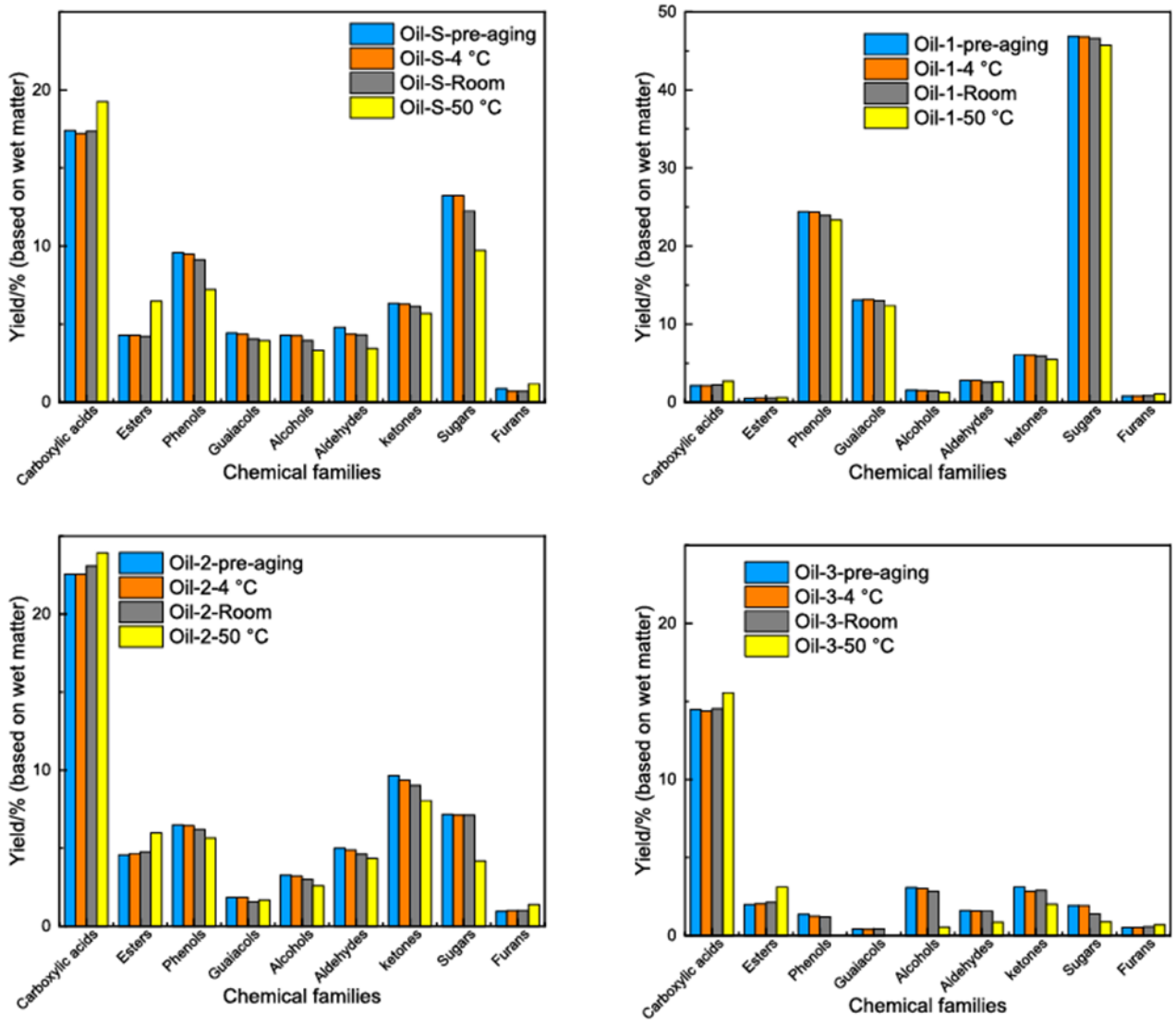

Figure 3. 4 Variations in the yield of chemical families of pre-aging and post-aging bio-oil products (Oil-S, Oil-1, Oil-2, and Oil-3) at various aging temperatures (4 °C, room temperature, and 50 °C) stored for 4 weeks (Average of triplicate runs with standard deviation < 3%.)

It can be concluded that all products stored at 4 °C and room temperature have high stability and can withstand the most severe aging process, whereas the bio-oils aging at 50 °C change significantly. Among them, Oil-1 has relatively high stability at 50 °C, which can be explained by the fact that Oil-1 has the lowest acid content and aliphatic compounds compared to other bio-oil products. Besides, Oil-S, Oil-2, and Oil-3 are not stable as Oil-1 due to their excessive content of acid and the carbonyl group compounds. Also, one can conclude that separating into

three fractions leads to less abrupt changes than a bio-oil even at 50°C, which can correspond to 1 year at room temperature.

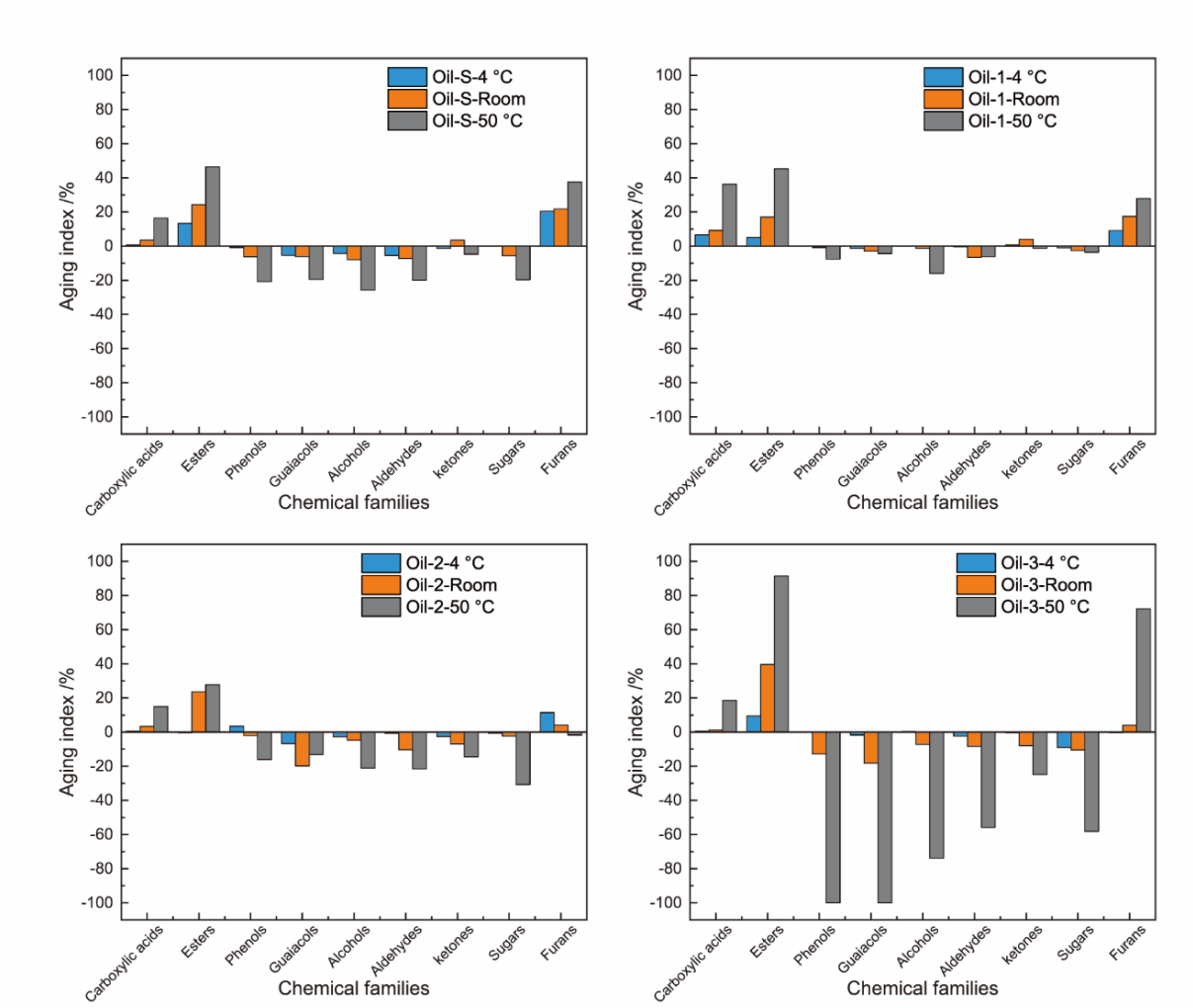

Figure 3. 5 Aging index of the content of chemical families of pre-aging and post-aging bio-oil products (Oil-S, Oil-1, Oil-2, and Oil-3) at various aging temperatures (4 °C, room temperature, 50°C) stored for 4 weeks

3.3.2 Accelerated aging of fractional condensation bio-oil products

3.3.2.1 Physicochemical properties of the aged bio-oil effect of aging time

The reaction mechanisms of different bio-oil fractions during accelerated aging were studied. **Table 3. 2** shows the variation in water content values of different fractions with aging time when the temperature was set as 50 °C. The aging index in water content after 4 weeks of storage is shown in **Figure 3. 6**. Regardless of the various bio-oil fractions, the water content increased gradually as the storage time increased. It should also be pointed out that, according to the aging index of water content, Oil-1 produces less water during aging. Wang et al. [238] stored bio-oil at 20 °C and indicated that aliphatic compounds with small molecular weights

participate more easily in esterification, cyclization, and polycondensation reactions to produce water. They also found that moisture growth was fast in the first 15 days. The same behavior was also observed in this study, during four weeks of aging time, the water was produced quickly in the first three weeks, then gradually slowed down in the last week. Concerning physical properties, the change in pH follows a similar trend as the water change for all fractions. The decrease in pH is probably due to the oxidation of organic components, forming carboxylic acids. The latter compound is a proton donor in the aqueous phase, increasing the acidity of the oil. The effect of aging time was discussed based on the changes in the physical and chemical composition of different bio-oil fractions when the aging temperature is fixed at 50 °C.

According to the aging index in pH shown in **Figure 3. 6**, regardless of chemical composition, the content of the major compounds from the pre-aging (Oil-1, Oil-2, and Oil-3) and post-aging oil have been listed to measure the changes (shown in the appendix). Oil-1 has the slowest decline rate in these bio-oil samples. The pH decreases during the aging process, indicating that the organic components are easily oxidized to form carboxylic acids. The latter compound dissociates in an aqueous phase and becomes a proton donor, increasing the acidity of the oil. Besides, the acidic environment may promote many aging reactions, such as esterification, etherification, and polymerization. Overall, Oil-1 has a relatively low aging index in both water content value and pH value, which demonstrates the excellent performance of Oil-1 in storage, even at 50 °C.

Table 3. 2 Water content and pH values at different aging times (aging at 50 °C)

Property	Bio-oil	Pre-age	Aging time			
			1 week	2 weeks	3 weeks	4 weeks
Water content wt%	Oil-S	33.33 ± 1.21	34.36 ± 1.03	34.93 ± 1.11	35.16 ± 0.79	35.33 ±1.19
	Oil-1	1.44 ± 0.20	1.46 ± 0.23	1.47 ± 0.34	1.48 ± 0.11	1.48 ±0.11
	Oil-2	37.37 ± 1.51	38.55 ± 0.78	38.79 ± 0.52	38.86 ± 1.16	38.91 ±0.60
	Oil-3	71.22 ± 1.10	73.99 ± 0.50	74.86 ± 0.90	76.27 ± 1.30	76.81 ±0.61
pH	Oil-S	4.05 ±0.01	3.98 ±0.01	3.95 ±0.01	3.90 ±0.01	3.89 ±0.01
	Oil-1	4.26 ±0.03	4.23 ±0.01	4.23 ±0.02	4.20 ±0.01	4.19 ±0.02
	Oil-2	2.46 ±0.02	2.42 ±0.01	2.39 ±0.01	2.36 ±0.01	2.35 ±0.01
	Oil-3	2.43 ±0.01	2.37 ±0.01	2.35 ±0.01	2.33 ±0.02	2.32 ±0.01

After 4 weeks of aging at 50 °C, chemical families like phenols, guaiacols, alcohols, aldehydes, sugars, and ketones decrease with increasing time, probably due to some reactions, such as esterification, hydrolysis, and condensation. Furans and carboxylic acids increase due to the hydrolysis of sugars.

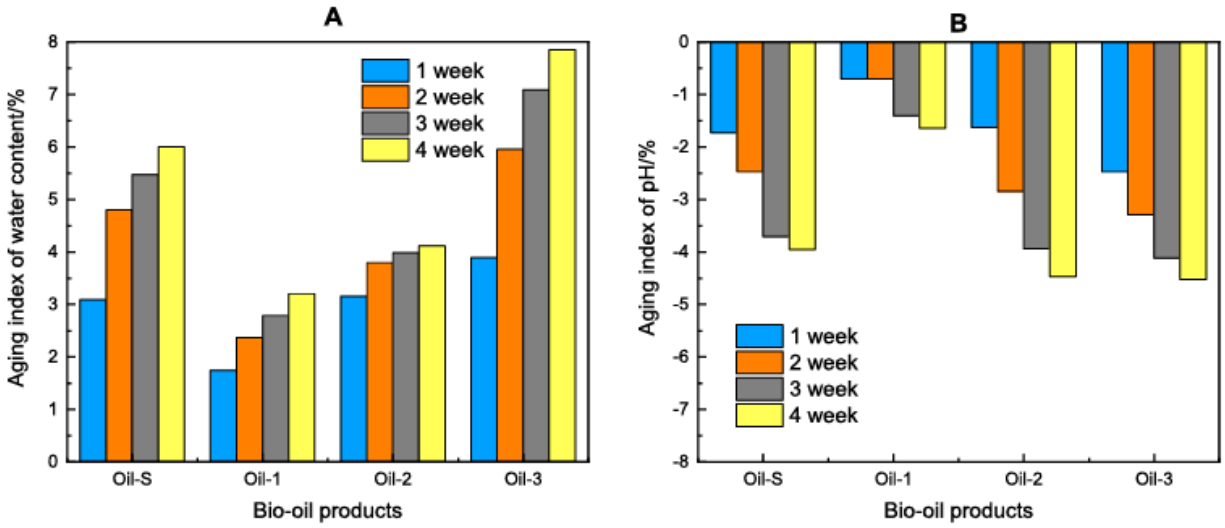

Figure 3. 6 The aging index in (A) water content and (B) pH value of bio-oil products aged at 50 °C for 4 weeks

Table 3. 3 Aging index of chemical families in bio-oil during 4 weeks aged at 50 °C

Chemical families	Aging index/ %											
	Oil-S			Oil-1			Oil-2			Oil-3		
	1 W	2 W	4 W	1 W	2 W	4 W	1 W	2 W	4 W	1 W	2 W	4 W
Carboxylic acids	0.10	11.33	10.62	-0.98	16.90	26.18	-0.05	4.40	6.05	-0.37	6.68	7.29
Esters	1.14	38.05	50.82	8.12	17.08	29.00	9.30	24.68	30.75	18.57	52.58	55.72
Phenols	-5.21	-22.22	-24.74	-0.17	-2.96	-4.27	-6.74	-8.95	-12.83	-73.20	-100.00	-100.00
Guaiacols	-2.25	-10.64	-11.25	-0.57	-2.22	-5.43	-2.79	-11.77	-9.55	-100.00	-100.00	-100.00
Alcohols	-11.18	-23.92	-22.13	-7.39	-14.10	-18.69	-4.29	-15.57	-20.96	-60.81	-72.46	-82.30
Aldehydes	-14.59	-27.61	-28.17	-2.07	-3.56	-6.38	-0.33	-9.79	-13.08	-17.93	-39.26	-46.48
Ketones	-4.73	-4.85	-10.31	-0.16	-9.20	-9.26	-1.86	-6.56	-16.52	-17.19	-25.71	-35.48
Sugars	-1.51	-23.92	-26.53	-0.90	-1.71	-2.33	-0.76	-30.24	-41.58	-6.61	-34.33	-53.86
Furans	0.00	32.45	33.37	-1.60	22.42	35.73	0.00	45.72	44.98	16.38	17.86	29.97

3.3.2.2 Chemical mechanisms of accelerated aging

According to the trend of the aging index of each bio-oil after 4 weeks of aging, the fluctuation of the dots in **Figure 3. 7**can determine the changes in the distribution of chemical compounds.

It is clear that the fluctuation of the Oil-1 curve remains relatively weak, while a severe fluctuation of the curve for Oil-3 is obtained. The change of Oil-2 is close to Oil-S depending on chemical families.

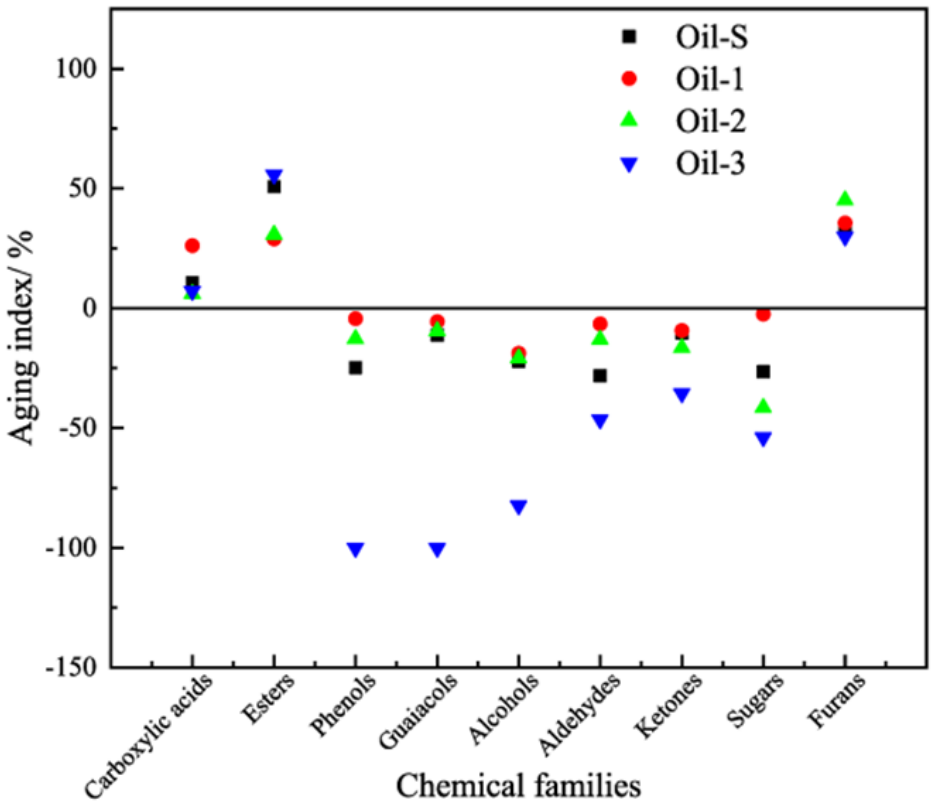

Figure 3. 7 The trend of the aging index of chemical families in bio-oils aged at 50 °C (4 weeks)

The aging index of sugars and carboxylic acids gradually become respectively more positive and more negative with time increasing, because of the formation of carboxylic acids from the decomposition of levoglucosan. The latter gradually decomposes with increasing aging time, as was observed by Ren et al. [231]. Levoglucosan mainly undergoes hydrolysis to form glucose in carboxylic acids and water medium [239]. According to the pH value and water content results discussed above, the composition of Oil-3 is more suitable to decompose sugars (53.86% of sugars consumed), whereas the sugars decrease slightly in Oil-1 (2.33% of sugars consumed). Glucose will be further degraded into various products through dehydration, retro-aldol condensation, and decomposition in the presence of acids, such as 5-(Hydroxymethyl) furfural (HMF), 2(5H)-furanone, 2-furanmethanol, 2-acetylfuran, furfural, furan, 2,5-dimethyl-, and acetic acid. HMF also undergoes further hydrolysis to produce levulinic acid and formic acid

[22], and the former then undergoes catalytic reduction to γ-valerolactone (GVL) (as described in **Figure 3. 8**).

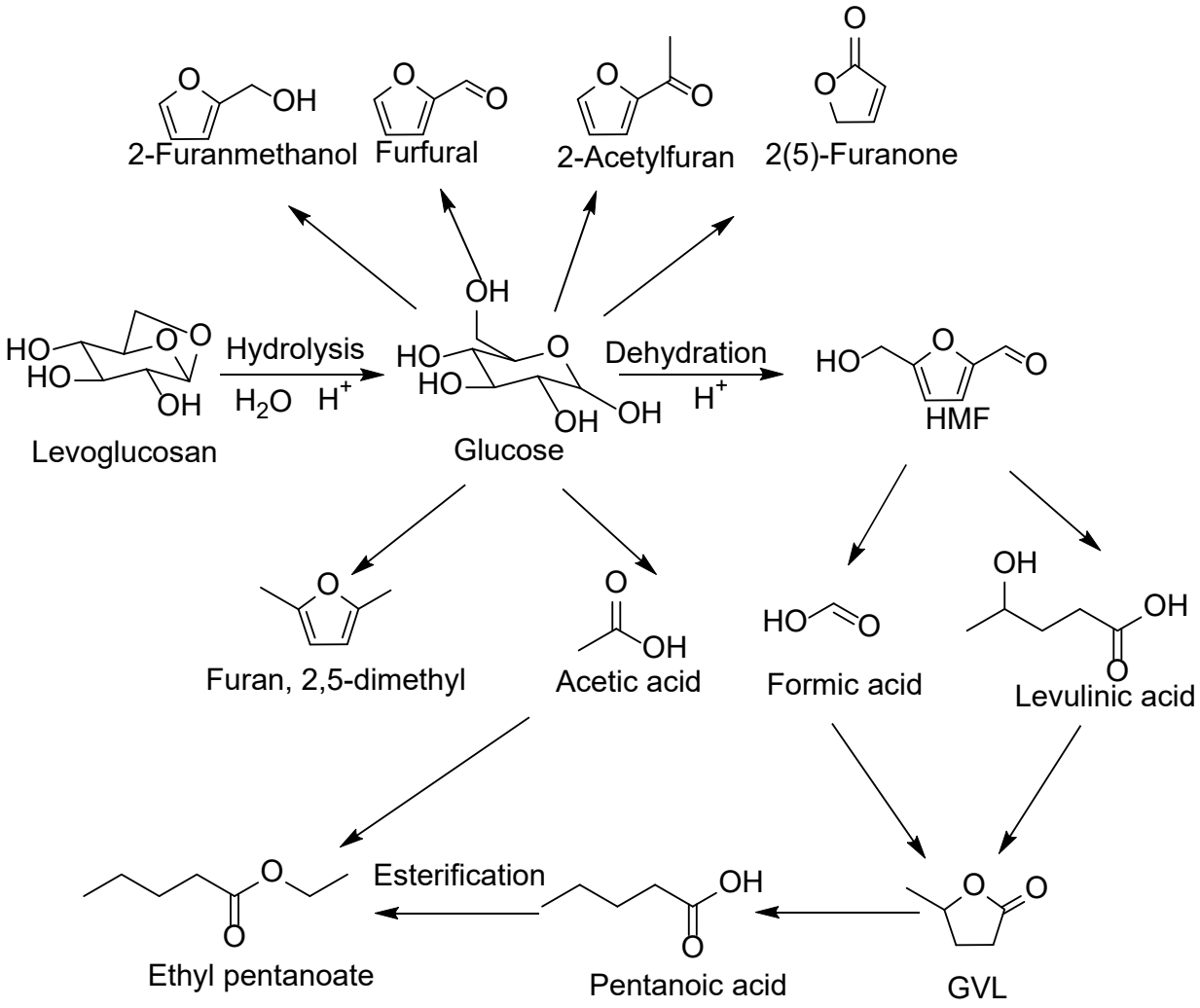

Figure 3. 8 The reaction pathway of levoglucosan in bio-oil during aging

This further explanation of the experimental results is reported in **Table A 2. 1**, where the content of GVL and 2(5H)-furanone increases during the aging process. It is difficult for them to participate in the polymerization reaction owing to the low reactivity of ester carbonyl in their stable structure of five-membered lactone ring. As an excellent platform compound, GVL can be formed by intramolecular esterification of hydroxy acid, or it can be converted by ring-opening and hydrogenated to produce pentanoic acid, as shown in **Figure 3. 8.** As indicated in **Table A 2. 1**, Oil-2 and Oil-3 produced more GVL than Oil-1 after aging. Furthermore, the production of the ethyl pentanoate in bio-oil products during aging was explained. Its fraction increased 57.49% in Oil-3 [231]. Butanedioic acid also increased, probably due to the oxidation

of succindialdehyde [98] (shown in **Figure 3. 9**). A decrease in the content of succindialdehyde seems to confirm this kind of reaction. Propanoic acid, 2-oxo-, methyl ester as a pathway ester can be produced by propanoic acid, 2-oxo- through esterification. These unsaturated carbonyl groups inside the structure can also undergo additional polymerization during aging. It seems that the presence of acetic acid is more inclined to provide a suitable environment for acid-catalyzed reactions than reactions that occur during the aging process, which is consistent with the results obtained by Sundqvist et al.[240].

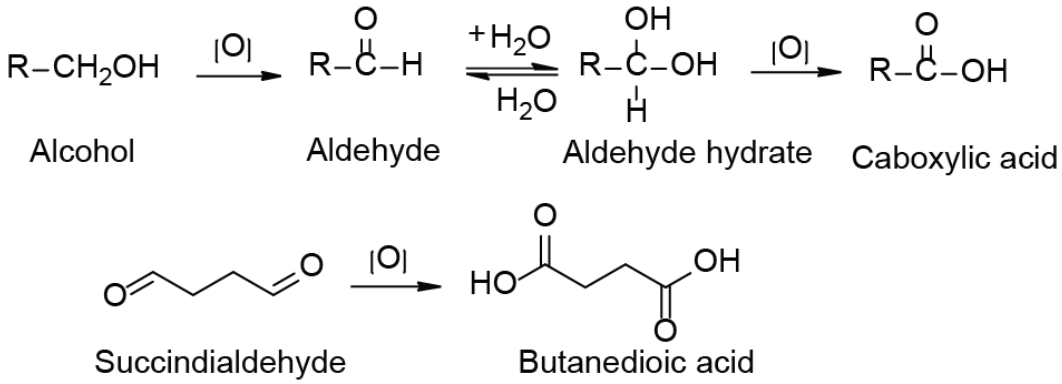

Figure 3. 9 The oxidation reactions of alcohol and aldehyde in bio-oil during aging

For instance, the content of alcohols in aged Oil-3 was reduced by 82.30%. Alcohols form esters with organic acids and can also form hemiacetals or acetals with aldehydes during aging [91]. Cyclic alcohols can be reduced to ketones described in **Figure 3. 10**. 2-furanmethanol, as the product of glucose hydrolysis, is the only alcohol with increasing content during aging. The number of ketones gradually decreased in bio-oil products, and their changes were more pronounced in Oil-2 and Oil-3 (16.52% and 35.48%, respectively). Consequently, hydroxyacetone, as the most prominent component of ketones, is very active. With three reactive sites, three kinds of reactions can occur aldol condensation involving a carbonyl group and active α-C, acetalization involving a carbonyl group and hydroxyl group, and etherification involving two hydroxyl groups. It is easy to polymerize with itself or with other reactive monomers [241].

All the aldehydes content listed in **Table A 2. 1** decreases during aging. Many reactions are possible, for example, aldehydes and water to form hydrates, aldehydes and alcohols to form hemiacetals or acetals, aldehydes to form oligomers and resins, and aldehydes and phenolics to form phenol aldehyde resins and water [91]. Glycolaldehyde and succindialdehyde are highly active compounds since they have two functional groups; thus, they can react via Michael

addition reactions [241] and aldol condensation and acetalization. These compounds not only self-polymerize but also interact with hydroxyl and carbonyl groups of other compounds.

The yield of phenols and guaiacols significantly decreased in the first two weeks of aging and continued to decrease with time, while it showed an upward trend by the end of 4 weeks. Phenolics could react with aldehydes in acid-catalyzed media to produce phenolic resin through condensation during aging [136]. The decreasing trend leveled off later, probably because thermodynamic equilibrium was reached [231]. The fluctuations and recovery of their content after 4 weeks of aging may be due to the reverse reaction of condensation and polymerization (**Figure 3. 10**). The rate of changes of phenols and guaiacols content during aging was in the following order: Oil-3 > Oil-S > Oil-2 > Oil-1. The significantly higher stability of phenols and guaiacols was observed in Oil-1 compared to Oil-3.

The quantity of esters increases during aging at 50 °C for 4 weeks. The maximum increase rate belongs to Oil-3 (55.72%). The esterification of organic acids and decomposition of large esters occurred [228], increasing the water content. Among them, many of the esters are acetates, such as 1-propen-2-ol, acetate, allyl acetate, acetic acid, (acetyloxy)- and 2-butanone, 1-(acetyloxy)-. Their content increased simultaneously during aging.

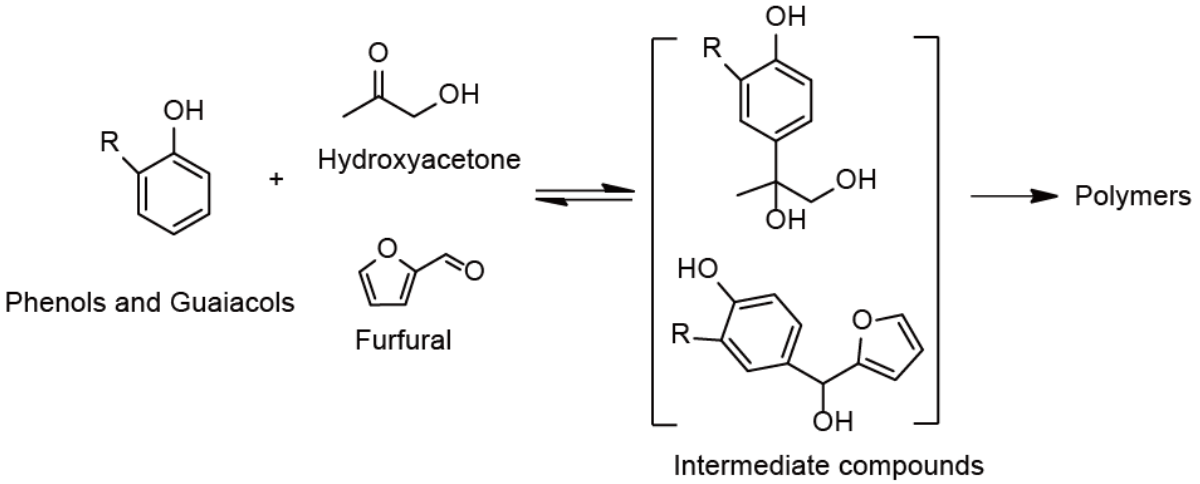

Figure 3. 10 The condensation reaction of phenolic compounds and aldehyde in bio-oil during aging

3.3.3 The effect of storage on water extraction of bio-oil products

The water extraction of bio-oil results in a water-soluble fraction and water-insoluble fraction. The former contains a large amount of easily soluble polar components while the latter is mostly insoluble non-polar components. In this study, the fractional condensation pyrolysis oils (Oil-1 and Oil-2) were used for water extraction. After separation, four water extraction fractions

are collected and stored at 50 °C for 4 weeks. The changes in the content of chemical families in the bio-oil products were studied.

Significant differences in the aging index of each chemical family were observed between the water-insoluble and water-soluble fractions, as shown in **Figure 3. 11**. It can be seen that the water-insoluble fractions are more stable than the water-soluble fractions during the 4 weeks of aging. Regardless of the carboxylic acids and aldehydes, the changes of all the chemical families in the composition of the Oil-1-WI fraction are very slight. The changes in the Oil-2-WI fraction are more obvious than in the Oil-1-WI faction, relying on its higher initial content of acids and carbonyl groups (**Chapter II Figure 2. 7**). The content of sugars, carboxylic acids, esters, alcohols, and aldehydes has undergone visible changes in the water-soluble fractions.

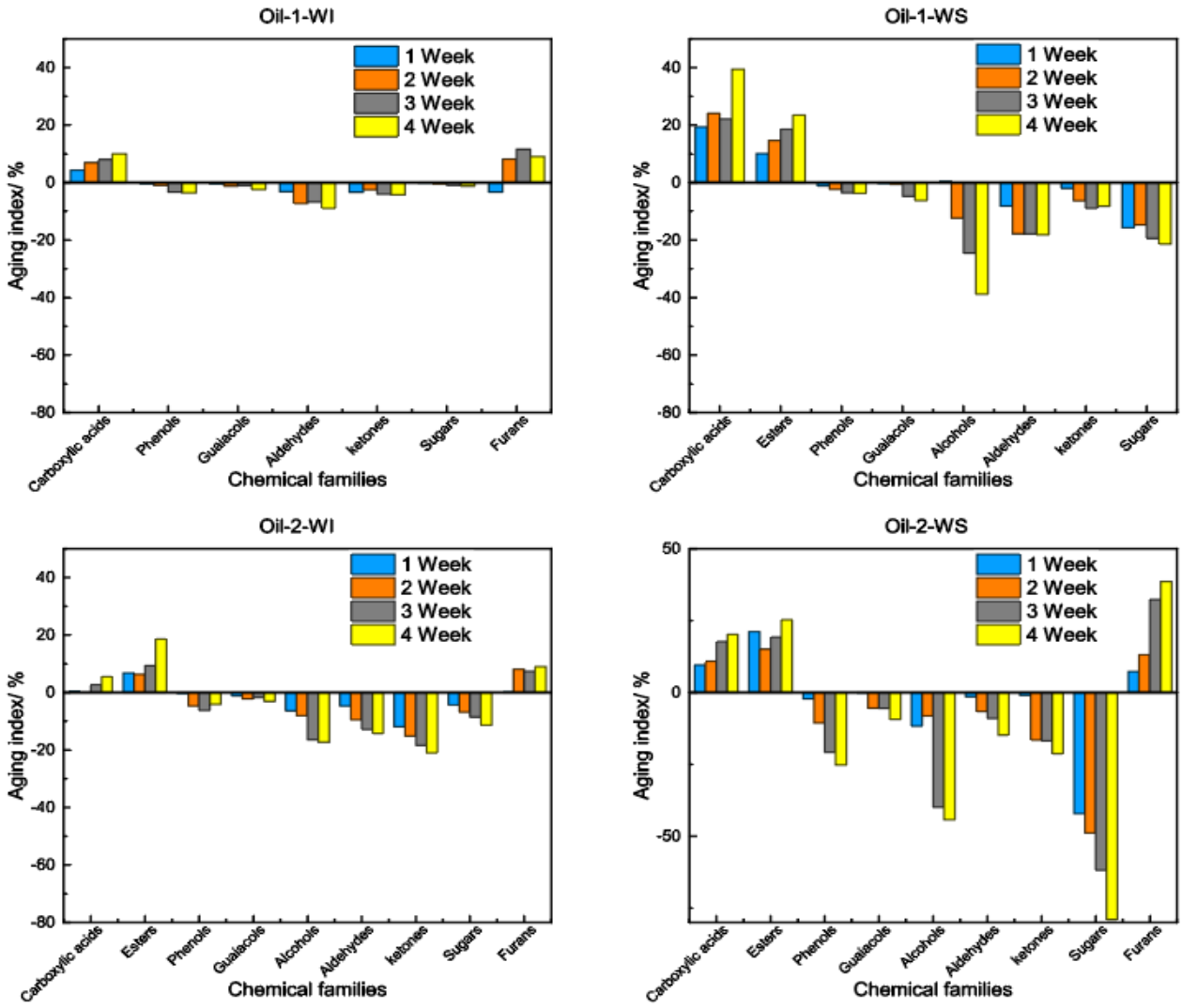

Figure 3. 11 The aging index of the content of chemical families in the bio-oil water-insoluble and water-soluble fractions

However, the changes between the two water-soluble fractions (Oil-1-WS and Oil-2-WS) are not the same. Moreover, sugars have the most obvious changes in Oil-2-WS, decreased by 79.06%. Hu et al. [239] found that, under an environment where water medium and acetic acid coexist, sugars were highly reactive and tended to polymerize. The high content of carboxylic acid and water obtained from the water extraction make the water-soluble fraction a suitable medium for the hydrolysis of sugars.

This contributes to the fact that the initial yield of carboxylic acids in Oil-2-WS (41.88 wt%) was higher than in Oil-1-WS (2.87wt%) and makes the changes in Oil-2-WS more obvious. Simultaneously, a lot of by-products (acetic acids, HMF, 2(5H)-furanone, furfural, furan, 2,5-dimethyl-, and GVL) were produced during sugar decomposition, as mentioned above (**Figure 3. 8**). A similar trend was reported in the literature that studied the aging of the water-soluble fraction and water-insoluble fraction at different temperatures by thermogravimetry [241].

To analyze more clearly the changes in the content of each family and compare them to the unaged fractional condensed bio-oils, **Table 3. 4** listed the aging index of the bio-oil products.

Table 3. 4 Aging index of the content of chemical families in water extraction bio-oil products after storage for 4 weeks at 50 °C

Aging index/%	Oil-1	Oil-1-WI	Oil-1-WS	Oil-2	Oil-2-WI	Oil-2-WS
Carboxylic acids	26.18	9.99	39.45	6.05	5.53	20.19
Esters	29.00	/	23.47	30.75	18.59	25.27
Phenols	-4.27	-3.63	-3.74	-12.83	-4.15	-25.24
Guaiacols	-5.43	-2.46	-6.27	-9.55	-3.09	-9.31
Alcohols	-18.69	/	-38.80	-20.96	-17.28	-44.23
Aldehydes	-6.38	-8.95	-18.14	-13.08	-14.27	-14.85
ketones	-9.26	-4.26	-8.25	-16.52	-21.01	-21.35
Sugars	-2.33	-1.22	-21.41	-41.58	-11.38	-79.06
Furans	27.71	9.08	/	21.86	9.00	38.62

It is obvious that after water extraction, the stability of some chemical families in the water-insoluble fractions was improved, such as carboxylic acids, alcohols, esters, phenols, guaiacols, as well as sugars. In particular, there is evidence that sugars change in the water-soluble fractions (-79.06% in Oil-2-WS, -21.41% in Oil-1-WS) compared to the water-insoluble

fractions (-11.38% in Oil-2-WI, -1.22% in Oil-1-WI). Moreover, the stability of some chemical families improved in both fractions, for example, phenols (-3.63% in Oil-1-WI, -3.74% in Oil-1-WS, and -4.27% in Oil-1) and guaiacols (-3.09% in Oil-2-WS, -9.31% in Oil-2-WS, and -9.55% in Oil-2).

Therefore, studying the aging reactions in the water-soluble fraction of Oil-2 can appear as a new approach to provide a perspective for the hydro-processing of pyrolysis oil to produce chemical compounds of interest (such as HMF, 2 (5H) -furanone, furfural, furan, 2,5-dimethyl-, and GVL).

3.3.4 The comparison and analysis of bio-oil fractions from both method

3.3.4.1 Effect of aging on the functional group in bio-oil

The FTIR spectra with the wavenumber range of 4000-500 cm^{-1} are presented in **Figure 3. 12** shows the evaluation and assignment of the FT-IR spectra represented functional group in bio-oil.

It shows a significant increase in intensity between various oil products and various aging temperatures at the peaks of 3338 cm^{-1}, 1720 cm^{-1}, 1633 cm^{-1}, 1363 $cm^{-1,}$ and 1220 cm^{-1}. Some decreases in the peak of 1089 cm^{-1} and 526 $cm^{-1}$are noticed. The increase in the concentration of carbonyl, ester, and ether families was characteristic of aging bio-oils associated with oxidation [237]. After aging at a temperature of 50 ° C, the functional families of the bio-oil have changed significantly, among which the changes of Oil-3 at 3400 cm^{-1} and 1720 cm^{-1} are most obvious due to the decomposition of sugars to form a large number of carboxylic acids during aging. Concerning the aging of the fractions obtained after additional water extraction, carboxylic acids and water were formed noticeably in both WI and WS, whereas there is no obvious evolution of water-insoluble fractions for other absorption peaks, in particular Oil-1-WI, compared with the original bio-oils. Through the water extraction and separation process, the stability of bio-oil can be improved, consisting of the result from GC analysis where the modification of several chemical families is identified in Oil-1-WI and Oil-2-WI after storage.

3.3.4.2 Effect of aging on the thermal stability of bio-oil

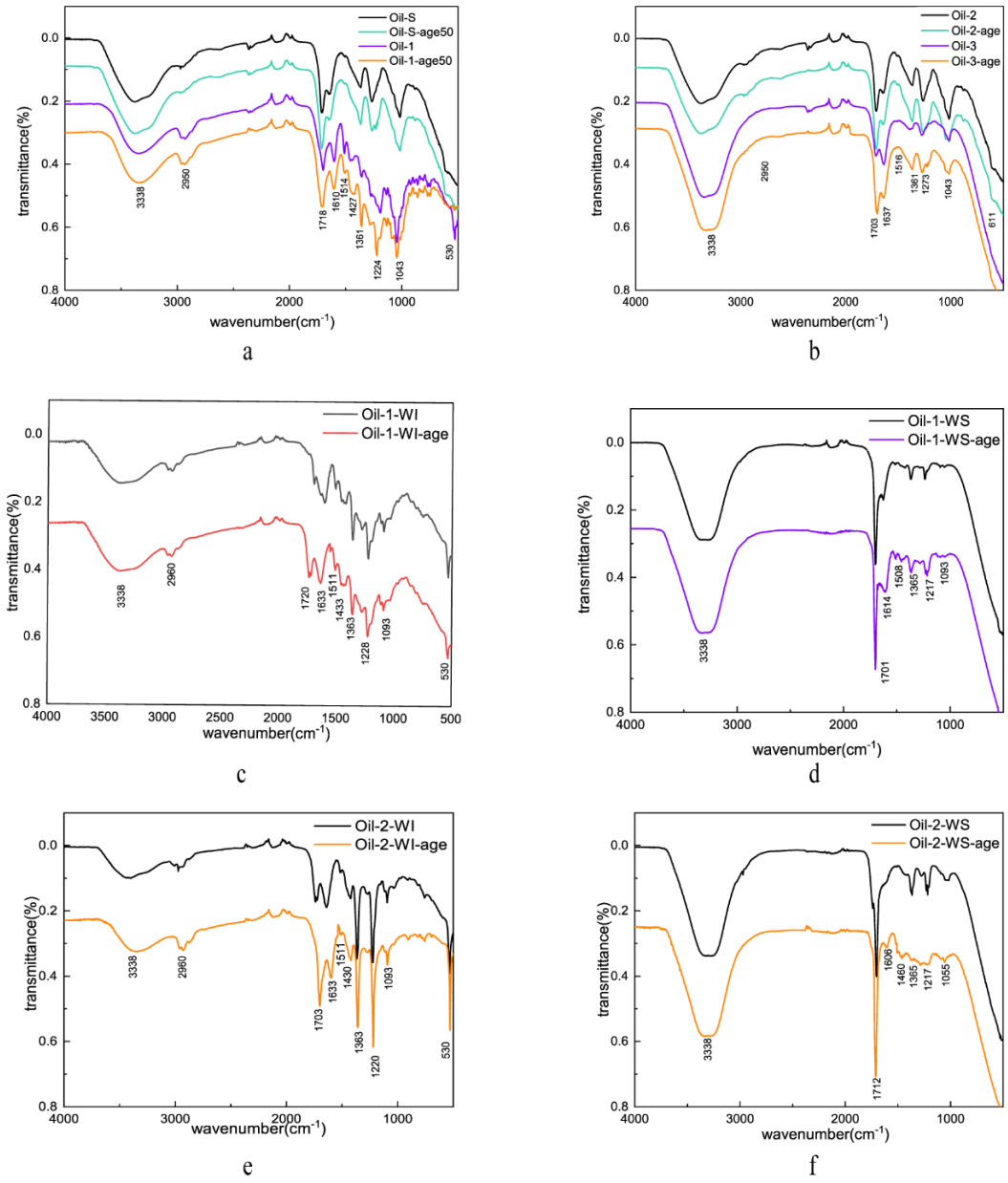

Figure 3. 12 FITR spectra of pre-aging and post-aging bio-oil products at aging temperature of 50 °C stored for 4 weeks

Considering the profiles of thermalgravimetric analysis (TGA), the evolution can be related to the boiling point distribution of the compounds of bio-oil, which can be regarded as a miniature distillation process.

The relationship between weight loss and temperature of bio-oil using TGA can evaluate the storage stability of bio-oil. The results of both pre-aging and post-aging bio-oil products are shown in **Figure 3. 13**.

According to the boiling point and GC-MS, GC-FID analysis of each component in the bio-oil, the weight losses are discussed comprehensively. These weight losses can be divided into main three stages.

First, (1) below 118°C is responsible for the evaporation of water and light volatiles with boiling points lower than this temperature, like acetic acid (boiling point 118°C) and some ketones, esters, aldehydes, and furans. Various products are generated by reacting with each other before 118°C, such as esters and water by esterification reaction, and some unstable carboxylic acid decomposition generating CO_2 [91].

Second, (2) 118–385°C, the major weight loss stage, including some high boiling volatiles components and especially phenol derivatives that have not previously been decomposed, continue to decompose into a small amount of gas. The weight losses of Oil-S, Oil-1, Oil-2and Oil-3 are 9.29%, 23.09%, 3.69% and 0.03% for pre-aging product, and 23.25%, 25.34%, 7.54%, 3.30% for the product aging at 50°C. During storage, bio-oil products at this stage can conserve more weight.

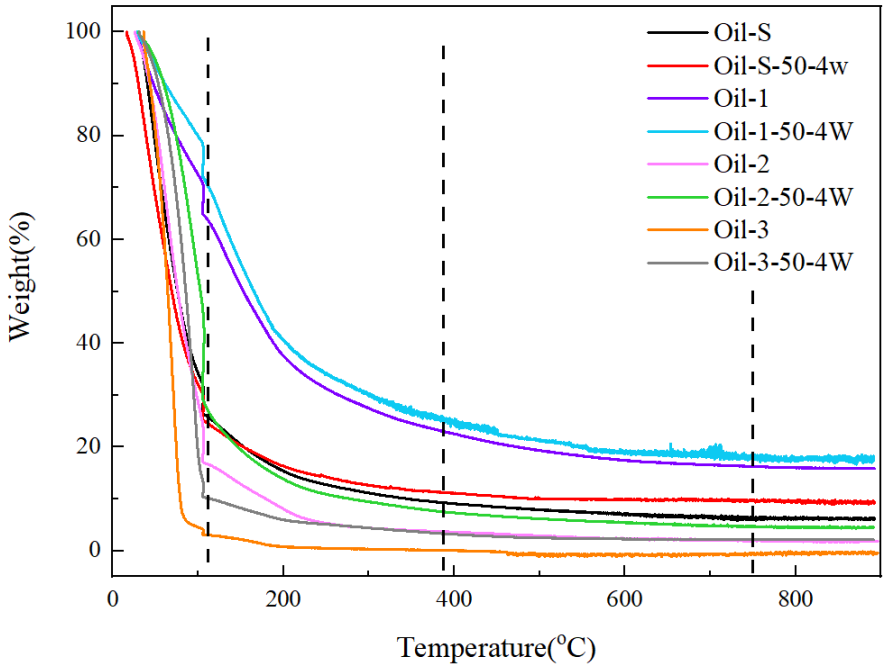

Figure 3. 13 TG graphs of the pre-aging and post-aging bio-oil samples

Third, (3) the coke was produced through the condensation and decarboxylation reactions of the residues at 385 °C–750 °C and levoglucosan was evaporated (boiling point 385°C). The

residual mass fraction did not obviously change after about 750°C. Therefore, the final residual mass fraction of the bio-oil can be used to evaluate the aging degree. The higher the final residue, the more polymer will be formed during the aging process and the sample will be more stable.

It can be discovered that, whether it is the aging of different products or the increase of the aging temperature, the final residue is increased, which further indicates that the bio-oil product produced obvious polymerization during the aging process. The maximum final residue has belonged to Oil-1 aging at 50℃.

3.4 Conclusion

The storage stability of bio-oil products obtained by fractional condensation has been evaluated by comparing the variation in the composition of aged samples with that of fresh bio-oil. An accelerated stability study has been done for 4 weeks using a temperature of 50 °C which would correspond to one year at room temperature. The main results showed that:

- The water content of each bio-oil fraction increased with time, whereas the pH value decreased
- The chemical analysis by GC chromatography and FTIR indicated that the content of some compounds increased, such as acetic acid, GVL, furan, 2,5-dimethyl-, 2(5H) -furanone, 2-furanmethanol, and 2-acetylfuran, while the content of levoglucosan decreased significantly, presumably due to its hydrolysis. Also, most of the alcohols, aldehydes, and ketones decreased, whereas esters increased, which may occur with esterification, oxidation, and polycondensation reactions.
- The products stored at 4 °C for 1 month have shown no fluctuation in composition. The bio-oil stored at ambient conditions presents relatively high stability, whereas the composition of samples aged at 50 °C changed significantly except for Oil-1. Oil-3 is more unstable compared to Oil-S due to its excessive acid and water content.
- The bio-oil fractions obtained by both condensation system and water extraction exhibit improved stability of most of the chemical families in the water-insoluble fractions, such as furans, phenols, guaiacols, alcohols, and aldehydes. However, the water-soluble fractions are not as stable as the initial fractions. In water-soluble fractions, sugars are more favorable for hydrolysis and for producing interesting chemical components such as HMF, 2(5H) -furanone, furfural, furan, 2,5-dimethyl-, and GVL.

Chapter IV

Synthesis and characterization of phenolic acetaldehyde resins based on pyrolysis bio-oil separated by fractional condensation and water extraction

Abstract:

In this chapter, the polymerization of phenol models (phenol, o-cresol, 2,6-dimethylphenol, m-cresol, and 4-ethylguaiacol) was studied to produce novolac model phenol acetaldehyde (MPA) resins. The mimic phenolics based on the composition of phenolic compounds in bio-oil were examined to produce novolac mimic acetaldehyde (mimic) resin. Bio-oil obtained from intermediate pyrolysis of biomass was added to synthesize bio-oil acetaldehyde (BOA) resins. DGEBA was used for the first time as a formaldehyde-free cross-linker for curing bio-oil based novolac resins. The kinetic parameters of the curing reaction with model-free methods using data obtained from DSC were determined. The physicochemical and thermal properties of resins before and after curing were compared, to evaluate the potential of bio-oil products obtained from fractional condensation and water extraction to effectively replace commercial phenols.

A part of this study has been published as an article (Xu J, Brodu N, Mignot M, Youssef B, Taouk B. Synthesis and characterization of phenolic resins based on pyrolysis bio-oil separated by fractional condensation and water extraction. Biomass Bioenergy 2022;159. https://doi.org/10.1016/j.biombioe.2022.106393

4.1 Introduction

In the first and second chapters, we used a drop tube reactor to produce beechwood bio-oil, which was then collected in a three-stage condensation system (temperature set as 110, 20, and -11 °C) to obtain three fractions of bio-oil. The latter was then upgraded using water extraction. Based on both separation methods, several types of phenol rich bio-oil precursors can be chosen by using: (1) the whole bio-oil to substitute petroleum-derived phenol [oil-S], (2) the bio-oil obtained from fractional condensation, or (3) the water-insoluble fraction of the bio-oil obtained from fractional condensation. The polymerization of phenol precursor will be studied to produce novolac model phenol acetaldehyde (MPA) resins to evaluate the feasibility of the replacement of polymer based on petrochemistry phenol resources.

The experimental result section of this chapter will separate into four parts. Firstly, model phenol acetaldehyde resins synthesis and characterization will be discussed. Secondly, various phenol-rich bio-oil precursors will be used to synthesize resin. The chemical and thermal properties will be compared with a mimic acetaldehyde resin to select the more favorable bio-oil fraction. A further study of the water-insoluble fraction of pyrolysis bio-oil phenol acetaldehyde resins catalyzed by 1% and 10% HCl will be led in the third part. The last section will focus on the kinetic properties of cured resin.

4.2 Experimental section

4.2.1 Materials

As a reminder of chapter 2, at the outlet of the pyrolysis reactor, three fractions of bio-oil, named OIL1, OIL2, and OIL3, were obtained at the condensation temperature of 110, 20, and -11 °C, respectively. A single condensation condenser (temperature set at -11 °C) was also used to produce a reference pyrolysis oil (OILS). The water-insoluble fractions (OILSWI, OIL1WI and OIL2WI) were collected after simply adding water. The selected bio-oils for resin polymerization precursors are OILS, OIL1, OIL2, OILSWI, OIL1WI and OIL2WI. Since OIL3 mainly contains a very small number of phenols, water and acids, it was not used in the experiments on resin synthesis.

Phenol (99%), o-cresol (99+%), m-cresol (≥ 98%), 4-ethylguaiacol (≥ 98%), 2,6-dimethylphenol (≥ 99%), acetaldehyde (99%, GC), HCl (37%), methanol (≥ 99.8%, HPLC grade), ethanol (≥ 99.8%, HPLC grade), acetone (≥ 99%), potassium hydroxide (KOH),

pyridine (≥ 99.5%, GC), dichloromethane (DCM) (≥ 99.8%, HPLC grade), acetic anhydride (≥ 99%), diglycidyl ether of bisphenol A (DGEBA) (≥ 99%), and triphenylphosphine (TPP) (≥ 95.0%) were purchased from Sigma Aldrich and used as received.

4.2.2 Synthesis of novolac resins

Polymerization tests of different phenolic precursors with acetaldehyde were carried out. The overview of the procedure was shown in **Figure 4. 1.** Phenol models, including phenol, o-cresol, 2,6-dimethylphenol, m-cresol, and 4-ethylguaiacol, were used alone and named phenol acetaldehyde (PA), o-cresol acetaldehyde (OCA), 2,6-dimethylphenol acetaldehyde (DPA), m-cresol acetaldehyde (MCA), and 4-ethylguaiacol acetaldehyde (EGA) resins, respectively. A mimic phenolic resin, consisting of the above five model phenols was studied as a reference for bio-oil synthesis to produce a mimic phenol acetaldehyde resin (mimic resin).

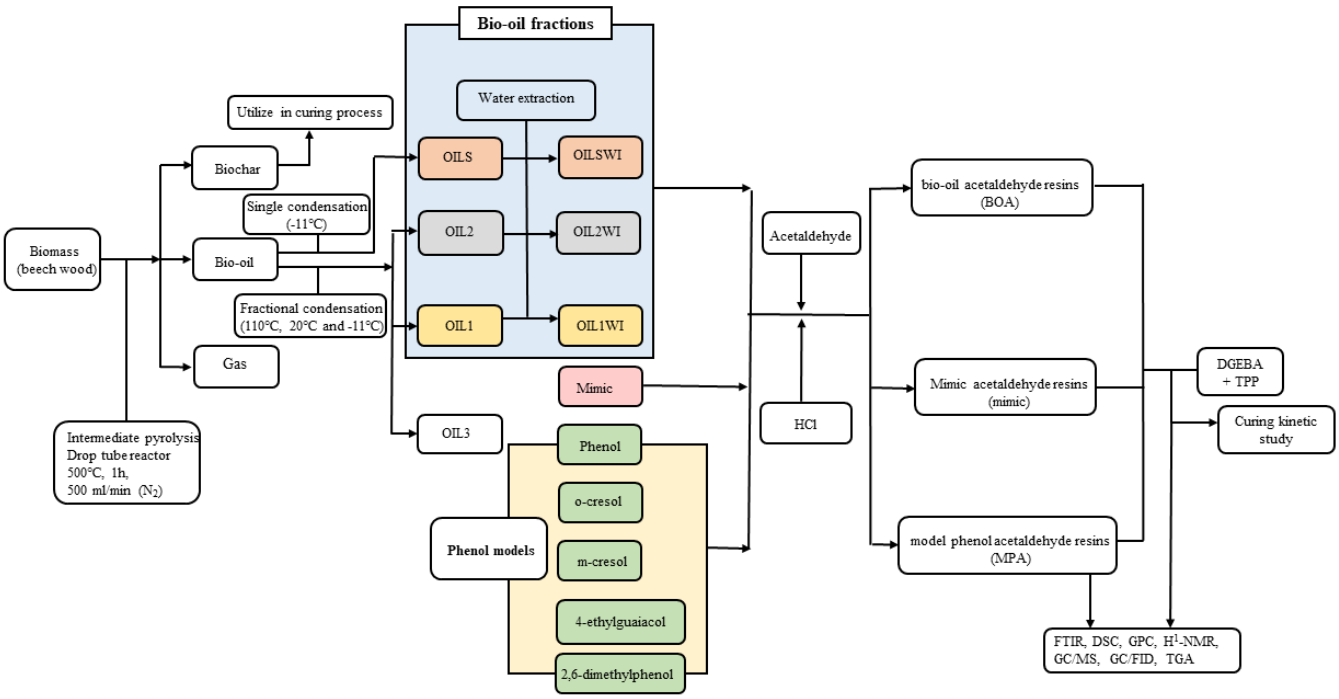

Figure 4. 1 The overview procedure of the model phenol, mimic and bio-oil acetaldehyde resins synthesis and analysis (for section 3.1 and 3.2)

The molar fraction of phenol models in mimic was based on the composition of these phenol compounds of the OIL1WI fraction, as shown in **Table 4. 1**. Bio-oil products, including OILS,

OIL1, OIL2, OILSWI, OIL1WI, and OIL2WI, were also used as the phenol precursors to synthesize BOA resins, which have different phenolic compounds concentration.

Table 4. 1 Molar fraction (mol.%) determined by GC-FID for the detected phenolic compounds in the oil and the mimic composition (Average of triplicate runs with standard deviation < 3%.)

Phenols in oil	mol. %						
	OILS	OIL1	OIL2	OILSWI	OIL1WI	OIL2WI	mimic
phenol	1.03	1.20	1.21	3.45	2.47	2.26	19.73
o-cresol	0.35	1.20	1.23	1.40	3.26	1.32	26.04
m-cresol	0.63	0.94	0.60	3.23	1.91	1.33	15.26
2,6-dimethylphenol	0.65	1.10	0.63	2.41	1.86	2.39	14.87
2,4-dimethylphenol	1.25	3.59	1.04	4.02	5.06	4.96	-
phenol, 3-ethyl-5-methyl-	0.47	1.00	0.39	2.46	2.42	3.03	-
3-methylcatechol	0.34	2.62	0.31	1.89	2.57	1.23	-
catechol	0.87	2.88	0.47	1.61	3.14	0.68	-
4-methylcatechol	0.43	1.88	-	1.83	3.08	-	-
4-ethylcatechol	0.47	1.69	-	1.80	5.52	-	-
guaiacol	0.82	-	0.61	3.86	-	2.87	-
creosol	0.44	1.69	0.34	2.00	3.58	1.83	-
4-ethylguaiacol	0.43	1.59	-	1.80	3.02	-	24.12
syringol	0.63	3.06	0.51	2.70	4.71	1.97	-
isoeugenol	0.45	1.55	-	1.78	3.21	1.30	-
2,4-dimethoxyphenol	0.30	1.30	-	1.26	4.62	0.95	-
Phenol concentration /mmol. g^{-1}	1.55	2.69	1.11	4.23	5.80	4.03	8.66

In section 3.3, various BOPA resins were prepared by using the bio-oil to gradually replace the commercial phenol that copolymerizes with acetaldehyde. The amount of the bio-oil water-insoluble fraction (only OIL1WI) added was increased from 0, 25, 50, 75, to 100 mol. % and the resulting resins were denoted PA, BO25PA, BO50PA, BO75PA, and BOA, respectively. Two different concentrations of the acid catalyst (1 and 10 mol. % of phenol) were also used in the synthesis, and two natures of BOPA resins were obtained. The production method and process are shown in **Figure 4. 2**. The chemical structure of phenol and schematic procedure of the bio-oil phenol resin procedure is based on the mechanism of phenol-acetaldehyde resin synthesis is displayed in appendix (**Figure A 3. 1**) [163]

Table 4. 1 shows the molar fraction (mol.%) of the major phenolic compounds in the bio-oil products and the total concentration of the phenolic compounds in each product prepared for the bio-oil synthesis calculations.

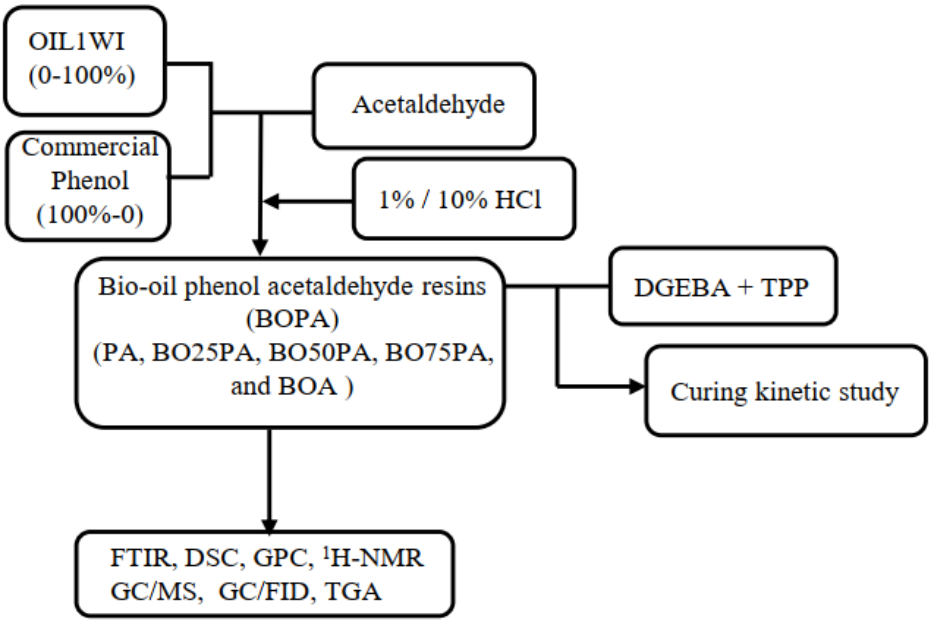

Figure 4. 2 Overview of the bio-oil based novolac resin procedure characterization methods

All the resin synthesis experiments were started at atmospheric pressure. The reaction was done in a 100 mL three-neck reactor with an oil bath preheated to a fixed temperature (80 °C) and stirred with a magnetic stirrer. The reactor was equipped with a condenser and nitrogen outlet in the middle neck, a nitrogen inlet, and a thermometer in two side necks, respectively. After the phenol precursors melted, hydrochloric acid (HCl) was added to obtain acidic conditions (1 mol.% HCl for phenol precursors for MPA and mimic resins, 1 mol.% and 10 mol.% HCl for phenol precursors for BOA resins). An aldehyde to phenol precursors molar ratio was 5:6, fixed for each experiment. Acetaldehyde was then added drop-wise through the addition funnel. The reaction mixture was heated for 4 h with continuous stirring. After the reaction, the resin products were washed with distilled water three times and vacuum dried at 125 °C for 24 h to remove the unreacted monomer and acid. Each experiment was repeated three times, and the average values of all the analyses were reported.

4.2.3 Curing treatment

The curing kinetics of the model phenol, mimic, and bio-oil resins were also studied using DSC (TA Q1000 instrument). Firstly, the vacuum dried resin samples were dissolved in acetone

and uniformly mixed with a certain percentage of the curing agent DGEBA and 2% TPP at room temperature for 12 h to evaporate all the solvent. Then, a sample of 4–5 mg of the mixture was placed in an aluminum hermetic crucible and heated in a nitrogen environment from 25 °C to 250 °C at various heating rates to obtain the heating cycles. The onset temperature of curing and curing energy was determined from the heating cycle. To optimize the amount of DGEBA, **Figure A 3. 1** shows the 20%, 30%, and 40% of PA resin by weight tested at a heating rate of 5 °C/min from 25 to 250°C in a nitrogen atmosphere to capture the maximum value of the glass transition temperature of cured resin. The result illustrates that 40% of DGEBA allows obtaining a high Tg resin, a curing reaction with a lower onset and peak temperature.

The non-isothermal DSC analysis is widely applied to study the curing behavior and kinetics for resin and polymer synthesis [187, 188, 242]. The results obtained from the DSC measurements are used to evaluate the kinetic parameters according to the model-free methods of Kissinger, Flynn–Wall–Ozawa (FWO), and Crane, which are illustrated by **Equation 4. 1, Equation 4. 2** and **Equation 4. 3**.

$$ln\left(\frac{\beta}{{T_P}^2}\right) = ln\left(\frac{AR}{E_a}\right) - \frac{E_a}{RT_P}$$

Equation 4. 1

$$log\,\beta = -\frac{0.4567E_a}{RT_P} + C$$

Equation 4. 2

$$\frac{dln\beta}{d(1/T_P)} = -\frac{E_a}{nR}$$

Equation 4. 3

where β is the heating rate (°C/min), T_p is the temperature of the maximum exothermic peak (K), E_a is the activation energy (kJ/mol), R is the gas constant (8.314 J/mol/K), A is the pre-exponential factor (min^{-1}), C is a constant, and n is the reaction order.

E_a and n can be calculated by plotting $ln(\beta/T_p^2)$ against $1/T_P$, $log\ \beta$ versus $1/T_p$, and $ln\ \beta$ versus $1/T_p$, respectively.

For characterization purposes, some resins were also thermally cured in the oven after mixing them with DGEBA in the same initial proportion as those used for the DSC experiment. The

curing temperature program was set at 120 °C for 30 min, 150 °C for 30 min, and 180 °C for 1 h [188].

4.2.4 Characterizations

4.2.4.1 Determination of conversion of reactant and yield of resin

The resin products after drying were weighed to determine the yield, which was calculated according to the following equation.

$$Yield\ (\%) = \frac{weight\ of\ final\ \ resin}{weight\ of\ reactant\ added} \times 100$$

Equation 4. 4

The conversion rate of phenols in the polymerization reaction was calculated by **Equation 4. 5**.

$$Conversion\ (\%) = \frac{Mole\ of\ reactant\ converted}{Mole\ of\ reactant\ added} \times 100$$

Equation 4. 5

The reactant converted and added was determined using gas chromatography (see **Chapter II**, **2.2.4.1**). Pure reference phenolic compounds were used for calibration. Standard solutions of each phenolic compound were prepared by dissolving them in acetone. Five-point straight line calibration curves (with $R^2 > 0.99$) were established for these pure compounds using nonane as the internal standard.

4.2.4.2 Chemical properties

4.2.4.2.1 Oligomer distribution

A high-performance liquid chromatography (HPLC) instrument Agilent 1100 was used to quantify the phenolic oligomers in the MPA resins. Gradient conditions were used: 50/50 methanol/water and then 100% methanol in 20 min, back to 50/50 in 0.5 min and for 5 min, a temperature of 30 °C, a flow rate of 1 mL/min, and a Kinetex C18 250 mm × 4.6 mm × 5 µm column. The detector was set at 280 nm. For identification of the oligomers, Liquid chromatography-mass spectrometry analysis was done with ISQ Single Quadrupole Mass Spectrometer from Thermo Scientific. Electrospray ionization (ESI) was used in negative mode.

Molecular weight distribution was monitored by gel permeation-chromatography (GPC) by a Waters Breeze gel permeation chromatography (Waters, Milford, MA, 1525 binary HPLC

pump, RI detector at 270 nm, Waters Styragel HR1 column at 40 ℃) with DCM as the eluent at a flow rate of 1 mL/min and polystyrene as the calibration standard. To improve the solubility of resins in the DCM solvent, all of the resin samples were subjected to acetylation by the dissolution of 0.2 g of resin in 10 mL of a mixture (1: 1 v/v) of pyridine and acetic acid followed by magnetic stirring at room temperature for 24 h. The acetylated products were obtained by precipitation in an ice-cooled 1.0 wt% HCl solution and then filtered, rinsed thoroughly with distilled water until pH = 7, and vacuum-dried at room temperature for 12 h [139].

4.2.4.2.2 Functional group determination

The hydroxyl number of the MPA, mimic, and BOPA resins were measured by the titration method [125], the number of hydroxyl groups determines the crosslinking ability of the resin, which is also very important characteristic of the novolac resin. In a 250 mL round-bottom flask equipped with a condenser and a magnetic stirring bar, 0.54 g of resin sample was mixed with 10 mL of acetylation mixture (1 V acetic anhydride and 10 V pyridine). The mixture was heated at 95 to 100 °C for 60 min. 2 mL of distilled water was then added. After 5 min, the funnel and neck of the flask were washed with 70 mL of cold water, which was then collected into the flask. A blank was run under the same condition without adding a resin sample. The resin sample and blank solution were titrated with a 0.5 mol/L potassium hydroxide ethanol solution using a pH meter to follow the pH value of the solution until the pH = 13. The hydroxyl number (OHN) was calculated by using (**Equation 4. 6**).

$$OHN = \frac{(V_b - V_S) \times C_{KOH}}{m_s}$$

Equation 4. 6

V_s = consummated volume (ml) of 0.5 mol/L potassium hydroxide solution in the main test

V_b = consummated volume (mL) of 0.5 mol/L potassium hydroxide solution in the blank test

C_{KOH} = The molar concentration of 0.5 mol/L potassium hydroxide solution

m_s = sample weight (g)

Nuclear magnetic resonance (^{1}H-NMR) was used to confirm the characterization of the resin, and the spectra were recorded on a Bruker AVANCE III (300 MHz) using DMSO-d as a solvent.

Attenuated total reflection Fourier-transform infrared (ATR-FTIR) spectroscopy was used to confirm the appearance of the organic functional groups present in the resin samples.

4.2.4.3 Thermal properties

Thermal analysis of the resins was conducted on a differential scanning calorimetry (DSC) TA Q1000 instrument using about 5 mg of sample in a sealed hermetic pan and nitrogen purge gas at 50 mL/min. Samples were cycled between 25 and 180 °C at a heating/cooling rate of 5 °C/min. After that, the glass transition temperature (T_g) was measured.

Thermogravimetric analysis (TGA) was used to monitor the thermal degradation of the uncured and cured resin. By using a TA Q600 TGA instrument, all the samples (5–10 mg) were analyzed with a heating rate of 10 °C/min from room temperature to 900 °C and a 5 min plateau at 105 °C.

4.3 Results and discussion

4.3.1 Model phenol resins synthesis and characterization

4.3.1.1 Resin synthesis

The conversion of phenol models after 1, 2, 3, and 4 h are shown in **Figure 4. 3** It is clear that the reaction of phenol, o-cresol, and m-cresol was very fast and the phenols were largely converted in the first hour. The final conversion was more than 88%. However, for 2,6-dimethylphenol and 4-ethylguaiacol the reaction was relatively slower, and the final conversions were 86.70% and 18.80%, respectively. **Table 4. 2** shows the yield of the model phenol resins. The yields of PA, OCA, and MCA are similar, whereas the yield of DPA and EGA is significantly lower than the other resins. The yield value of EGA is only 15.5% due to its unreactive alkyl and methoxy groups.

The conversion of the mimic of OIL1WI product (composition showed in Table 4. 1) is shown in Figure 4. 3**.** Compared to reaction with a single model compound, phenol, o-cresol, and m-cresol have a relatively low reaction rate in the first hour, whereas their final conversion was higher (above 90 %). The increase in conversion of DPA and EGA is more important. These results probably indicate that the mutual promotion mechanism of phenolics, the cross-linking reaction of more reactive phenols and less reactive phenols have occurred. As bio-oil has consisted of small molecules and various phenols, the polymerization reaction of all these compounds could be promoted when using bio-oil as the precursor.

Table 4. 2 The phenol monomer used, yield and hydroxyl number of the MPA resins

Resin name	Phenol monomer	Molar mass (g/mol)	Yield (wt %)	Hydroxyl number (mmol/g)	Theoretical hydroxyl number*
PA	phenol	94.11	82.21	8.56	8.33
OCA	o-cresol	108.14	82.17	7.67	7.45
MCA	m-cresol	108.14	83.39	7.78	7.45
DPA	2,6-dimethylphenol	122.16	76.06	6.18	6.75
EGA	4-ethylguaiacol	152.19	15.50	4.41	5.61

* Calculated from 1000/ (molecular mass of phenolic monomer + 26). 26 results from the addition of 1 molecule of acetaldehyde and the elimination of 1 molecule of water per molecule of phenolic monomer.

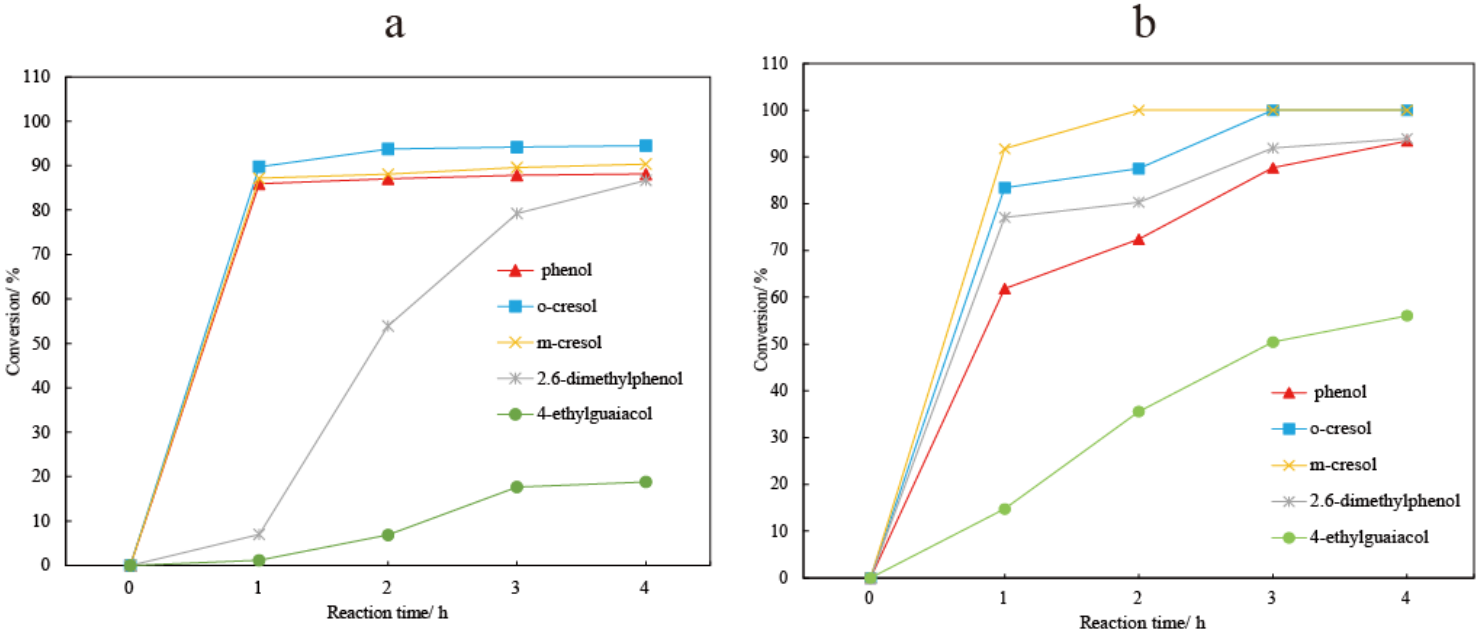

Figure 4. 3 The conversion of a. individual phenol models during the 4 h reaction with acetaldehyde. b. the phenolics in the mimic resin during the 4 h reaction with acetaldehyde.

4.3.1.2 Chemical characterization

After resinification and purification, the obtained PA resin has a dark amber color. The color of the model phenol resins like OCA and MCA is close to PA, whereas the resins like DPA, EGA, and mimic are darker than PA.

The FTIR spectra were shown in Figure 4. 4 illustrate the changes in the functional groups in the resins. The stretching modes at 2964, 1600, 1512, and 1450 cm^{-1} of the resins are attributed

to the methyl group (–CH_3), aromatic C=C, and methine (–CH–), respectively, which indicate the condensation reaction between the aldehyde in acetaldehyde and the phenol to form –$CH(CH_3)$– linkages. All peaks appearing here illustrate the successful synthesis of the MPA resins. The absorptions at 1050 cm^{-1} are due to C–O–C stretching, which reveals the methoxy of guaiacols, as evidenced by the strong absorption for EGA. The wide absorbance band at around 3300 cm^{-1} is due to O-H stretching, and the peaks located in the range of 1210 cm^{-1} are assigned to the C-O stretching of aromatics. Both of these peaks are assigned to the stretching vibration of active phenolic hydroxy in the resin structure, and they are clear and strong in all the MPA resins, whereas the peak of EGA is weaker than the others.

The hydroxyl number of resins can be more accurately quantified by the titration method (**Table 4.2)**. The rank of hydroxyl number of MPA resins was: PA ＞ MCA ＞ OCA ＞ DPA ＞ EGA. These results confirm those obtained by FTIR.

The oligomers in the resin samples were separated and identified by LC-MS [243]. As shown in **Figure 4. 5**, the monomer, dimer, trimer, tetramer, and pentamer were separated thoroughly and were present in all the MPA resins. (2.92%, 41.99%, 24.47%, 18.51% and 12.11% for PA resin, respectively). However, the methoxy and alkyl groups in the model phenols reduced the

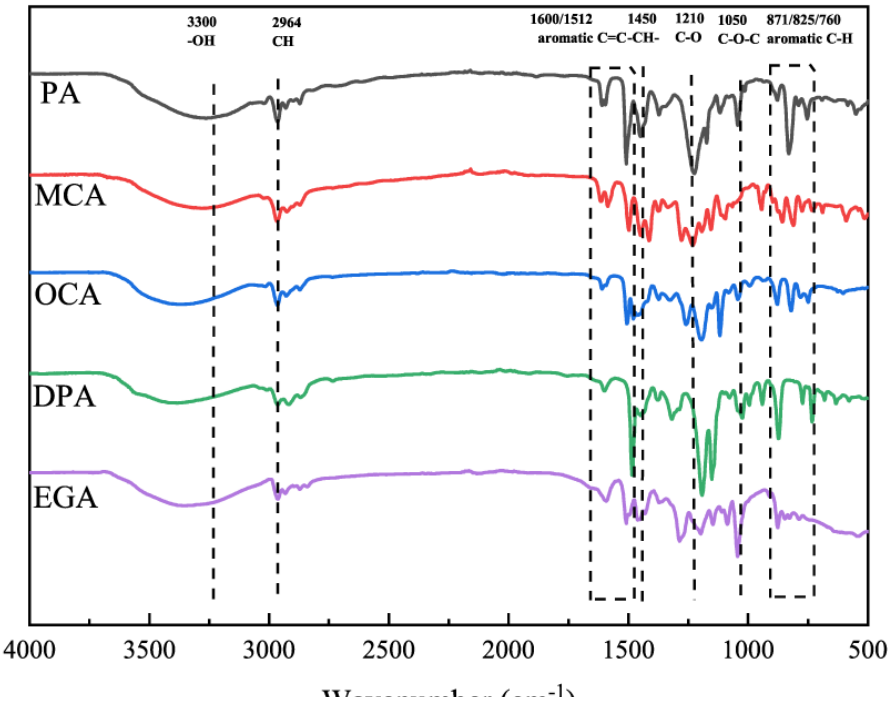

Figure 4. 4 FTIR graph of model phenol resins

solubility of the oligomers in the resins. As a result, their retention time is delayed compared with PA.

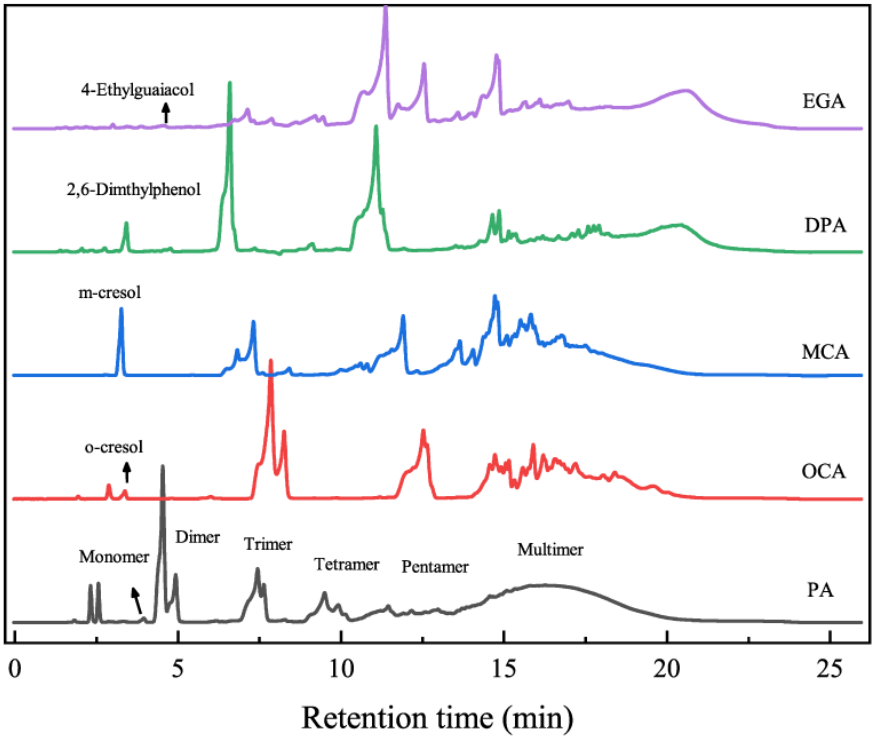

Figure 4. 5 Liquid chromatograms of model phenol resins.

4.3.1.3 Thermal Characterization of MPA resins

Glass transition temperature (T_g), initial decomposition temperature (5% weight loss-T_{d5}), the temperature of maximum decomposition rate (top of the peak of the thermogram derivative-T_{max}), and the char residue formed at 800 °C (R_{800}), were determined and their values are presented in **Table 4. 3**.

The T_g value of the novolac resins is in the range of 44 to 68 °C. A large difference between MPA resins is observed. Indeed, PA has the largest Tg value (67.7 °C) whereas EGA has the lowest one. T_g value seems to be correlated to the degree of polymerization.

The thermal stability of the non-volatile content of the resins was also evaluated by TGA. As shown in Table 3, the 5% weight loss of resin made by o-cresol, 2,6-dimethylphenol, and 4-ethylguaiacol is higher than that made by phenol. Furthermore, the most intense peak of the

thermogram derivative (DTG) also reflects the reaction degree of the resins. Indeed, 4-ethyl guaiacol and 2,6-dimethylphenol that a low degree of polymerization has a relatively weak value of T_{max} (220.0 °C and 279.5 °C, respectively).

Table 4. 3 Glass transition temperature (T_g), initial decomposition temperature (T_{d5}), the temperature of maximum decomposition rate (T_{max}), and char residue formed at 800 °C (R_{800}) of the MPA resins

Resin name	phenol monomer	T_g (°C)	T_{d5} (°C)	T_{max} (°C)	R_{800} (%)
PA	phenol	67.7	189.9	351.8	9.56
OCA	o-cresol	65.0	198.4	352.6	10.81
MCA	m-cresol	51.3	187.3	333.9	4.33
DPA	2,6-dimethylphenol	51.4	197.9	279.5	5.09
EGA	4-ethylguaiacol	44.5	202.5	220.0	9.59

4.3.2 Bio-oil and mimic acetaldehyde resins

4.3.2.1 Resin synthesis and characterization

Bio-oil fractions were selected as phenol precursors for bio-oil phenolic resin synthesis. A series of comparisons between traditional PA resin, mimic resin, and BOA resin was carried out. After purification, the obtained mimic resin has a deep amber color, darker than PA. All the BOA resins have a deep black color. ^{1}H NMR spectrum of BOA resin is shown in **Figure 4. 6**. The big peak at 2.06 ppm belongs to the solvent peak of d^6-acetone. The region between 8.5 and 6.5 ppm in the spectrum represents the protons of the aromatics derived from the phenolics of the bio-oil in the BOA resin. The peak around 9 ppm is the proton of the aldehyde group from free acetaldehyde and the bio-oil. The peak around 8 ppm is due to the proton of the phenol hydroxyl group. The resonances between 4.0 and 3.5 ppm represent protons belonging to the methoxy group, which is related to the existence of guaiacols. 3.0 and 2.2 ppm represent protons located in the alpha to ketones, aldehydes, or carboxyl groups and benzylic protons. Both peaks are due to the use of the bio-oil. The methine (–CH–) proton peak located around 4.3 ppm and the peak at 1.37 ppm were assigned to the methyl group ($–CH_3$) from $CH(CH_3)–$ linkages. This indicates the link between phenolics and acetaldehyde and confirms that the resin synthesis was successful [158, 166].

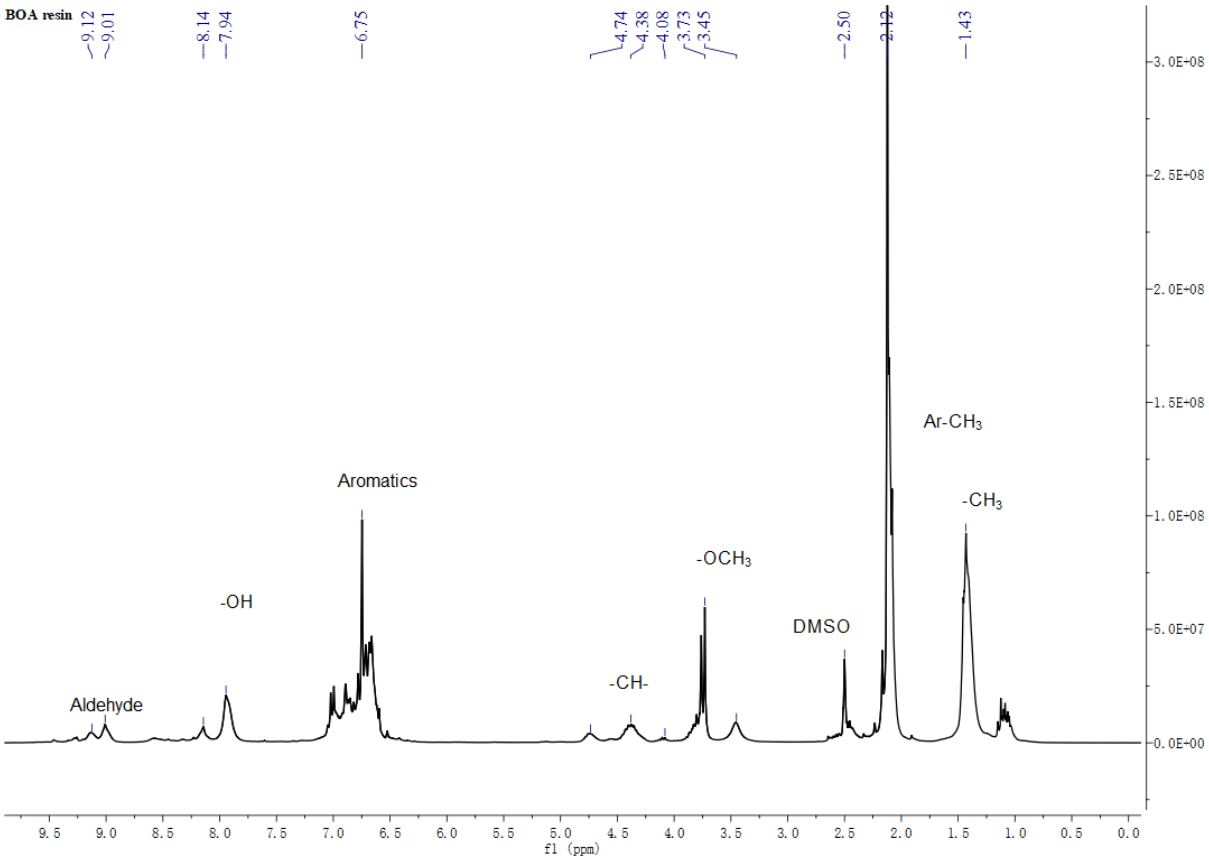

Figure 4. 6 ^{1}H NMR spectrum of BOA resin (10% HCl).

Figure 4. 7 shows the yield and yield by phenol for different resins based on phenol models, mimic, and bio-oil fractions. The yield of resin reflected the degree of the polymerization reaction. The determination "yield" is based on the mass of bio-oil whereas "yield (phenol)" refers to the mass of phenols in bio-oil. The difference value between "yield" and "yield (phenol)" indirectly emphasizes the cross-polymerization of chemical compounds different from phenols. The data show that the "yield (phenol)" of BOA resins is higher than that of "yield". This extra part of yield indicates that the cross-polymerization of compounds such as between aldehydes and ketones took place. Correspondingly, using fractional condensation, the bio-oil (OIL1) showed a higher yield (phenol) compared to the bio-oil water-insoluble fractions. The water extraction step efficiently removes small reactive compounds, promoting a larger proportion and a higher concentration of phenol compounds in the water-insoluble phase. Furthermore, compared with OILSWIA and OIL2WIA, yield and yield (phenol) values are close and near to the yield of PA.

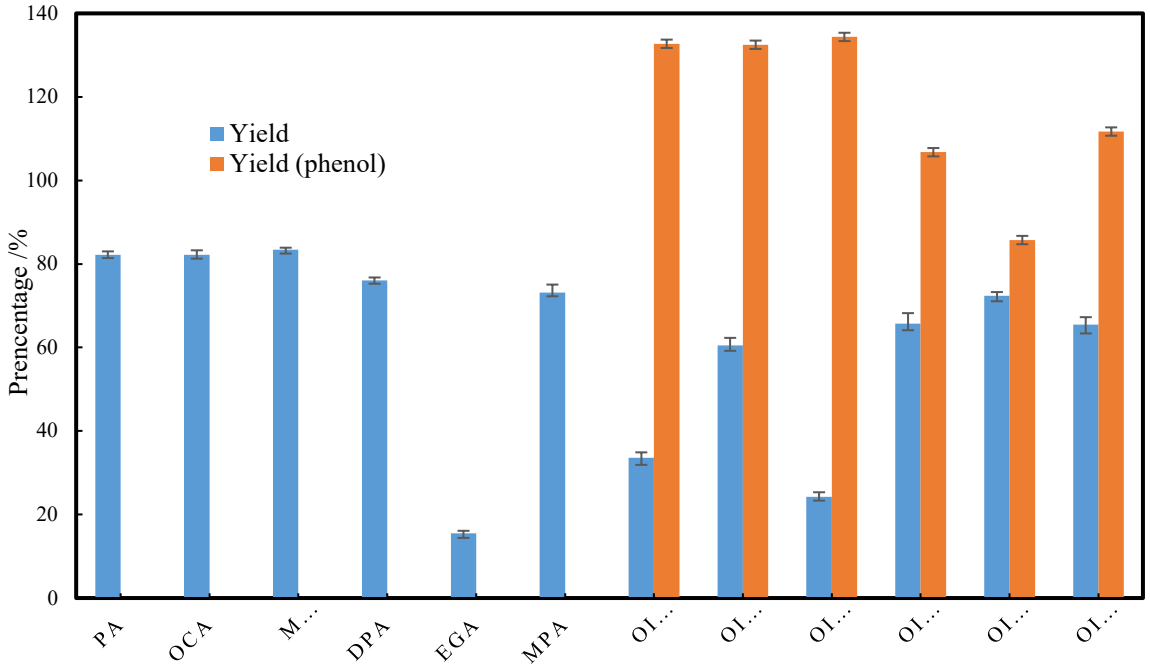

Figure 4. 7 The yield of PA, mimic, and BOA resins

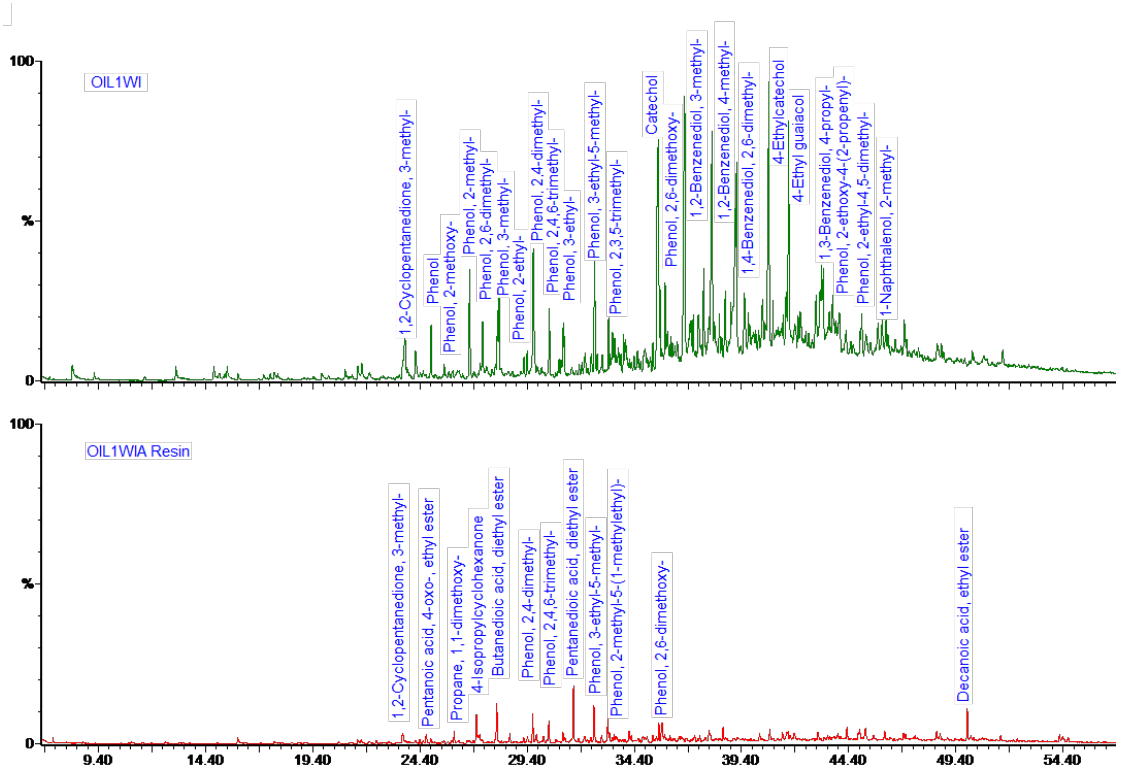

Figure 4. 8 GC-MS chromatograms of the OIL1WI and OIL1WIA resin

Thus, it is likely that the resin properties of OIL1WIA and PA resins are similar. As seen on GC/MS spectra of OIL1WI fraction and OIL1WIA resins (**Figure 4. 8**), few phenolic compounds were detected in the OIL1WIA resin, such as phenol, 2,4-dimethyl-, phenol, 2,4,6-trimethyl-, phenol, 3-ethyl-5-methyl-, phenol, 2,6-dimethoxy- and few new synthesized esters

were formed after the resinification. This qualitative observation seems to validate the yield analysis.

4.3.2.2 Properties comparison between bio-oil and model resin

Figure 4. 9 shows the FTIR spectra comparing the changes in the functional groups of the PA, mimic, and OIL1WIA resins. It is obvious that the peaks associated with the formation of the –$CH(CH_3)$– linkages (2964, 1600, 1512, and 1450 cm^{-1}), increase in the OIL1WIA resin compared to the bio-oil (OIL1WI). The mimic, and OIL1WIA resin have strong absorption at 1050 cm^{-1} due to the C–O–C stretching of guaiacols. The band at 1702 cm^{-1} was correlated with the aldehyde group in the bio-oil according to the incomplete separation of the families with the C=O group. The peaks at around 3300 cm^{-1} and 1210 cm^{-1} are assigned to the O-H and C-O of the phenolic hydroxy group in the resins. They became stronger in the PA resin than in the mimic resin and OIL1WIA resin. According to the titration method, the hydroxyl number of the PA and mimic resins is higher than the OIL1WIA resin, as shown in **Figure 4. 10**.

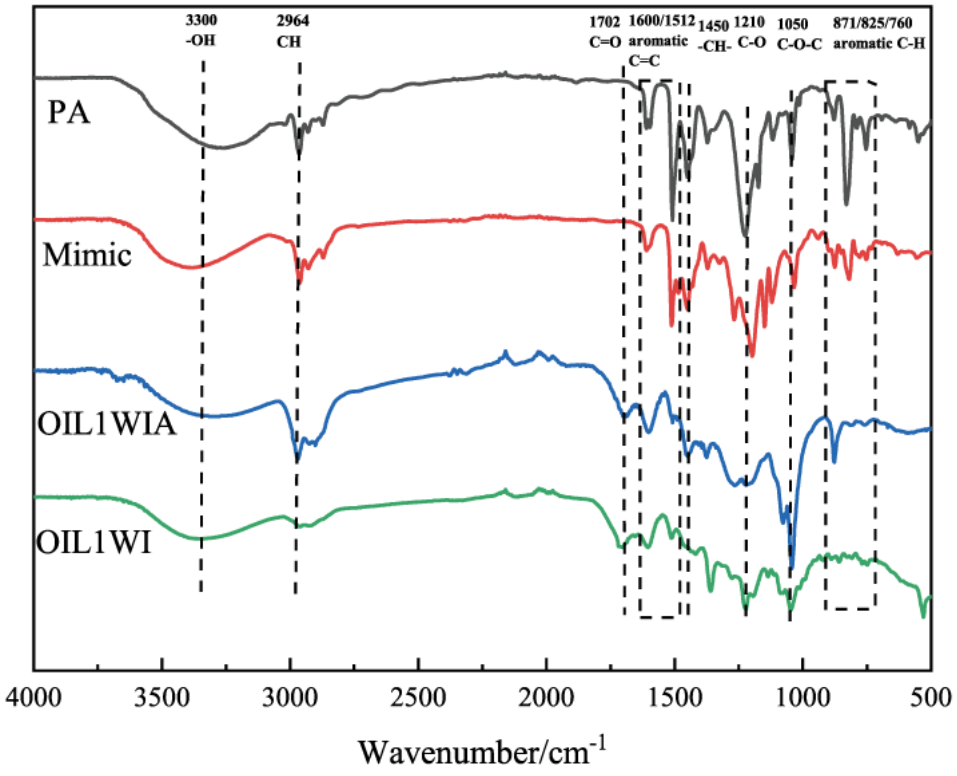

Figure 4. 9 FTIR graph of the PA, mimic, and OIL1WIA resin and bio-oil

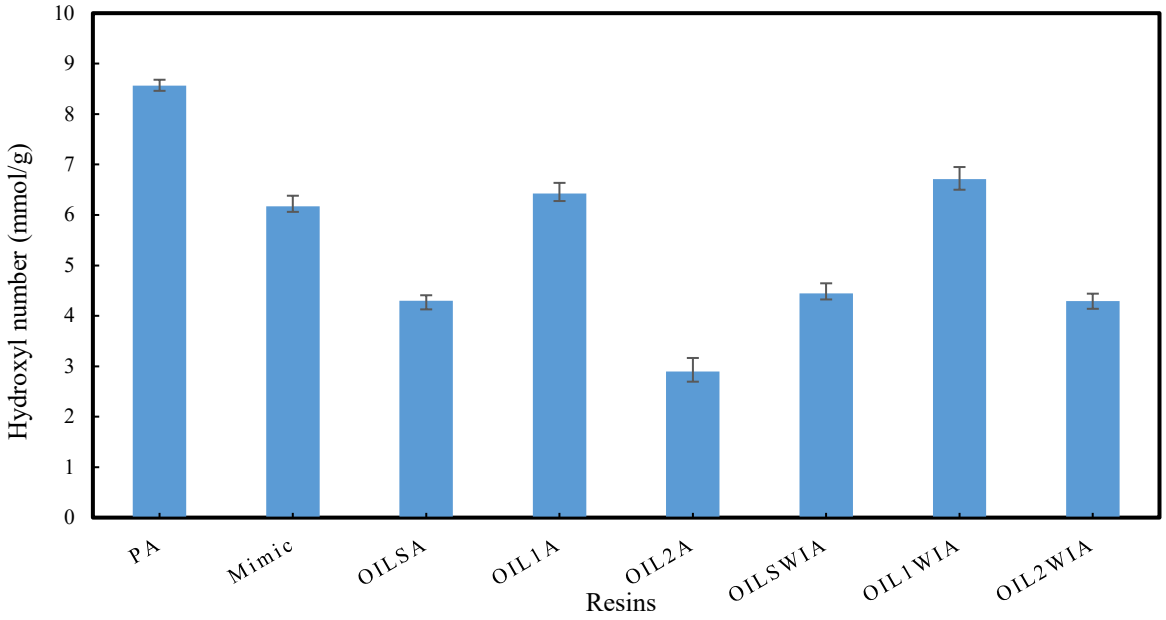

Figure 4. 10 The hydroxyl number of the resin

Furthermore, the use of water extraction fraction of the bio-oil as the phenol precursor conserved more hydroxyl groups than the other bio-oil product.

To analyze further the promising resin OIL1WA, the molecular weight distribution of this resin is compared with mimic and PA resin as indicated in **Table 4. 4**. GPC profiles of the OIL1WIA resin (**Figure 4. 11**) displayed a broader molecular weight distribution than that of the PA and mimic resin and had higher M_w and M_n values (Mw = 3494 g/mol, Mn = 1136 g/mol, polydispersity = 3.08). The reaction of phenols and aldehydes generally occurs in the ortho-para position of phenolic hydroxyl groups, and the reactivity of phenol models decreases with the increase in the substituents [244]. Since some of the ortho and para positions of the phenolic hydroxyl groups were occupied by the methoxy group, the polymerization of 4-ethylguaiacol, for example, became more complicated due to steric hindrance. Hence, the phenolics in the mimic resin have fewer reactive positions per molecule than the phenol, leading to the small length of the polymer.

Table 4. 4 GPC of the PA, mimic and OIL1WIA resin

Resin	M_n(g/mol)	M_w (g/mol)	Polydispersity
PA	831	1204	1.45
mimic	731	1147	1.57
OIL1WIA	1136	3494	3.08

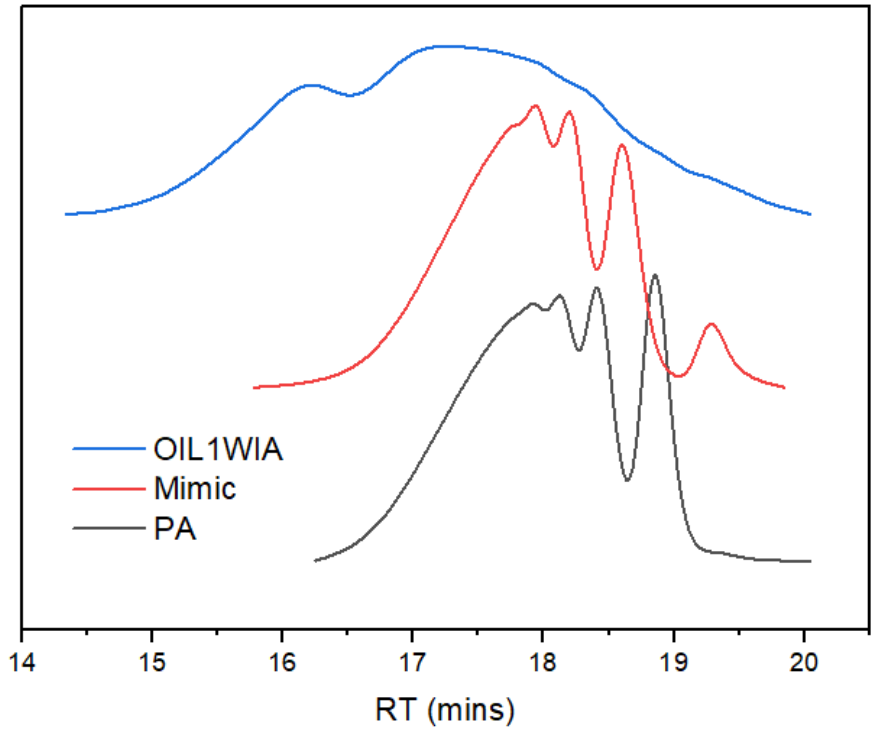

Figure 4. 11 GPC chromatograms of the PA, mimic, and OIL1WIA resin

Otherwise, The GPC profile of the OIL1WIA resin displayed a broader molecular weight distribution than that of the PA and mimic resin, resulting in larger dispersity (3. 08). The size of the resin is also larger (M_w = 3494 g/mol, M_n=1136 g/mol). Unlike the composition of the mimic only contains five kinds of phenols, a real bio-oil contains many small molecules and other more reactive phenols such as catechol, leading to a gap in characteristics.

4.3.2.3 Thermal characterization of resins

The thermal analysis results from DSC, TGA, and DTG (T_g, T_{d5}, T_{max}, and R_{800}) are listed in **Table 4. 5**. Concerning glass transition phenomena, the T_g value evolves according to the following sequence: PA > mimic > OIL1WIA > OILSA resin. It is clear that water extraction upgrading of the bio-oil can effectively improve the T_g value of the BOA resins as the latter gets closer to the value of the model resin. For clarifying the comparison, thermograms of the PA, mimic, and OIL1WIA resins are shown in **Figure 4. 12.** Moreover, as shown on the DSC thermogram the T_g of the PA and mimic resin is clear and sharp, whereas the bio-oil resin has a relatively lower glass transition temperature and the changes are moderate. The curve of the OIL1WIA resin has also a slight rise when the temperature increases. The bio-oil contains some unreacted small compounds, which increases the heterogeneity of formed resin, and some

plasticization reactions occurred simultaneously, making the OIL1WIA resin a very complex structure according to its molecular distribution mentioned above [160].

Table 4. 5 Glass transition temperature (T_g), initial decomposition temperature (T_{d5}), temperature of maximum decomposition rate (T_{max}), and char residue formed at 800 °C (R800) of the resins

Resin name	phenol monomer	T_g (°C)	T_{d5} (°C)	T_{max} (°C)	R_{800} (%)
PA	Phenol	67.7	189.9	351.8	9.56
mimic	Model phenols	63.6	181.6	338.7	5.62
OILSA	OILS	42.7	172.9	254.9	30.29
OIL1A	OIL1	43.3	200.0	291.7	32.24
OIL2A	OIL2	43.5	175.4	232.1	26.95
OILSWIA	OILSWI	58.9	199.7	332.1	29.35
OIL1WIA	OIL1WI	57.0	209.8	345.9	31.41
OIL2WIA	OIL2WI	57.3	205.4	336.4	30.90

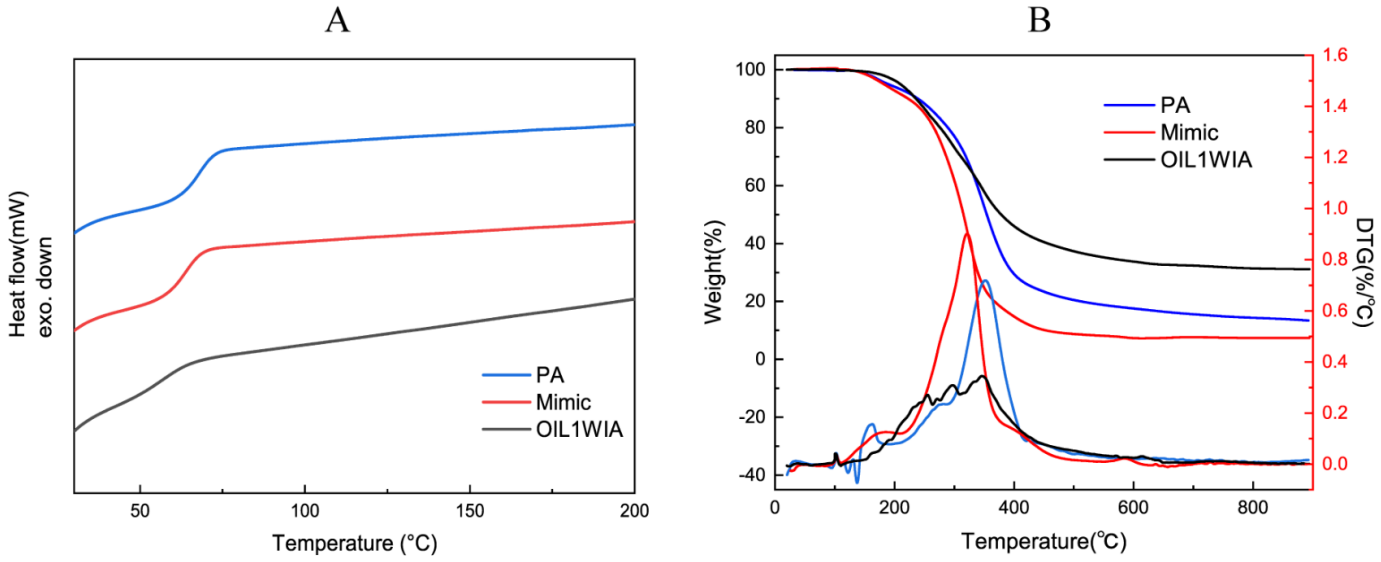

Figure 4. 12 A. DSC, B.TG and DTG profiles of the uncured PA, mimic, and OIL1WIA resin

The thermal stability of the non-volatile contents of the resins was also evaluated by TGA. As shown in **Table 4. 5**., the 5% weight loss temperature of the resin made by the bio-oil water-

insoluble fractions is higher than that of the bio-oils due to their higher reactivity demonstrated after separation. The mimic resin, which contains a large percentage of 4-ethylguaiacol and 2,6-dimethylphenol, has a relatively small T_{max} compared to the PA resin due to its incomplete polymerization, the comparison of yields illustrated this view (**Figure 4. 7**). The GPC result also reveals that the molecular weight of the mimic resin is lower than that of the PA resin, inducing a lower degradation temperature. In addition, the use of water extraction bio-oil fractions improved the thermal characteristic of the resin. Indeed, the T_{max} of OIL1WIA is the highest (345.9°C) and is the closest to the PA resin among all the BOA resins. As shown in **Table 4. 5**, the residual carbon content at 800 °C for the BOA resins was higher than for the MPA resins (comp. **Table 4. 3**). This is probably caused by the cross-linking of numerous side chains from the bio-oil molecules [160].

In summary, the comparison of various bio-oil precursor to produce a novolac resin demonstrate that OIL1WI is more suitable to produce phenol resin among the bio-oil products to achieve chemical characteristics approaching that of the PA resin. Moreover, OIL1WIA resin displayed a comparable thermal resistance to that of the pure PA resin and has a higher crosslinking ability.

4.3.3 Effect of bio-oil phenol ratio on novolac phenol acetaldehyde resins

Based on the previous part, OIL1WI is more suitable to produce phenol resin among the bio-oil products to achieve chemical characteristics approaching that of the PA resin. The partial incorporation of bio-oil phenol precursor in PA resin, as well as catalyst concentration, are further studied to evaluate its potentiality to replace the petrochemical source of phenol.

4.3.3.1 Resin synthesis

Figure 4. 13 illustrates the conversion of acetaldehyde and phenol as well as the yield of the resin synthesis for different concentrations of an acid catalyst. Overall, regardless of the amount of catalyst used, both bar charts have a similar trend in both conversion and yield. The conversion of acetaldehyde decreased when the ratio of the bio-oil increased, indicating that it is more difficult for the bio-oil to react with acetaldehyde than phenol. Moreover, the conversion of phenol grows with the increase in the bio-oil ratio because the addition of bio-oil brings some small molecules, improving the probability of multiple crosslinks and resulting in the decrease in phenol monomers. However, a higher acid concentration allows for increasing both acetaldehyde and phenol conversions. In addition, the acetaldehyde conversion in BOPA resins is closer to that of PA resins regardless of the proportion of bio-oil. It is also interesting to notice

that the free phenol cannot be detected in the case of BO75PA and BOA resins. Many phenols and their oligomers with long alkane chains or methoxy, such as guaiacol, do not react easily with acetaldehyde, while in a strong acid environment, the reaction is facilitated, leading to an increase in phenol conversion. As predicted, the high acid catalyst content can facilitate the cross-polymerization reaction between bio-oils and acetaldehyde, improving the conversion rate of acetaldehyde due to the addition of bio-oils.

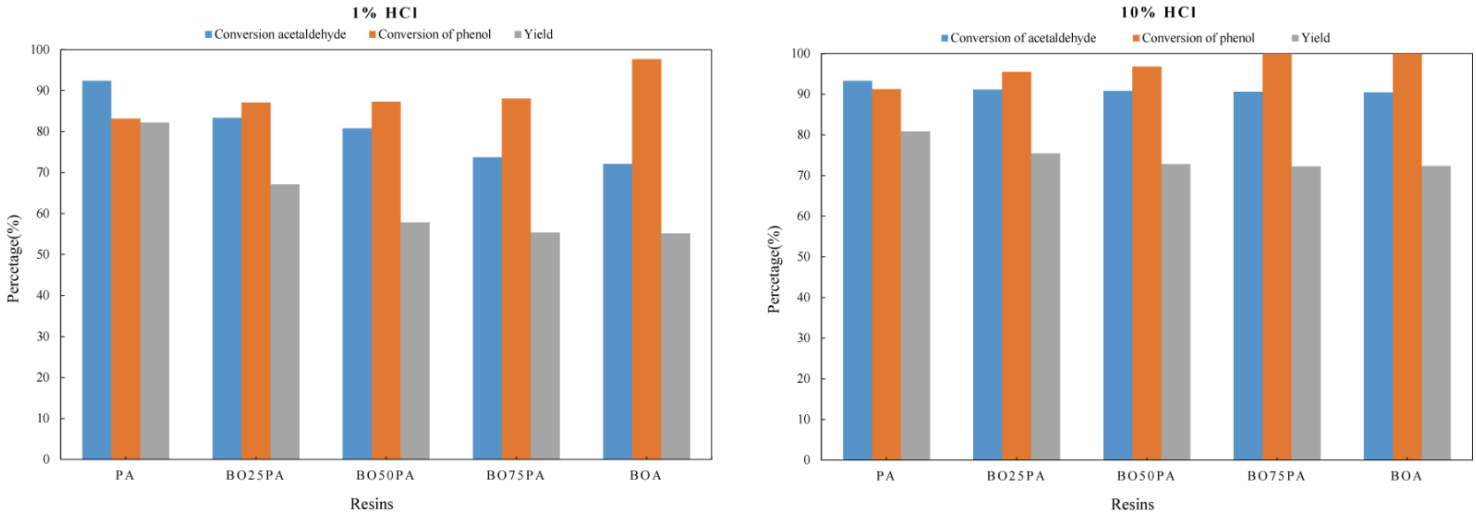

Figure 4. 13 The conversion of reagents and yield of BOPA resins with 1% and 10% HCl added

The resin yield reflected the degree of polymerization. It is noted that there is a diminution of the yield with the ratio of the bio-oil using 1% acid, which means the diverse oligomers in the bio-oil are less reactive than phenol. However, when 10% acid is present in the reactive media, the yield remains nearly unchanged (70%) and is close to the yield of the PA resin regardless of the ratio of the bio-oil added. The acid catalyst accelerates the reaction of unoccupied reactive sites of the bio-oil, such as alkyl and methoxy groups, significantly reducing the incomplete polymerization. There is no clear difference in the PA resins when 10% HCl is used, while there is a visible change between the BOPA resins. Overview, using high acid catalyst content can produce BOPA resins with lower free phenol, higher acetaldehyde conversion, and higher yield.

4.3.3.2 Characterization

Figure 4. 14 shows the FTIR profiles of the phenol-acetaldehyde resins and the bio-oil phenol resins with different ratios of bio-oils for both 1% and 10% acid catalyst. They illustrate the changes in the functional groups in the resin. The wide absorbance band at around 3300 cm^{-1} is due to O-H stretching, and the peaks located at 1210 cm^{-1} are assigned to the C-O stretching of aromatics. Both peaks are assigned to the stretching vibration of active phenolic hydroxy in the

resin structure. When the ratio of the bio-oil increases, the intensity of the signal is reduced, corresponding to a lower phenolic hydroxy content in the bio-oil phenol resin than that of the phenol resin. Furthermore, the improvement of condensation reactions is evidently using a high catalyst content (10% HCl) as peaks associated with the formation of –CH(CH_3)– linkages (2964, 1600, 1512, and 1450 cm^{-1}). The decrease in strength of the band correlated with the aldehyde group at (1702 cm^{-1}), also in the BOPA resins with 10% HCl was greater than with 1% HCl, which indicates that more crosslink reactions were happening.

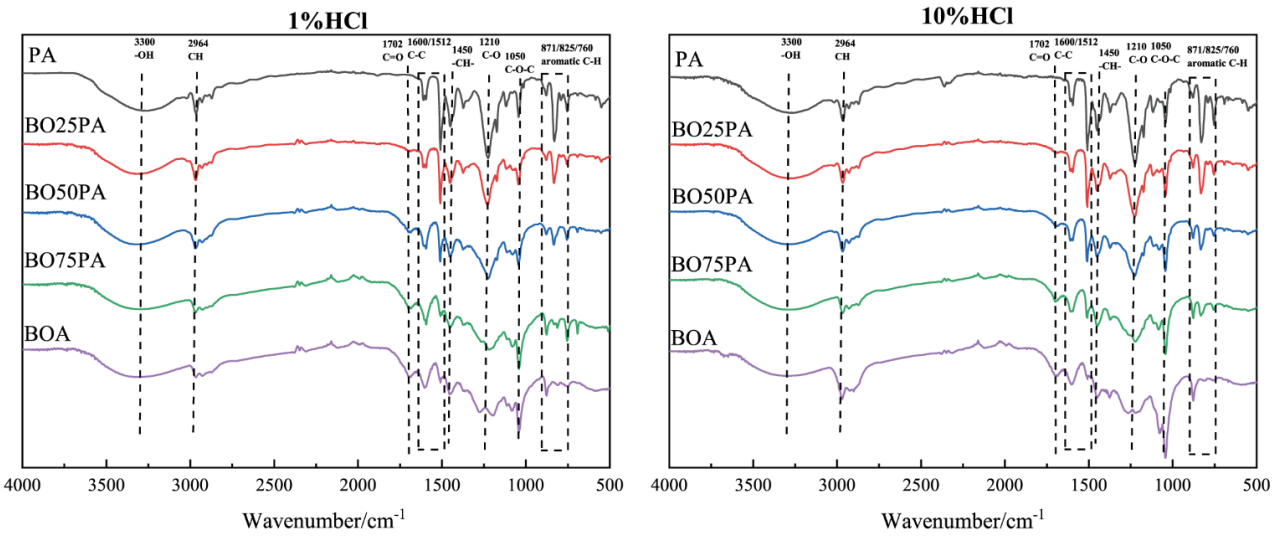

Figure 4. 14 FTIR graph of BOPA resins when 1% and 10% HCl are used as a catalyst.

The hydroxyl number of phenol from the OH titration, displayed in **Figure A 3. 2** is consistent with the FTIR results. Regardless bio-oil ratio, the use of high HCl content can maintain an interesting hydroxyl number close to those of the PA resins (8,69 vs 6,7 mmol/g for PA and BOA respectively). The molecular weight distribution of all resins was obtained from chromatograms, as shown in **Table A 3.2**. According to GPC these chromatograms presented in **Figure 4. 11**, the peak positions of the resins move to a lower retention time when the bio-oil ratio increases, and their profiles are broader than those of PA. In the resinification using 1% HCL, the GPC curves of PA, BO25PA, and BO50PA could be separated into two parts: oligomers and polymers. The increase in bio-oil directly results in a decrease in the oligomer peak. In addition, a high acid content also induces a decrease in the oligomer peak. Indeed, the oligomer peak disappeared and a new peak was generated in the high molecular weight part at the same time in the BO50PA, BO75PA, and BOA resins. Small molecules and phenolic compounds contained in bio-oil, very reactive can easily participate in the multi cross-polymerization reactions. Thus, the more bio-oil is added, the more the value of M_w and the

molecular weight distribution increase gradually, promoted by a high concentration in a catalyst.

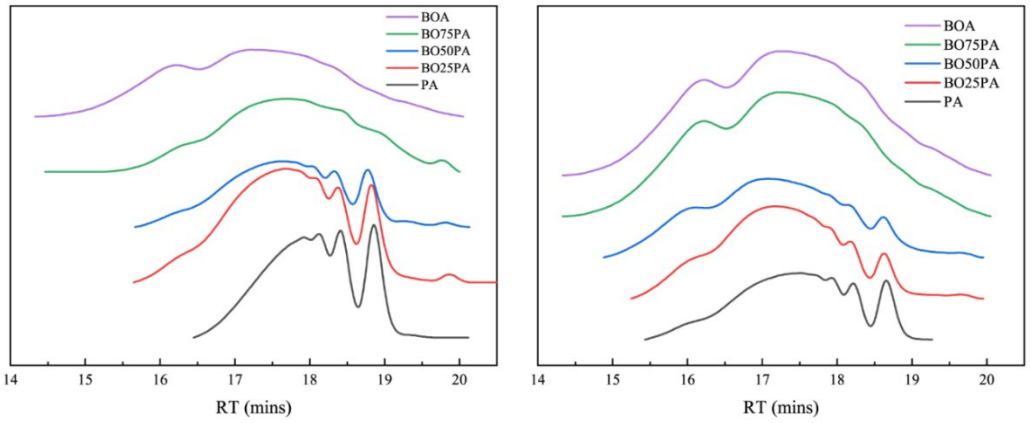

Figure 4. 15 GPC chromatograms of BOPA resins synthesized with 1% (left) and 10% HCl (right) as a catalyst.

4.3.3.3 Thermal characterization of resins

Table 4. 6 present the results of thermal analysis of PA and BOPA resins by using 1% and 10% HCl catalyst. The T_g values of the resins are in the range of 57 to 68 °C and decrease with the addition of the bio-oil in both acid environments. As discussed previously (**4.3.2.2**), the addition of small compounds present in bio-oil promotes the plasticization reactions making the structure of the BOPA resins very complex. Moreover, a high acid catalyst concentration favors cross-linking reaction that consumes more unreacted compounds, resulting in a higher glass transition temperature.

The thermal stability of the non-volatile contents of the resins was also evaluated by TGA. It is evidenced that the 5% weight loss of resins has an opposite trend with T_{max} when increasing the amount of bio-oil. The T_{d5} of the BOPA resins relies on the polymerization reaction between the phenolics and aldehyde. As the proportion of bio-oil increases, T_{d5} shows a rising tendency. Unlike the insignificant change in T_{d5}, T_{max} changes significantly under the two acidic conditions; in particular, the T_{max} of BOA resin reaches 235.2 °C in the case of 1% HCl and 345.9 °C for 10% HCl. The result indicates that high catalyst content aims to speed up the reaction by reducing the steric hindrance between aldehyde and the phenolic compounds contained in bio-oil. The higher crosslinking reaction occurrence in high acid content is confirmed by the higher residual carbon content obtained in these operating conditions.

Table 4. 6 DSC, TGA, and DTG results of PA and BOPA resins using 1% and 10% HCl catalyst

Catalyst (HCl)	Resin name	Molar ratio Phenol: Phenol (bio-oil)	T_g (°C)	T_{d5} (°C)	T_{max} (°C)	R_{800}(%)
1 mol.%	PA	100:0	67.7	190.1	351.9	9.6
	BO25PA	75:25	64.5	192.7	348.3	17.0
	BO50PA	50:50	59.0	196.1	295.6	26.7
	BO75PA	25:75	59.3	200.2	257.2	27.5
	BOA	0:100	56.1	206.8	235.2	29.8
10 mol.%	PA	100:0	67.8	194.9	359.9	10.4
	BO25PA	75:25	64.1	194.6	359.7	21.5
	BO50PA	50:50	63.4	200.9	357.1	27.9
	BO75PA	25:75	63.1	201.6	344.0	28.8
	BOA	0:100	57.0	209.8	345.9	31.4

4.3.4 Curing of PA, mimic and BOA resin

As shown in **Table 4. 7** and **Figure 4. 16**, all the temperatures of the curing reactions are between 98 and 200 °C, and OIL1WIA had a similar thermogram as PA resin. The mimic and BOA resin have a relatively lower initial onset temperature compared to PA, but the ranking of the peak temperature is mimic < PA < OIL1WIA resin. The use of a catalyst, such as triphenylphosphine (TPP), promotes this phenol–epoxy reaction, which is an adverse reaction. Furthermore, the chain-wise polymerization mechanisms of the novolac/DGEBA curing system using TPP as a catalyst included three main reaction steps: initiation, propagation, and branching [187]. The reaction mechanisms above are more adapted to the PA resin, while the reactions of DGEBA with the mimic as well as the OIL1WIA resin are more complex due to the existence of small compounds [242].

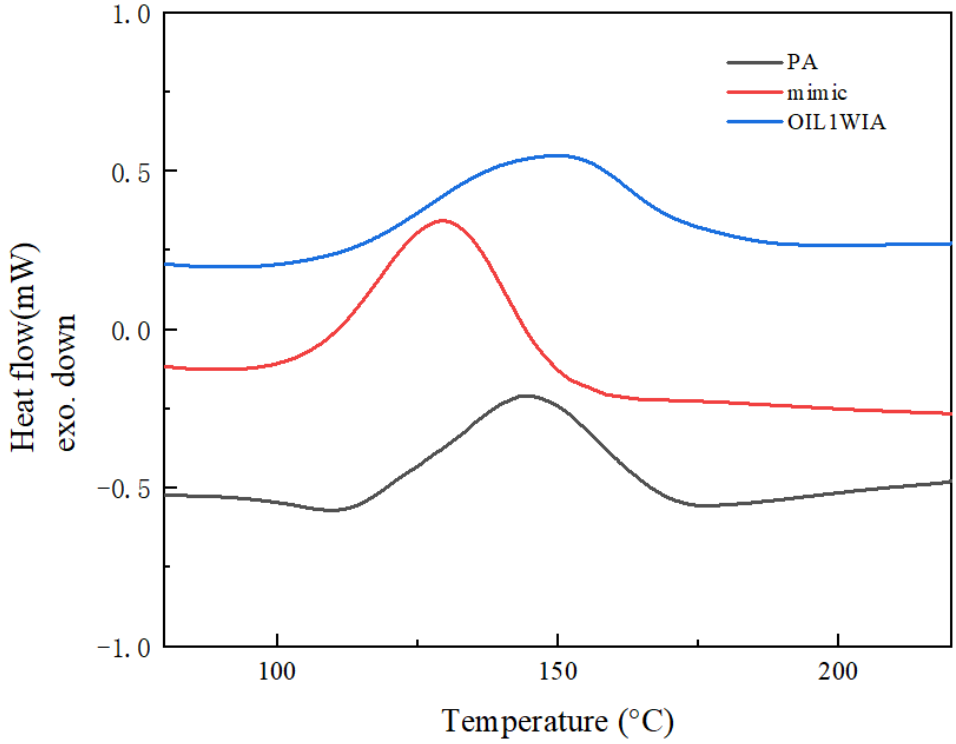

Figure 4. 16 DSC thermograms of PA, mimic and OIL1WIA resin at the heating rate 10 K/min

Table 4. 7 The kinetic parameters of the PA, mimic, and OIL1WIA resin curing with 40% DGEBA

Resin type		Heating rate (K/min)				Activation energy (kJ/mol)		n
		5	10	15	20	Kissinger	Flynn–Wall–Ozawa	
PA	Onset temp (°C)	107.7	117.9	124.4	126.1	94.9	96.8	0.95
	Peak temp (°C)	134.8	144.0	150.5	154.4			
Mimic	Onset temp (°C)	100.8	106.3	113.5	114.3	80.0	82.4	0.94
	Peak temp (°C)	118.8	130.2	136.0	140.3			
OIL1WIA	Onset temp (°C)	100.9	110.8	119.9	120.5	95.5	97.4	0.95
	Peak temp (°C)	138.4	147.5	154.8	157.8			

Table 4. 7 and **Figure 4. 17** show the values of activation energy E_a, order of the cure reaction n, and the correlation coefficient ($R^2 > 0.99$). The global curing reaction for all of the resins was

approximately first order ($n = 0.94 – 0.95$), which is consistent with previous studies [139, 245]. The mimic resin has the lowest value of E_a due to the presence of a lot of oligomers that make it easier to crosslink and cure with the epoxy groups. Additionally, the E_a value of the OIL1WIA resin is slightly larger than that of PA; this might be because the bio-oil contains a mixture of oligomers and polymers with a wide range of molecular weights, which have less unoccupied reactive sites and it is difficult for the hydroxyl group to participate in the curing reaction [139].

Overall, the utilization of the bio-oil as a phenol alternative to produce the phenol-acetaldehyde novolac resin can be a reasonable method to obtain a resin with a similar curing condition.

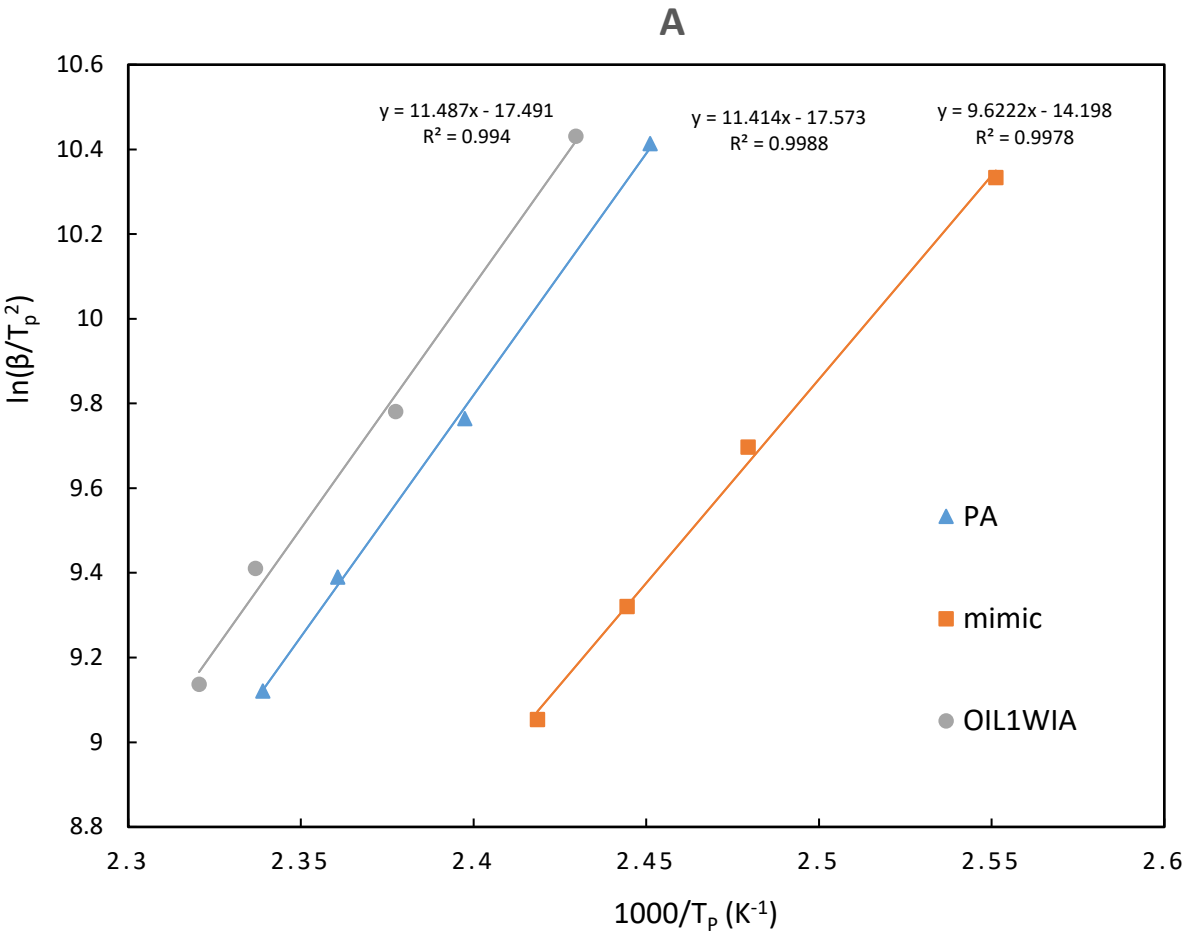

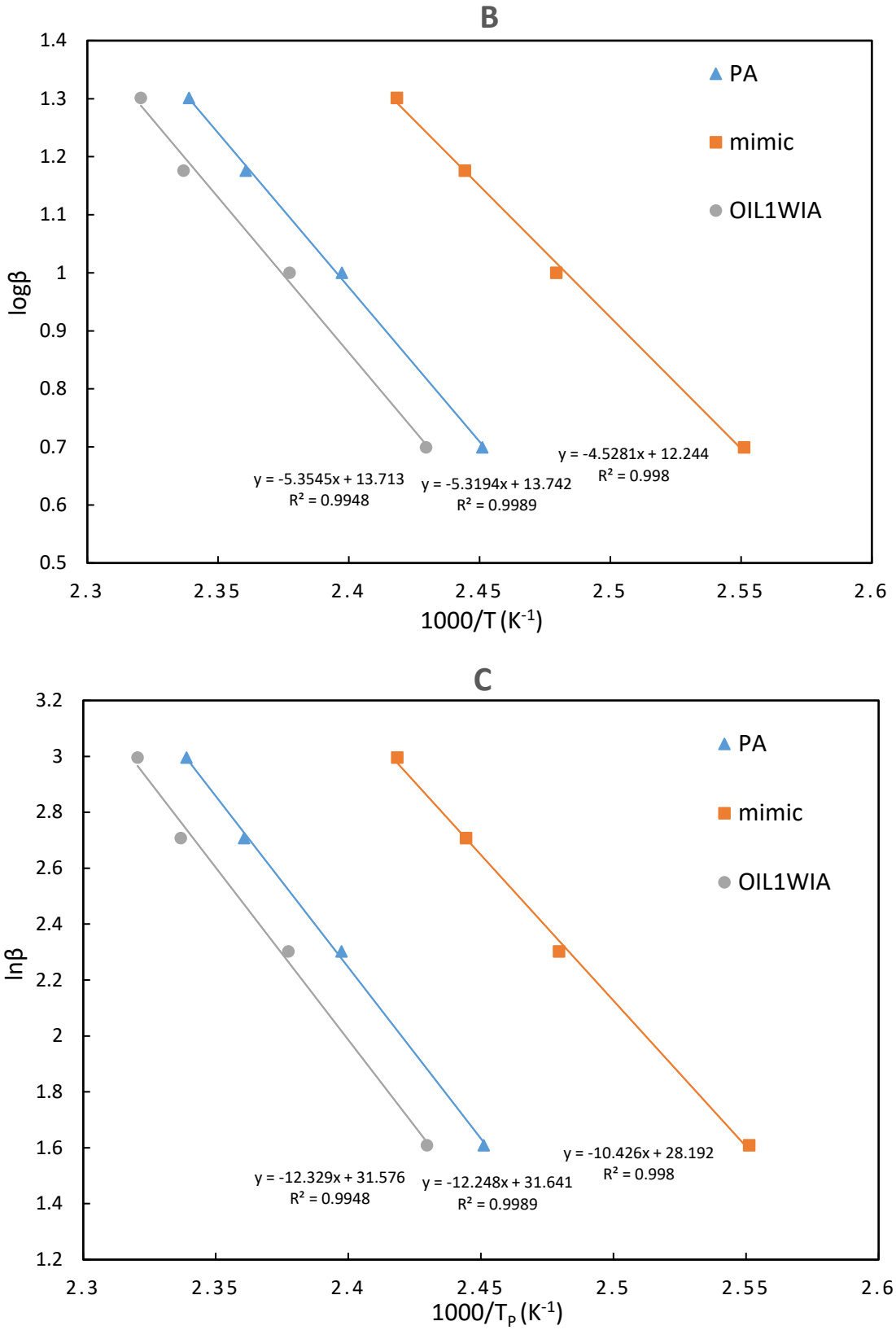

Figure 4. 17 Plots of the DSC kinetic analysis by the (A) Kissinger, and (B) Ozawa, and (C) Crane equations

4.3.5 Characterization of the cured novolac resins

FTIR spectra were also acquired to confirm the chemical structural characterization of the cured resin, as shown in **Figure 4. 18**. The pure DGEBA and the mixture of the OIL1WIA resin and DGEBA were used to study the curing reaction of the OIL1WIA resin. It is clear that the absorption band at 855 and 911 cm^{-1} corresponding to the characteristic peak of the oxirane ring was absent in the uncured and cured resins. In contrast, a strong and sharp peak was observed for pure DGEBA, which decreases when it is mixed with the OIL1WIA resin [120, 195]. After the curing procedure, the peak disappeared due to the reaction, indicating that almost all the epoxy groups were consumed in the curing process [197]. The increased absorption at 1030 cm^{-1} is due to the C–O–C stretching, which also confirms the presence of the ether groups in the cured resin.

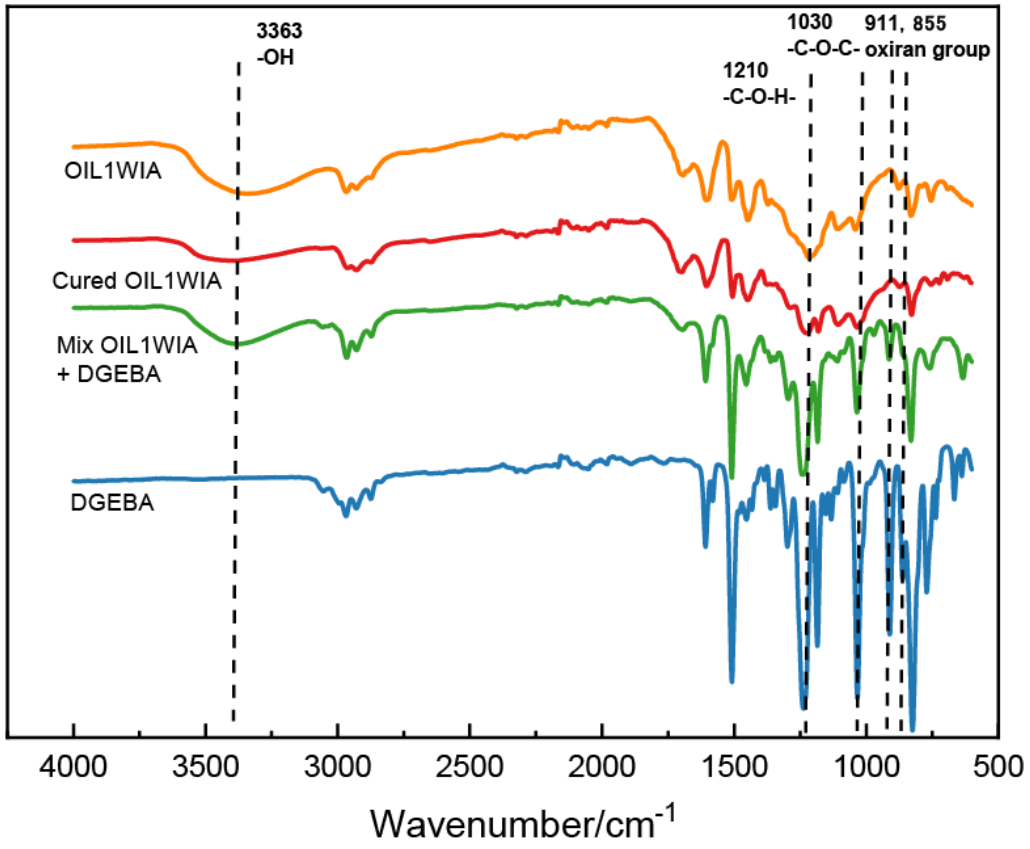

Figure 4. 18 FTIR spectra of the uncured OIL1WIA resin, cured OIL1WIA resin, the mixture of the OIL1WIA resin and DGEBA, and DGEBA

Also, both the wide peak around 3363 cm^{-1} (O-H stretching) and the peaks located in the range 1210 cm^{-1} (C-O stretching) indicate the reduction of the hydroxyl group. All the changes confirmed the curing mechanism: the reaction of phenol hydroxyl and the epoxy groups, as mentioned above.

Thermal stability is very important as a performance criterion of the cured resin and will ultimately affect its application value. The thermal stability of resins cured with 40% DGEBA was studied (**Table 4. 8)**. Compared to the thermal stability of the novolac resin, a significant improvement was obtained after curing. At the same DGEBA content, the cured PA, mimic, and OIL1WIA resin showed the highest initial and maximal thermal decomposition temperature as well as char yield at 800 °C. However, the trend of the initial thermal decomposition temperature of cured resins had some differences compared with the uncured ones. The T_{d5} of the PA and the mimic resin becomes higher than the OIL1WIA resin. Through curing, all resins are more stable, and the increase in the residue also explains the occurrence of cross-linking reactions.

Table 4. 8 Initial decomposition temperature (T_{d5}), the temperature of maximum decomposition rate (T_{max}), and char residue formed at 800 °C (R_{800}) of the cured resins

Resin	T_{d5} (°C)		T_{max} (°C)		R_{800} (%)	
	uncured	cured	uncured	cured	uncured	cured
PA	189.9	323.5	351.8	422.0	9.6	12.0
mimic	181.6	294.0	338.7	414.5	5.6	11.5
OIL1WIA	209.8	275.3	345.9	389.6	31.4	34.4

4.4 Conclusion

The polymerization of acetaldehyde with phenol models, mimic, and bio-oil products from fractional condensation (OIL1 and OIL2) and water extraction (OIL1WI and OIL2WI) were carried out successfully as confirmed by FTIR spectroscopy, HPLC, GPC, and GC analyses.

- Additional cross-polymerization has been put in evidence when bio-oil is used as a phenol precursor. Compared with the untreated bio-oil, the use of pyrolysis bio-oil from the high-temperature condenser obtained by fractional condensation upgraded with water extraction can significantly improve the chemical and thermal properties (T_g and thermal degradation) of the OIL1WIA resin. The latter is close to model phenol resin. This is due to its high content of phenolic compounds and fewer small compounds.

- The high catalyst content can shorten the difference and can produce excellent bio-oil-based resins with less free phenols and aldehydes, a higher degree of polymerization, and more phenolic hydroxyl groups. However, GPC analysis shows that the BOPA resins produced from 10% HCl had a broader and larger molecular weight distribution compared to resins produced from 1% HCl, which were closer to PA resins.
- The more environmentally friendly and effective curing agent, bisphenol A type epoxy (DGEBA), was used as a formaldehyde-free cross-linker for bio-oil-based phenol resins.
- The curing mechanism was investigated by DSC and FTIR analysis. The curing of the OILWIA resin and DGEBA started earlier than the PA resin (100.9 and 107.7 ℃), whereas the peak temperature has an opposite tendency at around 134.8 and 138.4 °C. The curing activation energy determined by Kissinger and FWO methods (E_a) is slightly higher for the curing of bio-oil resin at a bio-oil ratio higher than 75 wt%. The improved thermal stability of the DGEBA cured OIL1WIA resin demonstrates the potential feasibility of using water extraction pyrolysis oil to replace commercial phenol for producing a bio-based green material.

Chapter V

Synthesis and characterization of bio-oil-glyoxal novolac resins and bio-oil epoxy resins, and their curing system built

Abstract:

The synthesis of novolac uncured and cured with epoxy resin based on bio-oil fractions is discussed in this chapter. In particular, the replacement of aldehyde by glyoxal, a greener compound, was studied. Commercial phenol, mimic phenols and the water-insoluble part of bio-oil fractional condensation products were used to synthesize with glyoxal to produce the novolac type resins (PG, MPG, and BOG, respectively). Secondly, the water-insoluble fraction of bio-oil was used to synthesize the bio-oil based epoxy resin (BOE). The chemical structure of BOE was confirmed by FT-IR, GPC, and ^{1}H-NMR spectroscopy. In a third step, DGEBA and BOE will use as a formaldehyde-free cross-linker, and biochar was used for the first time as an additive for novolac resins curing to build a "greener" material. The kinetic parameters of the curing reaction and the physicochemical and thermal properties of PG, MPG and BOG resins before and after curing were compared.

5.1 Introduction

In addition to the replacement of phenol resources for producing a greener resin, researchers have focused on selecting a sustainable and less toxic alternative to formaldehyde for a phenol-formaldehyde resin over the past decade. Among potential and green aldehyde compounds (Hydroxymethylfurfural (HMF) [166], furfural [141], benzaldehyde [171], vanillin [135] and glyoxal), glyoxal with its two aldehyde groups, has high reactivity, is nontoxic and non-volatile [173]. Glyoxal is already proved to be an ideal substitute for formaldehyde in various applications [172].

Owing to the exceptional properties of epoxy resins [101, 102, 117, 118], the bio-based epoxy monomer or oligomer is developed to replace the commercial DGEBA, which consisted of bisphenol A [126, 127]. The bio-based epoxy resins are prepared from a variety of renewable resources such as vegetable oils [125, 128, 129]. The high purity bio-oil fraction with a large yield of phenolics will become a very effective alternative for commercial BPA in the field of bio-oil-based epoxy resin (BOE) production [201]. Biochar, a by-product produced in large amounts during the pyrolysis, will be used for the first time as an additive for novolac resins curing.

In this chapter, the first step consists of the study of the polymerization of glyoxal with commercial phenol, mimic phenols and the water-insoluble part of bio-oil of fractional condensation products to produce the novolac type resins (PG, MPG and BOG, respectively). In the second part, the bio-oil-based epoxy resin (BOE) is synthesized and characterized using different chemical analyses. Finally, curing of novolac resin using DGEBA and BOE as well as biochar as an additive is performed to build a "greener" material. The thermo-kinetic parameter and the physicochemical and thermal properties of different resins before and after curing are compared. The potential of bio-oil products to effectively replace commercial phenol is evaluated.

5.2 Experimental section

5.2.1 Materials.

Phenol (99%), o-cresol (99%), m-cresol (≥ 98%), 4-ethylguaiacol (≥ 98%), 2,6-dimethylphenol (≥ 99%), glyoxal (40%), oxalic acid (≥ 99%), ethanol, acetone (≥ 99%), sodium hydroxide (NaOH), potassium hydroxide (KOH), pyridine(≥ 99.5%, GC),

dichloromethane (≥ 99.8%, HPLC grade), acetic anhydride (≥ 99%), diglycidyl ether of bisphenol A (DGEBA) (≥ 99%), Triphenylphosphine (≥ 95.0%), epichlorohydrin (99%), benzyltriethylammonium chloride (TEBAC), were purchased from Sigma Aldrich and used as received. Distilled water was used in all experiments.

Based on the study of polymerization in **Chapter IV**, the OIL1WI fraction was selected as an interesting substituent of commercial phenol for resin polymerization. The physical and chemical properties of this fraction have been detailed previously (see **Chapter II**).

5.2.2 Synthesis of novolac resins

A resinification reaction between phenol models and glyoxal has been conducted. The three phenol precursors which include phenol, mimic phenol models and bio-oil water-insoluble fraction (OIL1WI) were shown in **Figure 5. 1**. The composition of five model phenols in mimic were shown in **Table 4. 1**(**Chapter IV**).

The OIL1WI fraction is aimed to be used as renewable phenolic precursors to replace phenol. The total concentration of identifiable phenolic compounds in the bio-oil product (OIL1WI) was used to polymerize with glyoxal and was estimated to be 5.80 mmol. g^{-1}. After the reaction, the products were named phenol-glyoxal (PG) resin, mimic phenol glyoxal (MPG) resin and bio-oil (OIL1WI) glyoxal (BOG) resin, respectively [244].

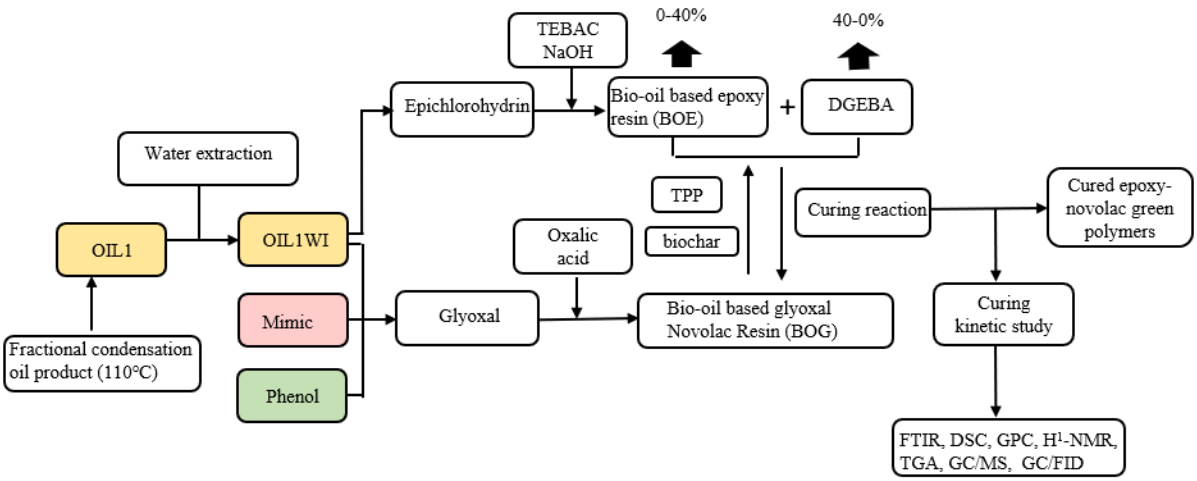

Figure 5. 1 Overview of synthesis procedure of the bio-oil based resins

All the resinification experiments were conducted in same experimental set-up presented in **Chapter IV**. The temperature was fixed at 125 °C. 10 % molar ratio of oxalic acid to phenol precursors is added to obtain acidic conditions, the molar ratio of glyoxal to phenol precursors is set as 0.5 and it was added drop-wise through the addition funnel. The reaction mixture was heated and stirred for 7 h. Then, the resin products wash with distilled water three times and vacuum dried at 125°C for 24 h to remove the unreacted monomer and acid. In addition, the resin products were weighed to determine the yield. The resin synthesis schematic was shown in **Figure A 4. 1.**

Thermal analysis experiments were performed on a TA Q1000 instrument DSC to evaluate the exothermic polymerization reaction from 25 to 300 °C. In this part, a similar medium mixture was prepared for carrying out DSC experiments. A 30 µL high-pressure steel crucible (Mettler ME-51140404) with a gold-plated copper seal (Mettler ME-51140403) as the sample pans that could withstand the relatively high pressure of about 15 MPa. Various heating rates (1, 2, 4, and 10 K/min) were used. A weight of about 8 mg of the sample was used for acquiring the experimental data. The test crucible was sealed manually by a special tool for Mettler's DSC high-pressure steel crucible. [205]. TA Universal analysis software was employed for acquiring the onset of curing exotherm and its linear integration respectively.

5.2.3 Synthesis of bio-oil based epoxy resin

The bio-oil based epoxy resins (BOE) were synthesized by a two-step glycidylation method [192, 196]. The resin synthesis schematic is shown in **Figure 5. 2**. About 2 g (1.52×10^{2} molar) of the water-insoluble fraction of bio-oil (OIL1WI) used as the alternative of phenol were added in a 100 mL three-neck reactor equipped with a condenser in the middle neck and a pressure-equalizing dropping funnel. Epichlorohydrin with 4M equivalents (eq/hydroxyl) was then added. The temperature was gradually increased to 100°C under a continuous stirring. Then, a phase transfer catalyst benzyltriethylammonium chloride (TEBAC) was introduced (0·012M eq/hydroxyl). The reaction was carried out for 1 h at 100°C. In the second step, the temperature was decreased to 30°C. The benzyltriethylammonium chloride (0·012M eq/hydroxyl) and 20 wt% aqueous solutions of sodium hydroxide (2M eq/hydroxyl) were mixed at the same time and added drop-wise through the pressure-equalizing dropping funnel, the reaction has been continued for 1-2 h at 30°C. The organic layer

was partitioned thrice with water and poured into an extraction funnel to separate the water and remove the salt. A rotary evaporator was used at 90°C to remove unreacted ECH. The resin products were dried and concentrated under 50 °C overnight. Each experiment was repeated three times, and the average values of all the analyses were reported.

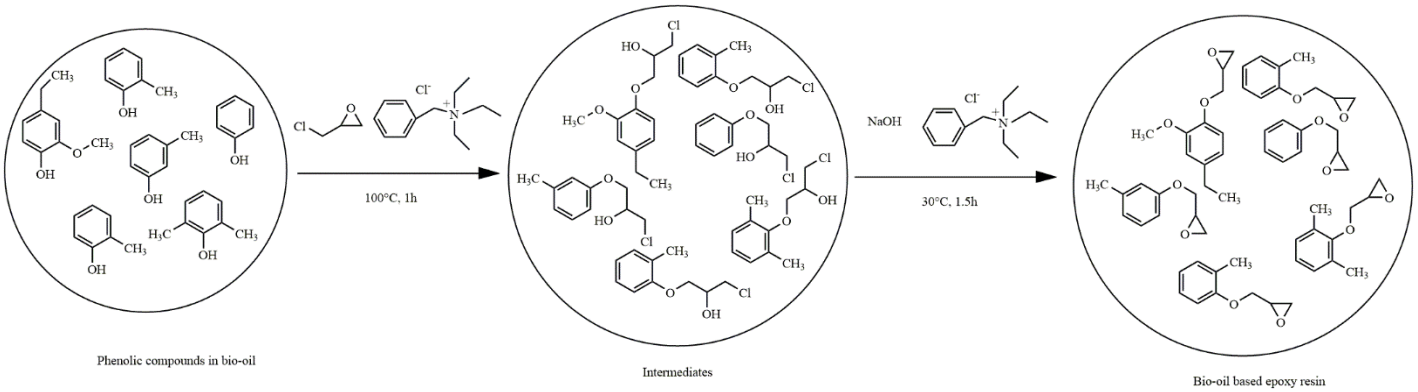

Figure 5. 2 Bio-based epoxy resin synthesis schematic

According to the literature [191], the epoxidation reaction can be divided in two steps as indicated in **Figure 5. 2**. In the first step, a phase transfer catalyst (TEBAC) consists of forming pairs of ions, which then undergo an addition reaction with ECH to open the epoxy ring, before reacting with the OH groups of the bio- oil. [120]. In the second step, the dehydrochlorination of the intermediates (ring-closing) and HCl neutralization have proceeded.

5.2.4 Curing process

The curing kinetics study of various systems: (1) novolac resin system with DGEBA and biochar, (2) BOG curing with the mixture of BOE and DGEBA were carried out using Differential scanning calorimetry (DSC). PG and BOG homemade resins were used to cure with 40% DGEBA or biochar as curing agents. The experimental method was detailed in **Chapter IV**, **4.2.3.** Firstly, the vacuum dried resin samples were dissolving in acetone uniformly mixed with a certain percentage of the curing agent DGEBA and 2% TPP as a catalyst as well as 5% biochar based on the weight of the resin. The sample is then kept for 12 h at room temperature until the solvent has completely evaporated. Then, 4.0–4.5 mg of the mixture was put in an aluminum

hermetic crucible and heated in a nitrogen environment from 25 °C to 250 °C at various heating rates (5, 10, 15, and 20 K/min) to obtain heating cycles. Onset and peak temperature of curing and curing enthalpy were determined from thermograms obtained. The amount of DGEBA was optimized to obtain a higher T_g of cured phenol resin (PG) and a lower curing reaction temperature. A ratio of DGEBA over resin of 40 wt.% has been selected for the curing treatment of all resins. **Table 5. 1** details the different novolac resins cured.

Table 5. 1 The measurements of resin curing in DSC

Resin curing	Resin use	DGEBA/Resin (wt.%)	Biochar/Resin (wt.%)	TPP (wt.%)	Sample mass/mg	Reaction temp.	Heating rates (K/min)
PG + 40%DGEBA	PG	40	0	2	4.0-4.5	120, 150, and 180	5, 10, 15, and 20
PG + 40% DGEBA +5%biochar	PG	40	5	2	4.0-4.5	120, 150, and 180	5, 10, 15, and 20
BOG + 40% DGEBA	BOG	40	0	2	4.0-4.5	120, 150, and 180	5, 10, 15, and 20
BOG + 40% DGEBA +5%biochar	BOG	40	5	2	4.0-4.5	120, 150, and 180	5, 10, 15, and 20

A large amount of cured resins was also prepared in an oven after mixing resin with the curing agent. The temperature set program was 120 °C for 30 min, 150 °C for 30 min, and 180 °C for 1 h [188].

5.2.5 Characterizations

The resins were characterized using ATR-FTIR, ^{1}H-NMR, Hydroxyl number, GPC of novolac resin, DSC and TGA which were presented in **4.2.4**. The analysis of the recovered bio-oil products was performed using GC–MS and GC-FID, the method was

shown in **2.2.4.1**.

5.2.5.1.Determination of conversion of reactant and yield of resin

The conversion of reactants in resin samples was analyzed by using the same method as for bio-oil samples. The conversion rate of phenols in the polymerization reaction was calculated according to **Equation 4. 5.**

The resins produced after drying were weighed to determine the yield, which was calculated according to **Equation 4. 4.**

The yield of the bio-oil based epoxy resins was determined according to the **Equation 5. 1** [123]:

$$Yield\ (\%) = \frac{S}{L\ (1 + 0.427)} \times 100\%$$

Equation 5. 1

where *S* is the weight of dried BOE, *L* is the weight of dried OIL1WI, and 0.427 g is the stoichiometric amount of epichlorohydrin for 1 g of OIL1WI.

5.2.5.2.Determination of the epoxy equivalent weight

Epoxy equivalent weight (EEW) is the weight of the resin (in grams) that contains 1g equivalent of the epoxide group. The epoxy equivalent of the bio-oil-based epoxy (BOE) resin was determined by a chemical assay based on the reaction with an aliquot of standard pyridine hydrochloride in excess pyridine at reflux and subsequent back titration with standard ethanol sodium hydroxide. About 0.25 g of BOE resin sample was taken in a 100 mL flask. 25 ml of a solution of 0.2 mol/L hydrochlorides in pyridine was prepared and added to the flask. The contents of the flask were stirred and heated under reflux at 115 ℃ for 20 min so as to dissolve the epoxy sample. After cooling down, the titration of the excess acid is carried out by a prepared 0.2 mol/L sodium hydroxide - ethanol solution using a pH meter to follow the pH value of the solution until the pH reaches 13. The pH value is recorded after adding every 1 ml, and a graph is drawn to determine the volume of solvent added when the maximum change of pH value appears. A blank assay is performed under the same conditions in the absence of

BOE resin. The epoxy equivalent weight (EEW) is calculated by. **Equation 5. 2.**

$$EEW = \frac{P \times 10^3}{(A - B) \times C_{NaOH}}$$

Equation 5. 2

P = BOE resin weight (g)

A = 0.2 mol/L NaOH volume (mL) for blank

B = 0.2 mol/L NaOH volume (mL) for prepolymer

C_{NaOH} = The molar concentration of 0.2 mol/L NaOH solution

5.2.6 Thermal risk assessment

The thermal hazards of the resin synthesis and curing process by using non-isothermal DSC were performed. **Figure 5. 3** describes the different steps required for thermal risk assessment of both reactions. The effect of the various reactants (phenol, bio-oil and biochar) on the process safety will be discussed.

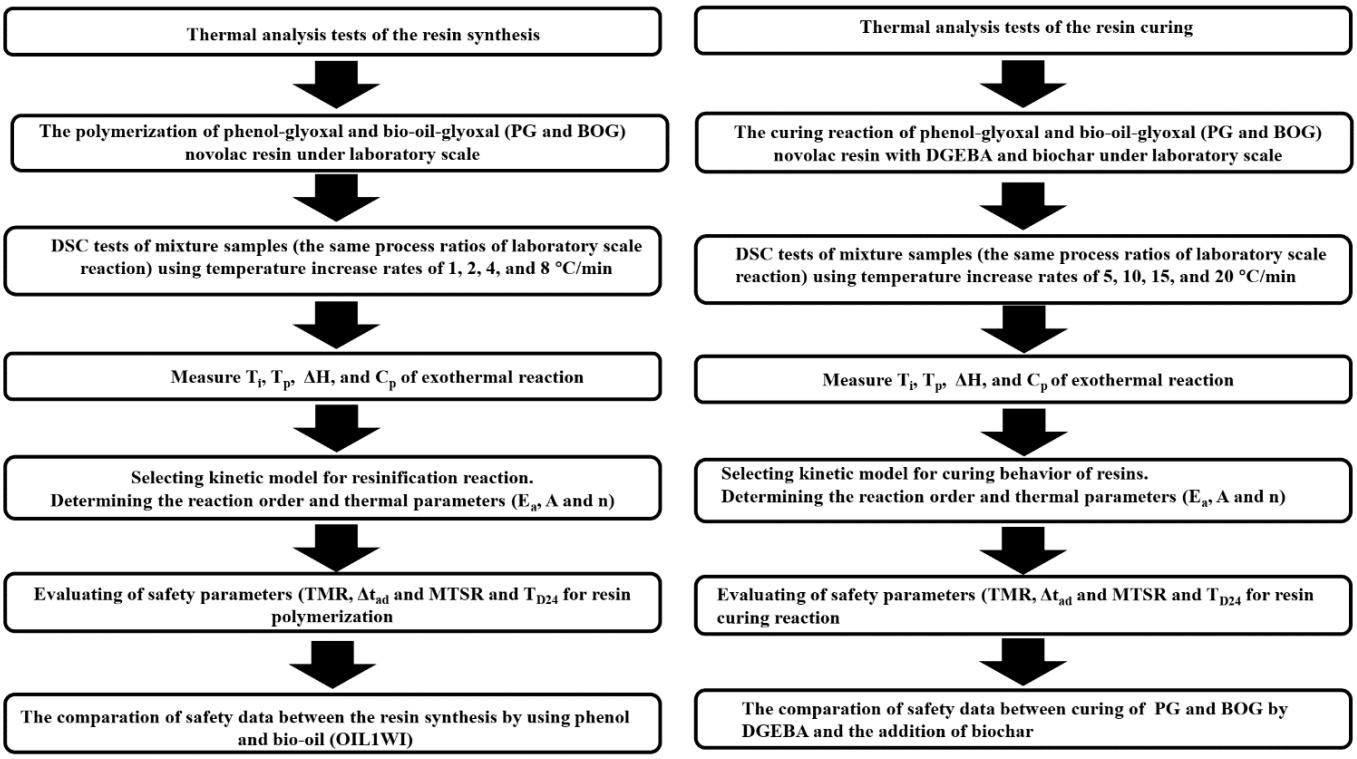

Figure 5. 3 Experimental design of thermal hazard analysis test

5.3 Results and discussion

5.3.1 Composition of bio-oil water extraction and biochar samples

The FTIR spectra of the bio-oil (OIL1WI) and biochar in **Figure 5. 4** show the visible wavenumber in the region 3,388–631 cm^{-1} and all assignments of the bands are reported in **Table 2. 6**.

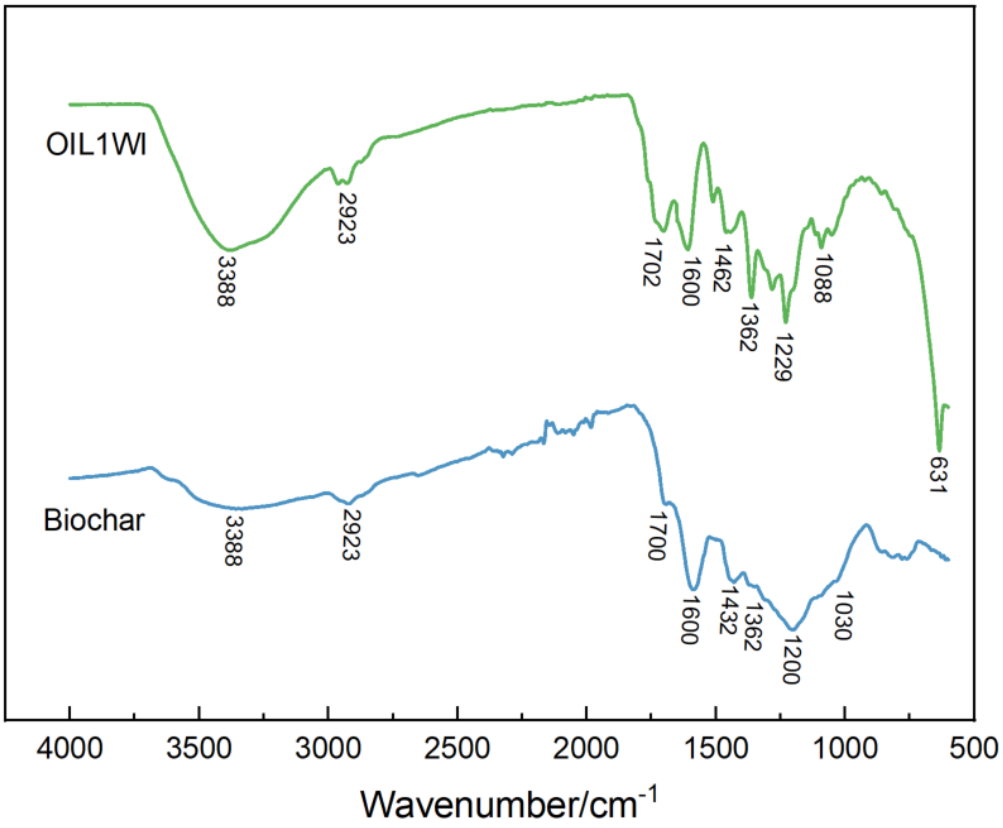

Figure 5. 4 FTIR spectra of OIL1WI and biochar

Compared to the bio-oil, the biochar presents peaks located at 3,388 cm^{-1} and 1,700 cm^{-1} with weaker intensity according to the less presence of -OH and C=O functions, respectively. However, the strong absorbance at 1,600 cm^{-1} indicated that biochar conserved more C=C functions [104]. Therefore, the presence of the fractional groups such as C=C, C=O and -OH of bio-oil and biochar confirmed that they have potential active sites for polymerization.

5.3.2 Characterization of novolac resins

5.3.2.1 Conversion and reaction yield

The conversion of reactant and yield of final resin were shown in **Table 5. 2.** The results

indicate that the conversion of phenol in PG is higher than in MPG. In order to understand the reactivity of different phenolic chemicals in MPG, the conversion of phenol models was shown in **Figure 5. 5.** It is clear that phenol, o-cresol, and m-cresol had a higher final conversion (> 89%), especially for m-cresol with a 96% conversion rate. However, 2,6-dimethylphenol and 4-ethylguaiacol have a relatively low conversion,84% and 78 % respectively. The chemical structure of both compounds presents additional alkyl and methoxy groups reducing their reactivity in the polymerization reaction and limiting their cross-linking capabilities. Thus, a low yield for MPG is observed compared with PG resin. The conversion of phenolic compounds in BOG is relatively higher than in the other two resins due to the cross-polymerization reaction of additional small compounds in bio-oil such as aldehydes and ketones. Moreover, acetic acid, present in bio-oil, does not participate in the polymerization reaction but can help to catalyze the reaction [246]. Thus, the resin, produced from OIL1WI, showed a higher yield than MPG resin.

Table 5. 2 Mw， Mn and polydispersity values of novolac resins using 10 % oxalic acid

Resin name	Phenol monomer	-OH (mmol/g)	Conversion of phenol (%)	Yield (%)	Mn(g/mol)	Mw (g/mol)	Polydispersity
PG	Phenol	8.08±0.06	91.48±1.52	90.41±0.93	863±78	1237±29	1.42
MPG	Model phenols	6.49±0.05	86.49±2.21	84.30±1.22	852±39	1126±84	1.32
BOG	OIL1WI	6.14±0.09	95.97±2.25	87.18±1.30	1095±61	3169±85	2.96

However, the yield of BOG resin had a lower value than PG resin due to the low reactivity of the complex structure of some phenolic compounds with several alkyl and methoxy groups in bio-oil.

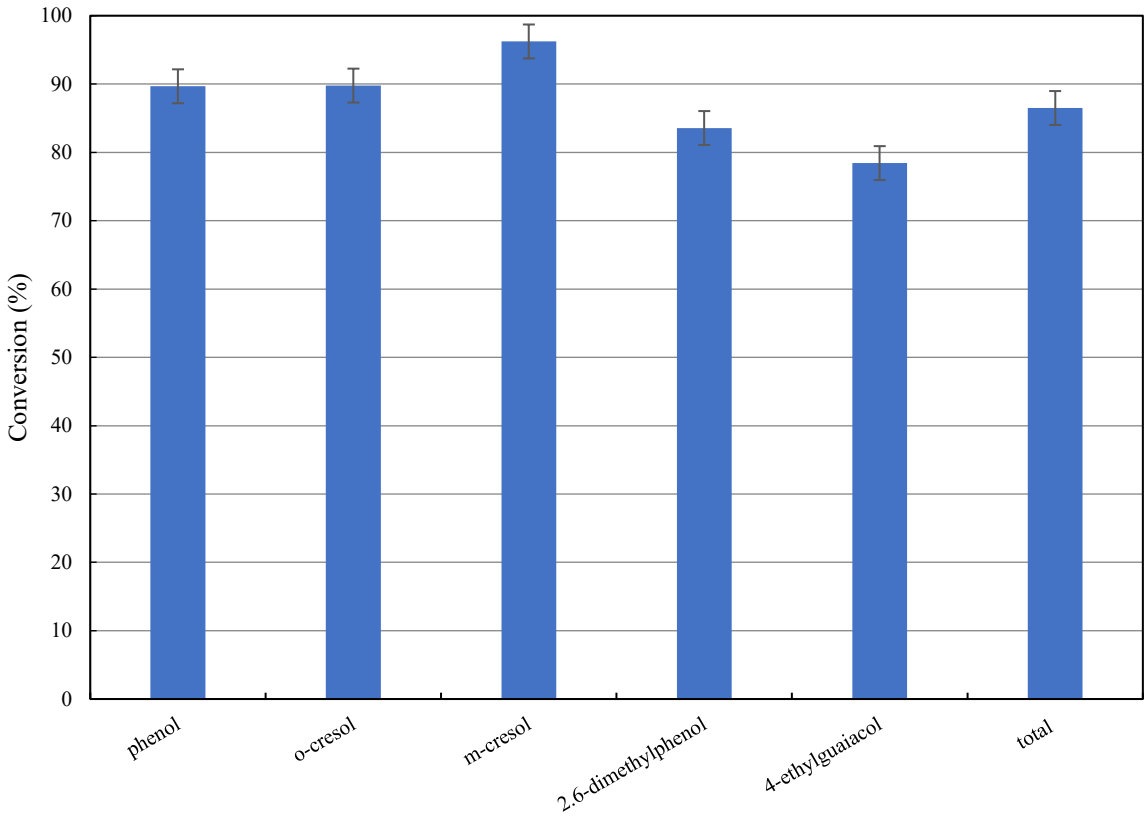

Figure 5. 5 The conversion of phenol models in mimic phenol glyoxal (MPG) resin

5.3.2.2 Chemical characterization

The FTIR spectra illustrating the functional groups in PG, MPG and BOG resins are shown in **Figure 5. 6**. The spectra of PG, MPG and BOG resins put in relief new peaks, demonstrating their successful synthesis. Indeed, compared with the bio-oil structure, an obvious increase in intensity is visible for the peaks located at 2962, 1440, 1702, 1600, 1512, and 1018 cm^{-1}, related to the methylene, aldehyde, carbon-carbon double bond, aromatic, and ether groups respectively. These functional groups can be associated with the condensation reactions between the aldehyde in glyoxal and phenolic compounds to form –CH2–C=O and –C=C–O–C=O linkages [172]. Their intensity is stronger in PG than in MPG and BOG.

The wide absorbance band at around 3300 cm^{-1} and the peaks located in the range 1210 cm^{-1} are assigned to the stretching vibration of active phenolic hydroxyl in the resin structure. The peak intensity varies according to the following rank: PG ＞ MPG ＞ BOG.

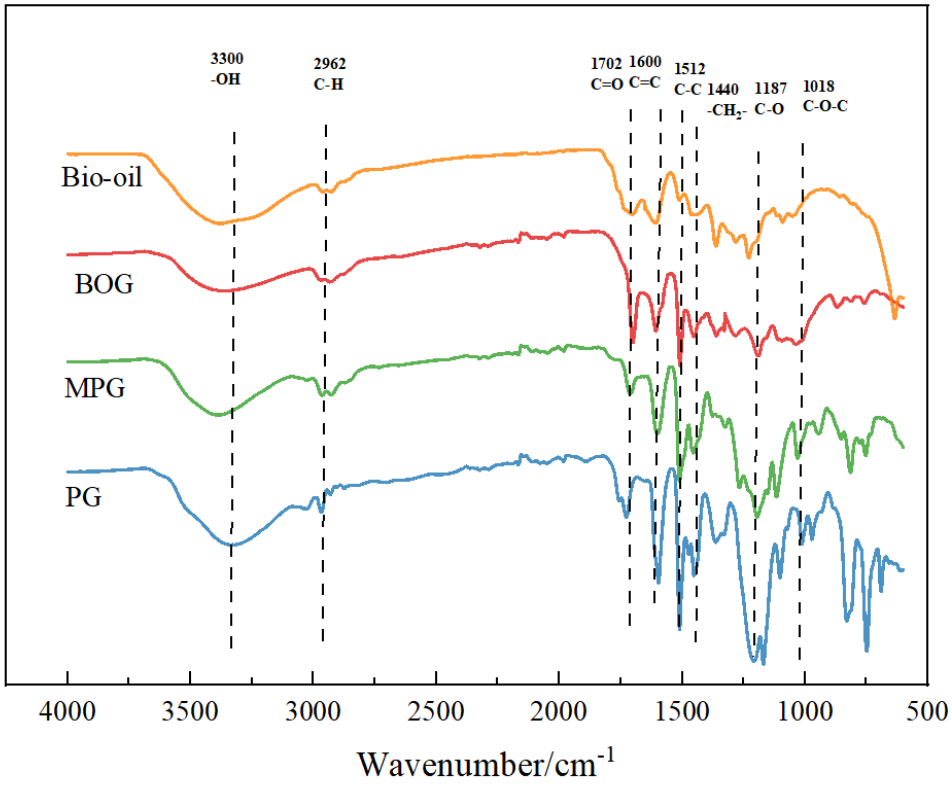

Figure 5. 6 FTIR graph of bio-oil and resins

The hydroxyl number of resins obtained by the titration method, shown in **Table 5. 2** confirms partially the trends observed by FTIR. The hydroxyl number of PG resins is larger than that of MPG whereas BOG resins have a similar amount.

Considering the complex structure of bio-oil, ^{1}H-NMR (**Figure 5. 7**) was used to confirm the partial condensation reaction in BOG resins. Indeed, the peaks around 10-9.5 ppm and around 9.2 were attributed to the proton of the residual oxalic acid and glyoxal respectively. The signal belongs to the protons of the structure (H–C=C–) located around 8.64 ppm and the peak around 3.8-4.5 were assigned to the formation of linkages between glyoxal and bio-oil phenolics according to the schematic of BOG (**Figure A 4. 1**) confirming the success of applying bio-oil for resin synthesis [158, 166, 172]. Other peaks can be linked to the aromatic structure of phenolic compounds (regions 8-6 ppm and 4.0- 3.5 ppm) as well as the small molecular aliphatic, due to the use of bio-oil. In particular, the strong signals between 2.5 and 0.5 ppm are ascribed to the protons of the aliphatic chain linked to the aromatic structure as well as the small aliphatic molecules.

The properties of resins (M_w， M_n and polydispersity values) obtained by the GPC chromatogram analysis software are listed in **Table 5. 2**.

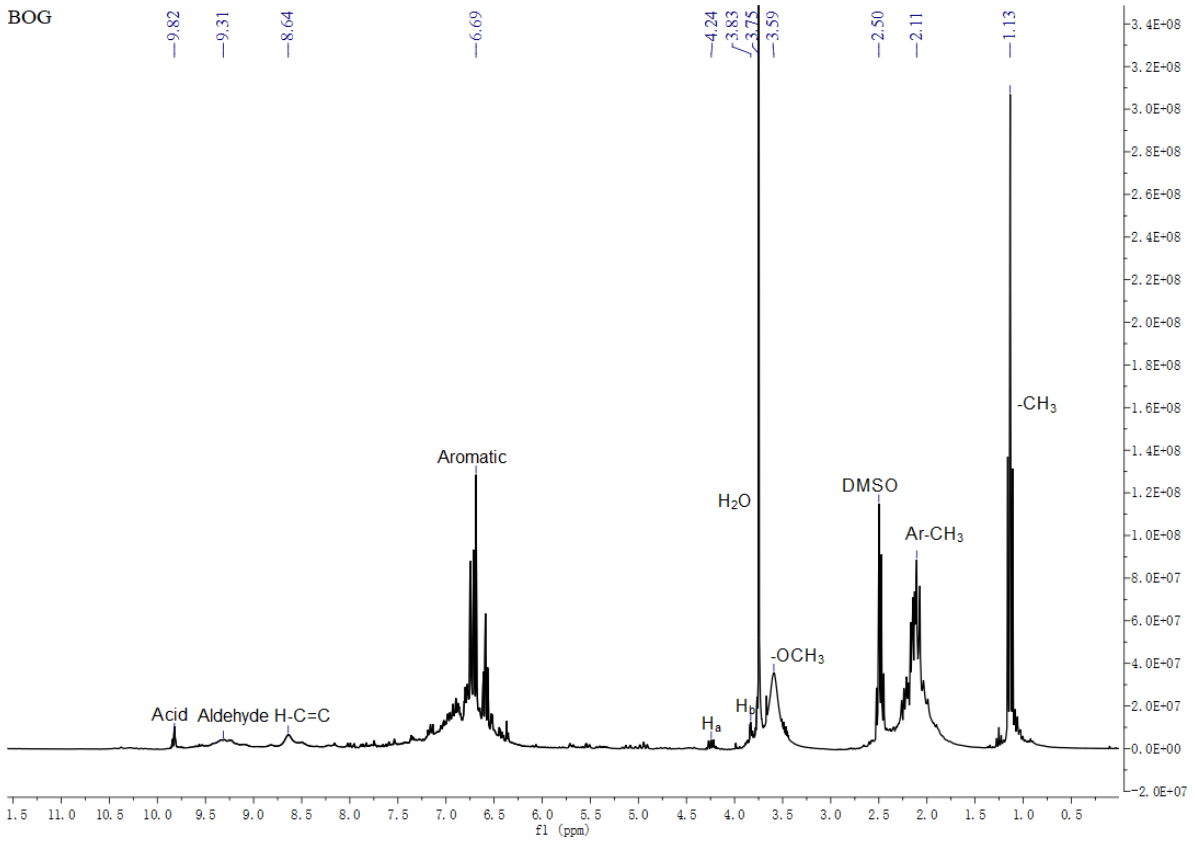

Figure 5. 7 ^{1}H NMR spectrum of BOG resin

PG and MPG resins show similar properties, whereas BOG resin shows a broader molecular weight distribution than that of PG and MPG resin as well as higher M_w and M_n values (M_w = 1095±61 g/mol, M_n=3169±85 g/mol, polydispersity= 2.96). The reaction of phenols and glyoxal generally occurs in the ortho-para position of phenolic hydroxyl groups, and the reactivity of phenol models decreases with the increase of substituents on the benzene ring due to steric hindrance. Since the active sites were occupied and the presence of additional alkyl and methoxy groups, the phenolic compounds in mimic and bio-oil have lower reactivity. As an uncomplete reaction (**Figure A 4. 2**), the residual phenolic compounds made the molecular weight of MPG slightly lower than PG. Unlike model resins, real bio-oil also contains many small molecule chemicals and other more reactive phenols such as catechol which help to build a complex network structure of macromolecules, probably resulting in broader molecular weight distribution and higher size of formed resin BOG.

5.3.2.3 Thermal Characterization of uncured resin

The thermal analysis techniques like DSC and TGA were used to provide valuable information on the thermal properties of uncured PG, MPG, and BOG resins and the curves are shown in **Figure 5. 8**. Moreover, the glass transition temperature (T_g), the 5% decomposition temperature (T_{d5}), the temperature of maximum decomposition rate (T_{max}) and char residue formed at 800℃ were determined and displayed in **Table 5. 3**.

The T_g values of the novolac resins are in the range of 75 to 93℃ following ascending order: PG> BOG> MPG resin. As also observed in the case of resin synthesized using acetaldehyde, the glass transition change of BOG resin is not as stable as those of the other resins due to its heterogeneity induced by the presence of small molecules and some plasticization reactions occur simultaneously [160].

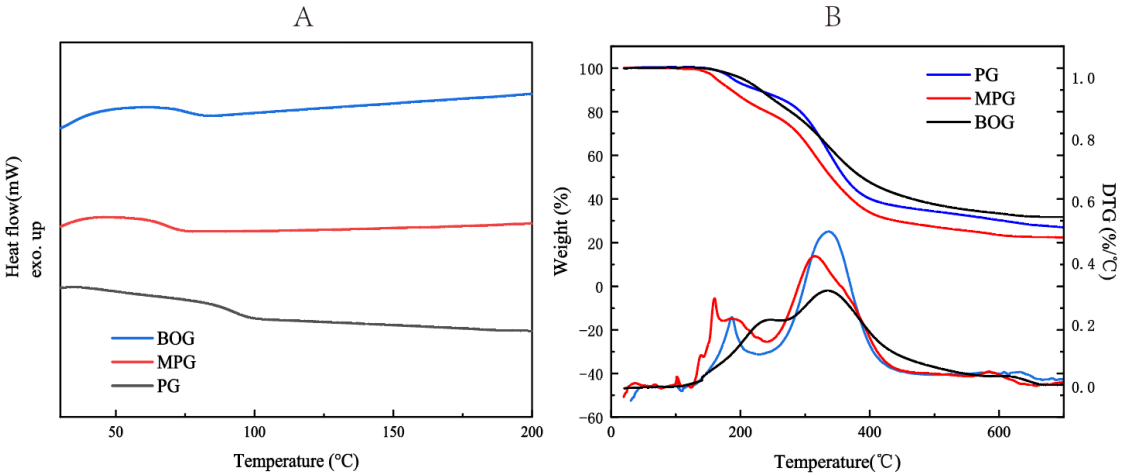

Figure 5. 8 DSC, TG, and DTG profiles of the uncured PG, mimic, and BOG resin

Table 5. 3 DSC, TGA, and DTG results of uncured PG, mimic, and BOG resins

Resin name	Phenol monomer	T_g (℃)	T_{d5} (℃)	T_{max} (℃)	R_{800} (%)
PG	Phenol	92.51	188.90	336.47	24.75
MPG	mimic	68.41	162.22	315.21	20.91
BOG	OIL1WI	75.79	203.71	334.97	30.90

Using bio-oil water-insoluble fraction to produce resin showed a higher 5% weight loss temperature (T_{d5}) than the other resins. T_{d5} of resin depends on the degree of polymerization. A hypothesis could be that small compounds participate to crosslink reactions, resulting in a complex resin structure as the GPC profile put in evidence (Appendix **Figure A 4. 2).** In the case of PG resin and MPG resin, T_{d5} is close to the melting point of the monomer. It is logical as the reaction was not complete. Furthermore, the tallest peak of the thermogram derivative also reflects the properties of resins. PG and BOG have similar T_{max} values at the opposite of MPG resin. Reasonably, in MPG resin, complex phenolic compounds having substituents on the aromatic ring such as 4-ethylguaiacol and 2,6-dimethylphenol produced a polymer having lower thermal stability. The residual carbon contents at 800°C for BOG resin were higher than for PG and MPG resins. This behavior can be explained by the cross-linking of many side chains of the bio-oil molecules and the reaction will be favored as the heating temperature increases.

In summary, BOG resins have similar thermal properties as PG as well as PA resins (chapter 4). Moreover, conversion and yield were also more important reaching an almost complete reaction. However, the size properties of BOG resin have a slightly larger molecular weight (M_n) and a larger distribution is observed.

5.3.2.4 Synthesis mechanism

The resin synthesis mechanism is shown in **Figure 5. 9**. Generally, the traditional novolac prepolymers are produced from formaldehyde and phenol with molar ratios of formaldehyde to phenol (F/P) between 0.7 and 0.9 [133, 137]. The polymerization reaction usually has two main stages: addition and condensation. The addition of formaldehyde to phenol is to form methylolphenols (e.g., 2-hydroxymethylphenol and 4-hydroxymethylphenol). With the introduction of phenol, the condensation step leads to the formation of dihydroxydiphenylmethane.

Next, finally, a global condensation leads to the linear novolac resin [210, 247, 248]. The polymerization of phenol and glyoxal using oxalic acid also follows a similar reaction mechanism as the traditional acid-catalyzed phenol-formaldehyde resins with excess phenol and then the novolac-type phenol-glyoxal resin is obtained. However, since glyoxal is a dialdehyde, the reaction is more complex. In addition, glyoxal is

typically solubilized in water and is in equilibrium with hydrated forms which will readily be converted into glycolic acid in the presence of an acidic catalyst [162, 249, 250]. In the resinification process, firstly, the additional products were formed between phenol and hydrated forms of glyoxal due to the catalytic role of oxalic acid. Under the condensation part, the dimers were formed first, however, since the hydrated forms are not very stable, a molecule of water is lost to form a double bond structure.

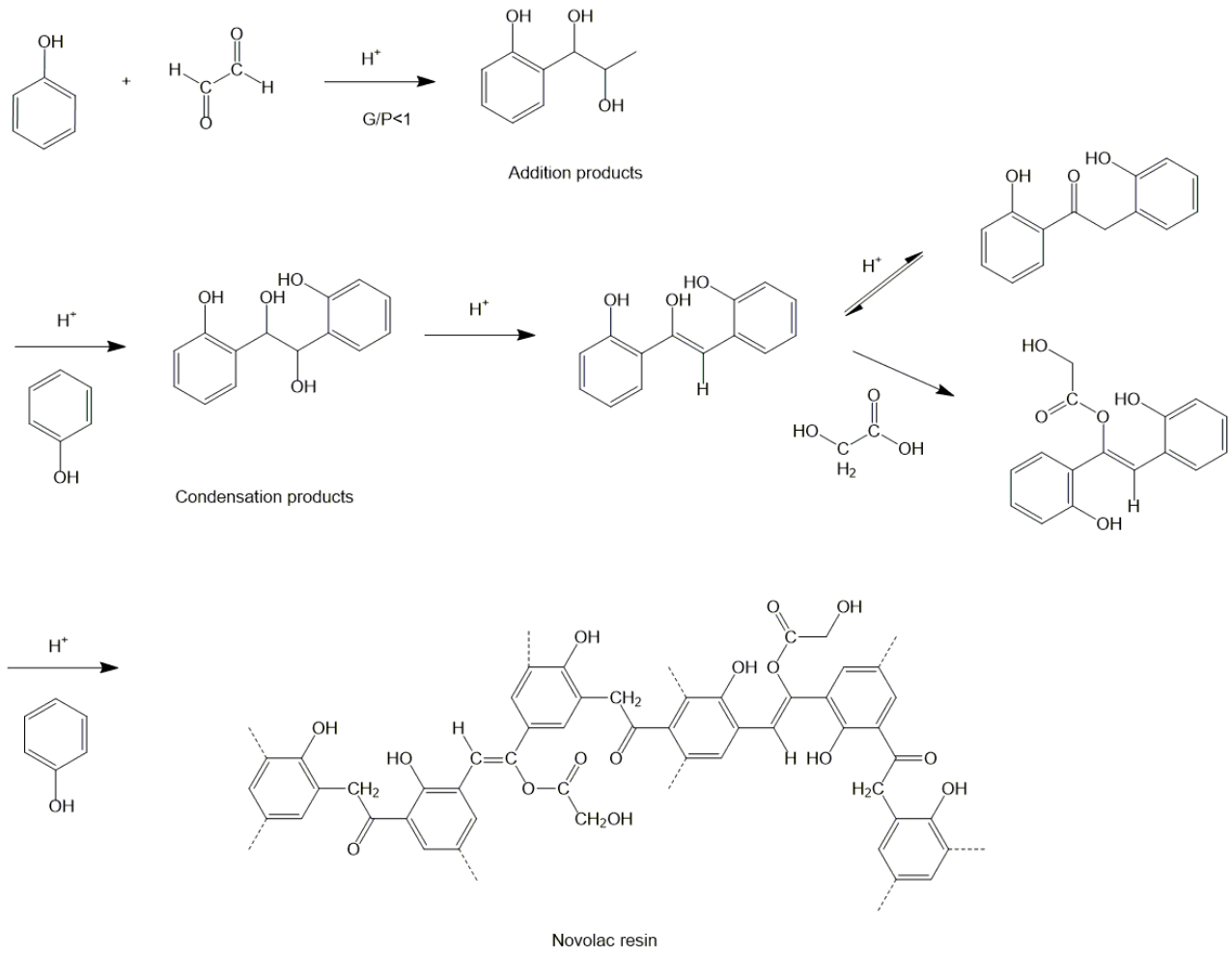

Figure 5. 9 Schematic of the resin synthesis mechanism

Additionally, the enolate structure product follows keto−enol tautomerism to form ketone products and aliphatic ketones mostly exist in the ketone form. The glycolic enol ester derivative is formed by esterification of residual glycolic acid with the enolate structure [162, 172]. Then, the more crosslink starts to form the linear novolac resin.

5.3.3 Bio-oil based epoxy resin synthesis and characterization

5.3.3.1 Epoxy structure

As same as bio-oil based novolac resin, the bio-oil based epoxy resin is also synthesized by treating bio-oil water-insoluble fractions with epichlorohydrin (see **Figure 5. 2**). After purification, the obtained BOE resin was semi-solid with black color.

Figure 5. 10 shows the FTIR spectra which allow identifying differences of functional groups between bio-oil based epoxy resin, epichlorohydrin, and their phenolic precursors. The signal at 911 and 855 cm^{-1} are belonging to the oxirane group [120, 195], clearly seen in ECH. However, no signal is detected in the spectrum of bio-oil, but the resulting BOE resin showed new peaks here which confirmed the success of the epoxidation reaction between phenols in bio-oil and epichlorohydrin, and the new epoxy ring in the resin structure. Similarly, deformation peaks were observed for C–O–C in the range 1225–1250 cm^{-1} and in the range 1026–1043 cm^{-1} for asymmetric and symmetric bending, respectively. Similarly, in both epoxy resin and bio-oil, the deformation peaks of C-O-C for asymmetric and symmetric bending were observed in the ranges of 1225-1250 cm^{-1} and 1026-1043 cm^{-1}, respectively. The broad peak around 3300 cm^{-1} assigned to the O–H stretching vibrations, is reduced in BOE resin compared with bio-oil due to the phenolic hydroxyl converted into glycidyl functionality. The band at 1702 cm^{-1} is associated with the aldehyde group in bio-oil, which also decreases after the reaction and indicates the occurrence of the condensation reaction.

The ^{1}H-NMR spectrum of bio-oil-based epoxy resin (BOE) confirmed the epoxidation reaction of bio-oil as shown in **Figure 5. 11**. Indeed, the signals around 3.30 and 2.82 ppm are attributed to the protons of oxirane moieties, the protons at a and b are on the epoxide CH_2(O)-CH- structure, and the peaks of the protons (c) on the -CH_2- next to the epoxy group around 4 ppm was observed as well [193, 194, 197, 198], which demonstrated that the target compounds were synthesized successfully. As detailed in the previous part, the other peaks are related mainly to phenolics compound recovered in BOE resin.

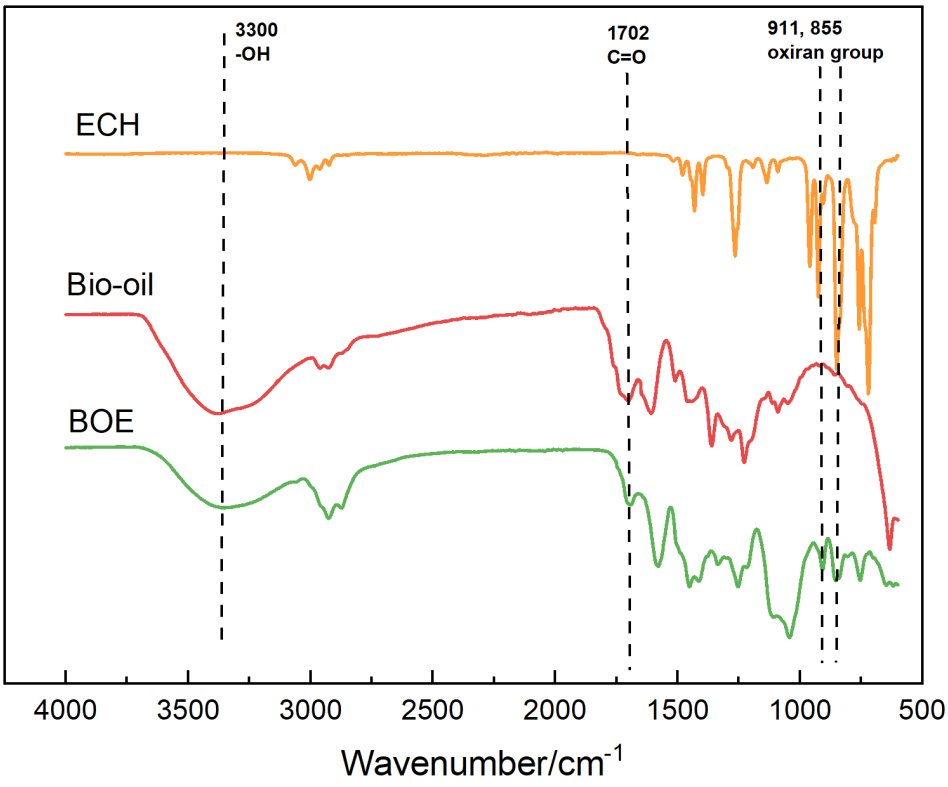

Figure 5. 10 FTIR spectra of epichlorohydrin, bio-oil (OIL1WI), and BOE resin

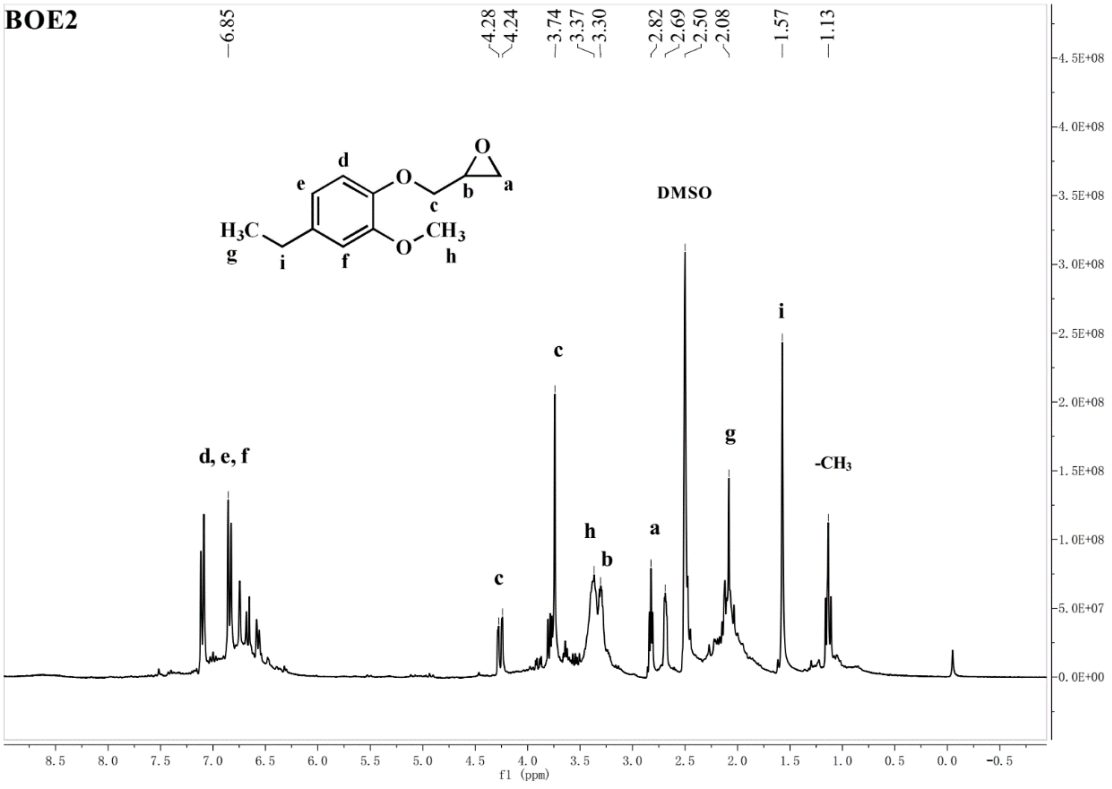

Figure 5. 11 ^{1}H-NMR spectrum of BOE resin

5.3.3.2 Resin properties and characterization

The yield and epoxy equivalent weight (EEW) of the epoxy resin are two important parameters. The yield reflects the degree of the polymerization reaction. The EEW value provides information on the reactivity of the epoxy resin; a lower EEW is desirable because it means a higher concentration of epoxy group attached to the resin. The reaction time of the second step has a crucial influence on yield and EEW [186, 251]. In order to optimize the reaction in the polymerization, the effect of reaction times (1.5, 2, and 2.5h) on yield and EEW was examined, the results are shown in **Table 5. 4**. It is evident that the longer the reaction time is, the higher the yield and the EEW value of epoxy resin. These results are in agreement with the literature [120, 251].

Table 5. 4 The yield and EEW of epoxy resins

Epoxy resin	Reaction time/h	Yield (%)	EEW (g/eq.)	Mn(g/mol)	Mw (g/mol)	Polydispersity
BOE1.5	1.5	87.3±2.2	310±3	303±20	723±15	2.39
BOE2	2.0	91.0±1.7	317±2	368±18	1019±31	2.77
BOE2.5	2.5	92.8±1.1	375±1	375±11	1108±33	2.96
DGEBA	-	-	181±1	-	-	-

As the OILWI fraction, is made of a mixture of monomeric, oligomeric, and macromolecular phenolic components, it has a higher molecular weight and lower phenolic hydroxyl reactivity than commercial phenols. As expected, EEW of synthetized BOE is twice higher than that of DGEBA (181 $g.equ^{-1}$) which is a commercially manufactured epoxy resin made with the desired EEW.

The molecular weight distribution of BOE resins is listed in **Table 5. 4** and the graph is shown in Appendix **Figure A 4. 3**. The difference between M_w and M_n values (M_w = 1019±31 g/mol, M_n=368±18 g/mol) resulted in large polydispersity (2.77). Various substituents on phenolic backbone such as methoxy group limit their participation in the further cross-linking reaction. Moreover, the strong presence of small molecules in bio-oil reduces the value of M_n. On the opposite, the glycidylation reaction occurred, leading to the formation of oligomers. And the newly formed glycidyl groups can react

with the phenolic group of another molecule to create higher-molecular-weight oligomers [122, 131]. This results in a large polydispersity of epoxy resin. When the reaction time increases, the growth of M_n and M_w values of BOE resins is obvious (especially for the M_w) resulting in a rise in polydispersity value. However, a longer reaction time allows for improving BOE yield.

5.4 Resin curing

In the first part, curing with commercial epoxy resin will be discussed. The char addition effect will be analyzed on the cured resin properties. In another part, homemade epoxy resin (BOE) will be investigated for curing BOG novolac resin. The latter material, a greener one, mainly consist of pyrolysis bio-oil resource. As a reminder, all the non-isothermal DSC experiments were led to study the curing behavior and kinetics of resins.

5.4.1 Curing mechanism of phenol glyoxal novolac resin with DGEBA

The curing reaction of phenol glyoxal novolac resin with DGEBA by using the reaction between phenolic–OH and epoxy groups to produce low moisture absorbing and void-free products[179]. Furthermore, the reaction is less difficult in the presence of TPP used as a catalyst, and the chain-wise polymerization mechanisms of the novolac/epoxy curing system included three main reaction steps: initiation, propagation, and branching [187], and the mechanism is illustrated in **Figure 5. 12**.

In the initial stage of curing the phenol hydroxyl-epoxy reaction is predominant, TPP opens the epoxy ring by generating a zwitter ion and a rapid proton transfer from the phenol to the secondary hydroxyl ion. In the propagation step, the primary epoxies are consumed quickly resulting in a greater number of secondary hydroxyl groups facilitating the ring-opening reaction. In the branching step, the secondary epoxy groups started reacting with the new hydroxyl groups that came from the primary epoxy [187, 242]

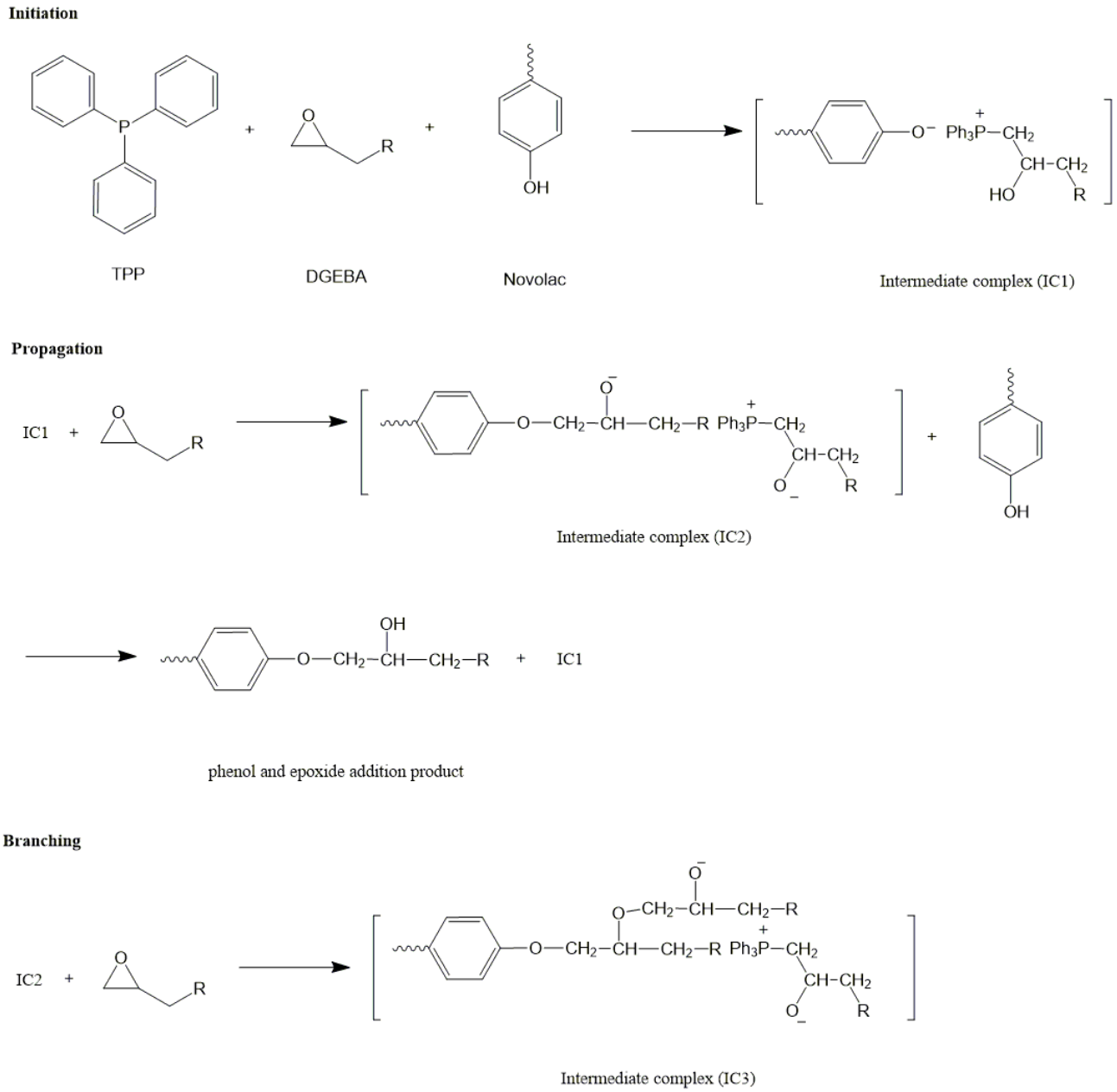

Figure 5. 12 Cure mechanism of epoxy/ novolac system catalyzed by TPP.

5.4.2 Curing PG, MPG, and BOG resin with DGEBA and biochar

The comparison was between the effect of using different resins (PG and BOG) and the effect of the curing additive (biochar). The obtained DSC thermograms were presented in **Figure 5. 13**. All the thermograms of both PG and BOG resin exhibit one main exothermic peak, the curing exothermic peak of PG is sharper than that of BOG and the profile of the sample containing biochar was sharper than this without biochar.

The onset and peak temperature of the curing reaction of PG, MPG and BOG resins are shown in **Table 5. 5**, all the temperatures of curing reactions are between 100-200°C.

BOG resin had a relatively lower initial onset temperature compared to PG resin at each heating rate. Additionally, the reaction enthalpy of PG and BOG curing with DGEBA and biochar is in the range of 80-100 J/g. These enthalpy values are close to that of the PF resin cured with the traditional curing agent HMTA [252].

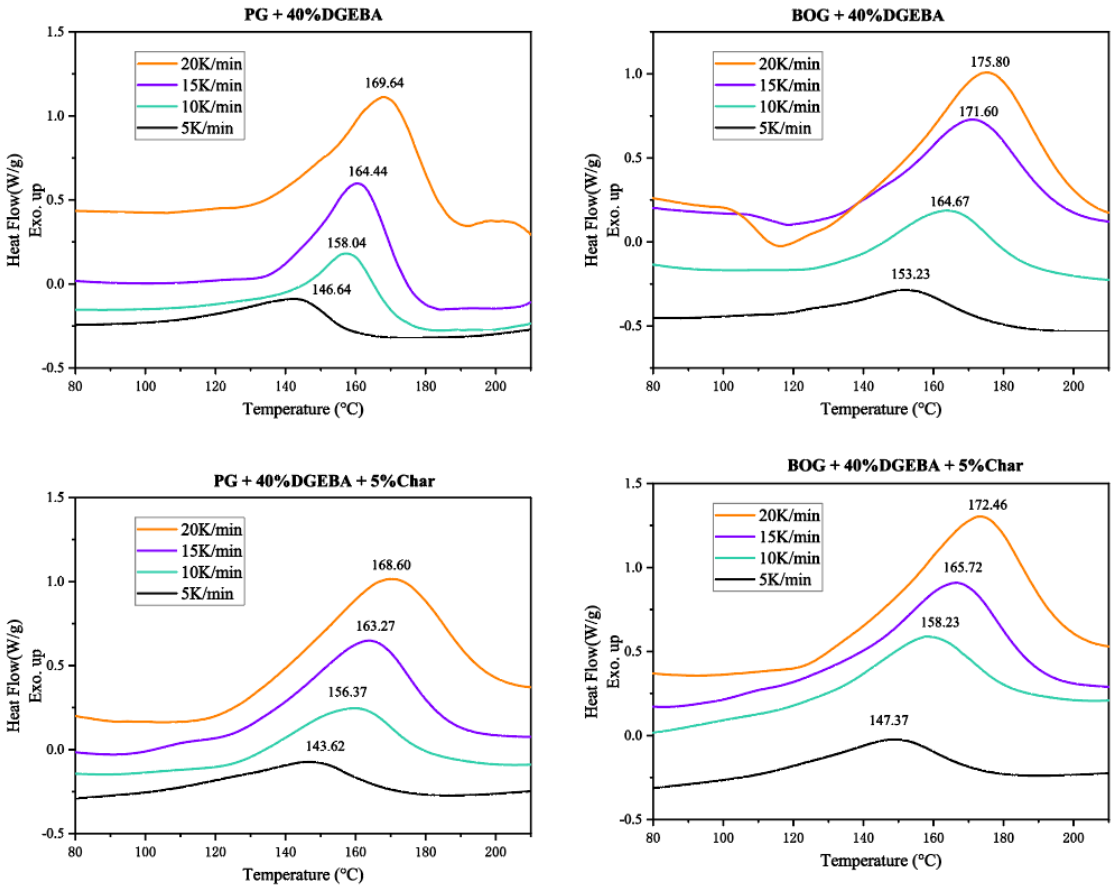

Figure 5. 13 DSC thermograms of novolac resin curing at heating rates of 5, 10, 15, and 20 K/min

The curing reaction mechanisms of MPG and BOG are not as simple as PG resin, probably due to the diversity of the nature of phenol precursors and the number of small compounds. The latter can ease the start of the reaction, resulting in a relatively lower initial onset temperature for MPG and BOE resins compared to PG resins. Nevertheless, the rank peak temperature is different from to onset temperature and varies in ascending order: MPG < PG < BOG resin. As also observed in the curing of acetaldehyde resin, the peak temperature seems to be linked to the active hydroxyl number available in the novolac resin-based curing reaction. The large variety of molecules in BOG resin could complicate the access of active sites such hydroxyl group leading to a higher reaction

temperature. It is worth mentioning that the addition of biochar as a curing additive clearly reduced the onset temperatures of the curing reaction and the peak temperature is also slightly decreased.

Table 5. 5 Onset temperature, Peak temperature, Activation Energy, and reaction order of PG, MPG, and BOG resin curing with 40% DGEBA, 2% TPP and the addition of 5% char

Resin type		Heating rate (°C/min)				Activation energy (kJ/mol)		n
		5	10	15	20	Kissinger	Flynn–Wall–Ozawa	
PG	Onset temp (°C)	123.25	138.57	144.25	148.39	86.41	88.98	0.944
	Peak temp (°C)	146.64	158.04	164.44	169.64			
PG +5%char	Onset temp (°C)	107.29	122.14	124.28	126.32	77.91	80.86	0.936
	Peak temp (°C)	143.62	156.37	163.27	168.60			
MPG	Onset temp (°C)	110.11	115.04	129.17	133.69	84.23	86.79	0.943
	Peak temp (°C)	139.48	150.55	157.23	162.18			
MPG +5% char	Onset temp (°C)	102.49	115.97	125.44	126.86	74.92	77.85	0.935
	Peak temp (°C)	133.20	145.15	153.78	156.96			
BOG	Onset temp (°C)	122.24	134.21	136.92	139.89	89.53	92.05	0.945
	Peak temp (°C)	153.23	164.67	171.60	175.80			
BOG + 5% char	Onset temp (°C)	100.27	116.92	126.87	132.04	79.58	82.51	0.937
	Peak temp (°C)	147.37	158.23	165.72	172.46			

Model-free methods (Kissinger, Flynn–Wall–Ozawa (FWO) and Crane equation) were used to evaluate kinetics parameters according to equations described in **4.3.4.** The value of activation energy (E_a) is ranged as follows: MPG < PG < BOG resin. MPG resin has the lowest E_a. MPG resin has the lowest molecular weight which means it contains a lot of oligomers and more unreacted hydroxyl groups, making it easier to crosslink with epoxy groups and reducing the energy barrier of the ring-opening reaction. Otherwise, the E_a value of BOG resin is slightly larger than that of PG. It is likely that because of the wide range of molecular weight compounds contained in bio-oil including several big molecular have fewer unoccupied reactive sites. As a consequence, the participation of the hydroxyl group could be more difficult in the curing reaction. The same behavior was observed in the case of bio-oil acetaldehyde resin. The addition of biochar not only reduces the curing temperature range but also reduces the activation energy of the curing reaction. As mentioned above, the C=C and

C=O bonds in biochar could combine with unreacted small molecules in bio-oil to promote a curing reaction.

The initiation, propagation, and branching are the three main reaction steps of chain-wise polymerization curing mechanisms of PG resin [187]. FTIR spectra (**Figure 5. 14**) show the chemical structural characterization of the reactants used and the cured BOG resin. The mixture of BOG resin and DGEBA were used to understand the curing reaction of BOG resin.

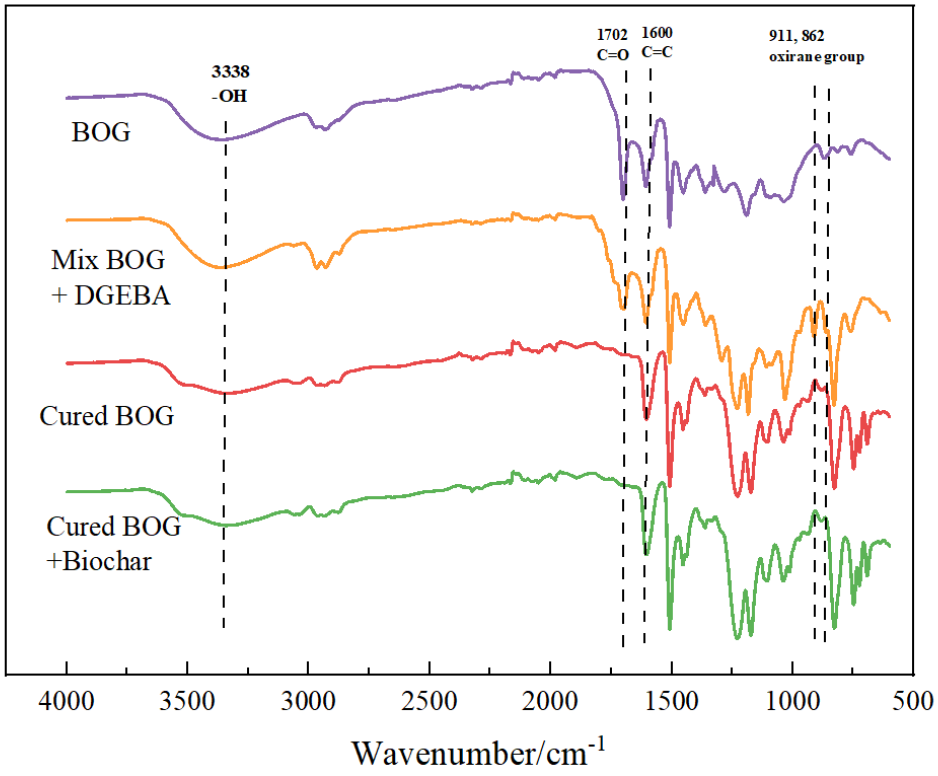

Figure 5. 14 FTIR spectra of BOG resin, mixture of BOG resin and DGEBA, BOG resin cured by DGEBA, and BOG resin cured by DGEBA and bio-char

It is clear that the absorption bands at 862 and 911 cm^{-1} correspond to the characteristic peak of the oxirane ring which is only present in the mixture [120, 195]. The peak disappeared after curing due to the consumption of oxirane [197]. The stretching modes at 1,702 and 1,600 cm^{-1} correspond to aldehyde group (C=O), carbon-carbon double bond (C=C) in glyoxal, bio-oil, and biochar, which decrease after the reaction indicating the occurrence of the condensation reaction. Both the wide peak around 3,363 cm^{-1} (O-H stretching) and the peaks located in the range of 1,233 cm^{-1} (C-O stretching) indicate the reduction of the hydroxyl group. All the changes confirmed the curing mechanism:

the main reaction pathway is performed between phenol hydroxyl and epoxy groups.

The thermal stability parameters (T_{d5}, $T_{max,}$ and R_{800}) of cured resins are shown in **Table 5. 6.** Compared to novolac resins, the thermal stability of the cured resins was significantly improved as demonstrated by the increase in initial and thermal decomposition temperatures as well as the increase in the char yield at 800℃ of the cured PG, MPG and BOG resin. The introduction of biochar has improved again the thermal stability. The increase of R_{800} can be explained by the cross-linking reaction favored by biochar. The result is consistent with Hu et al. [104] who found that biochar can be used to make carbon materials with high yields.

Table 5. 6 The thermal stability of the cured resins

Resin	T_{d5} (℃)	T_{max} (℃)	R_{800}(%)
PG	188.90	336.47	24.75
Cured PG	301.11	391.02	28.49
Cured PG-biochar	303.08	408.78	40.68
MPG	162.22	315.21	20.91
Cured MPG	278.34	411.42	22.36
Cured MPG-biochar	287.52	413.05	26.07
BOG	203.71	334.97	30.90
Cured BOG	283.12	390.59	39.66
Cured BOG-biochar	289.73	391.76	41.70

5.4.3 Kinetic study of BOE/DGEBA-BOG curing system

The curing reaction of BOG resins with 40 wt% BOE/DGEBA (based on the weight of BOG resin) were performed. **Figure 5. 15** displays the DSC curves of the

BOG+DGEBA/BOE curing system with a heating rate of 10 K/min. A single exothermic peak for all the curing systems is observed which corresponds to the complete progress of the thermal curing reaction [193]. Analysis of DSC profiles were gathered in the **Table 5. 7**. The exothermic peak temperature at various heating rate of curing reaction is between 84-180°C (**Table 5. 8**). The curing onset and peak temperature of BOG curing with BOE have significant change compared with only cured by DGEBA. The peak temperature of curing reaction decreases with the increase of BOE ratio, also the reaction enthalpy decreases. In a previous work, novolac-epoxy resin curing system were built basing on the OH–epoxy reaction [179].

Table 5. 7 Curing characteristics of BOG resins with 40 wt% BOE/DGEBA with a heating rate of 10 K/min.

Resin	Onset temp (°C)	Peak temp (°C)	Enthalpy(J/g)
BOG+40%DGEBA	134.2	164.7	83.4
BOG+30%DGEBA+10%BOE	106.5	148.7	78.9
BOG+20%DGEBA+20%BOE	107.8	147.3	73.6
BOG+10%DGEBA+30%BOE	104.2	141.5	69.9
BOG+40%BOE	106.1	135.3	63.1

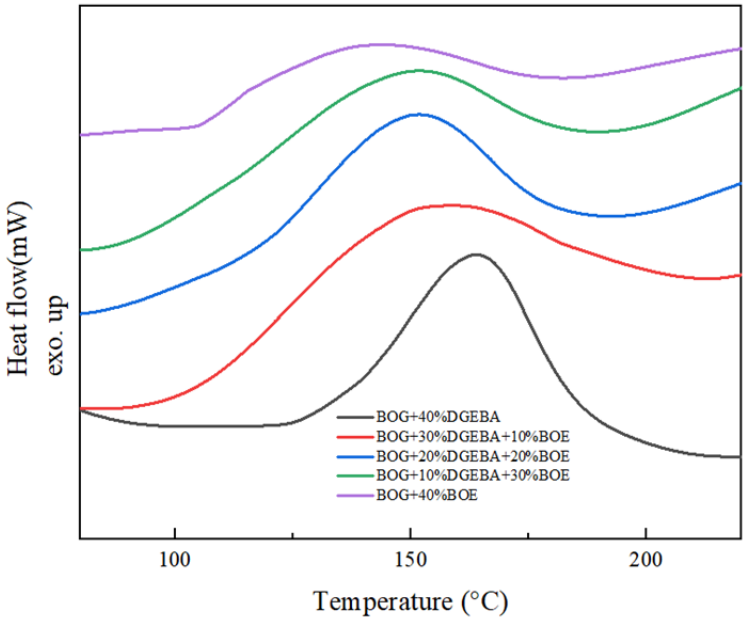

Figure 5. 15 DSC curves of BOG+DGEBA/BOE curing system with a heating rate of 10 K/min.

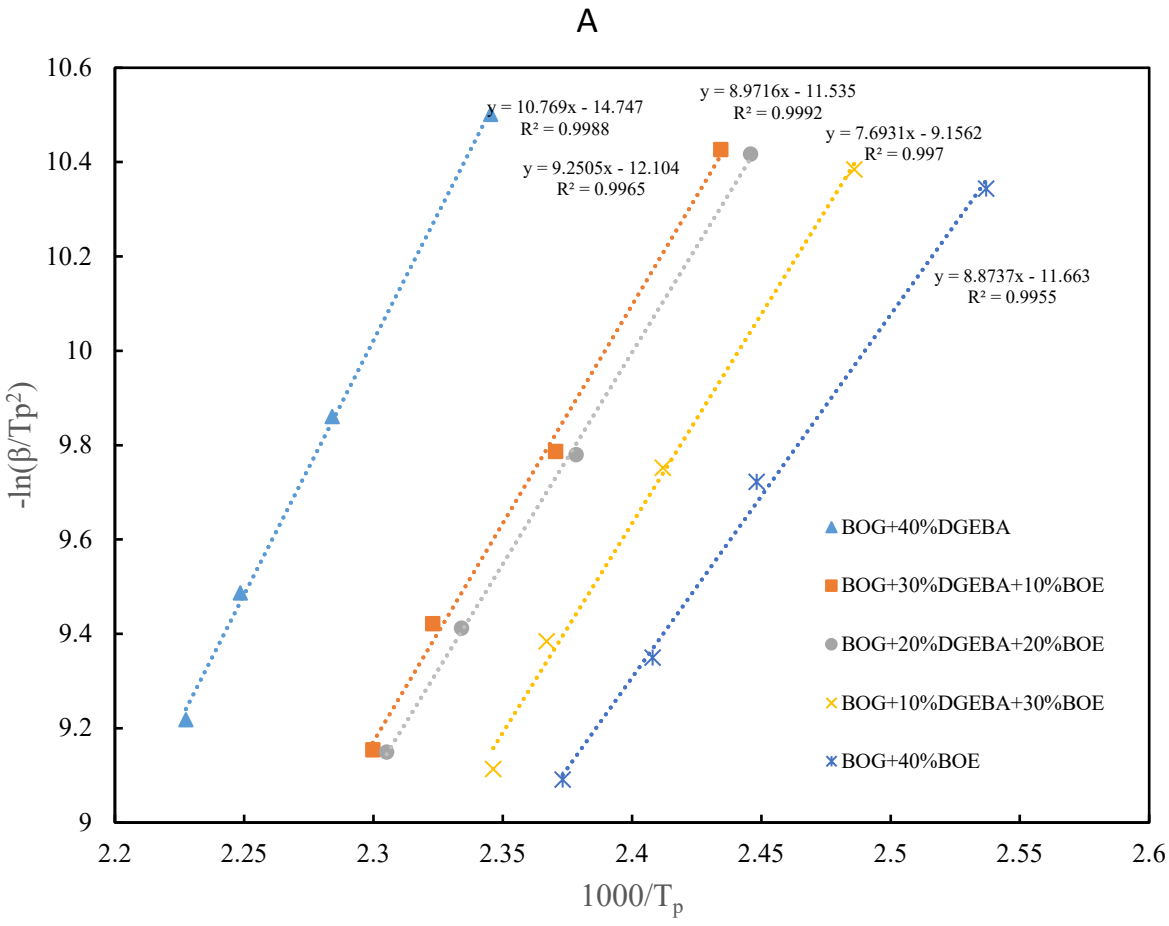

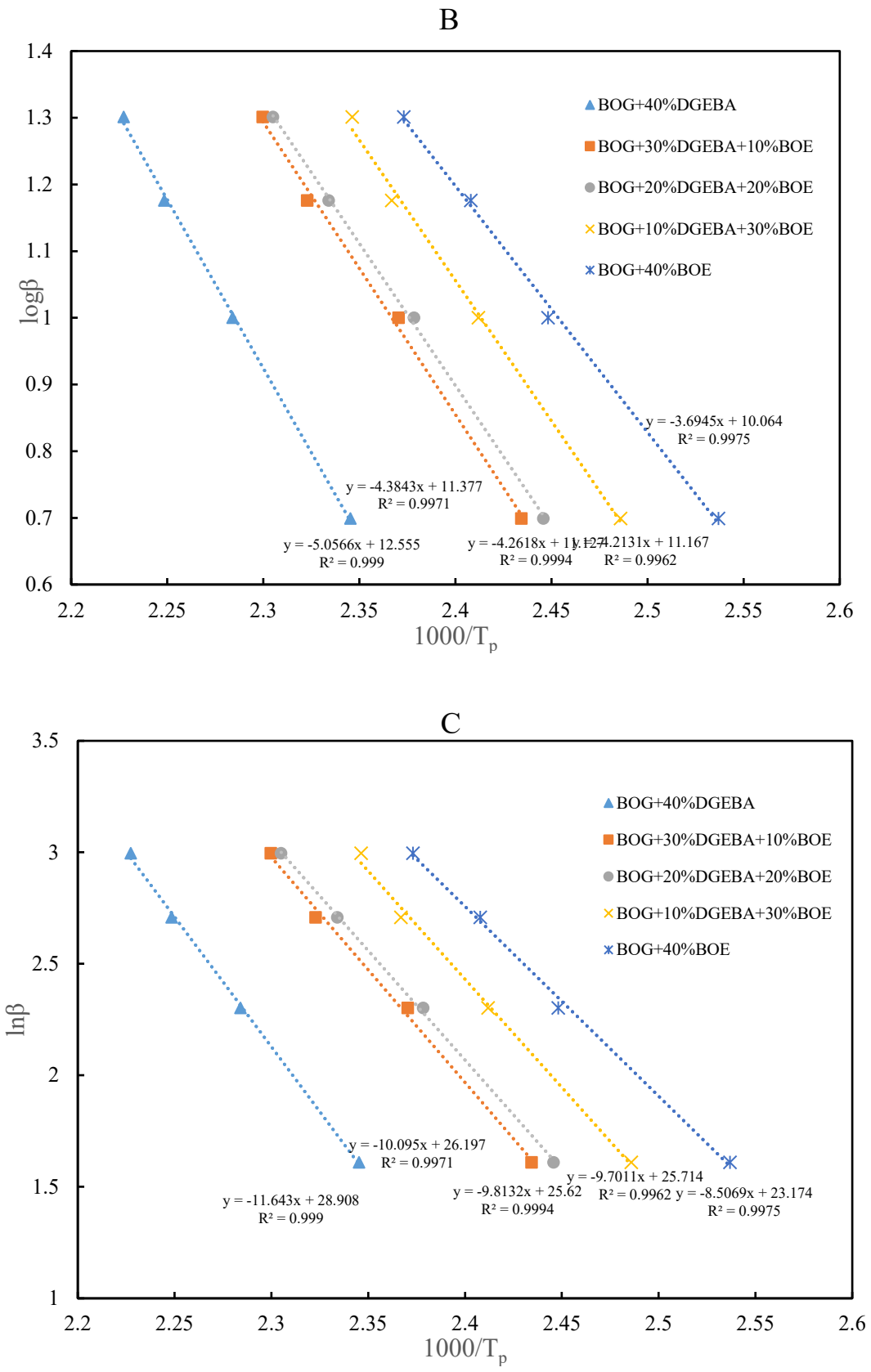

Figure 5. 16 Plots of DSC kinetic analysis by the (a) Kissinger and (b) Ozawa equations, and (c) Crane equations

Consistent with the result of the curing temperature, the E_a decreased with the increase in the ratio of BOE. This result indicates that the chemical reactivity of BOE with BOG is higher than with DGEBA. The increase of the percentage of BOE is creating a mixture of DGEBA and their apparent activation energy is necessarily between the two initial apparent activation energies. In correlation with the GPC result of BOE resin, it has a very high value of polydispersity. Although it has a larger average molecular weight, it still contains a large number of unreacted small compounds which include many reactive functional groups such as hydroxyl groups and aldehyde groups (Fig.3). Then, they can bring more unoccupied reactive sites, promoting cross-linking with BOG resin compared with using DGEBA.

Table 5. 8 The calculated thermal curing kinetic parameters

Resin type		Heating rate (°C/min)				Activation energy (kJ/mol)		n
		5	10	15	20	Kissinger	Flynn–Wall–Ozawa	
BOG+40%DGEBA	Onset temp (°C)	122.2	134.2	136.9	139.9	89.5	92.1	0.95
	Peak temp (°C)	153.2	164.7	171.6	175.8			
BOG+30%DGEBA+10%BOE	Onset temp (°C)	104.0	106.5	116.5	123.9	76.9	79.8	0.94
	Peak temp (°C)	137.6	148.7	157.4	161.7			
BOG+20%DGEBA+20%BOE	Onset temp (°C)	95.7	107.8	114.9	119.3	74.2	77.3	0.93
	Peak temp (°C)	135.7	147.3	155.3	160.7			
BOG+10%DGEBA+30%BOE	Onset temp (°C)	84.9	104.2	114.6	116.1	73.8	76.7	0.94
	Peak temp (°C)	129.1	141.5	149.3	153.1			
BOG+40%BOE	Onset temp (°C)	85.4	106.1	112.0	113. 8	64.0	67.3	0.92
	Peak temp (°C)	121.0	135.3	142.1	148.2			

Figure 5. 17 displays the DSC curves indicating the glass transitions of the 40 wt% BOE/DGEBA cured BOG resins obtained at a 5 °C/min heating rate. In order to ensure the complete crosslinking of polymers, the glass transition temperatures were determined in the second run of DSC analyses [192]. The glass transition temperature (T_g) values of the epoxy cured BOG resins were higher than that of the uncured BOG resin (75.8±1.1°C), with the range of 96.1−121.1 °C (**Table 5. 9**). However, higher

proportions of BOE resulted in a lower T_g. When only BOE was used as the curing agent the T_g reached the minimum value of 96.1 °C, because of the higher EEW of BOE (317.1) than DGEBA (160.65) [194], the unreacted small molecules from the bio-oil lower the Tg value, in agreement with other researchers [193]. Moreover, unlike DGEBA, which is a rigid molecule with only aromatic rings, BOE contains dimers and oligomers with rigid and flexible connections and, the flexible structure and methoxy in bio-oil may lower the T_g of cured resins.[190]. Besides, the curve of T_g gradually changes to a broader temperature range upon transition by the addition of BOE. In particular, when the amount of BOE added is more than 20%, the change in T_g is more obvious. Similarly, the presence of non-phenolic compounds in the BOE may influence the polymer T_g [192].

The thermal stability was investigated by TGA under nitrogen from room temperature to 900 °C and the profiles are shown in **Figure 5. 18**. Results including the initial degradation temperature for 5% weight loss (T_{d5}), the temperature of maximum decomposition rate (T_{max}), and the residue percentage at 800℃ (R_{800}), were determined and presented in **Table 5. 9**.

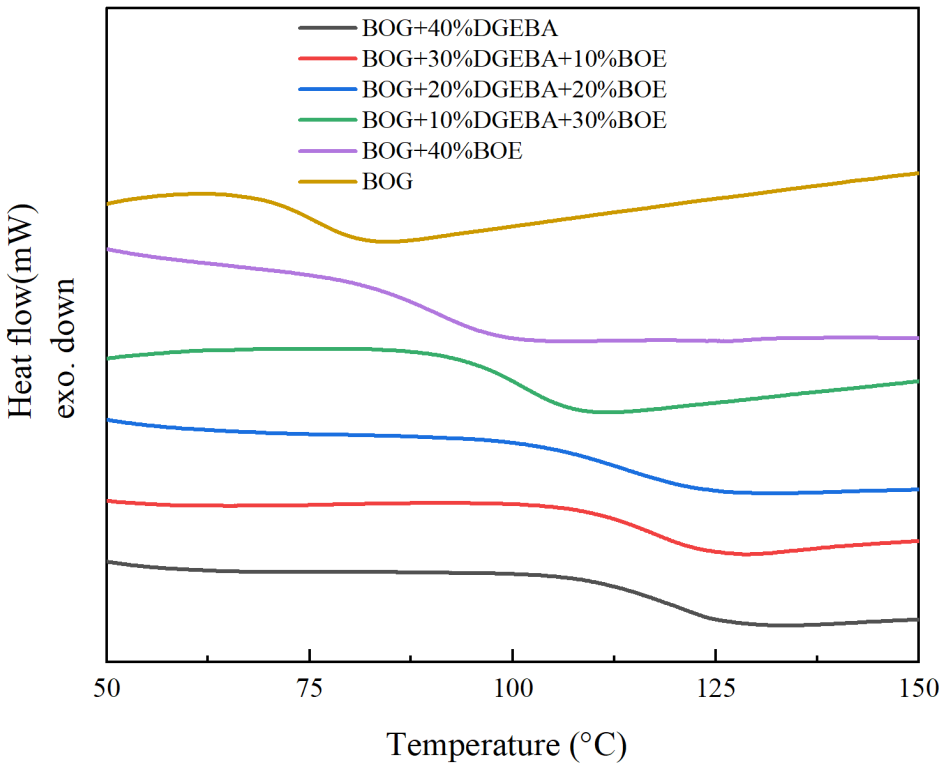

Figure 5. 17 DSC of BOE/DGEBA cured BOG resins

Table 5. 9 DSC, TGA, and DTG results of the cured BOG resins

Resin name	T_g (°C)	T_{d5} (°C)	T_{max} (°C)	R_{800} (%)
BOG	75.8±1.1	203.7±0.8	335.0±1.0	30.90±0.21
BOG+40%DGEBA	121.1±0.5	282.9±0.6	390.6±1.7	39.66±0.31
BOG+30%DGEBA+10%BOE	117.4±0.8	282.8±1.1	389.2±2.1	39.99±0.39
BOG+20%DGEBA+20%BOE	113.7±0.7	282.4±2.7	385.7±3.3	40.16±0.23
BOG+10%DGEBA+30%BOE	101.2±1.5	278.1±2.3	383.1±1.5	42.29±0.43
BOG+40%BOE	96.1±2.4	271.7±1.3	381.5±2.2	43.26±0.57

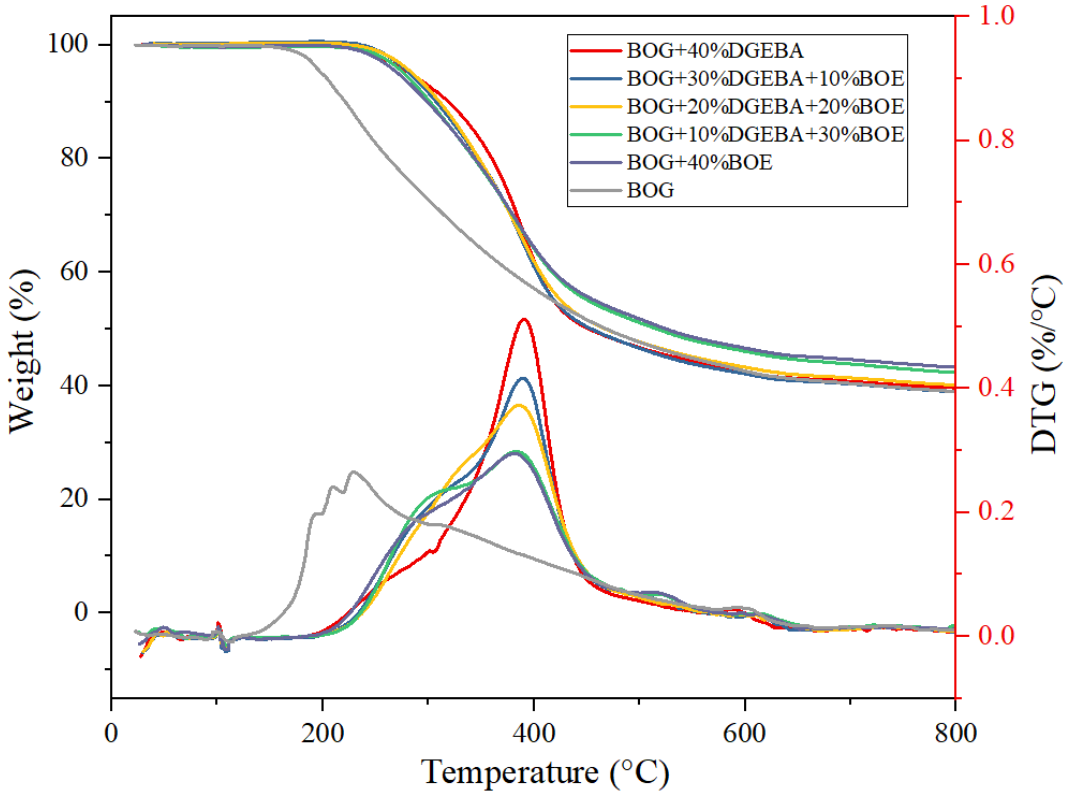

Figure 5. 18 Thermal decompositions of BOE/DGEBA cured BOG resins

As shown in **Table 5. 9**, compared to uncured BOG resin, the thermal stability of cured resins was significantly improved by observing the higher value of T_{d5}, T_{max}, and R_{800}.

With the increase of BOE content, T_{d5} and T_{max} of the cured resins gradually decrease, until reaching the lowest value when using 40% of BOE for curing (271.7 and 381.5, respectively). The decrease in thermal stability may be due to the presence of methoxy groups on the aromatic ring resulting from bio-oil-derived guaiacols. These groups are known to reduce thermal stability by donating electrons to the aromatic rings [190]. However, it can be founded in **Figure 5. 18** that adding BOE as a curing agent can obtain a relatively slower thermal decomposition rate.

The residual materials of the cured resins at 800°C are also listed in **Table 5. 9.** The presence of BOE resin leads to a significant increase in R_{800} value for the cured resins (43.26%) which is 9.1% higher than that of using pure DGEBA (39.66%) and indicates the positive effect of BOE by reducing resin decomposition. This is attributed to the rich aromaticity in the main chain between rigid rod-like aromatic linked by carbon-carbon double bonds inherent to BOE which is produced by bio-oil. These polymer fragments would be transformed into char at high temperatures [193]. It also explains that BOE and BOG have more cross-linking reactions under high-temperature conditions than DGEBA. The good thermal stability of BOE cured BOG resin illustrates that BOE is very attractive as a promising substitute for commercial DGEBA whose petroleum-based thermosetting resins.

5.5 Thermal assessment

The collected data of disasters in **Table 5. 10** show the frequent occurrence of explosions in resin factories from 2003-2021. Given the considerable production of resins and their wide field of application, the potential thermal risk of their manufacture is what we must pay attention permanently.

5.5.1 Thermal Risk parameters

From the characteristics of DSC, basic thermal dynamic parameters for unknown substances initially could be acquired and fitted to a rate equation to calculate runaway adiabatic behavior. The required data are the heat of reaction (ΔH), exothermic peak temperature (T_p), reaction order (n), and activation energy (E_a). [207, 253]. In addition, the safety parameters such as (Time to Maximum Rate) TMR_{ad}, ΔT_{ad} (adiabatic temperature increase) and MTSR (Maximum Temperature of Synthesis Reaction) could

be determined to evaluate the degree of thermal hazard during the reaction, storage, or transportation [219].

Table 5. 10 Disasters related to resins from 2003-2021.

Date	Material type	Location	Injury	Hazard	Cause
16/07/2021	PET Resin	SC, US	2 injured	Potential Dust Explosion	/
08/04/2021	alkyd polyester resin	Columbus, US	1 dead, 9 injured	Reactor explosion	/
03/11/2020	epoxy resin	Jiangsu, China	2 injured	Reactor explosion	BPA caused explosion
15/10/2019	PF resin	Guangxi, China	4 dead, 8 injured	Reactor explosion	/
01/09/2014	Silicone resin	Mie Ken, Japan	5 dead, 11 injured	explosion	release of extremely explosive hydrogen
21/09/2012	epoxy resin	Hyogo, Japan	1 dead, 30 injured	tank explosion	/
01/02/2003	phenolic resin	Laurel County, Ky., US	7 dead	explosion and fire	housekeeping violations

Thermal safety concerning severity in connection with an exothermic runaway scenario is described using the adiabatic temperature increase ΔT_{ad} calculated according to:

$$\Delta T_{ad} = \frac{\Delta H}{C_p}$$

Equation 5. 3

Where ΔH (J/g) represents the specific enthalpy of reaction. C_p (J/g/K) is the heat capacity of the reaction mixture determined using a DSC measurement.

The MTSR is the temperature reached if the synthesis reaction is suddenly left under

adiabatic conditions. If unconverted reactants are still present in the reaction mixture after the cooling failure, they will react in an uncontrolled way and lead to an adiabatic temperature increase. MTSR is calculated as:

$$MTSR = T_P + \Delta T_{ad}$$

Equation 5. 4

TMR is an indicating data used as a reference for planning emergency measurements. It indicates the time needed from a given temperature at which the runaway begins to the point of reaching the maximum reaction rate. The less the TMR, the higher the risk of the runaway reaction. Stoessel pointed out that the acceleration due to temperature increase dominates far over the effect of reactant depletion. Thus, the kinetics are often simplified to zero order. Generally, the zero-order reaction results in a shorter time to explosion than higher reaction orders. The following is the commonly used TMR equation for a zero-order reaction [203, 205, 208, 214, 217].

$$TMR_{ad}(T) = \frac{C_p R T^2}{q_{(T)}\, E_a}$$

Equation 5. 5

Where at the temperature to be assessed, according to **Equation 5.5**. the specific heat capacity (Cp), the specific heat release rate (q(T)) at temperature fixed (T), and the activation energy (Ea) is required. q(T) is obtained using:

$$q_{(T)} = (-r_A)V(-\Delta H)$$

Equation 5. 6

Where at the temperature (*T*), r_A (mol·L^{-1}·s^{-1}) represents the reaction rate. For a single n^{th}-order, the reaction rate can be expressed as [210]

$$-r_A = \frac{-dC_A}{dt} = kC_{A0}^n(1 - X_A)^n$$

Equation 5. 7

Where C_{A0} is the initial concentration (mol·L^{-1}), C_A is the concentration at any time *t* (mol·L^{-1}), X_A is the fractional conversion, and *k* is the reaction rate constant (s^{-1}).

According to the Arrhenius model, the rate constant *k* is an exponential function of temperature:

$$k = Ae^{-E_a/RT}$$

Equation 5. 8

Thus, the equation above can be converted under zero-order as follows:

$$-r_A = k = Ae^{-\frac{E_a}{RT}}$$

Equation 5. 9

Then, TMR can be expressed under zero-order as follows:

$$TMR_{ad}(T) = \frac{C_p RT^2}{E_a Ae^{-\frac{E_a}{RT}}}$$

Equation 5. 10

Non-isothermal DSC analysis performed at four heating rates is commonly applied to study the behavior and kinetics for polymerization and curing of resins [188]. The use model-free methods were employed to evaluate the kinetic parameters according to the equations of Kissinger, Ozawa and Crane as shown in **Chapter IV**. According to **Equation 5. 11**, the obtained activation energies were used to calculate the logarithm of the pre-exponential factor (log A/s^{-1}).

$$A = \beta \frac{E_a}{RT_p^2} exp\left(\frac{E_a}{RT_p}\right)$$

Equation 5. 11

5.5.2 Evaluation of safety parameters of resin synthesis

In order to examine the thermal behavior of the reaction DSC thermograms of phenol-glyoxal and bio-oil-glyoxal resin synthesis were presented in **Figure 5. 19** and **Figure 5. 20**, respectively. The exothermic characteristic of temperature and enthalpy of the reaction is shown in **Table 5. 11.** The thermograms of both PG and BOG resins exhibit just one main exothermic peak corresponding to the polymerization reaction between phenol or substituted phenol with glyoxal and catalyzed by acid to form addition products. Oligomers were then formed in the condensation part. By comparison, **Figure 5. 19** and **Figure 5. 20** indicate that the exothermic peak is sharper with using phenol than using bio-oil. Moreover, the polymerization reactions occur at temperatures between 109 and 210 °C for PG and BOG resins, respectively. According to details in **Table 5. 11,** the initial reaction temperatures seem not to be dependent on the phenolic source whereas the peak temperature of BOG was higher than PG for each heating rate. In our previous work [254], we identified the compounds in bio-oil and also the multiple phenolics which can participate in the polymerization of glyoxal.

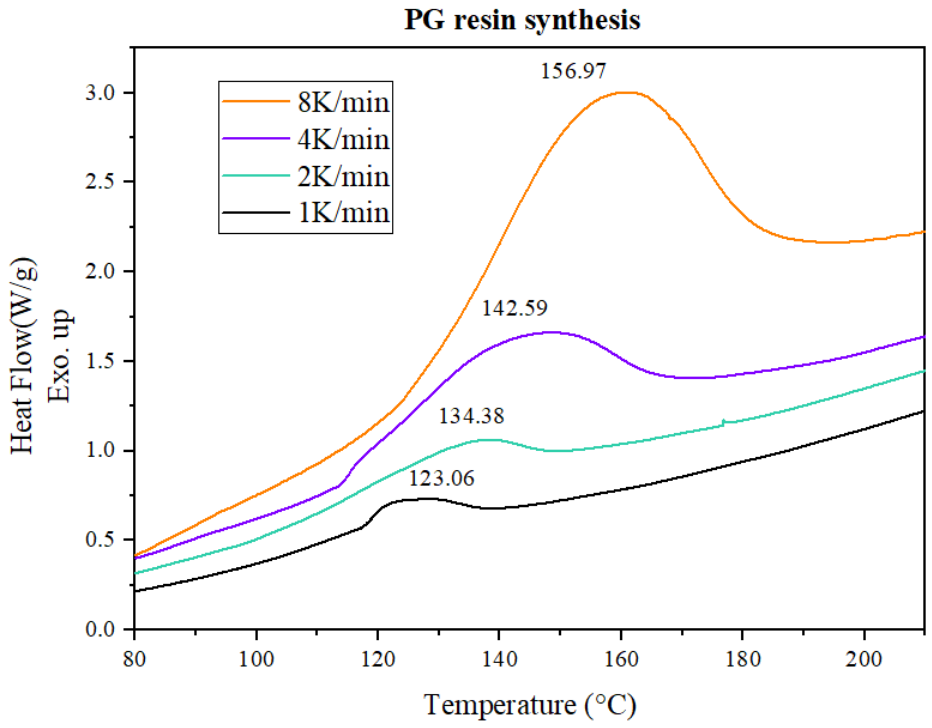

Figure 5. 19 DSC thermograms of PG resin synthesis at heating rates of 1, 2, 4, and 8 K min^{-1}

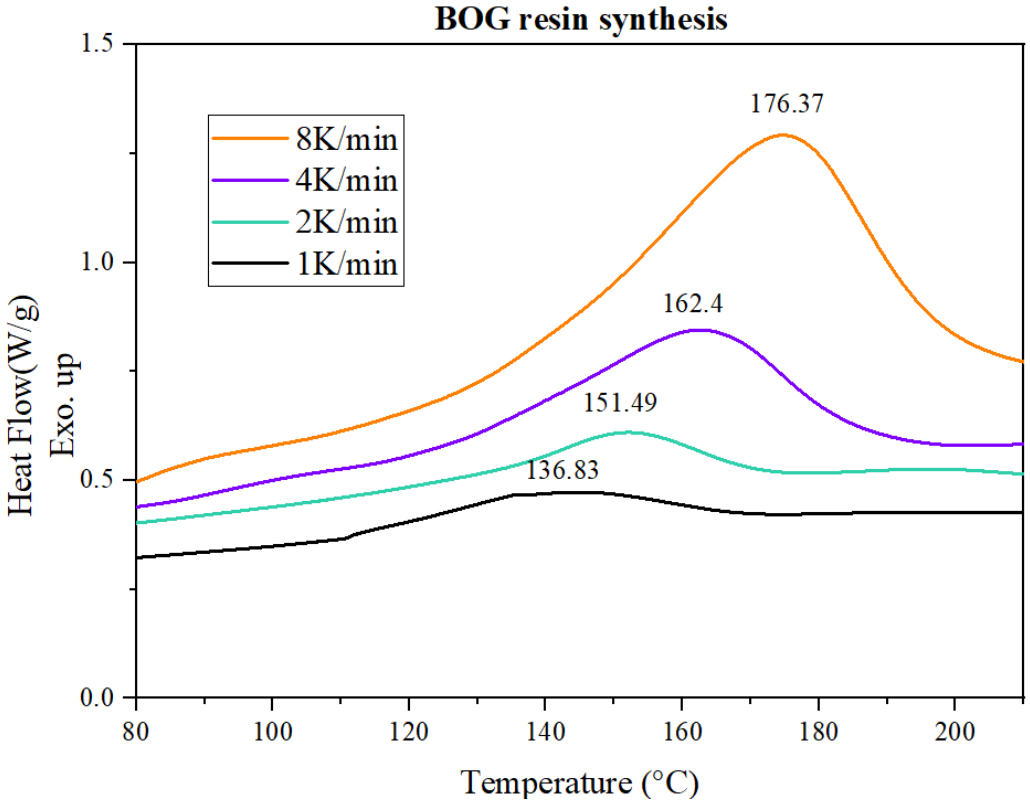

Figure 5. 20 DSC thermograms of resin synthesis at heating rates of 1, 2, 4, and 8 K min^{-1}

Table 5. 11 Measured and calculated parameters related to the reaction of resin polymerization using DSC

Resin	Heating rate (K/min)	Onset temp. (°C)	Peak temp. (°C)	Enthalpy(J/g)	The activation energy (J/mol)		Reaction order n	Pre-exponential factor A (S^{-1})
					Kissinger	FWO		
PG	1	112.59	123.06	254.1	81702	84221	0.943	6.217×10^{7}
	2	114.03	134.38	273.9				
	4	115.11	142.59	283.6				
	8	126.87	156.97	302.3				
BOG	1	109.52	136.83	174.5	74515	77642	0.933	2.652×10^{6}
	2	114.54	151.49	178.0				
	4	115.34	162.40	183.9				
	8	126.21	176.37	183.2				

The substituent of them which bring higher steric hindrance can increase the difficulty of the reaction [188].

In general, the enthalpy of acid-catalyzed phenol-formaldehyde resin synthesis reaction is higher than 300 J/g [210]. However, both the PG and BOG resins generated reaction exothermic heat lower than 300 J/g, indicating that the use of glyoxal reduces the reaction enthalpy. Additionally, the difference between reaction enthalpy values of PG and BOG is obvious (183.9 J/g for BOG and less than 283.6 J/g for PG resin).

For the kinetic study, the Kissinger, Flynn–Wall–Ozawa (FWO) and Crane equations were applied. The correlation coefficient (R^2) of each curve fitting was greater than 0.99, proving the accuracy of the linear fitting as demonstrated (**Figure A 4. 5**). The activation energy of PG and BOG polymerization was calculated by using both Kissinger (**Equation 4. 1**) and FWO (**Equation 4. 2**) methods and the reaction order was simply obtained by the Crane equation (**Equation 4. 3**). From the two methods, the E_a value of the BOG resin is lower than that of PG (74 515 and 81 702 J/mol by the Kissinger

method). The global polymerization reaction of the PG and BOG resins was approximately first order (n = 0.943 - 0.933), which is in agreement with previous studies of phenol-formaldehyde novolac resin synthesis [210, 211, 218].

The value of TMR_{ad} is determined by **Equation 5. 10**. with the temperature of resin synthesis used (125°C) which was derived for the zero-order reaction resulting in shorter TMR_{ad}. The variation of TMR_{ad} with different synthesis temperatures (**Figure 5. 21**) is also examined to determine $T_{D24,}$ temperature at which TMR_{ad} reaches 24h (**Table 5. 12)**. By observing **Figure 5. 21,** it is clear that BOG resin has higher TMR_{ad} value when the polymerization reaction temperature set as 125°C. Since the higher the TMR, the less the risk of the runaway reaction [205]. Using bio-oil for polymerization can reduce the risk of reaction.

The adiabatic temperature rise ΔT_{ad} is calculated according to **Equation 5. 3**. The average value of the PG reaction (86.02 K) is higher than the BOG one (75.58 K). The MTSR value of BOG synthesis is higher than PG resin due to the higher T_p of BOG resin. The results of the calculation with various heating rates are shown in Table A 4. 1.

Since the adiabatic temperature rise and time to maximum rate under adiabatic conditions are commonly used to evaluate the severity and probability of the runaway reaction, an assessment matrix (**Figure 1. 19**) was designed according to Stoessel method [203] to consider both reasons. The polymerization reactions of PG and BOG have belonged to the high-risk reactions.

Table 5. 12 Safety criteria of resin polymerization led at 125 °C (Average value)

Resin	C_{pm} (J/g/K)	TMR_{ad} at 120°C (min)	T_{D24} (°C)	MTSR (K)	ΔT_{ad} (K)
PG	3.23	2.6	39	497	86
BOG	2.37	8.7	46	508	76

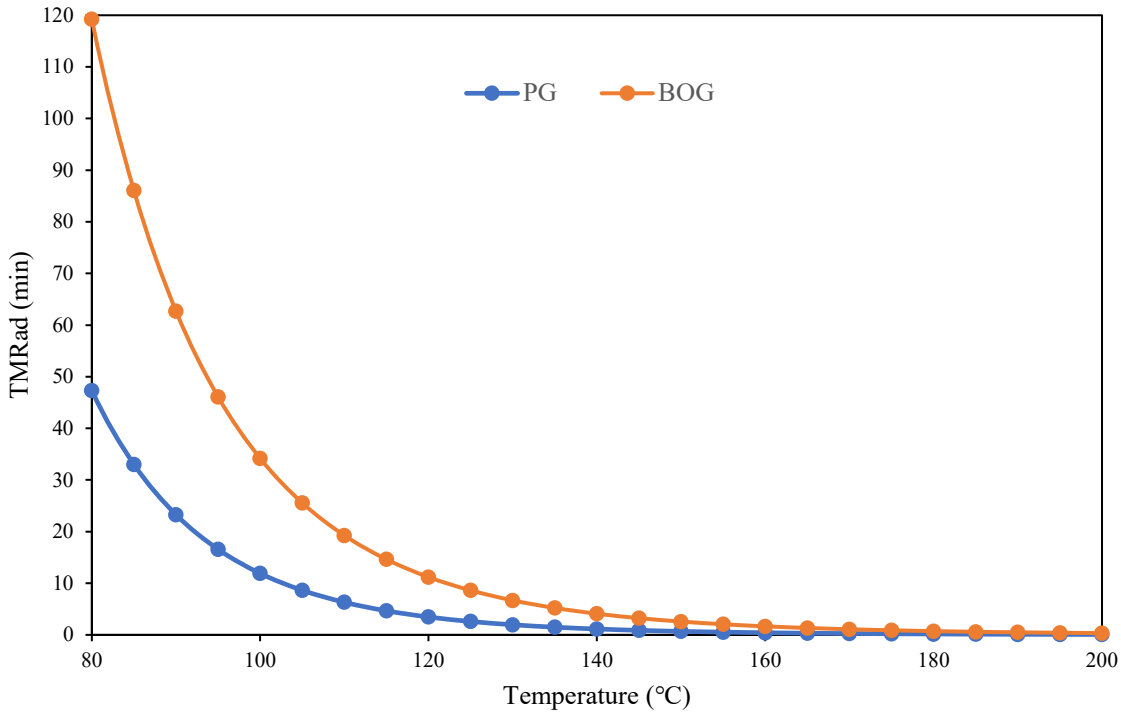

Figure 5. 21 Simulated TMR versus reaction temperature for PG and BOG synthesis (heating rate of 4K/min).

5.5.3 Evaluation of safety parameters of BOG resin curing

The curing kinetic of the Novolac resin was studied by many researchers [187, 245, 252], however, there is no report mentioning the evaluation of thermal hazards in novolac resin curing. In this study, the typical safety parameters such as TMR_{ad}, ΔT_{ad} and MTSR were calculated under various heating rates and shown in Appendix **Table A 4. 2.** The average values are shown in 错误!未找到引用源。**.** The value of $TMR_{ad,}$ determined according to **Equation 5. 10** at a typical curing temperature (120°C), is derived for a zero-order reaction. The variation of the value of TMR_{ad} as a function temperature of the curing reaction is shown in **Figure 5. 22** for the temperature range of 120-200°C. It is indicated that BOG resin curing has a higher TMR_{ad} value and the addition of biochar increases this value in both cases of cure of novolac resins.

At the various heating rate, ΔT_{ad} values of all the resins curing are close **(Table A 4. 2)**. The average ΔT_{ad} value of PG curing (53.18 K) is slightly higher than that of BOG (51.56 K). However, after adding 5% of biochar, both PG and BOG resins had an obvious decrease in the value of the adiabatic temperature rise (36.63 K for PG resin

and 34.62 K for BOG resin). It was worth mentioning that adding biochar can significantly increase the specific heat capacity of the sample mixture.

According to the safety assessment matrix in **Figure 1. 19,** both ΔT_{ad} and TMR were considered to evaluate the severity and probability of the runaway reaction. If only consider the TMR_{ad} value, the curing reaction of all the resins has belonged to a high probability of runaway reaction. Classifying severity level according to ΔT_{ad}, indicates that curing biochar is medium severity level ($50<\Delta T_{ad}<200$ K) while in the presence of biochar the severity level is low (<50 K). We can therefore conclude that the use of bio-oil and biochar for resin curing reaction can reduce the runaway risk of reaction.

Table 5. 13 Safety criteria of resin curing led at 120 °C (Average value)

Reaction mixture	C_{pm} (J/g/K)	TMR_{ad} at 120°C (min)	T_{D24}	MTSR (K)	ΔT_{ad}(K)
PG + 40%DGEBA	1.56	5.06	46.60	487.07	53.18
PG + 40%DGEBA+ 5%biochar	2.29	6.48	42.57	469.68	36.63
BOG + 40% DGEBA	1.65	7.96	53.54	491.12	51.65
BOG + 40% DGEBA + 5%biochar	2.48	8.12	46.53	470.16	34.62

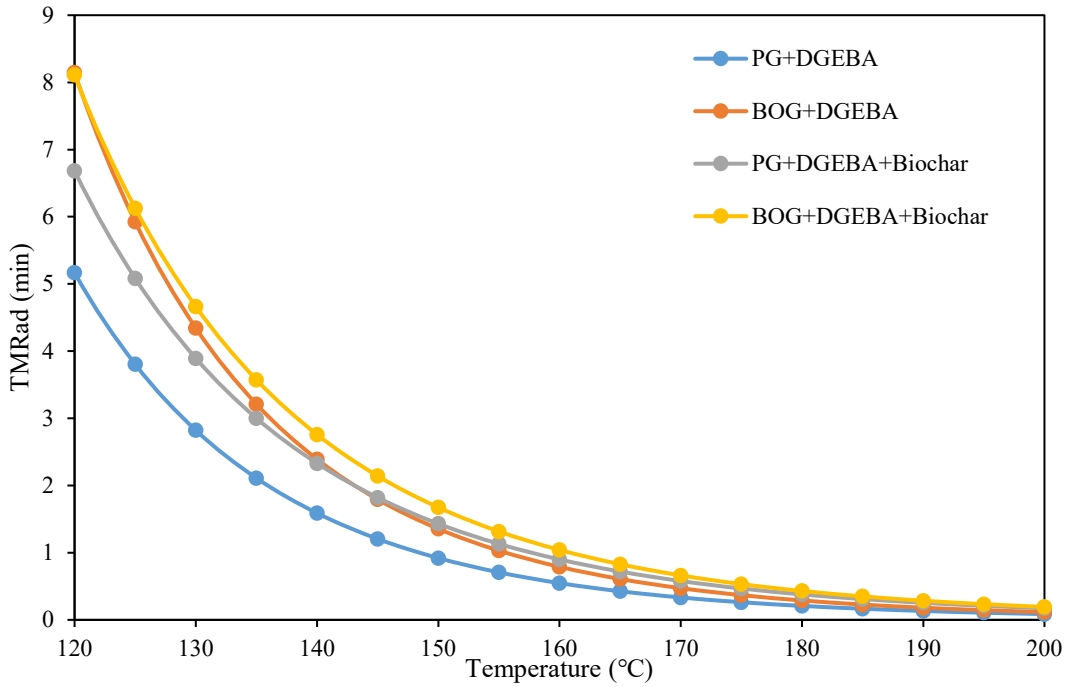

Figure 5. 22 Curve of resin curing time to the maximum rate at a heating rate of 10 K/min

5.6 Conclusion

- The polymerization of glyoxal with the water-insoluble fraction of fractional condensation of bio-oil (OIL1WI) catalyzed by oxalic acid was succeeded as confirmed by analysis of FTIR spectroscopy, ^{1}H-NMR, and GPC analyses. The resin produced by OIL1WI showed a higher phenol conversion and yield than the model phenol bio-oil fraction and was close to phenol resin. The BOG resin has a closer thermal behavior (T_g and thermal degradation) with PG resin than MPG, but the residual carbon contents at 800°C were higher than PG. E_a value for the BOG resin synthesis is lower than that of PG one.

- The synthesis of bio-based epoxy resin (BOE) from the water-insoluble fraction of beechwood pyrolysis oil and epichlorohydrin was successful and its chemical structure was confirmed by FT-IR and 1H-NMR spectroscopy. The resin synthesis mechanism was discussed and a schematic was proposed. The yield and epoxy equivalent weight (EEW) of the epoxy resin at various reaction times (1.5, 2, and 2.5h) of the second step were also discussed and the 2h was selected to obtain a relatively high yield (90.95%) and low EEW value (317.1) at the same time. BOE was shown a higher EEW than DGEBA (180.7) due to the complexity and lower phenolic hydroxyl reactivity of phenolic components in bio-oil than in commercial phenols.

- Bisphenol A type epoxy (DGEBA) was used as a formaldehyde-free cross-linker for bio-oil based phenol-glyoxal resins. The curing mechanism was investigated by DSC and FTIR measurements. The curing initial temperature of BOG is lower than PG whereas the peak temperature is higher than PG. The activation energy (E_a) is similar (86.41 and 89.53 kJ/mol for PG and BOG respectively). Biochar was employed as a curing additive. The curing of resins with biochar shows a lower initial and peak temperature than without biochar, and the E_a of BOG decreased from 89.5 to 79.6 KJ/mol.
- The more environment-friendly synthesized bio-based epoxy resin (BOE) was the first time to be used to gradually replace bisphenol A diglycidyl ether (DGEBA) equivalent (0-100%) as a formaldehyde-free cross-linker for bio-oil based glyoxal novolac resin (BOG). The curing reaction for all of the resins proved to be approximately first order. All of the cured resins were curable at a temperature of 84-176°C. Incorporating BOE resin was able to obtain a lower curing initial temperature, peak temperature, and activation energy compared to using DGEBA. This suggested that the presence of BOE resin promoted the curing reactions and the lowest E_a (64.0 kJ/mol via Kissinger method) reached 40% BOE cured BOG resin.
- The thermal properties of the BOE/DGEBA cured BOG resins are more stable than uncured BOG by observing the increase of T_g, T_{d5}, T_{max} and R800 values. By the increasing BOE content, T_g, $T_{d5,}$ and T_{max} of the cured resins decrease slightly. However, the R_{800} value increased until reached the lowest value at using 40% of BOE for curing indicating the positive effect of BOE on reducing resin decomposition. The good thermal stability of BOE cured BOG resin illustrates that BOE is very attractive as a promising substitute for commercial DGEBA.
- Finally, DSC analysis of non-isothermal experiments of the bio based novolac resin synthesis and curing reactions under various heating rates, were performed to evaluate its runaway risk and safety criteria. A comparison with PG resin was done. The BOG resin reaction leads to a higher TMR_{ad} value and lower ΔT_{ad} value. It is quite reasonable to conclude that the use of bio-oil as a phenol precursor, for resin synthesis, reduces the risk of runaway of resin synthesis. The decrease in thermal risks of the curing process of bio-oil resin is

also significant, improved also by the use of biochar as an additional curing agent.

General conclusions and perspectives

In this thesis, the combination of both fractional condensation and water extraction upgrading methods was accomplished to separate pyrolysis bio-oil. The storage stability of bio-oil fractions was also studied. Based on the results and discussions of the bio-oil composition and aging, different fractions of phenol rich bio-oil precursors obtained from woody biomass pyrolysis oil were used in the bio-based phenolic resin and epoxy resin synthesis to substitute petroleum-derived phenol: (1) raw bio-oil, (2) bio-oil obtained from fractional condensation, or (3) the water-insoluble fraction of the bio-oil obtained from fractional condensation.

Four experimental and/or modeling distinct parts have been led to answer these problems. Firstly, combining fractional condensation and water extraction has been proven to be an efficient and interesting method for the separation of bio-oil due to both the dew points and the solubility in water of chemical compounds. Compared with the single-stage condensation, a significant difference in the physicochemical properties of the bio-oil is noticed when using the three-stage condensation system.

- Phenolic compounds and sugars are mainly found in the first condenser, water is mainly recovered in the second and the third condensers.

- An increase in the first condenser temperature promotes the selectivity for sugars and phenolic compounds in Oil-1.

- The effect of additional separation of bio-oil by water was more beneficial for the fraction of the first condenser. Indeed, sugars can be separated efficiently in the WS fraction, whereas phenolics remain in the WI fractions.

The accelerated aging study of storage of bio-oil products obtained by fractional condensation and water extraction has been evaluated by comparing the variation in the composition of aged samples with that of fresh bio-oil and the oil obtained from single condensation. The chemical analysis indicated that:

- The changes in chemical compounds contents occurred presumably due to hydrolysis, esterification, oxidation, and polycondensation reactions.

- Concerning the effect of fractional condensation, the stability of Oil-1 has been improved, whereas Oil-3 is more unstable compared to Oil-S due to its

excessive acid and water content.

- The further separation by water extraction allowed an improvement of the stability of most of the chemical families in the water-insoluble fractions.

- The hydrolysis of sugars promotes the formation of valuable chemical components in the water-soluble fraction.

In the third step of this work, novolac resin synthesis of bio-oil products from fractional condensation and water extraction with acetaldehyde were realized with success, as confirmed by various characterization methods.

- Compared with the untreated bio-oil, the use of pyrolysis bio-oil from the high-temperature condenser obtained by fractional condensation and water extraction can significantly improve the thermal properties of the OIL1WIA resin.

- The high catalyst content can produce bio-oil-based resins close to commercial resins concerning a higher degree of polymerization, and phenolic hydroxyl groups but the distribution and the size of the bio-oil-based resin are larger than commercial resin.

- The improved thermal stability of the bisphenol A type epoxy (DGEBA) cured OIL1WIA resin demonstrates the potential feasibility of using water extraction pyrolysis oil to replace commercial phenol for producing a bio-based green material.

- The curing kinetics is slightly promoted at lower temperatures thanks to small molecules other than phenolic compounds available in bio-oil fractions but the hindrance effect can limit the efficiency of the reaction.

A greener novolac resin system was successfully synthesized consisting of glyoxal, a water-insoluble fraction of fractional condensation bio-oil product (OIL1WI), and oxalic acid. The resin showed a high phenol conversion, yield, and thermal behavior close to those of phenol resin.

The synthesis of bio-based epoxy resin (BOE) from the water-insoluble fraction of pyrolysis oil (OIL1WI) was carried out for producing a cross-linker for curing bio-oil-based phenol-glyoxal resins.

- The epoxy equivalent weight (EEW) of homemade epoxy resin was twice higher than commercial DGEBA epoxy resin.
- Incorporating BOE resin was able to induce a lower curing initial temperature, peak temperature, and activation energy compared to DGEBA-resin.
- The good thermal stability of BOE cured BOG resin illustrates that BOE is very attractive as a promising substitute for commercial DGEBA.
- The curing of resins with biochar shows a lower initial and peak temperature and E_a.

The evaluation of critical runaway conditions and safety criteria have been investigated based on the kinetic parameters of the novolac resin synthesis and curing reaction.

The BOG resin results from a higher TMR_{ad} value and lower ΔT_{ad} value when the polymerization reaction temperature is set as 125℃. Using bio-oil for polymerization can reduce the risk of reaction.

Under the curing process temperature of 120℃, BOG resin has a higher TMR_{ad} and lower ΔT_{ad} value than the curing with DGEBA. The addition of biochar results in increasing in TMR_{ad} value and decreasing ΔT_{ad}. Thus, using bio-oil glyoxal resin, bio-oil epoxy resin and biochar for resin curing reaction can significantly reduce the risk of reaction.

From chapters 2 to 6, some interesting ideas emerge on the basis of our results and some perspectives can be formulated for the future continuation of this work.

- According to the targeted compound, design the bio-oil extraction route to obtain more valuable bio-oil components

As demonstrated in this work, solvent extraction is a very efficient and environment-friendly method for upgrading bio-oil. From our results, it can be shown, that after the factional condensation of beechwood pyrolysis bio-oil, water was simply used as an extraction solvent and showed great ability in acquiring phenol-rich bio-oil fraction. However, there are still many valuable compounds worth extracting for further use. There are also some effective solvents with excellent extraction effects according to the work of some scholars [255] (ethyl acetate, dimethyl ether, water/methanol, dichloromethane…). An in-depth study of the use of these solvents will make it possible

to valorize a large number of the chemicals present in bio-oils (**Figure 6. 1**)

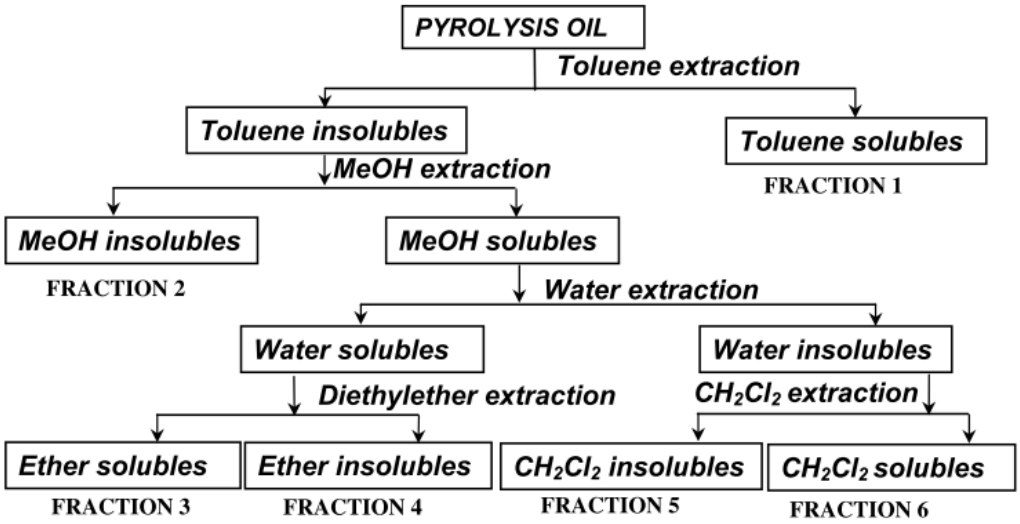

Figure 6. 1 Fractionation scheme for bio-oil chemical characterization

- The hydrolysis of bio-oil to produce HMF and some useful chemical compounds for direct use or application in polymers

1,6-anhydro-b-D-glucopyranose (levoglucosan), an anhydrosugar that can be hydrolyzed to glucose, is the most abundant sugar in the pyrolysis oil. Depending on the type of biomass used and the pyrolysis conditions the content of levoglucosan may have some differences. In our study, bio-oil can contain up to 10 wt% of levoglucosan, and since it has a high solubility in water, 10 wt% of levoglucosan can be founded in the water-soluble fraction of bio-oil, which is very promising for a further application. Bennett et al.[256] studied the acid-hydrolysis of levoglucosan into glucose, and the subsequent fermentation of this hydrolysate into ethanol.

A novel one-pot synthesis process for phenol-5- HMF resin using phenol and glucose was realized by using $CrCl_2$, $CrCl_3.6H_2O$, and TEAC as catalysts aiming to converse glucose to HMF, then undergoing condensation reaction with phenol (Zhong et al. [166]).

Here, we can replace glucose by directly using bio-oil water-insoluble fraction which includes a large quantity of levoglucosan. However, the most important and difficult task is to find an appropriate catalyst.

- The polymerization of bio-oil and furfural at a high-pressure reactor to obtain a green bio-based resin than to study the reaction kinetic

In chapters 4 and 5, we already used the phenol-rich fraction from bio-oil for the polymerization of bio-oil-acetaldehyde, bio-oil-glyoxal, and bio-oil based epoxy resin. We have fully demonstrated the possibility of producing phenolic resin from bio-oil. However, we did a lot of experiments with phenol-furfural without success. Since furfural is a biomass derived-chemical that can be used to replace petrochemicals, it is very promising to apply it to polymerization. Xu et al.[141] studied the cross-polymerization between furfural and phenolics using H_2SO_4 as the catalyst and an autoclave reactor at 30 bar and 200 °C. Based on this study, the use of a high-pressure reactor is required for investigating the polymerization of bio-oil and furfural.

- More mechanical testing and applications of this green material

It would be interesting in the continuation of this work to compare other properties in particular the mechanical properties of these materials such as tensile strength test, internal bonding testing, storage modulus E', loss modulus E'', internal friction tanδ, adhesion strength measurement.

Bibliography

[1] K.M. Zia, A. Noreen, M. Zuber, S. Tabasum, M. Mujahid, Recent developments and future prospects on bio-based polyesters derived from renewable resources: A review, Int. J. Biol. Macromol. 82 (2016) 1028-40.
[2] G.W. Huber, S. Iborra, A. Corma, Synthesis of transportation fuels from biomass: chemistry, catalysts, and engineering, Chem. Rev. 106(9) (2006) 4044-4098.
[3] D. Tilman, R. Socolow, J.A. Foley, J. Hill, E. Larson, L. Lynd, S. Pacala, J. Reilly, T. Searchinger, C. Somerville, Beneficial biofuels—the food, energy, and environment trilemma, Science 325(5938) (2009) 270-271.
[4] M. Stocker, Biofuels and biomass-to-liquid fuels in the biorefinery: catalytic conversion of lignocellulosic biomass using porous materials, Angew Chem Int Ed Engl 47(48) (2008) 9200-11.
[5] S.V. Vassilev, D. Baxter, L.K. Andersen, C.G. Vassileva, T.J. Morgan, An overview of the organic and inorganic phase composition of biomass, Fuel 94 (2012) 1-33.
[6] A.J. Ragauskas, C.K. Williams, B.H. Davison, G. Britovsek, J. Cairney, C.A. Eckert, W.J. Frederick, Jr., J.P. Hallett, D.J. Leak, C.L. Liotta, J.R. Mielenz, R. Murphy, R. Templer, T. Tschaplinski, The path forward for biofuels and biomaterials, Science 311(5760) (2006) 484-9.
[7] C. Mohabeer, L. Abdelouahed, S. Marcotte, B. Taouk, Comparative analysis of pyrolytic liquid products of beech wood, flax shives and woody biomass components, J. Anal. Appl. Pyrolysis 127 (2017) 269-277.
[8] P. McKendry, Energy production from biomass (part 2): conversion technologies, Bioresour. Technol. 83(1) (2002) 47-54.
[9] Q. Zhang, J. Chang, T. Wang, Y. Xu, Review of biomass pyrolysis oil properties and upgrading research, Energy Convers. Manage. 48(1) (2007) 87-92.
[10] L. Zhang, R. Liu, R. Yin, Y. Mei, Upgrading of bio-oil from biomass fast pyrolysis in China: A review, Renew. Sustain. Energy Rev 24 (2013) 66-72.
[11] T. Ai, Z. Wang, H. Zhang, F. Hong, X. Yan, X. Su, Novel Synthesis of Nitrogen-Containing Bio-Phenol Resin and Its Molten Salt Activation of Porous Carbon for Supercapacitor Electrode, Materials 12(12) (2019) 1986.
[12] K.M. Zia, A. Noreen, M. Zuber, S. Tabasum, M. Mujahid, Recent developments and future prospects on bio-based polyesters derived from renewable resources: A review, Int. J. Biol. Macromol. 82 (2016) 1028-1040.
[13] J.L. Easterly, M. Burnham, Overview of biomass and waste fuel resources for power production, Biomass Bioenergy 10(2-3) (1996) 79-92.
[14] M. Bajus, Pyrolysis of woody material, Petroleum & Coal 52(3) (2010) 207–214.
[15] S.V. Vassilev, D. Baxter, L.K. Andersen, C.G. Vassileva, An overview of the chemical composition of biomass, Fuel 89(5) (2010) 913-933.
[16] C.E. Wyman, B.E. Dale, R.T. Elander, M. Holtzapple, M.R. Ladisch, Y.Y. Lee, Coordinated development of leading biomass pretreatment technologies, Bioresour. Technol. 96(18) (2005) 1959-66.
[17] G.W. Huber, Breaking the chemical and engineering barriers to lignocellulosic biofuels: next generation hydrocarbon biorefineries, Citeseer2008.
[18] F.H. Isikgor, C.R. Becer, Lignocellulosic biomass: a sustainable platform for the production of bio-based chemicals and polymers, Polymer Chemistry 6(25) (2015) 4497-4559.
[19] Y.P. Zhang, Reviving the carbohydrate economy via multi-product lignocellulose biorefineries, J. Ind. Microbiol. Biotechnol. 35(5) (2008) 367-375.
[20] M. Crocker, Thermochemical conversion of biomass to liquid fuels and chemicals, Royal Society of Chemistry2010.
[21] Front Matter, Fast Pyrolysis of Biomass2017, pp. P001-P006.
[22] D.M. Alonso, J.Q. Bond, J.A. Dumesic, Catalytic conversion of biomass to biofuels, Green chemistry 12(9) (2010) 1493-1513.
[23] A. Oasmaa, I. Fonts, M.R. Pelaez-Samaniego, M.E. Garcia-Perez, M. Garcia-Perez, Pyrolysis Oil Multiphase Behavior and Phase Stability: A Review, Energy Fuels 30(8) (2016) 6179-6200.
[24] S.A. Archer, R. Steinberger-Wilckens, Systematic analysis of biomass derived fuels for fuel cells, Int. J. Hydrogen Energy 43(52) (2018) 23178-23192.
[25] R. Górecki, A. Piętak, M. Meus, M. Kozłowski, Biomass Energy Potential – Green Energy for the University of Warmia and Mazury in Olsztyn, Journal of KONES. Powertrain and Transport 20(4) (2015) 99-106.
[26] A.V. Bridgwater, Review of fast pyrolysis of biomass and product upgrading, Biomass Bioenergy 38 (2012) 68-94.
[27] W.-H. Chen, B.-J. Lin, Y.-Y. Lin, Y.-S. Chu, A.T. Ubando, P.L. Show, H.C. Ong, J.-S. Chang, S.-H. Ho, A.B. Culaba, A. Pétrissans, M. Pétrissans, Progress in biomass torrefaction: Principles, applications and challenges, Prog. Energy Combust. Sci. 82 (2021).

[28] C.Z. Zaman, K. Pal, W.A. Yehye, S. Sagadevan, S.T. Shah, G.A. Adebisi, E. Marliana, R.F. Rafique, R.B. Johan, Pyrolysis: A Sustainable Way to Generate Energy from Waste, Pyrolysis2017.
[29] Y. Lu, X.Y. Wei, J.P. Cao, P. Li, F.J. Liu, Y.P. Zhao, X. Fan, W. Zhao, L.C. Rong, Y.B. Wei, S.Z. Wang, J. Zhou, Z.M. Zong, Characterization of a bio-oil from pyrolysis of rice husk by detailed compositional analysis and structural investigation of lignin, Bioresour. Technol. 116 (2012) 114-9.
[30] A.K. Sakhiya, A. Anand, P. Kaushal, Production, activation, and applications of biochar in recent times, Biochar 2(3) (2020) 253-285.
[31] J. Koppejan, S. Van Loo, The handbook of biomass combustion and co-firing, Routledge2012.
[32] J.A. Okolie, S. Nanda, A.K. Dalai, J.A. Kozinski, Chemistry and Specialty Industrial Applications of Lignocellulosic Biomass, Waste and Biomass Valorization 12(5) (2020) 2145-2169.
[33] J. Waluyo, I.G.B.N. Makertihartha, H. Susanto, Pyrolysis with intermediate heating rate of palm kernel shells: Effect temperature and catalyst on product distribution, 2018.
[34] S. Li, S. Xu, S. Liu, C. Yang, Q. Lu, Fast pyrolysis of biomass in free-fall reactor for hydrogen-rich gas, Fuel Process. Technol. 85(8-10) (2004) 1201-1211.
[35] L. Wei, S. Xu, L. Zhang, C. Liu, H. Zhu, S. Liu, Steam gasification of biomass for hydrogen-rich gas in a free-fall reactor, Int. J. Hydrogen Energy 32(1) (2007) 24-31.
[36] B. Pidtasang, P. Udomsap, S. Sukkasi, N. Chollacoop, A. Pattiya, Influence of alcohol addition on properties of bio-oil produced from fast pyrolysis of eucalyptus bark in a free-fall reactor, Journal of Industrial and Engineering Chemistry 19(6) (2013) 1851-1857.
[37] C. Ndibe, J. Maier, G. Scheffknecht, Combustion, cofiring and emissions characteristics of torrefied biomass in a drop tube reactor, Biomass Bioenergy 79 (2015) 105-115.
[38] C. Guizani, S. Valin, J. Billaud, M. Peyrot, S. Salvador, Biomass fast pyrolysis in a drop tube reactor for bio oil production: Experiments and modeling, Fuel 207 (2017) 71-84.
[39] A. Pattiya, S. Sukkasi, V. Goodwin, Fast pyrolysis of sugarcane and cassava residues in a free-fall reactor, Energy 44(1) (2012) 1067-1077.
[40] K.-Q. Tran, X. Luo, G. Seisenbaeva, R. Jirjis, Stump torrefaction for bioenergy application, Applied Energy 112 (2013) 539-546.
[41] W.H. Chen, M.Y. Huang, J.S. Chang, C.Y. Chen, W.J. Lee, An energy analysis of torrefaction for upgrading microalga residue as a solid fuel, Bioresour Technol 185 (2015) 285-93.
[42] A. Sarvaramini, G.P. Assima, F. Larachi, Dry torrefaction of biomass – Torrefied products and torrefaction kinetics using the distributed activation energy model, Chemical Engineering Journal 229 (2013) 498-507.
[43] M. Strandberg, I. Olofsson, L. Pommer, S. Wiklund-Lindström, K. Åberg, A. Nordin, Effects of temperature and residence time on continuous torrefaction of spruce wood, Fuel Processing Technology 134 (2015) 387-398.
[44] Y. Mei, R. Liu, Q. Yang, H. Yang, J. Shao, C. Draper, S. Zhang, H. Chen, Torrefaction of cedarwood in a pilot scale rotary kiln and the influence of industrial flue gas, Bioresour Technol 177 (2015) 355-60.
[45] M. Atienza-Martínez, I. Fonts, J. Ábrego, J. Ceamanos, G. Gea, Sewage sludge torrefaction in a fluidized bed reactor, Chemical Engineering Journal 222 (2013) 534-545.
[46] H. Li, X. Liu, R. Legros, X.T. Bi, C.J. Lim, S. Sokhansanj, Torrefaction of sawdust in a fluidized bed reactor, Bioresour Technol 103(1) (2012) 453-8.
[47] R.W. Nachenius, T.A. van de Wardt, F. Ronsse, W. Prins, Residence time distributions of coarse biomass particles in a screw conveyor reactor, Fuel Processing Technology 130 (2015) 87-95.
[48] R.W. Nachenius, T.A. van de Wardt, F. Ronsse, W. Prins, Torrefaction of pine in a bench-scale screw conveyor reactor, Biomass and Bioenergy 79 (2015) 96-104.
[49] M.J. Wang, Y.F. Huang, P.T. Chiueh, W.H. Kuan, S.L. Lo, Microwave-induced torrefaction of rice husk and sugarcane residues, Energy 37(1) (2012) 177-184.
[50] Y.F. Huang, W.R. Chen, P.T. Chiueh, W.H. Kuan, S.L. Lo, Microwave torrefaction of rice straw and Pennisetum, Bioresour Technol 123 (2012) 1-7.
[51] A.E. Eseyin, P.H. Steele, C.U. Pittman Jr., Current Trends in the Production and Applications of Torrefied Wood/Biomass - A Review, 2015 10(4) (2015) 47.
[52] R. Lu, G.-P. Sheng, Y.-Y. Hu, P. Zheng, H. Jiang, Y. Tang, H.-Q. Yu, Fractional characterization of a bio-oil derived from rice husk, Biomass Bioenergy 35(1) (2011) 671-678.
[53] T. Chen, C. Wu, R. Liu, W. Fei, S. Liu, Effect of hot vapor filtration on the characterization of bio-oil from rice husks with fast pyrolysis in a fluidized-bed reactor, Bioresour. Technol. 102(10) (2011) 6178-85.
[54] J.-S. Kim, Production, separation and applications of phenolic-rich bio-oil–a review, Bioresour. Technol. 178 (2015) 90-98.
[55] N.S. Tessarolo, L.R. dos Santos, R.S. Silva, D.A. Azevedo, Chemical characterization of bio-oils using comprehensive two-dimensional gas chromatography with time-of-flight mass spectrometry, J.

Chromatogr. A 1279 (2013) 68-75.
[56] L. Leng, H. Li, X. Yuan, W. Zhou, H. Huang, Bio-oil upgrading by emulsification/microemulsification: A review, Energy 161 (2018) 214-232.
[57] D. Chiaramonti, M. Bonini, E. Fratini, G. Tondi, K. Gartner, A.V. Bridgwater, H.P. Grimm, I. Soldaini, A. Webster, P. Baglioni, Development of emulsions from biomass pyrolysis liquid and diesel and their use in engines—Part 1 : emulsion production, Biomass Bioenergy 25(1) (2003) 85-99.
[58] S. Xiu, A. Shahbazi, Bio-oil production and upgrading research: A review, Renew. Sustain. Energy Rev 16(7) (2012) 4406-4414.
[59] R.M. Baldwin, C.J. Feik, Bio-oil Stabilization and Upgrading by Hot Gas Filtration, Energy Fuels 27(6) (2013) 3224-3238.
[60] F. Mahfud, F. Ghijsen, H. Heeres, Hydrogenation of fast pyrolyis oil and model compounds in a two-phase aqueous organic system using homogeneous ruthenium catalysts, J. Mol. Catal. A: Chem. 264(1-2) (2007) 227-236.
[61] W. Yu, Y. Tang, L. Mo, P. Chen, H. Lou, X. Zheng, One-step hydrogenation-esterification of furfural and acetic acid over bifunctional Pd catalysts for bio-oil upgrading, Bioresour. Technol. 102(17) (2011) 8241-6.
[62] J. Wang, M. Jabbour, L. Abdelouahed, S. Mezghich, L. Estel, K. Thomas, B. Taouk, Catalytic upgrading of bio-oil: Hydrodeoxygenation study of acetone as molecule model of ketones, Can. J. Chem. Eng. 99(5) (2020) 1082-1093.
[63] J. Wang, L. Abdelouahed, J. Xu, N. Brodu, B. Taouk, Catalytic Hydrodeoxygenation of Model Bio-oils Using HZSM-5 and Ni2P/HZM-5 Catalysts: Comprehension of Interaction, Chem. Eng. Technol. 44(11) (2021) 2126-2138.
[64] M. Nokkosmäki, E. Kuoppala, E. Leppämäki, A. Krause, Catalytic conversion of biomass pyrolysis vapours with zinc oxide, J. Anal. Appl. Pyrolysis 55(1) (2000) 119-131.
[65] S. Czernik, R. French, C. Feik, E. Chornet, Hydrogen by catalytic steam reforming of liquid byproducts from biomass thermoconversion processes, Ind. Eng. Chem. Res. 41(17) (2002) 4209-4215.
[66] K. Takanabe, K.-i. Aika, K. Seshan, L. Lefferts, Sustainable hydrogen from bio-oil—Steam reforming of acetic acid as a model oxygenate, J. Catal. 227(1) (2004) 101-108.
[67] M. Saber, B. Nakhshiniev, K. Yoshikawa, A review of production and upgrading of algal bio-oil, Renew. Sustain. Energy Rev 58 (2016) 918-930.
[68] A.-C. Johansson, K. Iisa, L. Sandström, H. Ben, H. Pilath, S. Deutch, H. Wiinikka, O.G. Öhrman, Fractional condensation of pyrolysis vapors produced from Nordic feedstocks in cyclone pyrolysis, J. Anal. Appl. Pyrolysis 123 (2017) 244-254.
[69] A.S. Pollard, M.R. Rover, R.C. Brown, Characterization of bio-oil recovered as stage fractions with unique chemical and physical properties, J. Anal. Appl. Pyrolysis 93 (2012) 129-138.
[70] M. Chai, Y. He, C. Sun, R. Liu, Effect of fractional condensers on characteristics, compounds distribution and phenols selection of bio-oil from pine sawdust fast pyrolysis, J. Energy Inst. (2019).
[71] H. Sui, H. Yang, J. Shao, X. Wang, Y. Li, H. Chen, Fractional condensation of multicomponent vapors from pyrolysis of cotton stalk, Energy Fuels 28(8) (2014) 5095-5102.
[72] R. Yin, R. Liu, Y. Mei, W. Fei, X. Sun, Characterization of bio-oil and bio-char obtained from sweet sorghum bagasse fast pyrolysis with fractional condensers, Fuel 112 (2013) 96-104.
[73] C. Wang, Z. Luo, R. Diao, X. Zhu, Study on the effect of condensing temperature of walnut shells pyrolysis vapors on the composition and properties of bio-oil, Bioresour. Technol. 285 (2019) 121370.
[74] S. Papari, K. Hawboldt, P. Fransham, Study of selective condensation for woody biomass pyrolysis oil vapours, Fuel 245 (2019) 233-239.
[75] T. Chen, C. Deng, R. Liu, Effect of selective condensation on the characterization of bio-oil from pine sawdust fast pyrolysis using a fluidized-bed reactor, Energy Fuels 24(12) (2010) 6616-6623.
[76] S. Ma, L. Zhang, L. Zhu, X. Zhu, Preparation of multipurpose bio-oil from rice husk by pyrolysis and fractional condensation, J. Anal. Appl. Pyrolysis 131 (2018) 113-119.
[77] M. Sugimoto, Y. Kuramochi, A. Satake, Measurement of Solvation Ability of Solvents by Porphyrin-Based Solvation/Desolvation Indicators, ACS Omega 5(11) (2020) 6045-6050.
[78] A. Oasmaa, E. Kuoppala, S. Gust, Y. Solantausta, Fast Pyrolysis of Forestry Residue. 1. Effect of Extractives on Phase Separation of Pyrolysis Liquids, Energy Fuels 17(1) (2003) 1-12.
[79] X. Zhang, H. Ma, S. Wu, W. Jiang, W. Wei, M. Lei, Fractionation of pyrolysis oil derived from lignin through a simple water extraction method, Fuel 242 (2019) 587-595.
[80] A. Oasmaa, E. Kuoppala, Solvent fractionation method with brix for rapid characterization of wood fast pyrolysis liquids, Energy Fuels 22(6) (2008) 4245-4248.
[81] S. Ren, X.P. Ye, A.P. Borole, P. Kim, N. Labbé, Analysis of switchgrass-derived bio-oil and associated aqueous phase generated in a semi-pilot scale auger pyrolyzer, J. Anal. Appl. Pyrolysis 119 (2016) 97-103.

[82] D. Mohan, C.U. Pittman Jr, P.H. Steele, Pyrolysis of wood/biomass for bio-oil: a critical review, Energy Fuels 20(3) (2006) 848-889.
[83] A. Oasmaa, E. Kuoppala, S. Gust, Y. Solantausta, Fast pyrolysis of forestry residue. 1. Effect of extractives on phase separation of pyrolysis liquids, Energy Fuels 17(1) (2003) 1-12 %@ 0887-0624.
[84] X. Zhang, H. Ma, T. Li, S. Wu, Oligomers obtained from sequential fractionation of lignin pyrolysis oil, Energy Convers. Manage. 201 (2019).
[85] J.P. Cao, X.Y. Zhao, K. Morishita, L.Y. Li, X.B. Xiao, R. Obara, X.Y. Wei, T. Takarada, Triacetonamine formation in a bio-oil from fast pyrolysis of sewage sludge using acetone as the absorption solvent, Bioresour. Technol. 101(11) (2010) 4242-5.
[86] A. Oasmaa, K. Sipilä, Y. Solantausta, E. Kuoppala, Quality improvement of pyrolysis liquid: Effect of light volatiles on the stability of pyrolysis liquids, Energy Fuels 19(6) (2005) 2556-2561.
[87] L. Cesari, S. Namysl, L. Canabady-Rochelle, F. Mutelet, Phase equilibria of phenolic compounds in water or ethanol, Fluid Phase Equilib. 453 (2017) 58-66.
[88] K. Ramluckan, K.G. Moodley, F. Bux, An evaluation of the efficacy of using selected solvents for the extraction of lipids from algal biomass by the soxhlet extraction method, Fuel 116 (2014) 103-108.
[89] C.R. Vitasari, G.W. Meindersma, A.B. de Haan, Water extraction of pyrolysis oil: the first step for the recovery of renewable chemicals, Bioresour. Technol. 102(14) (2011) 7204-10.
[90] Z. Yang, A. Kumar, R.L. Huhnke, Review of recent developments to improve storage and transportation stability of bio-oil, Renew. Sustain. Energy Rev 50 (2015) 859-870.
[91] J.P. Diebold, A review of the chemical and physical mechanisms of the storage stability of fast pyrolysis bio-oils, National Renewable Energy Lab., Golden, CO (US), 1999.
[92] A. Oasmaa, E. Kuoppala, Fast pyrolysis of forestry residue. 3. Storage stability of liquid fuel, Energy Fuels 17(4) (2003) 1075-1084.
[93] J.P. Diebold, S. Czernik, Additives To Lower and Stabilize the Viscosity of Pyrolysis Oils during Storage, Energy Fuels 11(5) (1997) 1081-1091.
[94] M. Ikura, M. Stanciulescu, E. Hogan, Emulsification of pyrolysis derived bio-oil in diesel fuel, Biomass Bioenergy 24(3) (2003) 221-232.
[95] W.G. Etzkorn, S.E. Pedersen, T.E. Snead, Acrolein and Derivatives, Kirk‐Othmer Encyclopedia of Chemical Technology.
[96] B.-S. Kang, K.H. Lee, H.J. Park, Y.-K. Park, J.-S. Kim, Fast pyrolysis of radiata pine in a bench scale plant with a fluidized bed: Influence of a char separation system and reaction conditions on the production of bio-oil, J. Anal. Appl. Pyrolysis 76(1-2) (2006) 32-37.
[97] J. Meng, A. Moore, D.C. Tilotta, S.S. Kelley, S. Adhikari, S. Park, Thermal and storage stability of bio-oil from pyrolysis of torrefied wood, Energy Fuels 29(8) (2015) 5117-5126.
[98] D. Chen, J. Zhou, Q. Zhang, X. Zhu, Evaluation methods and research progresses in bio-oil storage stability, Renew. Sustain. Energy Rev 40 (2014) 69-79.
[99] S. Czernik, D.K. Johnson, S. Black, Stability of wood fast pyrolysis oil, Biomass Bioenergy 7(1-6) (1994) 187-192.
[100] Y. Zhang, Z. Yuan, C. Xu, Bio-based resins for fiber-reinforced polymer composites, Natural Fiber-Reinforced Biodegradable and Bioresorbable Polymer Composites2017, pp. 137-162.
[101] J. Wan, J. Zhao, X. Zhang, H. Fan, J. Zhang, D. Hu, P. Jin, D.-Y. Wang, Epoxy thermosets and materials derived from bio-based monomeric phenols: Transformations and performances, Prog. Polym. Sci. 108 (2020).
[102] S. Kumar, S.K. Samal, S. Mohanty, S.K. Nayak, Recent development of biobased epoxy resins: a review, Polymer-Plastics Technology and Engineering 57(3) (2018) 133-155.
[103] X. Hu, M. Gholizadeh, Progress of the applications of bio-oil, Renew. Sustain. Energy Rev 134 (2020) 110124.
[104] X. Hu, K. Nango, L. Bao, T. Li, M.D.M. Hasan, C.-Z. Li, High yields of solid carbonaceous materials from biomass, Green Chemistry 21(5) (2019) 1128-1140.
[105] I.O. Bakare, C. Pavithran, F.E. Okieimen, C.K.S. Pillai, Polyesters from renewable resources: Preparation and characterization, J. Appl. Polym. Sci. 100(5) (2006) 3748-3755.
[106] G.Z. Papageorgiou, V. Tsanaktsis, D.G. Papageorgiou, K. Chrissafis, S. Exarhopoulos, D.N. Bikiaris, Furan-based polyesters from renewable resources: Crystallization and thermal degradation behavior of poly(hexamethylene 2,5-furan-dicarboxylate), Eur. Polym. J. 67 (2015) 383-396.
[107] J.-W. Rhim, Preparation and characterization of vacuum sputter silver coated PLA film, LWT - Food Science and Technology 54(2) (2013) 477-484.
[108] A.F. Sousa, M. Matos, C.S.R. Freire, A.J.D. Silvestre, J.F.J. Coelho, New copolyesters derived from terephthalic and 2,5-furandicarboxylic acids: A step forward in the development of biobased polyesters, Polymer 54(2) (2013) 513-519.
[109] J. Dai, S. Ma, X. Liu, L. Han, Y. Wu, X. Dai, J. Zhu, Synthesis of bio-based unsaturated polyester

resins and their application in waterborne UV-curable coatings, Prog. Org. Coat. 78 (2015) 49-54.
[110] A. Hiroe, K. Ushimaru, T. Tsuge, Characterization of polyhydroxyalkanoate (PHA) synthase derived from Delftia acidovorans DS-17 and the influence of PHA production in Escherichia coli, J Biosci Bioeng 115(6) (2013) 633-8.
[111] J. Gharib, S. Pang, D. Holland, Synthesis and characterisation of polyurethane made from pyrolysis bio-oil of pine wood, Eur. Polym. J. 133 (2020).
[112] W. Lei, C. Fang, X. Zhou, Y. Cheng, R. Yang, D. Liu, Morphology and thermal properties of polyurethane elastomer based on representative structural chain extenders, Thermochim. Acta 653 (2017) 116-125.
[113] K. Mizera, J. Ryszkowska, Polyurethane elastomers from polyols based on soybean oil with a different molar ratio, Polym. Degrad. Stab. 132 (2016) 21-31.
[114] M. Zieleniewska, M.K. Leszczyński, M. Kurańska, A. Prociak, L. Szczepkowski, M. Krzyżowska, J. Ryszkowska, Preparation and characterisation of rigid polyurethane foams using a rapeseed oil-based polyol, Ind Crops Prod 74 (2015) 887-897.
[115] A. Lee, Y. Deng, Green polyurethane from lignin and soybean oil through non-isocyanate reactions, Eur. Polym. J. 63 (2015) 67-73.
[116] X. Kong, L. Zhao, J.M. Curtis, Polyurethane nanocomposites incorporating biobased polyols and reinforced with a low fraction of cellulose nanocrystals, Carbohydr. Polym. 152 (2016) 487-495.
[117] F. Ferdosian, Z. Yuan, M. Anderson, C.C. Xu, Thermal performance and thermal decomposition kinetics of lignin-based epoxy resins, J. Anal. Appl. Pyrolysis 119 (2016) 124-132.
[118] S. Kumar, S. Krishnan, S. Mohanty, S.K. Nayak, Synthesis and characterization of petroleum and biobased epoxy resins: a review, Polymer International 67(7) (2018) 815-839.
[119] E. Feghali, D.J. van de Pas, A.J. Parrott, K.M. Torr, Biobased Epoxy Thermoset Polymers from Depolymerized Native Hardwood Lignin, ACS Macro Lett. 9(8) (2020) 1155-1160.
[120] Y. Celikbag, S. Meadows, M. Barde, S. Adhikari, G. Buschle-Diller, M.L. Auad, B.K. Via, Synthesis and Characterization of Bio-oil-Based Self-Curing Epoxy Resin, Ind. Eng. Chem. Res. 56(33) (2017) 9389-9400.
[121] Z. Fang, M.C. Weisenberger, M.S. Meier, Utilization of Lignin-Derived Small Molecules: Epoxy Polymers from Lignin Oxidation Products, ACS Appl. Bio Mater. 3(2) (2020) 881-890.
[122] E. Feghali, D.J. van de Pas, K.M. Torr, Toward Bio-Based Epoxy Thermoset Polymers from Depolymerized Native Lignins Produced at the Pilot Scale, Biomacromolecules 21(4) (2020) 1548-1559.
[123] F. Ferdosian, Z. Yuan, M. Anderson, C. Xu, Synthesis of lignin-based epoxy resins: optimization of reaction parameters using response surface methodology, RSC Adv. 4(60) (2014) 31745-31753.
[124] E.D. Hernandez, A.W. Bassett, J.M. Sadler, J.J. La Scala, J.F. Stanzione, Synthesis and Characterization of Bio-based Epoxy Resins Derived from Vanillyl Alcohol, ACS Sustain. Chem. Eng. 4(8) (2016) 4328-4339.
[125] S. Benyahya, C. Aouf, S. Caillol, B. Boutevin, J.P. Pascault, H. Fulcrand, Functionalized green tea tannins as phenolic prepolymers for bio-based epoxy resins, Ind Crops Prod 53 (2014) 296-307.
[126] N. Khundamri, C. Aouf, H. Fulcrand, E. Dubreucq, V. Tanrattanakul, Bio-based flexible epoxy foam synthesized from epoxidized soybean oil and epoxidized mangosteen tannin, Ind Crops Prod 128 (2019) 556-565.
[127] C.-H. Chen, S.-H. Tung, R.-J. Jeng, M.M. Abu-Omar, C.-H. Lin, A facile strategy to achieve fully bio-based epoxy thermosets from eugenol, Green Chemistry 21(16) (2019) 4475-4488.
[128] J.R. Kim, S. Sharma, The development and comparison of bio-thermoset plastics from epoxidized plant oils, Ind Crops Prod 36(1) (2012) 485-499.
[129] X. Pan, P. Sengupta, D.C. Webster, Novel biobased epoxy compounds: epoxidized sucrose esters of fatty acids, Green Chemistry 13(4) (2011).
[130] T. Koike, Progress in development of epoxy resin systems based on wood biomass in Japan, Polym. Eng. Sci. 52(4) (2012) 701-717.
[131] Y. Zhang, H. Pang, D. Wei, J. Li, S. Li, X. Lin, F. Wang, B. Liao, Preparation and characterization of chemical grouting derived from lignin epoxy resin, Eur. Polym. J. 118 (2019) 290-305.
[132] S. Cheng, Z. Yuan, M. Anderson, M. Leitch, C.C. Xu, Synthesis of biobased phenolic resins/adhesives with methylolated wood-derived bio-oil, J. Appl. Polym. Sci. 126(S1) (2012) E431-E441.
[133] L. Pilato, Phenolic resins: a century of progress, Springer2010.
[134] M.H. Choi, H.Y. Byun, I.J. Chung, The effect of chain length of flexible diacid on morphology and mechanical property of modified phenolic resin, Polymer 43(16) (2002) 4437-4444.
[135] W. Yang, L. Jiao, X. Wang, W. Wu, H. Lian, H. Dai, Formaldehyde-free self-polymerization of lignin-derived monomers for synthesis of renewable phenolic resin, Int. J. Biol. Macromol. 166 (2021) 1312-1319.

[136] A. Effendi, H. Gerhauser, A.V. Bridgwater, Production of renewable phenolic resins by thermochemical conversion of biomass: a review, Renew. Sust. Energ. Rev. 12(8) (2008) 2092-2116.
[137] P.R. Sarika, P. Nancarrow, A. Khansaheb, T. Ibrahim, Bio-Based Alternatives to Phenol and Formaldehyde for the Production of Resins, Polymers 12(10) (2020) 2237-2260.
[138] Y. Zhang, Z. Yuan, C.C. Xu, Engineering biomass into formaldehyde-free phenolic resin for composite materials, AlChE J. 61(4) (2015) 1275-1283.
[139] S. Cheng, I. D'Cruz, Z. Yuan, M. Wang, M. Anderson, M. Leitch, C.C. Xu, Use of biocrude derived from woody biomass to substitute phenol at a high-substitution level for the production of biobased phenolic resol resins, J. Appl. Polym. Sci. 121(5) (2011) 2743-2751.
[140] A.U. Patel, S.S. Soni, H.S. Patel, Synthesis, Characterization and Curing ofo-Cresol – Furfural Resins, Int. J. Polymer. Mater. 58(10) (2009) 509-516.
[141] Q. Xu, K. Sun, Y. Shao, C. Zhang, S. Zhang, L. Zhang, P. Jia, S. Wang, Q. Liu, X. Hu, Cross-polymerisation between furfural and the phenolics of varied molecular structure in bio-oil, Bioresour. Technol. Rep. 8 (2019).
[142] M. Fraga-Corral, P. Otero, L. Cassani, J. Echave, P. Garcia-Oliveira, M. Carpena, F. Chamorro, C. Lourenco-Lopes, M.A. Prieto, J. Simal-Gandara, Traditional Applications of Tannin Rich Extracts Supported by Scientific Data: Chemical Composition, Bioavailability and Bioaccessibility, Foods 10(2) (2021).
[143] L. Puchot, Cardanol: a bio-based building block for new sustainable and functional materials, Cergy-Pontoise, 2016.
[144] P. Campaner, D. D'Amico, L. Longo, C. Stifani, A. Tarzia, Cardanol-based novolac resins as curing agents of epoxy resins, J. Appl. Polym. Sci. 114(6) (2009) 3585-3591.
[145] P. Rahmawati, A.H. Ramelan, S.D. Marliyana, N.S. Suharty, S. Wahyuningsih, Synthesis of Cardanol-Based Novolac Resin from Cashew Nut Shell Liquid, Journal of Engineering Science 15 (2019) 23-33.
[146] C. Li, J. Zhang, Z. Yi, H. Yang, B. Zhao, W. Zhang, J. Li, Preparation and characterization of a novel environmentally friendly phenol–formaldehyde adhesive modified with tannin and urea, Int. J. Adhes. Adhes. 66 (2016) 26-32.
[147] J. Li, A. Zhang, S. Zhang, Q. Gao, W. Zhang, J. Li, Larch tannin-based rigid phenolic foam with high compressive strength, low friability, and low thermal conductivity reinforced by cork powder, Composites Part B: Engineering 156 (2019) 368-377.
[148] J. Li, J. Zhang, Y. Zhou, Z. Zhou, H. Essawy, X. Zhou, G. Du, Preparation of an Abrasive Grinding Wheel Based on Tannin Resin Cross-Linked by Furfuryl Alcohol, Urea and Glyoxal, Journal of Renewable Materials 8(9) (2020) 1019-1032.
[149] M.C. Lagel, A. Pizzi, S. Giovando, A. Celzard, Development and Characterisation of Phenolic Foams with Phenol-Formaldehyde-Chestnut Tannins Resin, Journal of Renewable Materials 2(3) (2014) 220-229.
[150] M. Wang, M. Leitch, C. Xu, Synthesis of phenol–formaldehyde resol resins using organosolv pine lignins, Eur. Polym. J. 45(12) (2009) 3380-3388.
[151] J. Li, W. Wang, S. Zhang, Q. Gao, W. Zhang, J. Li, Preparation and characterization of lignin demethylated at atmospheric pressure and its application in fast curing biobased phenolic resins, RSC Adv. 6(71) (2016) 67435-67443.
[152] W.-J. Lee, K.-C. Chang, I.M. Tseng, Properties of phenol-formaldehyde resins prepared from phenol-liquefied lignin, J. Appl. Polym. Sci. (2011) n/a-n/a.
[153] W. Zhang, Y. Ma, C. Wang, S. Li, M. Zhang, F. Chu, Preparation and properties of lignin–phenol–formaldehyde resins based on different biorefinery residues of agricultural biomass, Ind Crops Prod 43 (2013) 326-333.
[154] N. Zhang, Z. Li, Y. Xiao, Z. Pan, P. Jia, G. Feng, C. Bao, Y. Zhou, L. Hua, Lignin-based phenolic resin modified with whisker silicon and its application, J. Bioresour. Bioprod. 5(1) (2020) 67-77.
[155] Y. Yu, P. Xu, C. Chen, J. Chang, L. Li, Formaldehyde emission behavior of plywood with phenol-formaldehyde resin modified by bio-oil under radiant floor heating condition, Build Environ 144 (2018) 565-572.
[156] M. Chaouch, P.N. Diouf, A. Laghdir, S. Yin, Bio-oil from whole-tree feedstock in resol-type phenolic resins, J. Appl. Polym. Sci. 131(6) (2014) n/a-n/a.
[157] E.S. Kokten, G. Özbay, N. Ayrilmis, Synthesis of biobased phenolic resins using catalytic pyrolysis oil and its effect on oriented strand board performance, J Adhes 96(5) (2018) 475-489.
[158] M. Aslan, G. Özbay, N. Ayrilmis, Adhesive characteristics and bonding performance of phenol formaldehyde modified with phenol-rich fraction of crude bio-oil, J. Adhes. Sci. Technol. 29(24) (2015) 2679-2691.
[159] Y. Yu, Y. Wang, P. Xu, J. Chang, Preparation and Characterization of Phenolic Foam Modified with

Bio-Oil, Materials 11(11) (2018).
[160] A.E. Vithanage, E. Chowdhury, L.D. Alejo, P.C. Pomeroy, W.J. DeSisto, B.G. Frederick, W.M. Gramlich, Renewably sourced phenolic resins from lignin bio-oil, J. Appl. Polym. Sci. 134(19) (2017) 44827-44836.
[161] K. Hirano, M. Asami, Phenolic resins—100years of progress and their future, React. Funct. Polym. 73(2) (2013) 256-269.
[162] I. Van Nieuwenhove, T. Renders, J. Lauwaert, T. De Roo, J. De Clercq, A. Verberckmoes, Biobased Resins Using Lignin and Glyoxal, ACS Sustain. Chem. Eng. 8(51) (2020) 18789-18809.
[163] G. Casiraghi, M. Cornia, G. Sartori, G. Casnati, V. Bocchi, G.D. Andreetti, Selective step-growth phenol-aldehyde polymerization, 1. Synthesis, characterization and X-ray analysis of linear all-ortho oligonuclear phenolic compounds, Die Makromolekulare Chemie 183(11) (1982) 2611-2633.
[164] Y. Zhang, M. Nanda, M. Tymchyshyn, Z. Yuan, C. Xu, Mechanical, thermal, and curing characteristics of renewable phenol-hydroxymethylfurfural resin for application in bio-composites, Journal of Materials Science 51(2) (2015) 732-738.
[165] Y. Zhang, Z. Yuan, N. Mahmood, S. Huang, C. Xu, Sustainable bio-phenol-hydroxymethylfurfural resins using phenolated de-polymerized hydrolysis lignin and their application in bio-composites, Ind Crops Prod 79 (2016) 84-90.
[166] Z. Yuan, Y. Zhang, C. Xu, Synthesis and thermomechanical property study of Novolac phenol-hydroxymethyl furfural (PHMF) resin, RSC Adv. 4(60) (2014) 31829-31835.
[167] Z. Xiong, Y. Chen, M.M. Azis, X. Hu, W. Deng, H. Han, L. Jiang, S. Su, S. Hu, Y. Wang, J. Xiang, Roles of furfural during the thermal treatment of bio-oil at low temperatures, Journal of Energy Chemistry 50 (2020) 85-95.
[168] R. Srivastava, D. Srivastava, Mechanical, chemical, and curing characteristics of cardanol–furfural-based novolac resin for application in green coatings, J. Coat. Technol. Res. 12(2) (2015) 303-311.
[169] F.B. Oliveira, C. Gardrat, C. Enjalbal, E. Frollini, A. Castellan, Phenol–furfural resins to elaborate composites reinforced with sisal fibers—Molecular analysis of resin and properties of composites, J. Appl. Polym. Sci. 109(4) (2008) 2291-2303.
[170] M. Fache, E. Darroman, V. Besse, R. Auvergne, S. Caillol, B. Boutevin, Vanillin, a promising biobased building-block for monomer synthesis, Green Chem. 16(4) (2014) 1987-1998.
[171] G. Foyer, B.-H. Chanfi, D. Virieux, G. David, S. Caillol, Aromatic dialdehyde precursors from lignin derivatives for the synthesis of formaldehyde-free and high char yield phenolic resins, Eur. Polym. J. 77 (2016) 65-74.
[172] E.C. Ramires, J.D. Megiatto, Jr., C. Gardrat, A. Castellan, E. Frollini, Biobased composites from glyoxal-phenolic resins and sisal fibers, Bioresour. Technol. 101(6) (2010) 1998-2006.
[173] P.L. de Hoyos-Martinez, E. Robles, A. Khoukh, F. Charrier-El Bouhtoury, J. Labidi, Formulation of Multifunctional Materials Based on the Reaction of Glyoxalated Lignins and a Nanoclay/Nanosilicate, Biomacromolecules 20(9) (2019) 3535-3546.
[174] Y. Celikbag, M. Nuruddin, M. Biswas, O. Asafu-Adjaye, B.K. Via, Bio-oil-based phenol–formaldehyde resin: comparison of weight- and molar-based substitution of phenol with bio-oil, J. Adhes. Sci. Technol. 34(24) (2020) 2743-2754.
[175] M.Z. Masli, S. Zakaria, C.H. Chia, R. Roslan, Polymeric reaction between aldehyde group in furfural and phenolic derivatives from liquefaction of oil palm empty fruit bunch fiber as phenol-furfural resin, 2016.
[176] A. Gardziella, L.A. Pilato, A. Knop, Phenolic resins: chemistry, applications, standardization, safety and ecology, Springer Science & Business Media2013.
[177] A. Knop, L.A. Pilato, Phenolic resins: chemistry, applications and performance, Springer Science & Business Media2013.
[178] B.M. Culbertson, Cyclic imino ethers in step-growth polymerizations, Prog. Polym. Sci. 27(3) (2002) 579-626.
[179] C. Nair, Advances in addition-cure phenolic resins, Prog. Polym. Sci. 29(5) (2004) 401-498.
[180] T. Takeichi, N. Furukawa, Epoxy Resins and Phenol-Formaldehyde Resins, Polymer Science: A Comprehensive Reference2012, pp. 723-751.
[181] A. Tejado, G. Kortaberria, C. Peña, J. Labidi, J.M. Echeverria, I. Mondragon, Isocyanate curing of novolac-type ligno-phenol–formaldehyde resins, Ind Crops Prod 27(2) (2008) 208-213.
[182] C. Ding, A.S. Matharu, Recent Developments on Biobased Curing Agents: A Review of Their Preparation and Use, ACS Sustain. Chem. Eng. 2(10) (2014) 2217-2236.
[183] Y. Fu, W.-H. Zhong, Cure kinetics behavior of a functionalized graphitic nanofiber modified epoxy resin, Thermochim. Acta 516(1-2) (2011) 58-63.
[184] W.G. Kim, J.Y. Lee, Contributions of the network structure to the cure kinetics of epoxy resin

systems according to the change of hardeners, Polymer 43(21) (2002) 5713-5722.
[185] R. Auvergne, S. Caillol, G. David, B. Boutevin, J.P. Pascault, Biobased thermosetting epoxy: present and future, Chem Rev 114(2) (2014) 1082-115.
[186] P.-Y. Kuo, L. de Assis Barros, M. Sain, J.S.Y. Tjong, N. Yan, Effects of Reaction Parameters on the Glycidyl Etherification of Bark Extractives during Bioepoxy Resin Synthesis, ACS Sustain. Chem. Eng. 4(3) (2016) 1016-1024.
[187] S.-p. Ren, Y.-x. Lan, Y.-q. Zhen, Y.-d. Ling, M.-g. Lu, Curing reaction characteristics and phase behaviors of biphenol type epoxy resins with phenol novolac resins, Thermochim. Acta 440(1) (2006) 60-67.
[188] Y. Zhang, F. Ferdosian, Z. Yuan, C.C. Xu, Sustainable glucose-based phenolic resin and its curing with a DGEBA epoxy resin, J. Taiwan Inst. Chem. Engrs. 71 (2017) 381-387.
[189] P. Chauhan, H. Chen, S. Roy Goswami, N. Yan, Improved mechanical properties of flexible bio-based polymeric materials derived from epoxy mono/di-abietic acid and soyabean oil, Ind Crops Prod 138 (2019).
[190] D.J. van de Pas, K.M. Torr, Biobased Epoxy Resins from Deconstructed Native Softwood Lignin, Biomacromolecules 18(8) (2017) 2640-2648.
[191] C. Aouf, C. Le Guernevé, S. Caillol, H. Fulcrand, Study of the O-glycidylation of natural phenolic compounds. The relationship between the phenolic structure and the reaction mechanism, Tetrahedron 69(4) (2013) 1345-1353.
[192] C. Aouf, S. Benyahya, A. Esnouf, S. Caillol, B. Boutevin, H. Fulcrand, Tara tannins as phenolic precursors of thermosetting epoxy resins, Eur. Polym. J. 55 (2014) 186-198.
[193] L. Shang, X. Zhang, M. Zhang, L. Jin, L. Liu, L. Xiao, M. Li, Y. Ao, A highly active bio-based epoxy resin with multi-functional group: synthesis, characterization, curing and properties, Journal of Materials Science 53(7) (2017) 5402-5417.
[194] S. Ma, X. Liu, L. Fan, Y. Jiang, L. Cao, Z. Tang, J. Zhu, Synthesis and properties of a bio-based epoxy resin with high epoxy value and low viscosity, ChemSusChem 7(2) (2014) 555-62.
[195] B. Sibaja, S. Adhikari, Y. Celikbag, B. Via, M.L. Auad, Fast pyrolysis bio-oil as precursor of thermosetting epoxy resins, Polym. Eng. Sci. 58(8) (2018) 1296-1307.
[196] M. Barde, S. Adhikari, B.K. Via, M.L. Auad, Synthesis and characterization of epoxy resins from fast pyrolysis bio-oil, Green Mater. 6(2) (2018) 76-84.
[197] Z. Wang, P. Gnanasekar, S. Sudhakaran Nair, R. Farnood, S. Yi, N. Yan, Biobased Epoxy Synthesized from a Vanillin Derivative and Its Reinforcement Using Lignin-Containing Cellulose Nanofibrils, ACS Sustain. Chem. Eng. 8(30) (2020) 11215-11223.
[198] H. Nouailhas, C. Aouf, C. Le Guerneve, S. Caillol, B. Boutevin, H. Fulcrand, Synthesis and properties of biobased epoxy resins. part 1. Glycidylation of flavonoids by epichlorohydrin, J. Polym. Sci., Part A: Polym. Chem. 49(10) (2011) 2261-2270.
[199] Y. Cui, J. Chang, W. Wang, Fabrication of Glass Fiber Reinforced Composites Based on Bio-Oil Phenol Formaldehyde Resin, Materials 9(11) (2016).
[200] Y. Cui, X. Hou, W. Wang, J. Chang, Synthesis and Characterization of Bio-Oil Phenol Formaldehyde Resin Used to Fabricate Phenolic Based Materials, Materials 10(6) (2017) 668-676.
[201] Y. Liu, B.K. Via, Y. Pan, Q. Cheng, H. Guo, M.L. Auad, S. Taylor, Preparation and Characterization of Epoxy Resin Cross-Linked with High Wood Pyrolysis Bio-Oil Substitution by Acetone Pretreatment, Polymers 9(3) (2017).
[202] S.-H. Liu, C.-M. Shu, H.-Y. Hou, Applications of thermal hazard analyses on process safety assessments, J. Loss Prev. Process Ind. 33 (2015) 59-69.
[203] F. Stoessel, Thermal safety of chemical processes: risk assessment and process design, John Wiley & Sons2021.
[204] S. Vyazovkin, A.K. Burnham, J.M. Criado, L.A. Pérez-Maqueda, C. Popescu, N. Sbirrazzuoli, ICTAC Kinetics Committee recommendations for performing kinetic computations on thermal analysis data, Thermochim. Acta 520(1-2) (2011) 1-19.
[205] C.-J. Wang, C.-M. Chang, J.-M. Tseng, Epoxy acrylic resin experimental analysis of runaway reaction, J. Therm. Anal. Calorim. 138(4) (2019) 2839-2851.
[206] S.-H. Wu, M.-L. Shyu, Y.-P. I, J.-H. Chi, C.-M. Shu, Evaluation of runaway reaction for dicumyl peroxide in a batch reactor by DSC and VSP2, J. Loss Prev. Process Ind. 22(6) (2009) 721-727.
[207] S.H. Liu, H.Y. Hou, J.W. Chen, S.Y. Weng, Y.C. Lin, C.M. Shu, Effects of thermal runaway hazard for three organic peroxides conducted by acids and alkalines with DSC, VSP2, and TAM III, Thermochim. Acta 566 (2013) 226-232.
[208] J.M. Tseng, M.Y. Liu, S.L. Chen, W.T. Hwang, J.P. Gupta, C.M. Shu, Runaway effects of nitric acid on methyl ethyl ketone peroxide by TAM III tests, J. Therm. Anal. Calorim. 96(3) (2009) 789-793.
[209] T.-S. Wang, S.-H. Liu, X.-M. Qian, M.-L. You, W.-L. Chou, C.-M. Shu, Isothermal hazards

evaluation of benzoyl peroxide mixed with benzoic acid via TAM III test, J. Therm. Anal. Calorim. 113(3) (2013) 1625-1631.
[210] K.T. Lu, K.M. Luo, S.H. Lin, S.H. Su, K.H. Hu, The Acid-Catalyzed Phenol–Formaldehyde Reaction, Process Safety and Environmental Protection 82(1) (2004) 37-47.
[211] K.-M. Luo, S.-H. Lin, J.-G. Chang, K.-T. Lu, C.-T. Chang, K.-H. Hu, The critical runaway condition and stability criterion in the phenol–formaldehyde reaction, J. Loss Prev. Process Ind. 13(2) (2000) 91-108.
[212] J.-M. Tseng, J.-Z. Lin, C.-C. Lee, C.-P. Lin, Prediction of TMCH thermal hazard with various calorimetric tests by green thermal analysis technology, AlChE J. 58(12) (2012) 3792-3798.
[213] M. Fujita, Y.-i. Izato, Y. Iizuka, A. Miyake, Thermal hazard evaluation of runaway polymerization of acrylic acid, Process Safety and Environmental Protection 129 (2019) 339-347.
[214] A. Kimura, T. Otsuka, Performance evaluation of differential accelerating rate calorimeter for the thermal runaway reaction of di-tert-butyl peroxide, J. Therm. Anal. Calorim. 113(3) (2013) 1585-1591.
[215] V.S. Smitha, M. Surianarayanan, H. Seshadri, N.V. Lakshman, A.B. Mandal, Reactive Thermal Hazards of Tributyl Phosphate with Nitric Acid, Ind. Eng. Chem. Res. 51(21) (2012) 7205-7210.
[216] X. Lu, Y. Wang, L. Estel, N. Kumar, H. Grénman, S. Leveneur, Evolution of Specific Heat Capacity with Temperature for Typical Supports Used for Heterogeneous Catalysts, Processes 8(8) (2020).
[217] Y.-C. Cheng, Y.-S. Huang, Y.-W. Wang, Evaluating time to maximum rate (TMR) and self-accelerating decomposition temperature (SADT) of self-polymerizing vinyl acetate monomer, J. Loss Prev. Process Ind. 71 (2021).
[218] C.-P. Lin, L.-T. Wang, C.-J. Wang, C.-M. Chang, J.-M. Tseng, Evaluation of thermal hazards in phenol-formaldehyde polymerization, J. Loss Prev. Process Ind. 49 (2017) 493-508.
[219] S.-H. Liu, H.-Y. Hou, C.-M. Shu, Thermal hazard evaluation of the autocatalytic reaction of benzoyl peroxide using DSC and TAM III, Thermochim. Acta 605 (2015) 68-76.
[220] D.S. Achilias, I.S. Tsagkalias, Investigation of radical polymerization kinetics of poly(ethylene glycol) methacrylate hydrogels via DSC and mechanistic or isoconversional models, J. Therm. Anal. Calorim. 134(2) (2018) 1307-1315.
[221] F. Bao, G. Zhang, S. Jin, C. Zhang, H. Niu, Thermal decomposition and safety assessment of 3,3′-dinitrimino-5,5′-bis(1H-1,2,4-triazole) by DTA and ARC, J. Therm. Anal. Calorim. 132(1) (2018) 805-811.
[222] <c 毕业论文.pdf>.
[223] J.T. Scanlon, D.E. Willis, Calculation of flame ionization detector relative response factors using the effective carbon number concept, J. Chromatogr. Sci. 23(8) (1985) 333-340.
[224] W. Cai, N. Kang, M.K. Jang, C. Sun, R. Liu, Z. Luo, Long term storage stability of bio-oil from rice husk fast pyrolysis, Energy 186 (2019) 115882.
[225] C.R. Vitasari, G.W. Meindersma, A.B. De Haan, Water extraction of pyrolysis oil: The first step for the recovery of renewable chemicals, Bioresour. Technol. 102(14) (2011) 7204-7210.
[226] W.-H. Chen, Y.-Y. Lin, H.-C. Liu, T.-C. Chen, C.-H. Hung, C.-H. Chen, H.C. Ong, A comprehensive analysis of food waste derived liquefaction bio-oil properties for industrial application, Appl. Energy 237 (2019) 283-291.
[227] F. Stankovikj, A.G. McDonald, G.L. Helms, M. Garcia-Perez, Quantification of bio-oil functional groups and evidences of the presence of pyrolytic humins, Energy Fuels 30(8) (2016) 6505-6524.
[228] R. Sakthivel, K. Ramesh, P.M. Shameer, R. Purnachandran, Experimental investigation on improvement of storage stability of bio-oil derived from intermediate pyrolysis of Calophyllum inophyllum seed cake, J. Energy Inst. 92(3) (2019) 768-782.
[229] E. Stefanis, C. Panayiotou, Prediction of Hansen solubility parameters with a new group-contribution method, Int. J. Thermophys. 29(2) (2008) 568-585.
[230] W. Yi, X. Wang, K. Zeng, H. Yang, J. Shao, S. Zhang, H. Chen, Improving bio-oil stability by fractional condensation and solvent addition, Fuel 290 (2021).
[231] S. Ren, X.P. Ye, Stability of crude bio-oil and its water-extracted fractions, J. Anal. Appl. Pyrolysis 132 (2018) 151-162.
[232] A. Oasmaa, T. Sundqvist, E. Kuoppala, M. Garcia-Perez, Y. Solantausta, C. Lindfors, V. Paasikallio, Controlling the Phase Stability of Biomass Fast Pyrolysis Bio-oils, Energy Fuels 29(7) (2015) 4373-4381.
[233] A. Oasmaa, D. Meier, Norms and standards for fast pyrolysis liquids: 1. Round robin test, J. Anal. Appl. Pyrolysis 73(2) (2005) 323-334.
[234] T.-S. Kim, J.-Y. Kim, K.-H. Kim, S. Lee, D. Choi, I.-G. Choi, J.W. Choi, The effect of storage duration on bio-oil properties, J. Anal. Appl. Pyrolysis 95 (2012) 118-125.
[235] J.V. Ortega, A.M. Renehan, M.W. Liberatore, A.M. Herring, Physical and chemical characteristics of aging pyrolysis oils produced from hardwood and softwood feedstocks, J. Anal. Appl. Pyrolysis 91(1) (2011) 190-198.

[236] E. Alsbou, B. Helleur, Accelerated aging of bio-oil from fast pyrolysis of hardwood, Energy Fuels 28(5) (2014) 3224-3235.
[237] Y. Mei, M. Chai, C. Shen, B. Liu, R. Liu, Effect of methanol addition on properties and aging reaction mechanism of bio-oil during storage, Fuel 244 (2019) 499-507.
[238] C. Wang, H. Ding, Y. Zhang, X. Zhu, Analysis of property variation and stability on the aging of bio-oil from fractional condensation, Renew. Energy 148 (2020) 720-728.
[239] X. Hu, Y. Wang, D. Mourant, R. Gunawan, C. Lievens, W. Chaiwat, M. Gholizadeh, L. Wu, X. Li, C.Z. Li, Polymerization on heating up of bio‐oil: A model compound study, AlChE J. 59(3) (2013) 888-900.
[240] T. Sundqvist, Y. Solantausta, A. Oasmaa, L. Kokko, V. Paasikallio, Heat Generation during the Aging of Wood-Derived Fast-Pyrolysis Bio-oils, Energy Fuels 30(1) (2015) 465-472.
[241] D. Luo, W. Yin, S. Liu, N. Yang, S. Xia, P. Ma, Pyrolysis oil polymerization of water-soluble fraction during accelerated aging, Fuel 230 (2018) 368-375.
[242] W.S. Choi, A.M. Shanmugharaj, S.H. Ryu, Study on the effect of phenol anchored multiwall carbon nanotube on the curing kinetics of epoxy/Novolac resins, Thermochim. Acta 506(1-2) (2010) 77-81.
[243] P. Zhang, S. Wang, X. Zhang, X. Jing, The effect of free dihydroxydiphenylmethanes on the thermal stability of novolac resin, Polym. Degrad. Stab. 168 (2019) 108946.
[244] J.F. Stanzione, P.A. Giangiulio, J.M. Sadler, J.J. La Scala, R.P. Wool, Lignin-Based Bio-Oil Mimic as Biobased Resin for Composite Applications, ACS Sustain. Chem. Eng. 1(4) (2013) 419-426.
[245] M. Wang, L. Wei, T. Zhao, Cure study of addition-cure-type and condensation–addition-type phenolic resins, Eur. Polym. J. 41(5) (2005) 903-912.
[246] Q. Xu, L. Zhang, K. Sun, Y. Shao, H. Tian, S. Zhang, Q. Liu, G. Hu, S. Wang, X. Hu, Cross-polymerisation between the model furans and carbohydrates in bio-oil with acid or alkaline catalysts, J. Energy Inst. 93(4) (2020) 1678-1689.
[247] P. Zhang, S. Wang, X. Zhang, X. Jing, The effect of free dihydroxydiphenylmethanes on the thermal stability of novolac resin, Polym. Degrad. Stab. 168 (2019).
[248] H. Jiang, J. Wang, S. Wu, Z. Yuan, Z. Hu, R. Wu, Q. Liu, The pyrolysis mechanism of phenol formaldehyde resin, Polym. Degrad. Stab. 97(8) (2012) 1527-1533.
[249] T. Ohshima, Y. Yamamoto, U. Takaki, Y. Inoue, T. Saeki, K. Itou, Y. Maegawa, T. Iwasaki, K. Mashima, Theoretical study of Al(III)-catalyzed conversion of glyoxal to glycolic acid: dual activated 1,2-hydride shift mechanism by protonated Al(OH)3 species, Chem Commun (Camb) (19) (2009) 2688-90.
[250] Z.C. Sun, W. Eli, T.Y. Xu, Y.G. Zhang, Oxidation of Glyoxal with Hydroperoxide Compounds Prepared from Maleic Acid by Ozonation To Produce Glyoxylic Acid, Ind. Eng. Chem. Res. 45(6) (2006) 1849-1852.
[251] F. Wang, J. Kuai, H. Pan, N. Wang, X. Zhu, Study on the demethylation of enzymatic hydrolysis lignin and the properties of lignin–epoxy resin blends, Wood Sci. Technol. 52(5) (2018) 1343-1357.
[252] C. Zhang, W.K. Binienda, L. Zeng, X. Ye, S. Chen, Kinetic study of the novolac resin curing process using model fitting and model-free methods, Thermochim. Acta 523(1-2) (2011) 63-69.
[253] K.-Y. Chen, S.-H. Wu, Y.-W. Wang, C.-M. Shu, Runaway reaction and thermal hazards simulation of cumene hydroperoxide by DSC, J. Loss Prev. Process Ind. 21(1) (2008) 101-109.
[254] J. Xu, N. Brodu, M. Mignot, B. Youssef, B. Taouk, Synthesis and characterization of phenolic resins based on pyrolysis bio-oil separated by fractional condensation and water extraction, Biomass Bioenergy 159 (2022).
[255] Y.H. Chan, S.K. Loh, B.L.F. Chin, C.L. Yiin, B.S. How, K.W. Cheah, M.K. Wong, A.C.M. Loy, Y.L. Gwee, S.L.Y. Lo, S. Yusup, S.S. Lam, Fractionation and extraction of bio-oil for production of greener fuel and value-added chemicals: Recent advances and future prospects, Chem. Eng. J. 397 (2020).
[256] N.M. Bennett, S.S. Helle, S.J. Duff, Extraction and hydrolysis of levoglucosan from pyrolysis oil, Bioresour. Technol. 100(23) (2009) 6059-63.

Appendices

Appendix 1

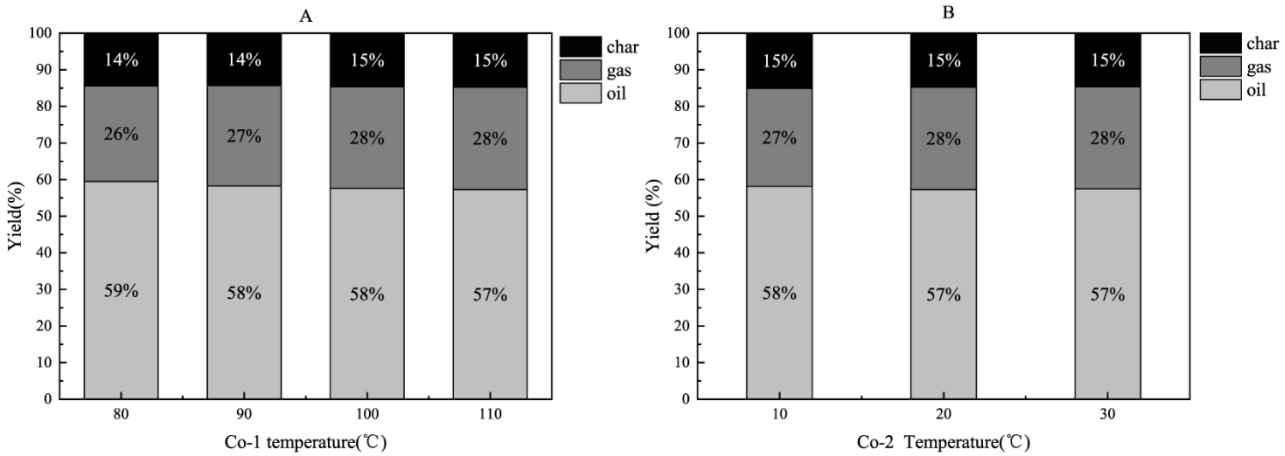

Figure A 1. 1 Distribution of biomass pyrolysis products A. Co-1 temperature increasing (Co-2 set as 20 ℃) and B. Co-2 temperature increasing (Co-1 set as 100 ℃)

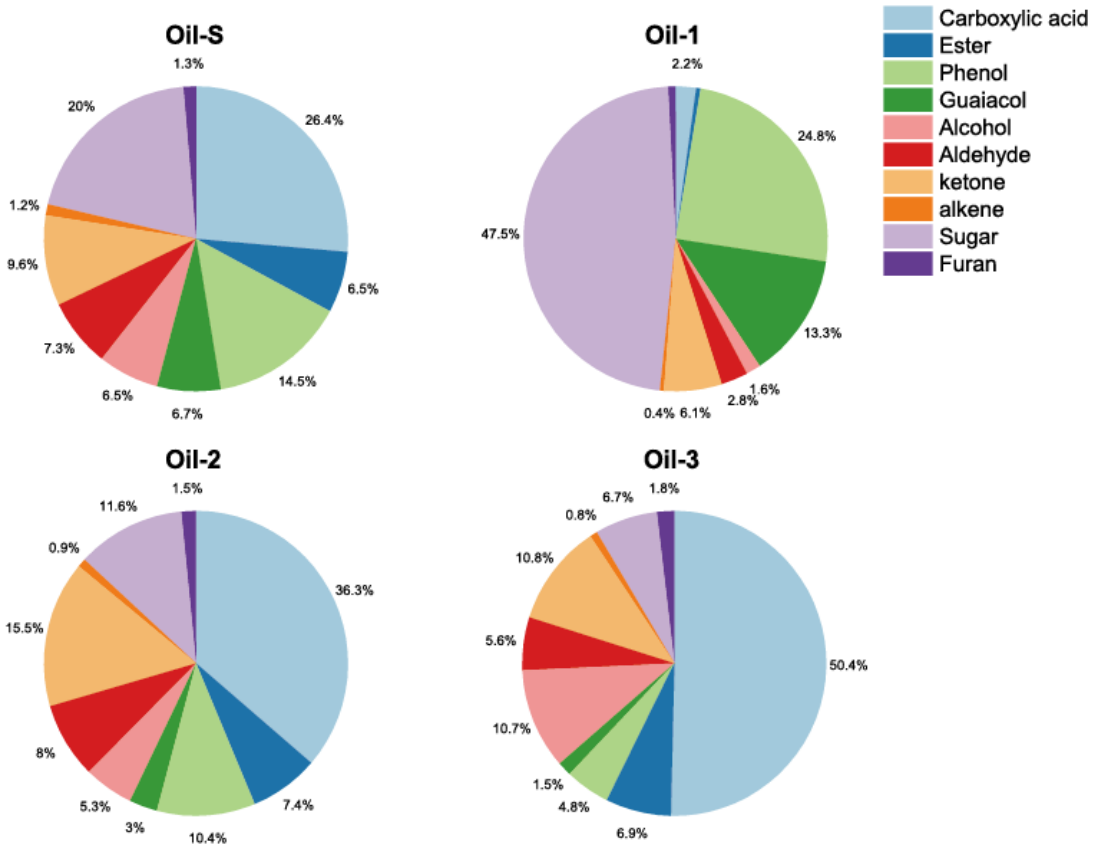

Figure A 1. 2 Distribution of chemical compounds in bio-oil obtained from pyrolysis at 500 ºC of beech wood in DTR (wt. %) (Single-stage condensation and three-stage condensation with the first stage at 110 ºC; the second stage at 20 ºC and third stage at -11 ºC).

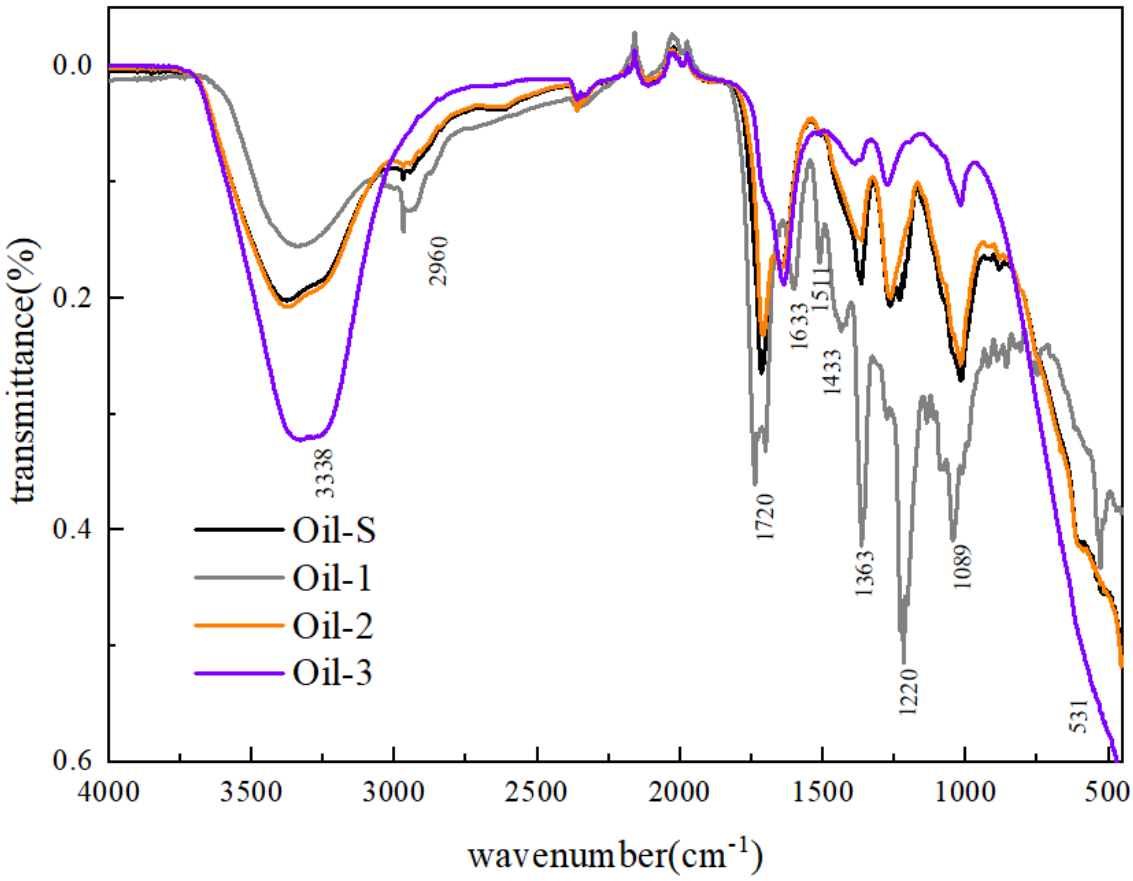

Figure A 1. 3 FTIR graph of bio-oils obtained from pyrolysis at 500 °C of beech wood in DTR (Single-stage condensation and three-stage condensation with the first stage at 110 °C; the second stage at 20 °C and third stage at -11 °C).

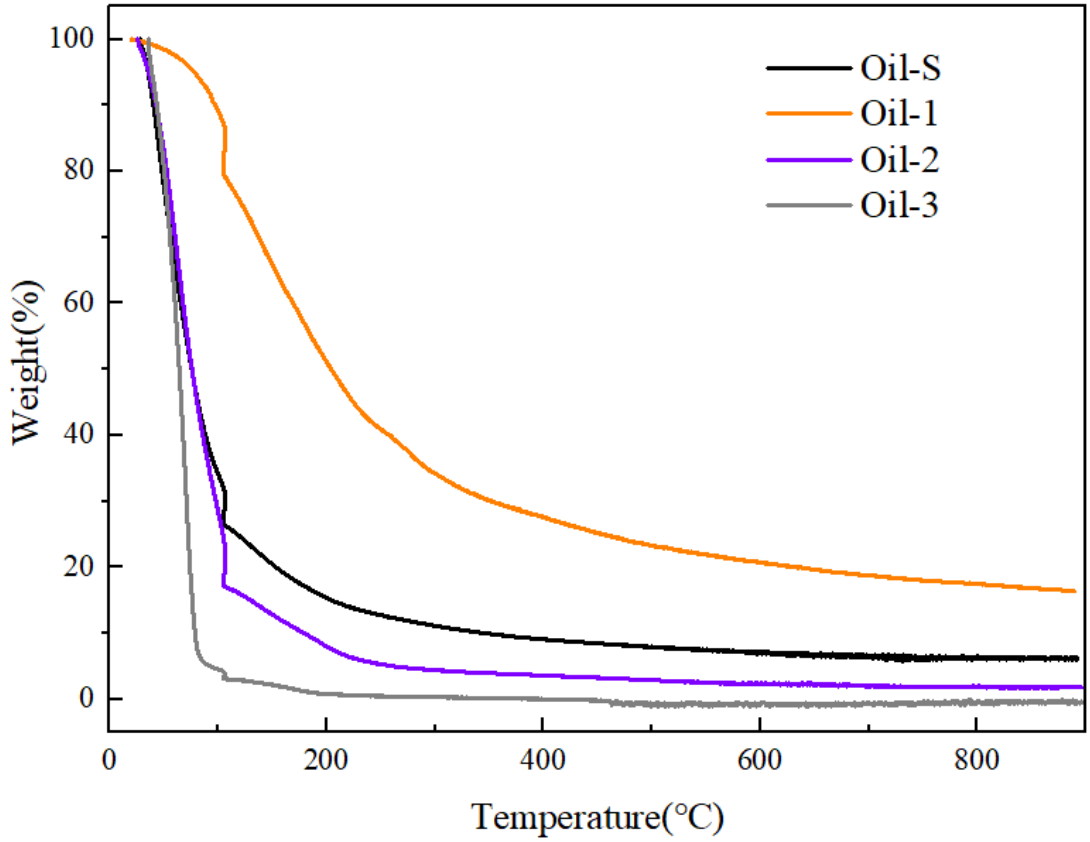

Figure A 1. 4 TGA graph of bio-oils obtained from pyrolysis at 500 °C of beech wood in DTR (Single-stage condensation and three-stage condensation with the first stage at 110 °C; the second stage at 20 °C and third stage at -11 °C).

Appendix 2

Reaction of alcohols, acids

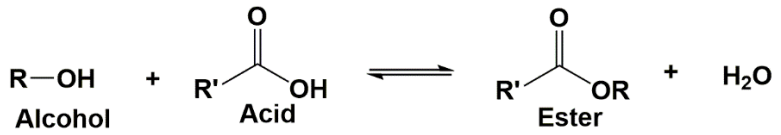

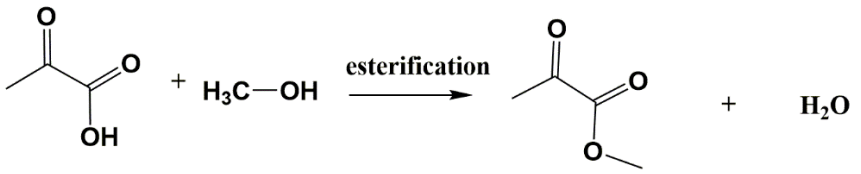

Propanoic acid, 2-oxo- Methanol Propanoic acid, 2-oxo-, methyl ester

Reaction of alcohols and ketones

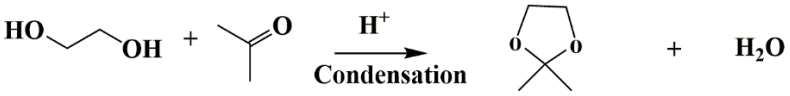

1,2-Ethanediol Acetone 1,3-Dioxolane, 2,2-dimethyl

Reaction of ketones, aldehyde

Aldol condensation

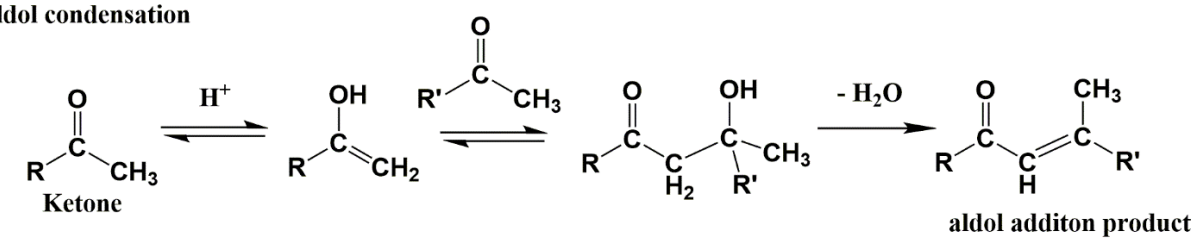

Acetalization

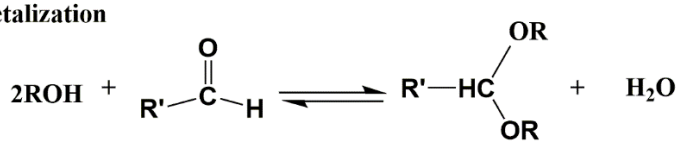

Homopolymerization

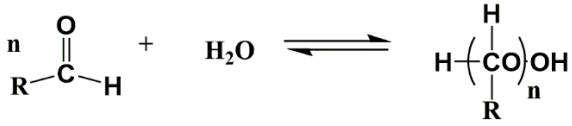

Figure A 2. 1 Some possible reaction mechanisms in bio-oil aging

Table A 2. 1 GC results of major compounds in samples Oil-1, Oil-2, and Oil-3 (aged 4 weeks at 50 °C)

Compound	Formula	MM (g/mol)	Yield/%					
			Oil-1		Oil-2		Oil-3	
			pre	post	pre	post	pre	post
Carboxylic acids								
Acetic acid	C2H4O2	60	1.65	1.85	19.18	20.39	12.29	12.91
Propanedioic acid	C3H4O4	104	-	-	0.62	0.60	0.78	0.73
Propanoic acid	C3H6O2	74	0.47	0.46	1.92	1.90	1.07	0.99
Propanoic acid, 2-oxo-	C3H4O3	88	-	-	0.31	-	-	-
Butanedioic acid	C4H6O4	118	-	-	-	0.34	-	0.47
Esters								
1-Propen-2-ol, acetate	C5H8O2	100	-	-	0.33	0.37	0.18	0.27
Allyl acetate	C5H8O2	100	-	-	0.32	0.30	0.23	0.25
Propanoic acid, 2-oxo-, methyl ester	C4H6O3	102	-	-	0.18	0.17	0.20	0.20
Acetic acid, (acetyloxy)-	C4H6O4	118	-	-	0.82	1.13	0.51	0.69
Ethyl pentanoate	C7H14O2	130	-	-	1.08	1.29	0.37	0.58
g-Valerolactone	C5H8O2	100	1.04	1.05	0.58	0.77	0.33	0.40
2(5H)-Furanone	C4H4O2	84	0.60	0.63	0.25	0.36	0.18	0.38
2-Butanone, 1-(acetyloxy)-	C6H10O3	130	-	-	0.19	0.33	-	-
Furans								
Furan, 2,5-dimethyl-	C6H10O	98	0.79	1.11	0.77	1.12	0.53	0.59
Alcohols								
1,2-Cyclopentanediol, trans-	C5H10O2	102	0.90	0.88	0.46	0.43	0.39	0.20
2-Furanmethanol	C5H6O2	98	-	-	0.24	0.25	0.24	0.24
1,2-Cyclopentanediol, 3-methyl-	C6H12O2	116	-	-	0.23	0.23	0.23	-
1,2-Ethanediol	C2H6O2	62	0.64	0.56	0.15	0.10	0.17	0.11
Aldehydes								
Glycolaldehyde	C4H6O	70	0.40	0.32	2.48	1.69	0.34	0.21
Succindialdehyde	C4H6O2	86	-	-	0.68	0.64	0.35	0.20
Furfural	C5H4O2	96	0.50	0.47	0.49	0.44	0.33	0.17
Ketones								
Hydroxyacetone	C3H6O2	74	0.46	0.40	5.01	4.04	0.81	0.45
2-Acetylfuran	C6H6O2	110	-	-	0.39	0.40	0.26	0.28
1,2-Cyclopentanedione	C8H12O2	140	0.95	0.81	0.69	0.38	0.40	0.17
1,2-Cyclopentanedione, 3-methyl-	C6H8O2	112	1.21	1.18	0.49	0.39	0.35	0.20
Phenols								
Phenol	C6H6O	94	0.75	0.72	0.84	0.73	0.28	-
O-Cresol	C7H8O	108	0.86	0.82	0.56	0.49	0.27	-
2,4-Dimethylphenol	C8H10O	122	2.90	2.88	0.94	0.88	0.33	-
2-Allyl-4-methylphenol	C10H12O	148	1.23	1.18	0.19	0.14	-	-
3-Methylcatechol	C7H8O2	124	2.16	2.09	0.28	0.23	-	-
Catechol	C6H6O2	110	2.10	1.94	0.38	0.33	0.27	-
2,5-Dimethylresorcinol	C8H10O2	138	2.13	2.10	0.00	-	-	-
4-Ethylcatechol	C8H10O2	138	1.54	1.49	0.00	-	-	-
Guaiacols								
Guaiacol	C7H8O2	124	-	-	0.56	0.20	-	-
Creosol	C8H10O2	138	1.55	1.49	0.35	0.20	-	-
4-Ethylguaiacol	C9H12O2	152	1.60	1.57	-	-	-	-
Syringol	C8H10O3	154	3.12	2.99	0.58	0.48	0.43	-
Isoeugenol	C9H12O3	168	1.69	1.61	-	-	-	-
trans-4-Propenylsyringol	C11H14O3	194	2.27	2.21	-	-	-	-
Sugars								
Levoglucosan	C6H10O5	162	21.37	20.80	2.93	0.64	1.93	0.60

- represents non-detectable

Appendix 3

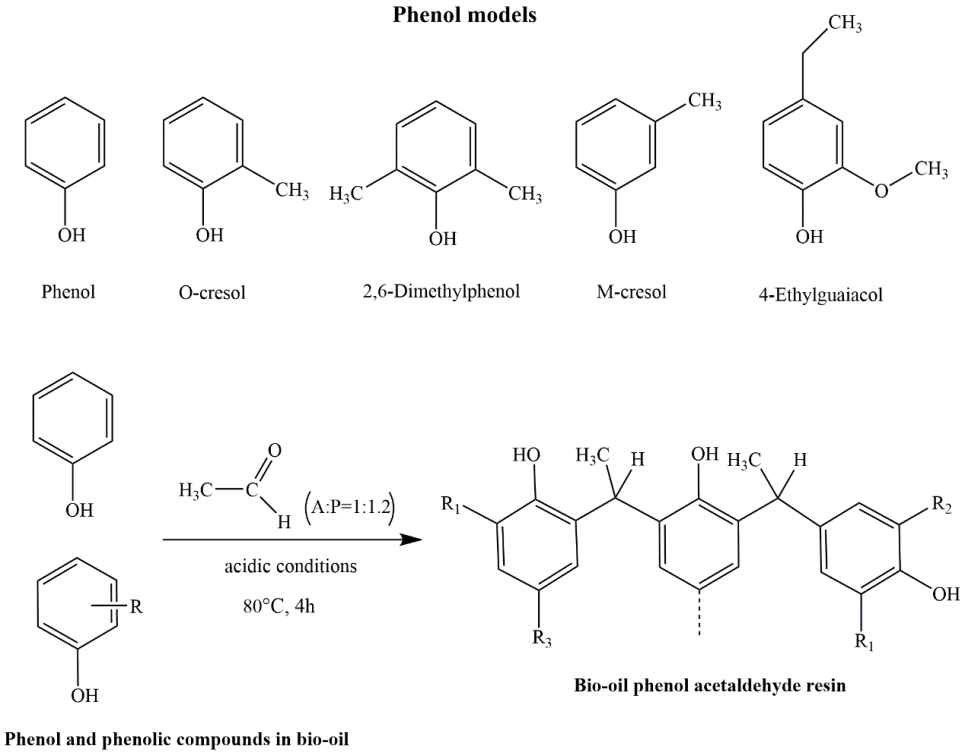

Figure A 3. 1 Chemical structures of the phenol models (phenol, o-cresol, 2,6-dimethylphenol, m-cresol, and 4-ethylguaiacol) and schematic of bio-based phenol acetaldehyde resin

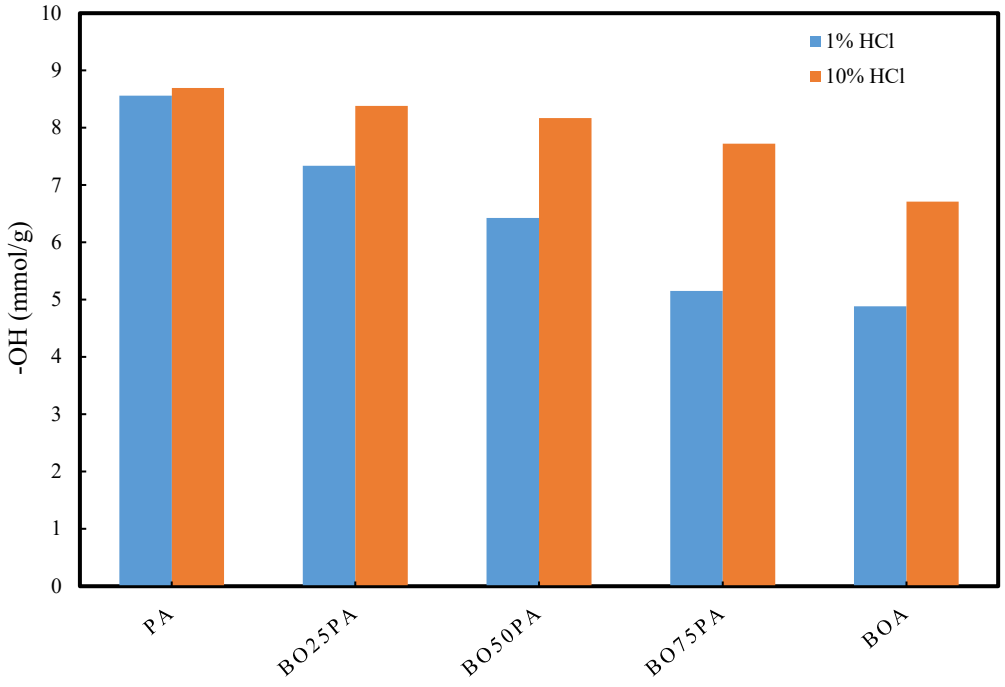

Figure A 3. 2 The hydroxyl number of resins as a function of bio-oil percentage and the amount of acid catalyst.

Table A 3. 1 PA resin (1%HCl) curing test with different concentration of DGEBA

Curing agent (%)	β (°C/min)	Tg (°C)	Ti (°C)	Tp (°C)	δH(J/g)
20% DGEBA	5	94.2	121.9	137.59	18.74
30% DGEBA	5	93.6	119.4	139.73	45.00
40% DGEBA	5	97.2	107.6	134.83	62.54

Table A 3. 2 GPC of PA and BOPA resins synthesized with 1% and 10% HCl catalyst

Catalyst (HCl)	**Resin name**	**Molar ratio Phenol: Phenol(bio-oil)**	**Mn(g/mol)**	**Mw (g/mol)**	**Polydispersity**
1 mol.%	PA	100:0	831	1204	1.45
	BO25PA	75:25	834	1663	1.99
	BO50PA	50:50	841	1838	2.19
	BO75PA	25:75	805	1861	2.31
	BOA	0:100	869	2232	2.57
10 mol.%	PA	100:0	853	1264	1.48
	BO25PA	75:25	1092	2318	2.12
	BO50PA	50:50	1181	3027	2.56
	BO75PA	25:75	1186	3334	2.82
	BOA	0:100	1136	3494	3.08

Table A 3. 3 PA and BOPA resins cured with 40% DGEBA: Onset and peak temperatures, activation energy, and reaction order.

Resin type		Heating rate (°C/min)				Activation energy (kJ/mol)		n
		5	10	15	20	Kissinger	Flynn–Wall–Ozawa	
PA-10%HCl	Onset temp (°C)	103.9	117.6	121.5	122.6	94.9	96.8	0.95
	Peak temp (°C)	134.4	144.6	149.7	154.5			
BO25PA-10%HCl	Onset temp (°C)	96.4	99.5	114.2	116.6	90.3	92.4	0.95
	Peak temp (°C)	126.9	138.0	144.1	147.8			
BO50PA-10%HCl	Onset temp (°C)	95.4	99.0	100.8	103.4	89.3	91.3	0.95
	Peak temp (°C)	119.7	128.5	135.0	139.0			
BO75PA-10%HCl	Onset temp (°C)	99.6	110.2	116.0	116.8	91.7	93.8	0.95
	Peak temp (°C)	133.5	143.8	149.3	153.9			
BOA-10%HCl	Onset temp (°C)	100.9	110.8	119.9	120.5	95.5	97.4	0.95
	Peak temp (°C)	138.4	147.5	154.8	158.3			
BOA-1%HCl	Onset temp (°C)	113.1	125.1	125.5	130.7	98.6	100.5	0.95
	Peak temp (°C)	140.5	149.3	156.3	159.6			

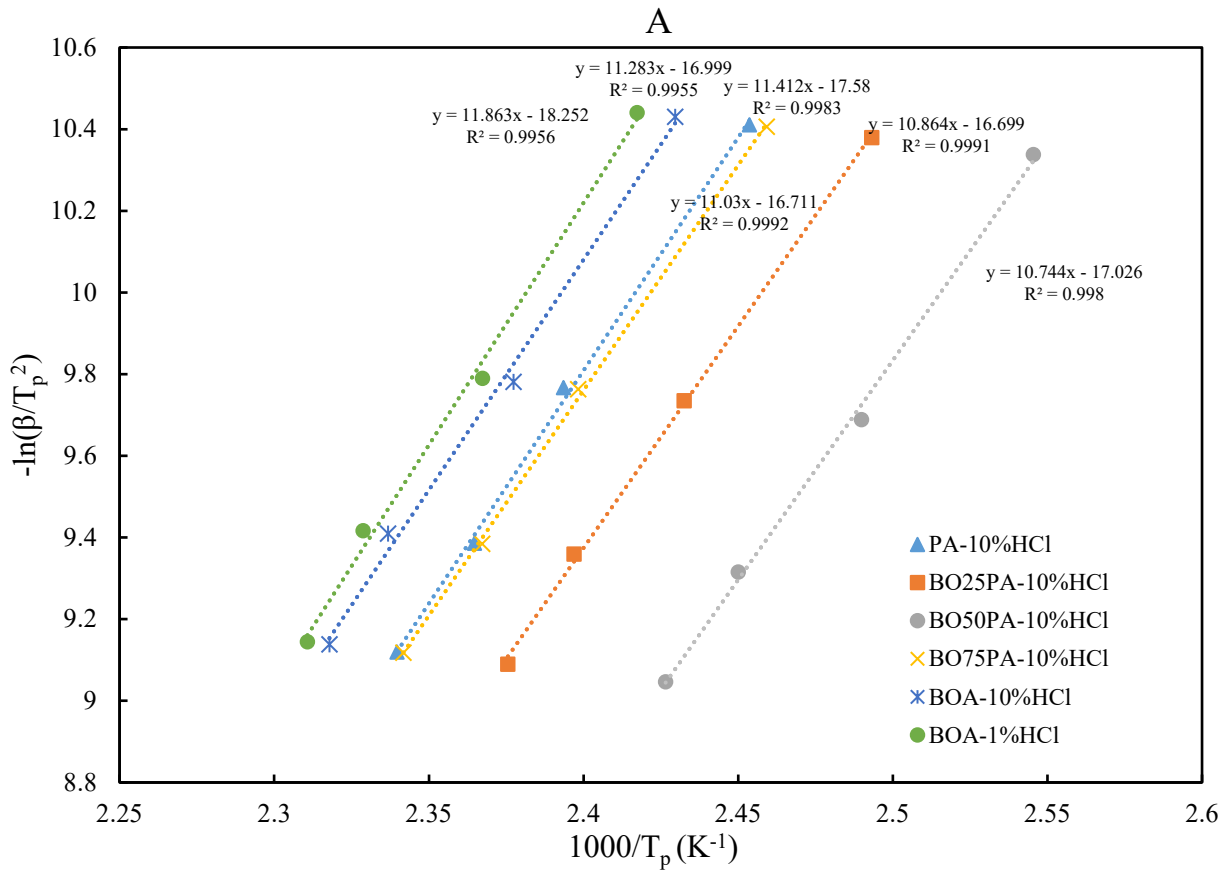
A
y = 11.283x - 16.999
R² = 0.9955
y = 11.412x - 17.58
R² = 0.9983
y = 11.863x - 18.252
R² = 0.9956
y = 10.864x - 16.699
R² = 0.9991
y = 11.03x - 16.711
R² = 0.9992
y = 10.744x - 17.026
R² = 0.998
PA-10%HCl
BO25PA-10%HCl
BO50PA-10%HCl
BO75PA-10%HCl
BOA-10%HCl
BOA-1%HCl
-ln(β/T_p^2)
1000/T_p (K^-1)

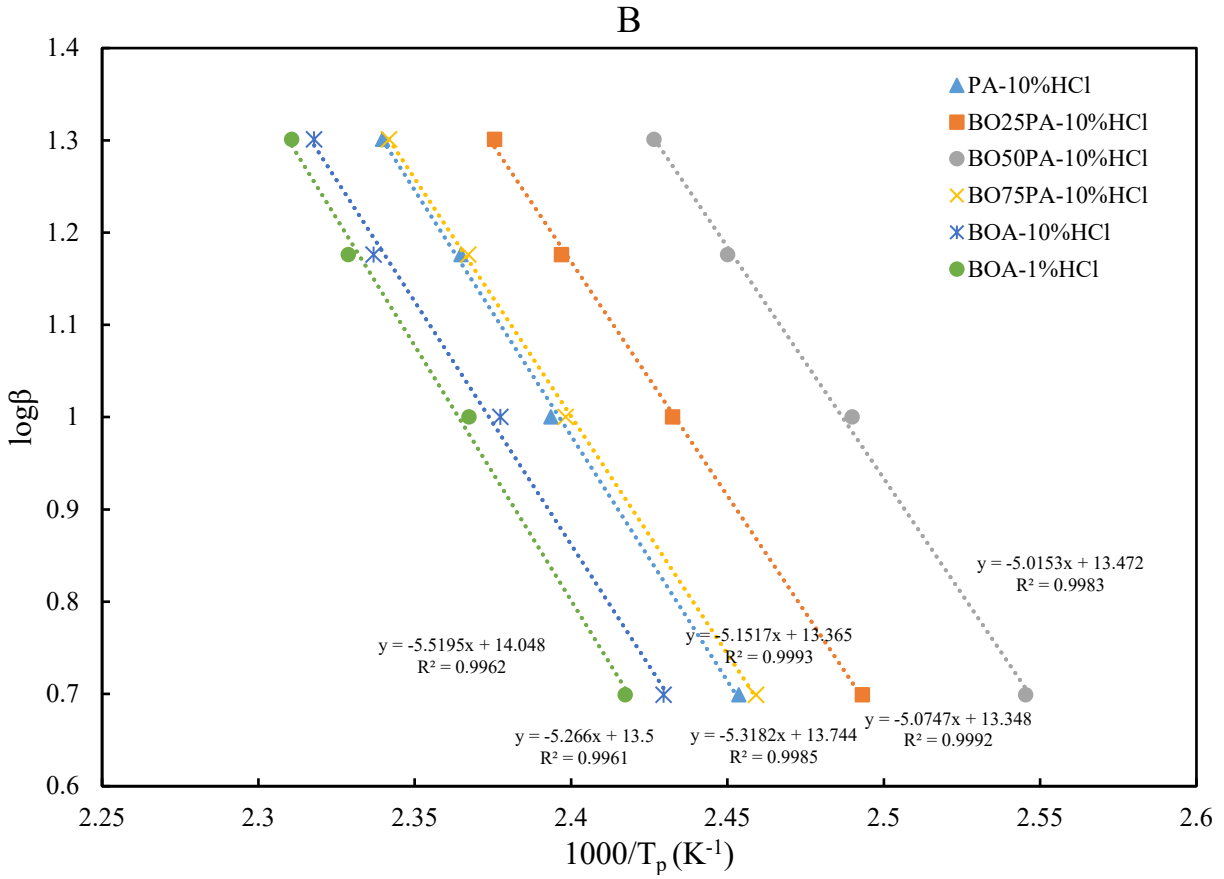
B
PA-10%HCl
BO25PA-10%HCl
BO50PA-10%HCl
BO75PA-10%HCl
BOA-10%HCl
BOA-1%HCl
y = -5.0153x + 13.472
R² = 0.9983
y = -5.5195x + 14.048
R² = 0.9962
y = -5.1517x + 13.365
R² = 0.9993
y = -5.0747x + 13.348
R² = 0.9992
y = -5.266x + 13.5
R² = 0.9961
y = -5.3182x + 13.744
R² = 0.9985
logβ
1000/T_p (K^-1)

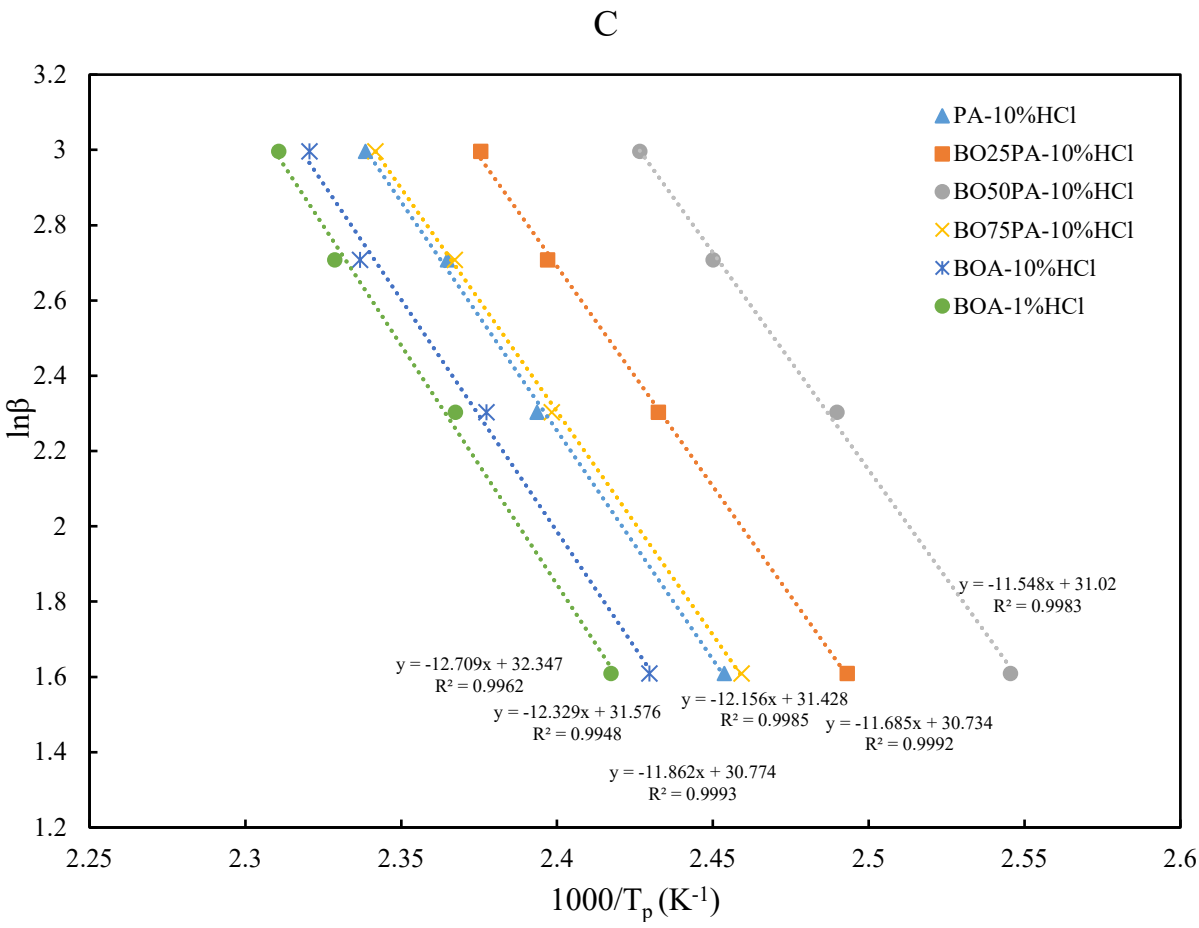

Figure A 3. 3 Plots of the DSC kinetic analysis by the (A) Kissinger, (B) Ozawa, and (C) Crane equations.

The cross-linking reactions show a single exothermic peak and all the temperatures of the curing reactions are between 95–160 °C. The onset temperature follows this order: BO50PA < BO25PA < BO75PA < BOA < PA. The peak temperature of the resins had a similar order as the onset temperature, while the T_p of BOA is higher than that of PA resin. With the addition of the bio-oil, the T_P decreases first and reaches its lowest value at 50%. When the bio-oil content is more than 50%, the value of T_P begins to increase. Moreover, when comparing the two BOPA resins polymerized at 1% and 10% HCl, it can be determined that using 10% HCl gives the lowest T_p and T_i.

Therefore, the BOA resin when using a 1% molar fraction of acid catalyst has a relatively larger E_a value than that when a 10% molar fraction is used. According to the results from GPC, the reaction under a high acid concentration leads to the resin with a broader molecular weight distribution including multiple reaction sites and a higher hydroxyl number, which is the main group that reacts with the epoxy groups (5.89 in

BOA1H, 7.49 in BOA10H). For the 10% of an acidic catalyst, a high reactivity resin having more hydroxyl groups can be produced, so it is easier to be cured by DGEBA.

Table A 3. 4 The thermal stability of the cured BOPA resins

Resin name	T_{d5} (°C)	T_{max} (°C)	R_{800}(%)
PA-10%HCl	323.5	422.0	12.0
BO25PA-10%HCl	309.8	412.4	22.2
BO50PA-10%HCl	304.1	398.3	30.8
BO75PA-10%HCl	295.1	396.3	30.9
BOA-10%HCl	275.3	389.6	34.4
BOA-1%HCl	265.2	386.2	34.1

The thermal stability of the cured BOPA resins was also studied to know their performance, which will further affect their application value. The results from TGA including the initial and highest thermal decomposition temperature and char yield at 800°C of the resins. Compared to uncured resins, the thermal stability of BOPA resins after curing significantly improved and is closer to PA resin. At the same DGEBA content, by increasing the bio-oil content, T_{d5} and T_{max} (°C) of the BOPA resins decrease after curing and follow the same sequence as the uncured resins. However, the trend of the char yield at 800 °C of the resins reached the highest point at BOA. Furthermore, the change in the thermal stability of the resin caused using different concentrations of acid catalysts is also reduced after curing. Thus, it seems to be possible to use a low concentration of acid catalyst for BOA resin synthesis. Through curing, all resins are more stable, and the increase in the residue also explains the occurrence of the cross-linking reaction between novolac resins and DGEBA.

Appendix 4

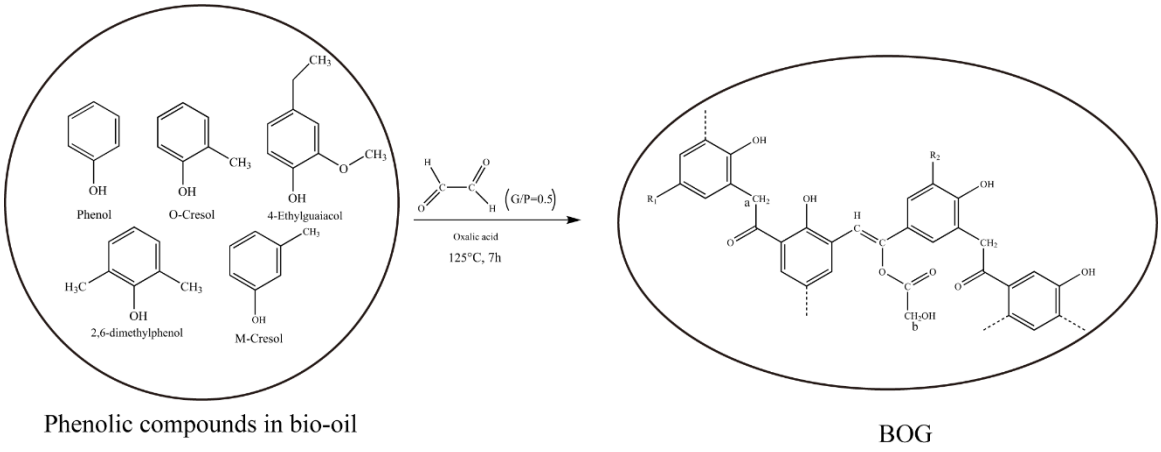

Figure A 4. 1 Schematic of the resin synthesis procedure

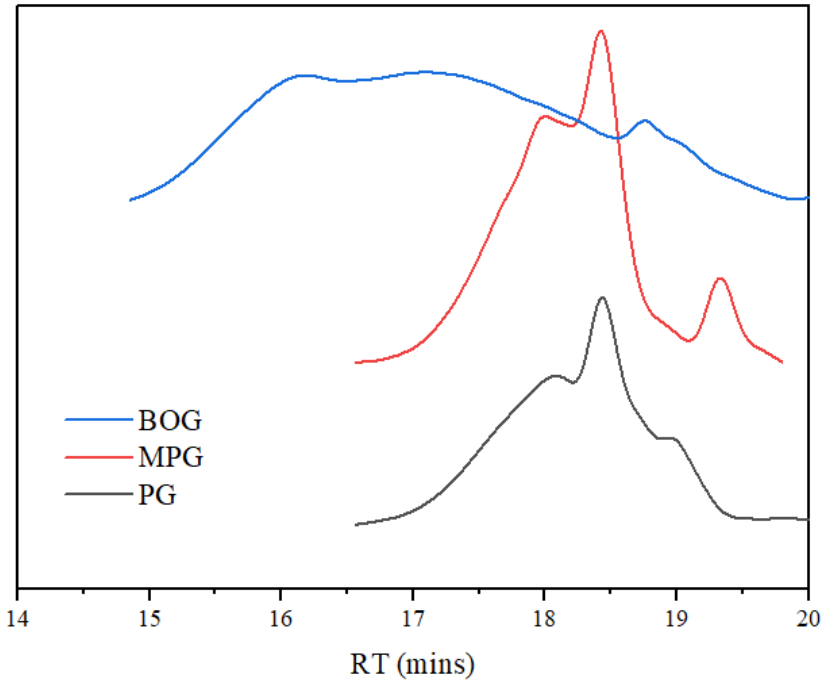

Figure A 4. 2 GPC chromatograms of PG, mimic and BOG resins

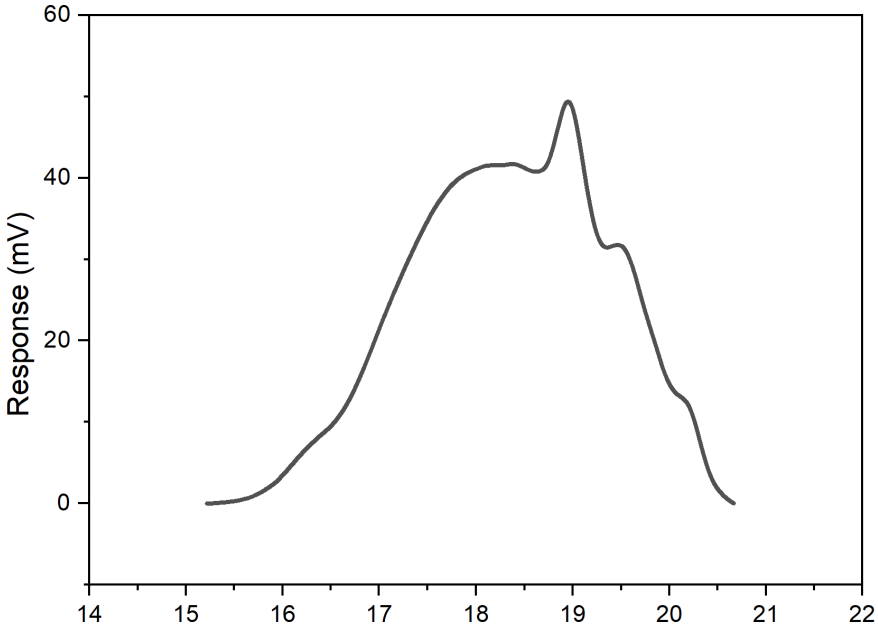

Figure A 4. 3 GPC chromatograms of BOE resin

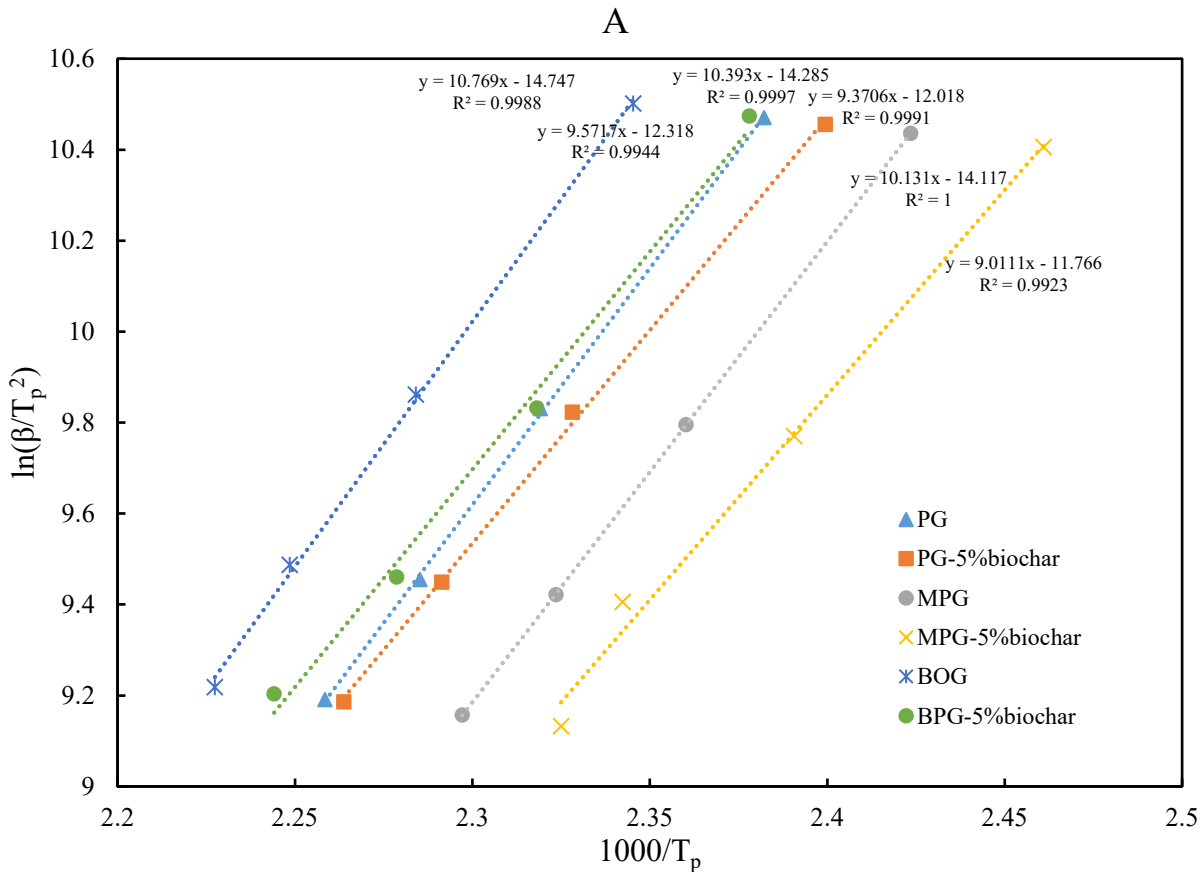

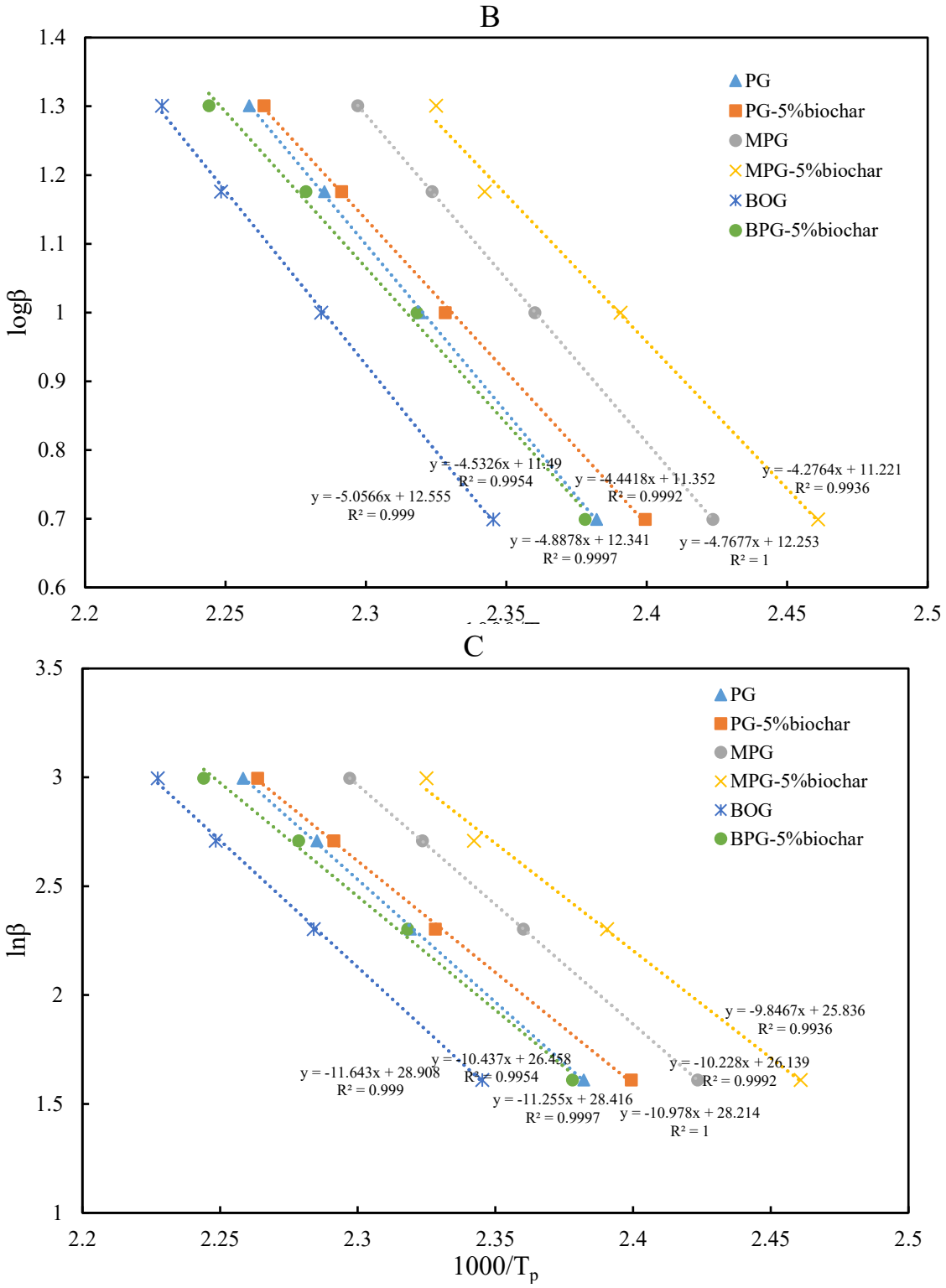

Figure A 4. 4 Plots of DSC kinetic analysis of PG, MPG and BOG by the (A) Kissinger and (B) Ozawa and (C) Crane equations

A. Kissinger

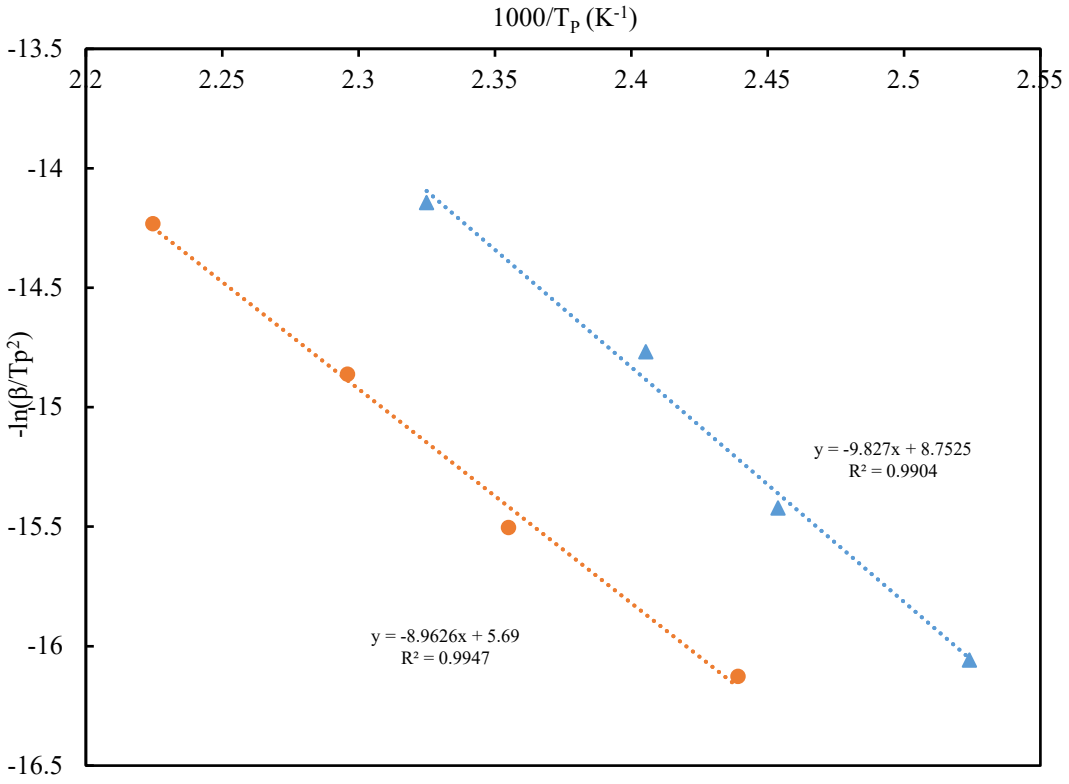

B. FWO

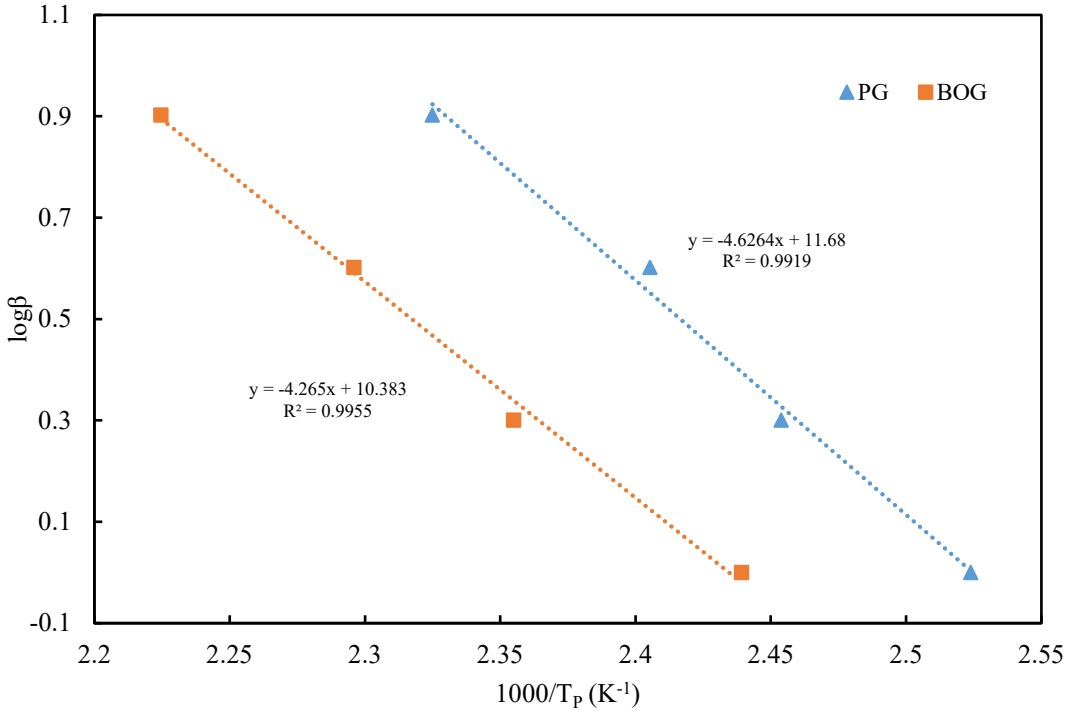

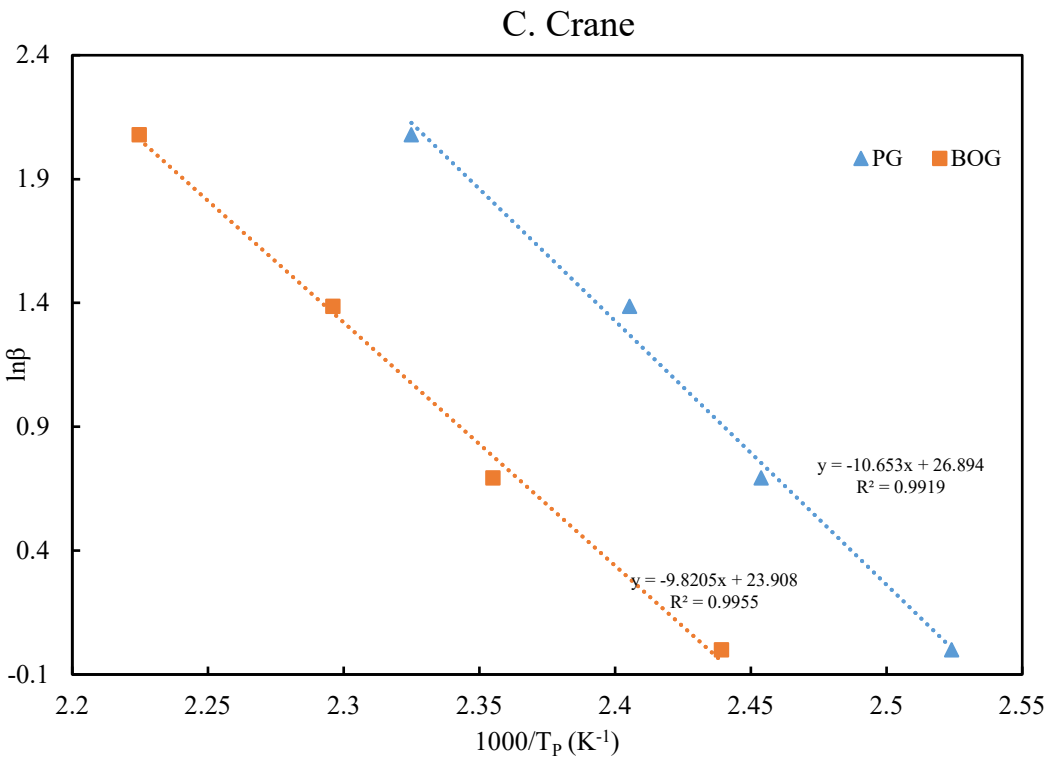

Figure A 4. 5 Plots of DSC kinetic analysis of (A) Kissinger and (B) Ozawa and (C) Crane equations for PG and BOG resin polymerization

Table A 4. 1 Safety criteria of resin polymerization at the various heating rate (125 °C)

Resin	Rate (℃/min)	C_{pm}(J/g/K)	TMR_{ad} at 125℃ (min)	T_{D24}	MTSR (K)	ΔT_{ad}(K)
PG	1	3.10	2.75	39.51	478.12	81.91
	2	3.22	2.65	39.12	492.52	85.00
	4	3.27	2.60	38.91	502.49	86.75
	8	3.34	2.49	38.46	514.76	90.41
BOG	1	2.37	8.97	46.59	486.76	73.63
	2	2.32	8.64	46.13	504.19	76.47
	4	2.40	8.62	46.10	516.61	76.64
	8	2.38	8.59	46.06	525.44	76.90

Table A 4. 2 Safety criteria of resin curing at various heating rate (120 °C)

Resin	Rate (K/min)	C_{pm}(J/g/K)	TMR_{ad} at 120°C (min)	T_{D24}	MTSR (K)	Δt_{ad}(K)
PG + 40%DGEBA	5	1.56	5.17	46.84	474.91	51.96
	10	1.58	5.17	46.83	480.99	52.02
	15	1.57	4.96	46.39	491.82	54.23
	20	1.54	4.93	46.34	500.55	54.49
PG + 40% DGEBA +5%biochar	5	2.28	6.45	42.52	453.05	36.78
	10	2.34	6.69	42.93	464.78	35.49
	15	2.24	6.31	42.26	475.39	37.61
	20	2.30	6.48	42.57	485.51	36.62
BOG + 40% DGEBA	5	1.66	8.11	53.75	476.99	50.61
	10	1.65	8.15	53.80	488.20	50.38
	15	1.65	7.94	53.52	496.46	51.71
	20	1.65	7.62	53.09	502.83	53.88
BOG + 40% DGEBA +5%biochar	5	2.49	8.25	46.72	457.52	34.02
	10	2.48	8.11	46.52	468.17	34.63
	15	2.47	8.18	46.62	473.14	34.34
	20	2.46	7.92	46.25	481.82	35.47